

Carbon allocation and tree growth under hydraulic  
constraints in Scots pine (*Pinus sylvestris* L.)

Federico Magnani

Ph.D.  
The University of Edinburgh  
1999



I want to dedicate this work to my wife Sabrina, to her calm quest for beauty and excellence that lights my life, thanking her for her patience during my stay in Edinburgh (and even more, I guess, after my return home). And to my parents, for their continuous support and for seeding a spirit of search and endeavor deep in my heart.

I want to thank Prof. Marco Borghetti, who initiated me to the wonders of scientific research, for continuous critical discussion and encouragement, and Prof. Frits Mohren, who trusted a young scientist, waiting for years for promises to bear fruit.

But even more, I want to thank my supervisor, Prof. John Grace, for his spirit of marvel in front of nature and life, the greatest gift a teacher can give to his students.

I also wish to thank Dr. James Irvine, Dr. Maurizio Mencuccini and Dr. Mauro Centritto for their practical help and for stimulating night-time discussions.

I hereby certify that this Thesis is the result of my original work for a Ph.D. degree at the University of Edinburgh. Although some of the experimental data analyzed have been kindly provided by colleagues at the University of Edinburgh, as clearly acknowledged in the Thesis, my contribution to the work has been substantial

Federico Magnani

## Abstract

Minimum leaf water potential has been found to be rather constant in coniferous species over a range of environmental conditions and developmental stages. Such a functional homeostasis requires the balanced growth of transpiring foliage, absorbing roots and conductive sapwood, with profound implications for resource allocation, plant allometry and productivity. Although central to the maintenance of plant structure, the process of growth allocation is still poorly understood.

The observation of a functional homeostasis in water transport has led to formulate a novel hypothesis of optimal plant growth under hydraulic constraints. The hypothesis has been tested against field and literature data of forest function and growth, choosing *Pinus sylvestris* as a model coniferous species.

The newly developed hypothesis delineates a common framework that seems to explain conveniently changes in growth allocation both over the lifetime of the plant and in response to the environment, helping to explain the variability in forest growth observed at the regional scale as well as the age-related decline in forest productivity.

A detailed process model of forest growth (HYDRALL) was developed, centered on the hypothesis of optimal carbon allocation under hydraulic constraints, and applied to the prediction of *P. sylvestris* growth patterns across Europe. The model was found to predict conveniently several of the growth patterns reported in the literature. Changes in carbon allocation were found to be most important under dry conditions.

Information on root hydraulic characteristics under natural conditions is scarce. Part of the research effort was therefore devoted to the development of a new technique for the measurement of the hydraulic resistance of entire root systems of soil-grown plants, a parameter central to the newly developed model.

## Summary

Chapter		Page
<b>1</b>	General introduction	8
<b>1.1</b>	Relevance of growth allocation	8
<b>1.2</b>	Approaches in modelling growth allocation	9
<b>1.3</b>	Functional homeostasis in water transport	11
<b>1.4</b>	The hypothesis of optimal growth under hydraulic constraints	12
<b>1.5</b>	Implications of the hypothesis: age-related decline in forest productivity	14
<b>1.6</b>	Implications of the hypothesis: response of allocation and growth to the environment	15
<b>1.7</b>	Reducing the uncertainty: measuring root hydraulic characteristics	16
<b>1.8</b>	Conclusions	17
<b>2</b>	Age-related decline in stand productivity: the role of structural acclimation under hydraulic constraints	25
<b>2.1</b>	Introduction	25
<b>2.2</b>	Theory	27
	<b>2.2.1</b> Implications of structural developmental changes	27
	<b>2.2.2</b> The hydraulic constraint	29
	<b>2.2.3</b> Optimal allometry under hydraulic constraints	32
<b>2.3</b>	Materials and methods	34
	<b>2.3.1</b> Site description	34
	<b>2.3.2</b> Leaf and xylem characteristics	35
	<b>2.3.3</b> Stand $P_a$	35
	<b>2.3.4</b> Fine root biomass	35
	<b>2.3.5</b> Fine root characteristics	36
<b>2.4</b>	Results and discussion	36
<b>2.5</b>	Conclusions	43
<b>App. 2.1</b>	Variables, parameters and units used in the	

	model	49
App. 2.2	An analysis of the components of below-ground productivity	51
3	On the causes of the age-related decline of forest growth. A meta-analysis of data from <i>Pinus sylvestris</i> L.	52
3.1	Introduction	52
3.2	Material and methods	53
3.3	Results and discussion	55
3.4	Conclusions	61
4	Acclimation of coniferous tree structure to the environment under hydraulic constraints	66
4.1	Introduction	66
4.2	Theory	68
4.2.1	Optimal tree allometry under hydraulic constraints	68
4.2.2	Response of allometry to key environmental parameters	72
4.2.3	Growth allocation under hydraulic constraints	76
4.3	Materials and methods	78
4.3.1	Test of the hypothesis of functional homeostasis	78
4.3.2	Test of forest growth model	79
4.4	Results and discussion	80
4.4.1	Test of the hypothesis of functional homeostasis	80
4.4.2	Implications for stand development	83
4.4.3	Response of plant structure to soil water availability	84
4.4.4	Response of plant structure to air humidity	85
4.4.5	Response of plant structure to temperature	87
4.4.6	Response of plant structure to climate	89
4.5	Conclusions	90

<b>App. 4.1</b>	Variables, parameters and units used in the model	97
<b>App. 4.2</b>	Combination of hydraulic, carbon and height constraints	99
<b>App. 4.3</b>	Analytical solution of cubic equation	100
<b>5</b>	Growth patterns of <i>Pinus sylvestris</i> across Europe. A functional analysis using the Hydrall model	102
<b>5.1</b>	Introduction	102
<b>5.2</b>	Model description	104
	<b>5.2.1</b> Light absorption by the canopy	105
	<b>5.2.2</b> Vertical functional gradients	106
	<b>5.2.3</b> Aerodynamic decoupling	106
	<b>5.2.4</b> Stand gas-exchange and respiration	106
	<b>5.2.5</b> Understorey gas-exchange and site water balance	107
	<b>5.2.6</b> Foliage water relations	108
	<b>5.2.7</b> Stand growth and allocation	108
	<b>5.2.8</b> Stand density	110
	<b>5.2.9</b> Soil carbon dynamics	110
	<b>5.2.10</b> Weather simulation	111
<b>5.3</b>	Model results	112
<b>5.4</b>	Discussion	116
<b>5.5</b>	Conclusions	120
<b>App. 5.1</b>	Summary of parameter values used in computations	126
<b>6</b>	Measurement of apoplastic and cell-to-cell components of root hydraulic conductance by a pressure clamp technique	127
<b>6.1</b>	Introduction	127
<b>6.2</b>	Theory	130
<b>6.3</b>	Materials and methods	136
	<b>6.3.1</b> Plant material	136
	<b>6.3.2</b> Description of the instrument	136

	<b>6.3.3</b>	Data analysis	139
<b>6.4</b>		Results	139
<b>6.5</b>		Discussion	143
<b>7</b>		General discussion	153
<b>7.1</b>		Introduction	153
<b>7.2</b>		Summary of key results	154
<b>7.3</b>		Functional homeostasis in water transport and optimal growth: a critique	157
<b>7.4</b>		Hydraulic limitations and tree function: model comparison	159
<b>7.5</b>		Future developments: optimal stomatal conductance and allocation under hydraulic constraints	161
<b>7.6</b>		Future developments: combining hydraulic and nutrient constraints	162
	<b>7.6.1</b>	Functional balance in carbon and nutrient uptake	163
	<b>7.6.2</b>	Effects of nitrogen on leaf and root function	165
<b>App. 1</b>		Plant energetics and population density. Comments to the paper 'Allometric scaling of plant energetics and population density' by Enquist B.J., Brown J.H. and West G.B. (Nature 395, 163-165. 1998)	170
<b>App. 2</b>		HYDRALL model source code	172

## Chapter 1. General introduction

I've read all the books but one  
Only remains sacred: this  
Volume of living wonders, open  
Always before my eyes

Kathleen Raine

### 1.1 Relevance of growth allocation

Higher organisms consist of complex, self-organizing networks of cells and tissues mutually interacting, each relying on the others for acquisition of resources and survival. This is particularly evident in trees, where a green photosynthesizing canopy is spatially divided from stem and root tissues, which are primarily responsible for the acquisition and transport of inorganic nutrients and water, as well as for mechanical support. The energy harnessed in the canopy through photosynthesis is channelled through phloem to all other heterotrophic tissues, resulting in the balanced growth of the entire organism. Although central to the maintenance of plant structure, this process of growth allocation is still poorly understood (Komor 1994; McDonald & Davies 1996). The processes of phloem loading, transport and unloading have been the subject of very detailed research (Lang 1983; Van Bel 1993; Patrick 1997), but the basic information gained appears still insufficient to understand and represent the entire process.

Yet, a clear representation of allocation and its response to the environment could prove central to our understanding of plant and forest function.

Allocation to root growth can take up more than 60 % of stand net primary productivity (Cannell 1985), but with large variability among different conditions (Santantonio 1989; Beets & Whitehead 1996). The balance between foliage and fine roots, for example, is known to be strongly affected by nutrient and water availability, light, carbon dioxide and temperature and to vary among developmental stages (Wilson 1988). Allocation to sapwood is also variable, reflecting in changes in the foliage-to-sapwood area ratio. The balance is known to be modulated by the environment (Nilsson



& Albrektson 1993; Mencuccini & Grace 1995) and to change with age (Albrektson 1984; Mencuccini & Grace 1996b) and in response to thinning (Margolis *et al.* 1988; Pothier & Margolis 1991), with important effects on plant carbon balance and productivity (Gower, McMurtrie & Murty 1996). A review of environmental effects on carbon allocation in conifers can be found in Gower *et al.* (1995) and Dewar *et al.* (1994).

Moreover, the ability to explain and predict the acclimation of tree structure to the environment would greatly increase the generality of forest growth models (Sharpe 1990), overcoming the need for site-specific parameterisation of structural characteristics.

In conclusion, there appears to be a need for reliable models of growth allocation (Landsberg *et al.* 1991).

## **1.2 Approaches in modelling growth allocation**

Several alternative approaches have been proposed over the years, as reviewed by Cannell (1985), Wilson (1988), Santantonio (1990) and more recently by Cannell and Dewar (1994).

Most of the attention has concentrated on the balance between foliage and fine roots, mainly focusing on the trade-offs between carbon assimilation and nutrient absorption. The empirical observation of rather constant allometric relations has been the basis of earliest models, and the same approach has been later extended by assuming fixed allocation functions, irrespective of age and environment, or by prescribing the response of allocation to these factors.

More recently, the observation of a functional balance between foliage photosynthesis and nutrient absorption by the roots has set the ground for a more realistic representation of plant function. The balance between foliage and fine root biomass is suggested to be inversely proportional to tissue activity, itself a complex function of the environment, so as to achieve a functional balance and maintain tissue nutrient contents at a constant level. According to Cannell and Dewar (1994), the nitrogen productivity approach of Ågren and Ingestad (1987) would also fit in this group.

A constant tissue nutrient content was also assumed by Reynolds and Thornley (1982)

in their teleonomic approach, based on the assumption of co-limitation of growth by carbon and nutrient content in the substrate. Optimal growth was on the contrary assumed as a teleonomic goal in a later similar model (Johnson & Thornley 1987).

A fully mechanistic approach has also been proposed by Thornley (1972), based on the assumptions of co-limitation of meristem growth by carbon and nitrogen and of an opposite flux of carbon and nitrogen through the plant, driven by concentration gradients divided by resistances to flow. Although many parameters in the model cannot be independently measured, the approach has been successfully applied in a forest and generic ecosystem model by Rastetter *et al.* (1991). Alternative limitation by either carbon or nitrogen was assumed, on the contrary, in the mechanistic model proposed by Cheeseman (1993).

In a later development, the Thornley (1972) model has been extended by Dewar (1993) to take into account the combined limitations imposed on carbon allocation and plant growth by nutrient and water availability. A linear reduction with decreasing water potential in the relative growth rate of both leaves and fine roots was assumed; this was found to account for the often observed increase in root-shoot ratio under drought conditions (Wilson 1988).

An alternative approach to the modelling of carbon allocation under drought conditions was proposed by Givnish (1986), based on the hypothesis of a direct detrimental effect of leaf water potential on assimilation. As a result, an excessive allocation to photosynthesizing foliage was found to be detrimental to growth, as it resulted in a more than proportional reduction in assimilation per unit foliage biomass. Optimal growth (Bloom, Chapin & Mooney 1985; Parker & Maynard Smith 1990) was achieved, on the contrary, through a balanced development of transpiring foliage and absorbing roots.

All of the approaches reviewed so far focus on the balance between foliage and fine roots only, but fail to consider the process of carbon allocation to sapwood. Wood production, however, is of the highest relevance in forest trees, both because of its role in storing carbon over long periods and because of its economic relevance.

Functional balance in water transport between foliage and sapwood area has been the basis of many recent models of forest growth. Leonardo da Vinci already observed that "all the branches of a tree at every stage of its height, when put together, are equal in

thickness to the trunk below them" (Richter 1989). This empirical observation has been later extended to the balance between foliage and the area of conducting sapwood (Shinozaki *et al.* 1964a) and attributed to the hydraulic demands of water transport. According to the pipe model (Shinozaki *et al.* 1964b; Margolis *et al.* 1995), the sapwood can be viewed as a bundle of conducting pipes, extending from the roots to the canopy, each supporting with water and nutrients a unit amount of transpiring foliage. And a rather constant foliage-to-sapwood area ratio has indeed been observed in many tree species (Whitehead 1978; Waring, Schroeder & Oren 1982; Long & Smith 1988; Long & Smith 1989; Shelburne, Hedden & Allen 1993).

Valentine (1985) first explored the implications of the pipe model for carbon allocation and tree growth. The analysis was further extended by Makela (1986), by assuming that the functional allometry of the plant can be wholly captured by the principle of functional balance: in nutrient uptake and photosynthesis, which regulates allocation between leaves and fine roots, and in water transport, which in accordance to the pipe model dictates the balance between foliage and sapwood. The commonly observed age-related decline in forest stand productivity (Ryan, Binkley & Fownes 1997) was also partly predicted by the model, as a consequence of the increasing costs of sapwood production and respiration in ageing stands.

The pipe model also constitutes the basis for the analysis by Friend (1993) of the functional determinants of maximum attainable tree height, together with the Givnish (1986) optimization approach. Tree height not only determines the balance between assimilating foliage and respiring sapwood biomass; it also affects foliage water potential, through its gravitational component and because of the increased resistance of conducting pipes, so shifting the optimum balance between foliage and absorbing roots. The maximum height attainable by a tree was therefore expected to be a function of local environmental conditions and to be curbed, for example, by soil drought and high transpiration rates in dry air.

### **1.3 Functional homeostasis in water transport**

In his review on plant water relations, Passioura (1982) noted that "the hydraulic resistance of a whole plant has often been found to be variable, with a tendency to keep

leaf water potential constant over a wide range of transpiration rates". This tendency has been observed on herbaceous plants in response to changes both in air humidity (Tinklin & Weatherley 1966; Stoker & Weatherley 1971) and in root water potential (Macklon & Weatherley 1965), and Boyer (1985) noted that such a pattern is probably associated with growth processes. More recently, Whitehead *et al.* (1983) extended this observation to *Pinus radiata* seedlings acclimated to different air humidity conditions, coming to the conclusion that minimum leaf water potential is conserved irrespective of transpiration rates, as long as long-term changes are considered. All this evidence points to the existence of a functional homeostasis in water transport.

The empirical observation of such a homeostatic behavior in plant function (as opposed to structure, as predicted by the pipe model) led Whitehead *et al.* (1984a) to speculate of the likely implications for the response of tree allometry to the environment. They reasoned that, if the hydraulic resistance to water flow is assumed to be located in the stem and to be linearly related to tree height and inversely related to sapwood permeability and to foliage-to-sapwood area ratio, minimum leaf water potential can be kept constant only by adjusting plant allometry to local environmental conditions (Margolis *et al.* 1995) (as explained in more detail in **Chapter 2 and 4**). The experimental evidence they presented seemed to support this view, both at the population and at the interspecific level. From their analysis, the balance between transpiring foliage and conductive sapwood area should also change with tree height .

#### **1.4 The hypothesis of optimal growth under hydraulic constraints**

The approaches of Givnish (1986), as extended to forest growth by Friend (1993), and Whitehead *et al.* (1984a) both focus on the effects on allocation and growth of hydraulic constraints. They can be viewed as complementary: whilst Friend (1993) explored the implications for the balance between transpiring leaves and absorbing roots, under the assumption of a constant foliage-to-sapwood area ratio, Whitehead *et al.* (1984a) neglected the role of roots in water transport, concentrating on the contrary on interactions within the shoot. Both points of view could be misleading: in Scots pine (*Pinus sylvestris* L.), for example, considerable changes in the foliage-to-sapwood area ratio have been observed both over the lifetime of the stand (Albrektson 1980;

Albrektson 1984; Mencuccini & Grace 1996a) and in response to the environment (Mencuccini & Grace 1995); the contribution of the root system and the soil to total plant hydraulic resistance, on the other hand, has been reported to exceed 50% (Roberts 1977) and cannot be safely neglected.

The main objective of the present work was to merge the two approaches, exploring at length the implications of functional homeostasis in water transport. This has led to formulate a novel hypothesis of optimal plant growth under hydraulic constraints (**Chapter 2 and 4**).

Evolution is assumed to have resulted in an allocation strategy that maximizes plant fitness within the limits imposed by the species' functional characteristics and by the environment (Parker & Maynard Smith 1990). Foliage production has been chosen as a fitness criterion to be maximized, because of its correlation with height increments (Ludlow, Randle & Grace 1990) and the pivotal role of tree height in interindividual competition and plant survival in closed canopies (Vanclay 1994; Oliver & Larson 1996). Were all resources to be allocated to foliage growth, however, this would result in extremely negative values of leaf water potential over the course of the year, which would pose a threat to the integrity of the entire system, possibly because of the risk of diffuse xylem embolism (Tyree & Sperry 1989). Minimum leaf water potential, on the contrary, has been found to be rather constant in coniferous species over a range of environmental conditions and developmental stages (as reviewed for *P. sylvestris* in **Chapter 4**). If this functional homeostasis is to be maintained, resources have to be allocated to the production of new sapwood and fine roots. Optimal height growth, on the other hand, requires that resources be allocated among transport tissues in an efficient way, in order to increase hydraulic conductance at the lowest possible carbon cost. An analysis of marginal costs and returns of sapwood and fine roots allocation (**Chapter 2 and 4**) demonstrates that this optimal balance is strongly affected both by tree height and by environmental conditions, more carbon being allocated for example to feeder roots in tall stands and under stress conditions.

In testing the model, Scots pine has been chosen as a model coniferous species both for its relevance in British and European forests (Christie & Lines 1979; Boratynski 1991) and because of the great deal of functional information on the species that has been gained at the University of Edinburgh over the years (Jarvis 1976; Whitehead 1978;

Waring, Whitehead & Jarvis 1979; Beadle, Talbot & Jarvis 1982; Whitehead, Jarvis & Waring 1984b; Beadle *et al.* 1985b; Beadle *et al.* 1985a; Beadle *et al.* 1985c; Pena & Grace 1986; Grace & Norton 1990; Borghetti *et al.* 1991; Sobrado, Grace & Jarvis 1992; Edwards *et al.* 1994; James, Grace & Hoad 1994; Berninger *et al.* 1995; Jackson, Irvine & Grace 1995a; Jackson, Irvine & Grace 1995b; Jackson *et al.* 1995; Mencuccini & Grace 1995; Mencuccini & Grace 1996a, 1996b; Mencuccini, Grace & Fioravanti 1997; Irvine *et al.* 1998).

### **1.5 Implications of the hypothesis: age-related decline in forest productivity**

The age-related decline in above-ground net primary productivity that is usually observed in forest stands has been variously attributed to respiration, nutrient or hydraulic limitations (Gower, McMurtrie & Murty 1996; Ryan, Binkley & Fownes 1997). The relevance of age-related changes in forest function has been the subject of a scientific correspondence by the Author to *Nature* (Magnani 1999), which is reported at the end of the thesis as **Appendix A**.

The newly proposed model was found to explain the phenomenon and the co-occurring changes in the balance between foliage, conducting sapwood and fine roots (**Chapter 2**). As the plant grows taller, allocation is predicted to shift from foliage to transport tissues; higher respiration and fine root turnover would then result in the observed decline in above-ground net primary productivity. The predictions of the model have been successfully compared with experimental data from a chronosequence of *P. sylvestris* stands in Thetford Forest (Suffolk, UK; Mencuccini & Grace 1996a, 1996b): the observed reduction in above-ground productivity is well explained by concurrent modifications in leaf area index and plant structure. In turn, changes in allometry and shoot hydraulic conductance with age are conveniently predicted by the principle of functional homeostasis.

To test the generality of model predictions for this model tree species, additional experimental evidence has been derived from the literature (**Chapter 3**), comparing data-sets relating to different environmental conditions throughout Europe (Ovington 1957; Mälkönen 1974; Albrektson & Valinger 1985; Mencuccini & Grace 1996b). The commonly observed reduction in aboveground net primary production with age has

been found to result from a combination of declining stand leaf area index and light interception, on the one hand, and lower light utilization coefficients, on the other. Both the extent and the speed of the productivity decline appeared to increase with site productivity. The observed reduction in leaf area index was found to be largely the result of stand self-thinning, which more than compensates the increase in tree foliage biomass with age. Changes in resource allocation with age were found to be most likely responsible for the observed decline in light use efficiency: in all the stands analyzed, the functional balance between foliage, sapwood and fine roots changes with age, less carbon being invested in foliage in old, taller trees. This observation is in good agreement with the hypothesis of functional homeostasis in water transport that has just been outlined.

#### **1.6 Implications of the hypothesis: response of allocation and growth to the environment**

The implications of the hypothesis of optimal growth under hydraulic constraints for the response to key environment factors of carbon allocation and forest growth were then explored (**Chapter 4**). A simple carbon balance model allowed to analyze not only tree allometric relationships, but also stand growth dynamics in a simple way. The effects of temperature, air humidity and soil water content were analyzed in detail. Because of the well known relationship between temperature and water viscosity, hydraulic resistances were predicted to decline under warmer conditions, so allowing a larger foliage area to be sustained by a given amount of sapwood or fine roots as observed by Berninger and Nikinmaa (1997) and Palmroth *et al.* (1999). Air vapour pressure deficit, determining the rate of transpiration per unit foliage area, was also predicted to affect carbon allocation, although the effect was expected to be partly countered by parallel changes in air temperature often observed under field conditions. Soil water content, eventually, was predicted to influence sapwood and root allocation to a different extent, the net effect largely depending on soil texture. Despite its simplicity, the model was found to explain in a coherent way the effects of climate on Scots pine allometry reported by Mencuccini and Grace (1995), as well as several other literature reports.

This simple analysis set the ground for the prediction of *P. sylvestris* growth patterns across Europe (**Chapter 5**). A detailed process model of forest growth (HYDRALL: HYDRaulic constraints on ALLocation) was developed, centered on the hypothesis of optimal carbon allocation under hydraulic constraints. The representation of other key forest functions was based on the latest understanding (Farquhar, von Caemmerer & Berry 1980; Westoby 1984; Campbell 1985; Ryan 1991; Lloyd & Taylor 1994; Leuning 1995; De Pury & Farquhar 1997; Wang & Leuning 1998), trying to find a balance between model reality, simplicity and generality (Sharpe 1990). The source code of the resulting model is reported in **Appendix B**. Model simulations, based on long-term climatological data for Europe (Hulme *et al.* 1995), analyzed the growth of Scots pine stands across two regional transects, exploring a temperature and a humidity gradient. The model was found to predict conveniently several (although not all) of the growth patterns reported by Christie and Lines (1979) and Ineson *et al.* (1984). Interestingly, changes in carbon allocation were found to be most important under dry conditions, whilst temperature-induced photosynthetic limitations played a larger role under boreal conditions. This could explain why the issue has been often neglected in previous models of forest growth, developed for nordic countries. The representation of structural acclimation to the environment, on the other hand, could greatly extend the generality and the applicability of process models.

### **1.7 Reducing the uncertainty: measuring root hydraulic characteristics**

Both ecophysiological research and process growth models have traditionally focused on above-ground processes, often neglecting the role of root function and belowground processes (Santantonio 1989; Santantonio 1990; Waisel, Eshel & Kafkafi 1991). Root functionality in water transport is, on the contrary, central to the newly developed model. Unfortunately, information on root hydraulic characteristics under natural conditions is scarce. Part of the research effort was therefore devoted to the development of a new technique for the measurement of the hydraulic resistance of entire root systems of soil-grown plants (**Chapter 6**; Magnani *et al.* 1996).

A novel pressure clamp technique (Zhu & Boyer 1992) was devised for the direct measurement of cell-to-cell and apoplasmic components of root hydraulic conductance;



the experimental results were analyzed in terms of a theoretical model of water and solute flow, based on a composite membrane model of the root (Steudle 1994). When water was forced under a constant pressure into a cut root system, an exponential decay of flow was observed, until a constant value was attained; when pressure was released, a reverse water flow out of the root system was observed, showing a similar exponential behavior. The model assumes that the transient flow occurs through a cell-to-cell pathway and the observed decrease is the result of accumulation of solutes in front of the root semi-permeable membrane, whilst the steady-state component results from the movement of water through the parallel apoplastic pathway. Root conductance components of potted cherry (*Prunus avium* L.) seedlings could be estimated by fitting the model to experimental data.

It is hoped that the technique, although not yet applied to *P. sylvestris*, will help fill this gap in present knowledge.

## 1.8 Conclusions

Changes in allocation patterns could provide a mechanism of structural acclimation to the environment, so reducing the vulnerability of forest ecosystems to projected Climate Change (Intergovernmental Panel on Climate Change 1996). Several models have been proposed over the last few years to explain the mechanisms of carbon allocation and structural acclimation. The newly developed hypothesis of optimal growth under hydraulic constraints delineates a common framework that seems to explain conveniently changes in growth allocation both over the lifetime of the plant and in response to the environment, helping to explain the variability in forest growth observed at the regional scale as well as the age-related decline in forest productivity.

The analysis highlights the ubiquitous effects of water availability and water relations on plant function and growth, not only under extreme drought conditions. The many aspects of plant function are strongly integrated and it could be that the long-held simplifying assumption that growth is limited only by the most limiting factor ("Liebig rule") has to be reconsidered.

This new perspective, however, should be viewed as complementary rather than alternative to existing hypotheses, as many processes superimpose to a various extent

under different environments. Further research is required to explore the interactions between water and nutrients in driving structural acclimation and between structural and stomatal responses in preventing the onset of diffuse embolism and tissue damage (Yoder *et al.* 1994; Waring & Silvester 1994; Ryan, Binkley & Fownes 1997).

## References

- Albrektson A. (1980) Relations between tree biomass fractions and conventional silvicultural measurements. *Ecological Bulletins* **32**, 315-327.
- Albrektson A. (1984) Sapwood basal area and needle mass of Scots pine (*Pinus sylvestris* L.) trees in central Sweden. *Forestry* **57**, 35-43.
- Albrektson A. & Valinger E. (1985) Relations between tree height and diameter, productivity and allocation of growth in a Scots pine (*Pinus sylvestris* L.) sample tree material. In *Crop Physiology of Forest Trees* (eds. P.M.A. Tigerstedt, P. Puttonen & V. Koski), pp. 95-105. University of Helsinki, Helsinki.
- Ågren G.I. & Ingestad T. (1987) Root:shoot ratio as a balance between nitrogen productivity and photosynthesis. *Plant Cell and Environment* **10**, 579-586.
- Beadle C.L., Jarvis P.G., Talbot H. & Neilson R.E. (1985a) Stomatal conductance and photosynthesis in a mature Scots pine forest. 2. Dependence on environmental variables of single shoots. *Journal of Applied Ecology* **22**, 573-586.
- Beadle C.L., Neilson R.E., Talbot H. & Jarvis P.G. (1985b) Stomatal conductance and photosynthesis in a mature Scots pine forest. 1. Diurnal, seasonal and spatial variation in shoots. *Journal of Applied Ecology* **22**, 557-571.
- Beadle C.L., Talbot H., Neilson R.E. & Jarvis P.G. (1985c) Stomatal conductance and photosynthesis in a mature Scots pine forest. 3. Variation in canopy conductance and canopy photosynthesis. *Journal of Applied Ecology* **22**, 587-595.
- Beadle C.L., Talbot H. & Jarvis P.G. (1982) Canopy structure and leaf area index in a mature Scots pine forest. *Forestry* **55**, 105-123.
- Beets P.N. & Whitehead D. (1996) Carbon partitioning in *Pinus radiata* stands in relation to foliage nitrogen status. *Tree Physiology* **16**, 131-138.
- Berninger F., Mencuccini M., Nikinmaa E., Grace J. & Hari P. (1995) Evaporative demand determines branchiness of Scots pine. *Oecologia* **102**, 164-168.
- Berninger F. & Nikinmaa E. (1997) Implications of varying pipe model relationships on Scots pine growth in different climates. *Functional Ecology* **11**, 146-156.
- Bloom A.J., Chapin F.S. & Mooney H.A. (1985) Resource limitation in plants. An economic analogy. *Annual Review Ecology Systematics* **16**, 363-392.
- Boratynski A. (1991) Range of natural distribution. In *Genetics of Scots Pine* (eds. M. Giertych & C. Matyas), pp. 19-30. Elsevier, Amsterdam.
- Borghetti M., Edwards W.R.N., Grace J., Jarvis P.G. & Raschi A. (1991) The refilling of embolized xylem in *Pinus sylvestris* L. *Plant Cell and Environment* **14**, 357-369.

- Boyer J.S. (1985) Water transport. *Annual Review of Plant Physiology and Plant Molecular Biology* **36**, 473-516.
- Campbell G.S. (1985) *Soil Physics with BASIC. Transport Models for Soil-Plant Systems*. Elsevier, Amsterdam.
- Cannell M.G.R. (1985) Dry matter partitioning in tree crops. In *Attributes of Trees as Crop Plants* (eds. M.G.R. Cannell & J.E. Jackson), pp. 160-193. ITE-NERC,
- Cannell M.G.R. & Dewar R.C. (1994) Carbon allocation in trees: a review of concepts for modelling. *Advances in Ecological Research* **25**, 50-104.
- Cheeseman J.M. (1993) Plant growth modelling without integrating mechanisms. *Plant Cell and Environment* **16**, 137-147.
- Christie J.M. & Lines R. (1979) A comparison of forest productivity in Britain and Europe in relation to climatic factors. *Forest Ecology and Management* **2**, 75-102.
- De Pury D.G.G. & Farquhar G.D. (1997) Simple scaling of photosynthesis from leaves to canopies without the errors of big-leaf models. *Plant Cell and Environment* **20**, 537-557.
- Dewar R.C. (1993) A root-shoot partitioning model based on carbon-nitrogen-water interactions and Munch phloem flow. *Functional Ecology* **7**, 356-368.
- Dewar R.C., Ludlow A.R. & Dougherty P.M. (1994) Environmental influences on carbon allocation in pines. *Ecological Bulletins* **43**, 92-101.
- Edwards W.R.N., Jarvis P.G., Grace J. & Moncrieff J.B. (1994) Reversing cavitation in tracheids of *Pinus sylvestris* L. under negative water potentials. *Plant Cell and Environment* **17**, 389-397.
- Farquhar G.D., von Caemmerer S. & Berry J.A. (1980) A biochemical model of photosynthetic CO<sub>2</sub> assimilation in leaves of C<sub>3</sub> species. *Planta* **149**, 78-90.
- Friend A.D. (1993) The prediction and physiological significance of tree height. In *Vegetation Dynamics & Global Change* (eds. A.M. Solomon & H.H. Shugart), pp. 101-115. Chapman & Hall, New York.
- Givnish T.J. (1986) Optimal stomatal conductance, allocation of energy between leaves and roots, and the marginal cost of transpiration. In *On the Economy of Plant Form and Function* (ed. T.J. Givnish), pp. 171-213. Cambridge University Press, Cambridge.
- Gower S.T., Isebrands J.G. & Sheriff D.W. (1995) Carbon allocation and accumulation in conifers. In *Resource Physiology of Conifers* (eds. W.K. Smith & T.M. Hinckley), pp. 217-254. Academic Press, San Diego.
- Gower S.T., McMurtrie R.E. & Murty D. (1996) Aboveground net primary production decline with stand age: potential causes. *Trends in Ecology & Evolution* **11**, 378-382.
- Grace J. & Norton D.A. (1990) Climate and growth of *Pinus sylvestris* at its upper altitudinal limit in Scotland. Evidence from tree growth-rings. *Journal of Ecology* **78**, 601-610.
- Hulme M., Conway D., Jones P.D., Jiang T., Barrow E.M. & Turney C. (1995) Construction of a 1961-1990 European climatology for climate change modelling and impact applications. *International Journal of Climatology* **15**, 1333-1363.

- Ineson P., Jones H.F. & Heal O.W. (1984) Regional aspects of forests in Europe: a preliminary study of *Pinus sylvestris*. In *State and Change of Forest Ecosystems. Indicators in Current Research* (ed. G.I. Ågren), pp. 315-332. Swed. Univ. Agric. Sci., Dept. Ecology & Environmental Research, Report No. 13.
- Intergovernmental Panel on Climate Change (1996) *Climate Change 1995. Impacts, Adaptations and Mitigation of Climate Change: Scientific-Technical Analyses*. Cambridge University Press, Cambridge.
- Irvine J., Perks M.P., Magnani F. & Grace J. (1998) The response of *Pinus sylvestris* to drought: stomatal control of transpiration and hydraulic conductance. *Tree Physiology* **18**, 393-402.
- Jackson G.E., Irvine J. & Grace J. (1995a) Xylem cavitation in Scots pine and Sitka spruce saplings during water stress. *Tree Physiology* **15**, 783-790.
- Jackson G.E., Irvine J. & Grace J. (1995b) Xylem cavitation in two mature Scots pine forests growing in a wet and a dry area of Britain. *Plant Cell and Environment* **18**, 1411-1418.
- Jackson G.E., Irvine J., Grace J. & Khalil A.A.M. (1995) Abscisic-acid concentrations and fluxes in droughted conifer saplings. *Plant Cell and Environment* **18**, 13-22.
- James J.C., Grace J. & Hoad S.P. (1994) Growth and photosynthesis of *Pinus sylvestris* at its altitudinal limit in Scotland. *Journal of Ecology* **82**, 297-306.
- Jarvis P.G. (1976) The interpretation of the variations in leaf water potential and stomatal conductance found in canopies in the field. *Philosophical Transactions of the Royal Society of London Series B- Biological Sciences* **273**, 593-610.
- Johnson I.R. & Thornley J.H.M. (1987) A model of shoot:root partitioning with optimal growth. *Annals of Botany* **60**, 133-142.
- Komor E. (1994) Regulation by futile cycles: the transport of carbon and nitrogen in plants. In *Flux Control in Biological Systems* (ed. E.-D. Schulze), pp. 153-201. Academic Press, San Diego.
- Landsberg J.J., Kaufmann M.R., Binkley D., Isebrands J.G. & Jarvis P.G. (1991) Evaluating progress toward closed forest models based on fluxes of carbon, water and nutrients. *Tree Physiology* **9**, 1-15.
- Lang A. (1983) Turgor-regulated translocation. *Plant Cell and Environment* **6**, 683-689.
- Leuning R. (1995) A critical appraisal of a combined stomatal-photosynthesis model for C<sub>3</sub> plants. *Plant Cell and Environment* **18**, 339-355.
- Lloyd J. & Taylor J.A. (1994) On the temperature dependence of soil respiration. *Functional Ecology* **8**, 315-323.
- Long J.N. & Smith F.W. (1988) Leaf area-sapwood area relations of lodgepole pine as influenced by stand density and site index. *Canadian Journal of Forest Research* **18**, 247-250.
- Long J.N. & Smith F.W. (1989) Estimating leaf area of *Abies lasiocarpa* across ranges of stand density and site quality. *Canadian Journal of Forest Research* **19**, 930-932.

- Ludlow A.R., Randle T.J. & Grace J.C. (1990) Developing a process-based growth model for Sitka spruce. In *Process Modeling of Forest Growth Responses to Environmental Stress* (eds. R.K. Dixon, R.S. Meldahl, G.A. Ruark & W.G. Warren), pp. 249-262. Timber Press, Portland, Oregon.
- Macklon A.E.S. & Weatherley P.E. (1965) Controlled environment studies of the nature and origins of water deficits in plants. *New Phytologist* **64**, 414-427.
- Magnani F. (1999) Plant energetics and population density. *Nature* **398**, 572
- Magnani F., Centritto M. & Grace J. (1996) Measurement of apoplasmic and cell-to-cell components of root hydraulic conductance by a pressure clamp technique. *Planta* **199**, 296-306.
- Makela A. (1986) Implications of the pipe model theory on dry matter partitioning and height growth in trees. *Journal of Theoretical Biology* **123**, 103-120.
- Margolis H., Oren R., Whitehead D. & Kaufmann M.R. (1995) Leaf area dynamics of conifer forests. In *Ecophysiology of Coniferous Forests* (eds. W.K. Smith & T.M. Hinckley), pp. 181-223. Academic Press, San Diego.
- Margolis H.A., Gagnon R.R., Pothier D. & Pineau M. (1988) The adjustment of growth, sapwood area, heartwood area, and sapwood saturated permeability of balsam fir after different intensities of pruning. *Canadian Journal of Forest Research* **18**, 723-727.
- Mälkönen E. (1974) Annual primary production and nutrient cycle in some Scots pine stands. *Communicationes Instituti Forestalis Fenniae* **84**.
- McDonald A.J.S. & Davies W.J. (1996) Keeping in touch: responses of the whole plant to deficits in water and nitrogen supply. *Advances in Botanical Research* **22**, 229-300.
- Mencuccini M. & Grace J. (1995) Climate influences the leaf area-sapwood area ratio in Scots pine. *Tree Physiology* **15**, 1-10.
- Mencuccini M. & Grace J. (1996a) Developmental patterns of aboveground xylem conductance in a Scots pine (*Pinus sylvestris* L.) age sequence. *Plant Cell and Environment* **19**, 939-948.
- Mencuccini M. & Grace J. (1996b) Hydraulic conductance, light interception and needle nutrient concentration in Scots pine stands and their relations with net primary productivity. *Tree Physiology* **16**, 459-468.
- Mencuccini M., Grace J. & Fioravanti M. (1997) Biomechanical and hydraulic determinants of tree structure in Scots pine: anatomical characteristics. *Tree Physiology* **17**, 105-113.
- Nilsson U. & Albrektson A. (1993) Productivity of needles and allocation of growth in young Scots pine trees of different competitive status. *Forest Ecology and Management* **62**, 173-187.
- Oliver C.D. & Larson B.C. (1996) *Forest Stand Dynamics*. John Wiley and Sons, New York.
- Ovington J.D. (1957) Dry-matter production by *Pinus sylvestris* L. *Annals of Botany* **21**, 287-314.
- Palmroth S., Berninger F., Nikinmaa E., Lloyd J., Pulkkinen P. & Hari P. (1999) Structural adaptation rather than water conservation was observed in Scots pine over a range of wet to dry climates. *Oecologia* **121**, 302-309

- Parker G.A. & Maynard Smith J. (1990) Optimality theory in evolutionary biology. *Nature* **348**, 27-33.
- Passioura J.B. (1982) Water in the soil-plant-atmosphere continuum. In *Encyclopedia of Plant Physiology* Vol. 12B (eds. O.L. Lange, P.S. Nobel, C.B. Osmond & H. Ziegler), pp. 5-33. Springer-Verlag, Berlin.
- Patrick J.W. (1997) Phloem unloading. Sieve element unloading and post-sieve element transport. *Annual Review of Plant Physiology and Plant Molecular Biology* **48**, 191-222.
- Pena J. & Grace J. (1986) Water relations and ultrasound emissions of *Pinus sylvestris* L. before, during and after a period of water stress. *New Phytologist* **103**, 515-524.
- Pothier D. & Margolis A. (1991) Analysis of growth and light interception of balsam fir and white birch saplings following precommercial thinning. *Annales des Sciences Forestieres* **48**, 123-132.
- Rastetter E.B., Ryan M.G., Shaver G.R., Melillo J.M., Nadelhoffer K.J., Hobbie J.E. & Aber J.D. (1991) A general biogeochemical model describing the response of the C and N cycles in terrestrial ecosystems to changes in CO<sub>2</sub>, climate, and N deposition. *Tree Physiology* **9**, 101-126.
- Reynolds J.F. & Thornley J.H.M. (1982) A shoot-root partitioning model. *Annals of Botany* **49**, 585-597.
- Richter J.P. (1989) *The notebooks of Leonardo da Vinci (1452-1519), compiled and edited from the original manuscripts*. Dover, New York.
- Roberts J. (1977) The use of tree-cutting techniques in the study of the water relations of mature *Pinus sylvestris* L. *Journal of Experimental Botany* **28**, 751-767.
- Ryan M.G. (1991) A simple method for estimating gross carbon budgets for vegetation in forest ecosystems. *Tree Physiology* **9**, 255-266.
- Ryan M.G., Binkley D. & Fownes J.H. (1997) Age-related decline in forest productivity: pattern and processes. *Advances in Ecological Research* **27**, 213-262.
- Santantonio D. (1989) Dry-matter partitioning and fine root production in forests. New approaches to a difficult problem. In *Biomass Production by Fast-Growing Trees*. (eds. J.S. Pereira & J.J. Landsberg), pp. 57-72. Kluwer Academic Publishers,
- Santantonio D. (1990) Modeling growth and production of tree roots. In *Process Modelling of Forest Growth Responses to Environmental Stress*. (eds. R.K. Dixon, R.S. Meldahl, G.A. Ruark & W.G. Warren), pp. 124-141. Timber Press, Portland.
- Sharpe P.J.H. (1990) Forest modeling approaches: compromises between generality and precision. In *Process Modeling of Forest Growth Responses to Environmental Stress* (eds. R.K. Dixon, R.S. Meldahl, G.A. Ruark & W.G. Warren), pp. 180-190. Timber Press, Portland.
- Shelburne V.B., Hedden R.L. & Allen R.M. (1993) The effects of site, stand density, and sapwood permeability on the relationship between leaf area and sapwood area in loblolly pine (*Pinus taeda* L.). *Forest Ecology and Management* **58**, 193-209.

- Shinozaki K., Yoda K., Hozumi K. & Kira T. (1964a) A quantitative analysis of plant form. The pipe model theory. I. Basic analyses. *Japanese Journal of Ecology* **14**, 97-105.
- Shinozaki K., Yoda K., Hozumi K. & Kira T. (1964b) A quantitative analysis of plant form. The pipe model theory. II. Further evidence of the theory and its application in forest ecology. *Japanese Journal of Ecology* **14**, 133-139.
- Sobrado M.A., Grace J. & Jarvis P.G. (1992) The limits to xylem embolism recovery in *Pinus sylvestris* L. *Journal of Experimental Botany* **43**, 831-836.
- Stedle E. (1994) The regulation of plant water at the cell, tissue, and organ level: role of active processes and of compartmentation. In *Flux Control in Biological Systems. From Enzymes to Populations and Ecosystems* (ed. E.-D. Schulze), pp. 237-299. Academic Press, San Diego.
- Stoker R. & Weatherley P.E. (1971) The influence of the root system on the relationship between the rate of transpiration and depression of leaf water potential. *New Phytologist* **70**, 547-554.
- Thornley J.H.M. (1972) A model to describe the partitioning of photosynthate during vegetative plant growth. *Annals of Botany* **36**, 419-430.
- Tinklin R. & Weatherley P.E. (1966) On the relationship between transpiration rate and leaf water potential. *New Phytologist* **65**, 509-517.
- Tyree M.T. & Sperry J.S. (1989) Vulnerability of xylem to cavitation and embolism. *Annual Review of Plant Physiology and Plant Molecular Biology* **40**, 19-38.
- Valentine H.T. (1985) Tree-growth models. Derivations employing the pipe model theory. *Journal of Theoretical Biology* **117**, 579-585.
- Van Bel A.J.E. (1993) Strategies of phloem loading. *Annual Review of Plant Physiology and Plant Molecular Biology* **44**, 253-281.
- Vanclay J.K. (1994) *Modelling Forest Growth and Yield*. CAB International, Wallingford.
- Waisel Y., Eshel A. & Kafkafi U. (eds) (1991) *Plant Roots: the Hidden Half*. M. Dekker, New York.
- Wang Y.P. & Leuning R. (1998) A two-leaf model for canopy conductance, photosynthesis and partitioning of available energy. I. Model description and comparison with a multi-layered model. *Agricultural and Forest Meteorology* **91**, 89-111.
- Waring R.H., Schroeder P.E. & Oren R. (1982) Application of the pipe model theory to predict canopy leaf area. *Canadian Journal of Forest Research* **12**, 556-560.
- Waring R.H. & Silvester W.B. (1994) Variation in foliar  $\delta^{13}\text{C}$  values within the crowns of *Pinus radiata* trees. *Tree Physiology* **14**, 1203-1213.
- Waring R.H., Whitehead D. & Jarvis P.G. (1979) The contribution of stored water to transpiration in Scots pine. *Plant Cell and Environment* **2**, 309-317.
- Westoby M. (1984) The self-thinning rule. *Advances in Ecological Research* **14**, 167-225.
- Whitehead D. (1978) The estimation of foliage area from sapwood basal area in Scots pine. *Forestry* **51**, 137-149.

- Whitehead D., Edwards W.R.N. & Jarvis P.G. (1984a) Conducting sapwood area, foliage area, and permeability in mature trees of *Picea sitchensis* and *Pinus contorta*. *Canadian Journal of Forest Research* **14**, 940-947.
- Whitehead D., Jarvis P.G. & Waring R.H. (1984b) Stomatal conductance, transpiration, and resistance to water uptake in a *Pinus sylvestris* spacing experiment. *Canadian Journal of Forest Research* **14**, 692-700.
- Whitehead D., Sheriff D.W. & Greer D.H. (1983) The relationship between stomatal conductance, transpiration rate and tracheid structure in *Pinus radiata* clones grown at different water vapour saturation deficits. *Plant Cell and Environment* **6**, 703-710.
- Wilson J.B. (1988) A review of evidence on the control of shoot:root ratio, in relation to models. *Annals of Botany* **61**, 433-449.
- Yoder B.J., Ryan M.G., Waring R.H., Schoettle A.W. & Kaufmann M.R. (1994) Evidence of reduced photosynthetic rates in old trees. *Forest Science* **40**, 513-527.
- Zhu G.L. & Boyer J.S. (1992) Enlargement in *Chara* studied with a turgor clamp. Growth rate is not determined by turgor. *Plant Physiology* **100**, 2071-2080.



## **Chapter 2. Age-related decline in stand productivity: the role of structural acclimation under hydraulic constraints**

Philosophy is written in this grand book - I mean the universe - which stands continually open to our gaze, but it cannot be understood unless one first learns to comprehend the language and interpret the characters in which it is written. It is written in the language of mathematics, and its characters are triangles, circles, and other geometrical figures, without which it is humanly impossible to understand a single word of it.

Galileo Galilei

### **2.1 Introduction**

The decline with age in aboveground forest stand productivity ( $P_a$ ) has long been known to forest ecologists (Kira & Shidei 1967; Gower, McMurtrie & Murty 1996). This process is only partly explained by the often observed decline in leaf area index and light interception: productivity per unit foliage biomass is also reduced (Ryan, Binkley & Fownes 1997).

Because of prolonged meristematic activity and of a continuous tissue turnover, the detrimental effects of cell ageing do not appear to play the same role in polycarpic plants as they do in animals (Nooden 1988). Rather, the explanation seems to be found in the shifting balance between photosynthesis, respiration and tissue turnover.

Kira and Shidei (1967) first hypothesized that the decline in net primary production with stand age was due to the continuous increase in respiring tissues. Direct observations, however, have recently demonstrated that increasing sapwood respiration accounts for only a small proportion of the  $P_a$  decline (Ryan & Waring 1992; Ryan *et al.* 1995).

An increased belowground allocation has also been proposed as a possible explanation, as a consequence of the reduced availability of nutrients that are increasingly immobilized in litter during stand development (Murty, McMurtrie & Ryan 1996). A higher fine root-to-foliage biomass ratio with age has indeed been often observed (Grier *et al.* 1981; Santantonio 1989; Ryan & Waring 1992; Usol'tsev & Vanclay 1995;

Vanninen *et al.* 1996).

The photosynthetic rates of young and old trees have also been observed to differ (Kull & Koppel 1987; Grulke & Miller 1994; Schoettle 1994; Yoder *et al.* 1994). The decline in photosynthesis per leaf area observed in ageing stands has been attributed either to a reduced foliar nitrogen concentration (Field & Mooney 1986), as a result of nutrient limitations, or to the increased hydraulic resistance of longer stems and branches in mature trees: in order to avoid extreme leaf water potentials and diffuse xylem cavitation, stomatal conductance and gas exchange would have to be reduced so as to maintain a functional homeostasis (Yoder *et al.* 1994; Saliendra, Sperry & Comstock 1995). However Sperry *et al.* (1993) reported that, following the artificial reduction of xylem hydraulic conductance, diffuse xylem embolism and foliage dieback could be prevented only temporarily by stomatal closure, but an increased production of xylem was required in the longer term.

Also over the lifetime of the stand, structural changes contribute to the maintenance of a functional homeostasis in water transport: not only by the already mentioned increase in fine root-to-foilage ratio, but also through an altered balance between the area of conductive sapwood and transpiring foliage (Albrektson 1984; van Hees & Bartelink 1993; Vanninen *et al.* 1996) that partly counterbalances the effects of increasing height on shoot hydraulic resistance (Mencuccini & Grace 1996a). As a result, hydraulic conductance per unit leaf area is remarkably constant with age. A shift of resource allocation from leaves to conductive structures in the stem and in the roots, reducing photosynthesis and increasing both respiration and turnover, could help explain the observed reduction in  $P_a$ .

Aboveground productivity has often been assumed as an indirect criterion of plant fitness, in particular in forest species that are strongly limited by competition for light (Bloom, Chapin & Mooney 1985; Parker & Maynard Smith 1990). One could then expect plants to have evolved a strategy of optimal growth under hydraulic constraints, whereby hydraulic safety is achieved through the minimum possible investment in sapwood and fine roots, so as to allocate as many resources as possible to the production of assimilating leaves and maximize  $P_a$ .

Two questions were therefore addressed in the present analysis. First, can the decline in aboveground net primary production observed in a chronosequence of Scots pine

(*Pinus sylvestris* L.) be explained by changes in the functional and allometric structure of the stand, even without a reduction in gas exchange and light use efficiency? Second, can the observed structural changes be explained by a strategy of optimal plant growth under the hydraulic limitations imposed by the risk of diffuse xylem embolism? A new mathematical model was developed to answer these questions.

## 2.2 Theory

### 2.2.1 Implications of structural developmental changes

The effects of structural changes on stand  $P_a$  and growth can be explored by a simple carbon balance analysis. Above-ground net primary production  $P_a$  can be expressed as:

$$P_a = (A - R_m) \cdot (1 - r_g) - P_b \quad (2.1)$$

where  $A$  is stand assimilation,  $R_m$  is maintenance respiration,  $r_g$  is specific growth respiration and  $P_b$  is stand below-ground net primary productivity. All variables and parameters are defined in Appendix 2.1.

Stand assimilation can be assumed to be proportional to the cumulated photosynthetic active radiation intercepted by the foliage over the growing season (McMurtrie *et al.* 1994):

$$A = \varepsilon_0 \cdot I \cdot [1 - \exp(-k \cdot \sigma \cdot W_f)] \quad (2.2)$$

where  $\varepsilon_0$  is stand gross light utilization coefficient,  $I$  is incoming photosynthetically active radiation,  $\sigma$  is specific leaf area,  $W_f$  is stand foliage biomass and  $k$  is a light extinction coefficient for the canopy.

A simple formulation can be used for both respiration and turnover of tree compartments (Thornley & Johnson 1990). Maintenance respiration of each plant compartment is assumed to be proportional to its biomass:

$$R_m = r_f^m \cdot W_f + r_s^m \cdot W_s + r_r^m \cdot W_r \quad (2.3)$$

where  $W_s$  is sapwood biomass (inclusive of coarse roots > 5 mm diameter),  $W_r$  is fine root biomass (< 5 mm diameter) and the specific respiration rates  $r_i^m$  are a function of tissue nitrogen content  $N_i$  and annual average temperature and variability (Ryan 1990, 1991).

Stand below-ground net primary production is the sum of root turnover  $T_r$  (equal to root mortality) plus any changes in root biomass taking place over the year ( $\Delta W_r$ ). Because of the high turnover rate of fine roots (Schoettle & Fahey 1994; Eissenstat & Yanai 1997),  $\Delta W_r$  can be assumed to be negligible in comparison with root mortality and  $P_b$  can be therefore expressed as:

$$P_b = \Delta W_r + T_r \approx \frac{W_r}{l_r} \quad (2.4)$$

where root mortality has been expressed as the ratio between fine root biomass and longevity. Detailed allometric data from a Scots pine chronosequence (Vanninen *et al.* 1997) support the simplification introduced in Eq. 2.4, as well as the assumption that fine root dynamics predominate over coarse root increments (as discussed in Appendix 2.2).

An age-related decline in  $P_a$  can be partly explained by the decline in leaf area index and light interception that is commonly observed in ageing stands (Gholz, Linder & McMurtrie 1994). However, stand growth efficiency ( $E_g$ ; stand  $P_a$  per unit foliage biomass; Waring 1983) is also reported to decline concurrently (Ryan, Binkley & Fownes 1997). When Eqns. 2.1-2.4 are combined,  $E_g$  can be expressed as the sum of carbon gain and costs per unit foliage biomass:

$$E_g = \frac{P_a}{W_f} = \frac{A}{W_f} \cdot (1 - r_g) \quad (\text{unit carbon gain})$$

$$- \left( r_f^m + r_s^m \frac{W_s}{W_f} + r_{fr}^m \frac{W_r}{W_f} \right) \cdot (1 - r_g) \quad (\text{unit respiratory costs}) \quad (2.5)$$

$$- \left( \frac{1}{l_r} \cdot \frac{W_r}{W_f} \right) \quad (\text{unit belowground costs})$$

Assimilation per unit leaf biomass (i.e. the unit carbon gain term) may even increase in old stands, because of reduced self-shading of foliage. A decline in growth efficiency, on the contrary, could result from changes in the balance between photosynthesizing foliage, conducting sapwood and fine roots with stand development, resulting in higher unit respiratory and belowground costs.

Such a structural acclimation, often reported in the literature (Persson 1983; Albrektson 1984; Usol'tsev & Vanclay 1995; Vanninen *et al.* 1996), could result from the need to maintain a functional homeostasis in water transport and prevent the negative effects of extreme water potentials.

### 2.2.2 The hydraulic constraint

The movement of water from the soil through the plant is customarily described in analogy to Ohm's law (Slatyer 1967). At equilibrium, the water potential of the leaves will differ from soil water potential  $\Psi_{soil}$  by a gravitational component ( $\Psi_{grav}$ ) that is a linear function of tree height  $h$ . Transpiration will induce an additional loss of water potential, since water has to overcome in its movement through the plant an hydraulic resistance  $R_{tot}$ , consisting of a root ( $R_{root}$ ) and a shoot component ( $R_{shoot}$ ) arranged in series. If any differences in transpiration and hydraulic resistance among leaves within the canopy are neglected, all fluxes and resistances can be expressed on a ground area basis and the minimum water potential experienced by the foliage ( $\Psi_{leaf}$ ) can then be represented as:

$$\begin{aligned}\Psi_{leaf} &= \Psi_{soil} - \Psi_{grav} - R_{tot} \cdot E_s = \\ &= \Psi_{soil} - (h \cdot g \cdot \rho_w) - (R_{root} + R_{shoot}) \cdot E_s\end{aligned}\quad (2.6)$$

where  $E_s$  is maximum stand transpiration over the year,  $h$  is tree height and  $\rho_w$  and  $g$  are water density and acceleration due to gravity, respectively.

Both stand transpiration and hydraulic resistances are to a large extent a function of stand structure. Scots pine canopies are generally open and aerodynamically well-coupled to the atmosphere (Jarvis, James & Landsberg 1976) and environmental

gradients through the canopy are consequently small; vertical gradients in stomatal conductance, transpiration and photosynthesis per unit foliage biomass are also reasonably small (Kellomäki & Hari 1980; Troeng 1981). Transpiration can be therefore assumed to be linearly proportional to stand foliage biomass  $W_f$ :

$$E_s = E_{un} \cdot \sigma \cdot W_f \quad (2.7)$$

where  $\sigma$  is specific leaf area and  $E_{un}$  is maximum transpiration per unit leaf area, assumed to be a constant function of site environmental conditions.

The hydraulic resistance of the root system is mainly determined by the radial resistance of fine roots (Weatherley 1982; Magnani, Centritto & Grace 1996) and is therefore inversely related to the surface and, in first instance, to the biomass of feeder roots:

$$R_{root} = \frac{1}{k_r \cdot W_r} \quad (2.8)$$

where  $k_r$  is fine root hydraulic conductance per unit biomass.

The hydraulic resistance of the shoot can be expressed as a function of plant height  $h$  and sapwood area  $A_s$  (Whitehead, Edwards & Jarvis 1984; Whitehead, Jarvis & Waring 1984). If the simple assumption is introduced that the cumulative cross-sectional area of the sapwood in stem and branches is constant all along the plant (Shinozaki *et al.* 1964; Makela 1986), then shoot resistance can be expressed as:

$$R_{shoot} = \frac{h}{k_s \cdot A_s} = \frac{h^2 \cdot \rho_s}{k_s \cdot W_s} \quad (2.9)$$

where  $k_s$  and  $\rho_s$  are sapwood specific hydraulic conductivity and density, respectively. As already mentioned, the minimum water potential experienced by the leaf is rather conservative for any species, changing little with plant age and site conditions (as reviewed in the Discussion section). This minimum appears to correspond to the critical value that would induce runaway xylem embolism and foliage dieback (Tyree

& Sperry 1988; Sperry & Pockman 1993):

$$\Psi_{leaf} = \bar{\Psi} \quad (2.10)$$

This functional homeostasis has profound implications for the hydraulic architecture of the plant, as it requires that hydraulic resistance per unit leaf area ( $R_{tot}^u$ ) does not exceed a limit given by (Eq. 2.7-2.8):

$$R_{tot}^u = (W_f \cdot \sigma) \cdot (R_{shoot} + R_{root}) \leq \frac{\Psi_{soil} - (h \cdot g \cdot \rho_w) - \bar{\Psi}}{E_{un}} \quad (2.11)$$

When shoot and root resistances are expressed as a function of plant allometry (Eq. 2.8-2.9), the principle of functional homeostasis results in a general hydraulic constraint on plant structure:

$$R_{tot}^u = (W_f \cdot \sigma) \cdot \left( \frac{1}{k_r \cdot W_r} + \frac{h^2 \cdot \rho_s}{k_s \cdot W_s} \right) \leq \frac{\Psi_{soil} - (h \cdot g \cdot \rho_w) - \bar{\Psi}}{E_{un}} \quad (2.12)$$

The principle of optimality (Bloom, Chapin & Mooney 1985) requires that  $R_{tot}^u$  not only does not exceed, but exactly matches the limit imposed by Eq. 2.12: if higher values would result in extensive cavitation and foliage dieback, lower values on the other hand could only be achieved if a lower leaf area were produced than can be safely sustained, so limiting light interception and photosynthesis and ultimately plant growth and fitness.

But for the minor effects of gravitational potential, Eq. 2.12 therefore predicts an age-independent value of hydraulic resistance per unit foliage area in the soil-plant continuum. Experimental evidence (reviewed in the Discussion section) seems to suggest that  $R_{tot}^u$  is indeed rather conservative over the lifetime of the plant, despite major changes in plant dimensions.

### 2.2.3 Optimal allometry under hydraulic constraints

According to Equation 2.12, when new transpiring foliage is produced, the plant will support its needs with enough absorbing roots and conducting sapwood to keep the minimum water potential within a safety range. The principle of optimality, moreover, requires that a reduction in hydraulic resistance is achieved at the lowest possible cost, so as to reserve as many resources as possible for foliage growth and maximize plant fitness (Parker & Maynard Smith 1990).

In order to decrease hydraulic resistance, the investment of carbon in fine roots or sapwood yields to the plant very different returns, both because of different hydraulic conductivities and because of the strong impact of plant height on shoot resistance. On the other hand, fine roots and sapwood have markedly different longevities and the cost of production, discounted for turnover, will differ accordingly.

Optimal growth under hydraulic constraints requires that the ratio of marginal hydraulic returns to marginal annual cost for carbon investment in either roots or sapwood be the same (Bloom, Chapin & Mooney 1985; Case & Fair 1989), i.e.:

$$\frac{\partial R_{tot}}{\partial W_r} \bigg/ \frac{1}{l_r} = \frac{\partial R_{tot}}{\partial W_s} \bigg/ \frac{1}{l_s} \quad (2.13)$$

where  $l_s$  is sapwood longevity, assumed to be constant. From Eqs. 2.8-2.9, this corresponds to:

$$\frac{1}{k_r \cdot W_r^2} \cdot \frac{k_s \cdot W_s^2}{h^2 \cdot \rho_s} = \frac{l_s}{l_r} \quad (2.14)$$

from which the allometric constraints can be derived:

$$\frac{W_s}{W_r} = c \cdot h \quad (2.15)$$

$$\frac{A_s}{W_r} = \frac{c}{\rho_s} \quad (2.16)$$



where it is:

$$c = \sqrt{\frac{k_r \cdot l_s}{k_s \cdot l_r} \cdot \rho_s} \quad (2.17)$$

Equation 2.16 predicts a constant ratio, under any environmental conditions, between conductive sapwood and absorbing roots, suggesting the existence of a functional balance in water transport. Such a constant balance, though, would not extend to foliage. When Equation 2.15 is combined with the hydraulic constraint of Equation 2.12, the allometric relationship between sapwood area and foliage biomass can be expressed as:

$$\frac{A_s}{W_f} = \left( \frac{\sigma \cdot h}{R_{tot}^u \cdot k_s} \right) + \left( \frac{\sigma \cdot l_s}{R_{tot}^u \cdot k_s \cdot c \cdot l_r} \right) \quad (2.18)$$

According to Eq. 2.18, the ratio between sapwood and foliage biomass is not constant, as suggested by the pipe model theory, but increases with height. The relationship would be linear, were it not for the effects of gravitational potential on  $R_{tot}^u$ . It is interesting to note that the first term in brackets is the allometric ratio that would be expected if all the hydraulic resistance were located in the shoot, as assumed in the hydraulic model of Whitehead *et al.* (1984). Because of a positive root resistance, however, the optimality model predicts a rather large sapwood-to-foliage ratio even in small seedlings (second term in brackets in Eq. 2.18).

The ratio of fine root-to-foliage biomass will also increase with stand height:

$$\frac{W_r}{W_f} = \left( \frac{\sigma}{k_r \cdot R_{tot}^u} \right) \cdot \left( 1 + h \cdot c \cdot \frac{l_r}{l_s} \right) \quad (2.19)$$

The first term in brackets in Eq. 2.19 represents the constant allometric ratio that would be expected if all the hydraulic resistance were located in fine roots, as predicted

for herbaceous plants by Givnish (1986). In the case of trees, however, because of the longitudinal resistance in the shoot, the principle of optimality requires an almost linear shift in the root-leaf balance as tree height increases.

A result of the allometric changes of Eq. 2.19 is the progressive decline of fine root hydraulic resistance per unit foliage area over the lifetime of the stand. However, this reduction will be matched by a parallel increase with height of the shoot component, so as to maintain an almost constant value of total resistance per unit foliage area, as predicted by Eq. 2.12:

$$R_{shoot}^u = R_{shoot} \cdot (W_f \cdot \sigma) = R_{tot}^u \cdot \left[ 1 - \left( 1 + h \cdot c \cdot \frac{l_r}{l_s} \right)^{-1} \right] \quad (2.20)$$

As height increases, this shoot component will approach asymptotically the maximum value of plant hydraulic resistance per unit leaf imposed by the threat of foliage dieback.

## 2.3 Materials and methods

### 2.3.1 Site description

The predictions of the model were tested against a chronosequence of *P. sylvestris*

Age years	Density trees ha <sup>-1</sup>	<i>D</i> cm	<i>H</i> m
7	3285	6.9	2.2
14	3133	12.8	7.7
18	3883	10	9.9
32	1560	19.9	16.9
33	1783	18.6	18.4
43	796	25.6	19.5
46	732	25.8	19.1
58	430	32.2	24.2
59	398	34.8	21.7

**Table 2.1** Summary of stand density, diameter at breast height (*D*) and top height (*H*) of the chronosequence of *P. sylvestris* stands.

stands, part of an extensive plantation in Thetford Forest, East Anglia, U.K. (Mencuccini & Grace 1996a, 1996b).

Average summer precipitation is 170 mm and average July temperature is 17 °C.

Despite local differences, soil nutrition is not considered to be a limiting factor for tree growth at the site (Corbett 1973).

The forest has been thoroughly studied over the years so that most of the parameters required by the model could be attributed species- as well as site-

specific values (Appendix 2.1). Nine study sites were selected in even-aged stands of Scots pine, with tree age ranging from 7 to 59 years and densities comprised between 3285 and 398 trees per hectare (Table 2.1). Stands were selected according to origin so as to minimize genetic variability. No thinning had been performed over the last 10 years and stands less than 33-years old had never been thinned.

### **2.3.2 Leaf and xylem characteristics**

At each site, three dominant trees were felled. Tree sapwood area and biomass, leaf biomass and area were determined by stratified sampling, as described by Mencuccini and Grace (1996b). Tree aboveground hydraulic resistance per unit foliage area ( $R''_{shoot}$ ) was derived from direct measurements in the laboratory, as described by Mencuccini and Grace (1996a). All measurements were conveniently scaled-up to the stand level, based on observed empirical relationships with sapwood area and tree diameter (Mencuccini & Grace 1996b).

### **2.3.3 Stand $P_a$**

Shoot biomass growth (above- plus belowground, excluding fine roots below 5 mm) was computed for the felled trees and scaled-up to the stand level as described in Mencuccini and Grace (1996b). Stand aboveground net primary production was computed as the sum of shoot growth and annual litterfall, assumed to be a constant fraction of foliage biomass (Jalkanen *et al.* 1994).

### **2.3.4 Fine root biomass**

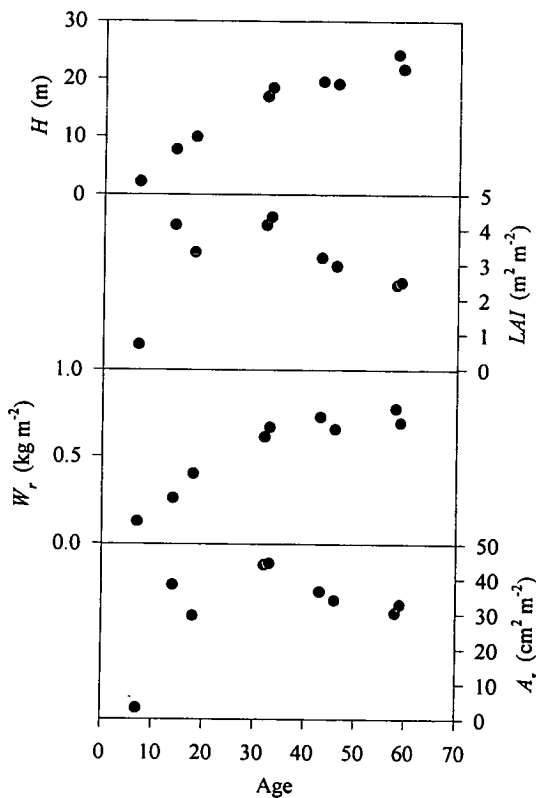
Fine root biomass was not directly measured, but derived from the empirical model proposed for Scots pine by Usol'tsev and Vanclay (1995), relating tree fine root biomass to plant age, diameter and height. The model fitted very well the experimental data reported by Vanninen *et al.* (1996) for Finnish stands and by Ovington (1957) for Thetford Forest itself ( $R^2 = 0.96$  and  $0.99$ , respectively). Site-specific parameter values were therefore used to estimate the root biomass (< 5 mm) of felled trees, that was then scaled-up to the stand level on a basal area basis.

### 2.3.5 Fine root characteristics

A value for fine root longevity in *P. sylvestris* was derived from Persson (1980); the highest of the two figures reported ( $l_r = 0.55$  and  $0.65$ ) was chosen, since the study referred to finer roots ( $< 2$  mm diameter) than considered here. Similar values have been reported in the literature for several pine species (Santantonio 1989; Schoettle & Fahey 1994).

The hydraulic conductance per unit biomass of fine roots could not be directly determined, but was derived from the literature. Roberts (1977) measured by the tree-cutting technique the hydraulic conductance of entire root systems of *P. sylvestris* trees growing in Thetford. The fine root length of the same stand was measured by Roberts (1976) and was translated into an appropriate figure for fine root biomass assuming a specific root length of  $25 \text{ m g}^{-1}$  (George *et al.* 1997). A value for the specific hydraulic

**Figure 2.1** Developmental changes in top height ( $H$ ), leaf area index ( $LAI$ ), estimated fine root biomass ( $W_r$ ) and sapwood area ( $A_s$ ) in a chronosequence of *P. sylvestris* stands.



conductance of fine roots could then be derived from Eq. 2.8. The estimated figure was in rather good agreement with experimental data for pine seedlings reported by Sands *et al.* (1982) and Smit-Spinks *et al.* (1984).

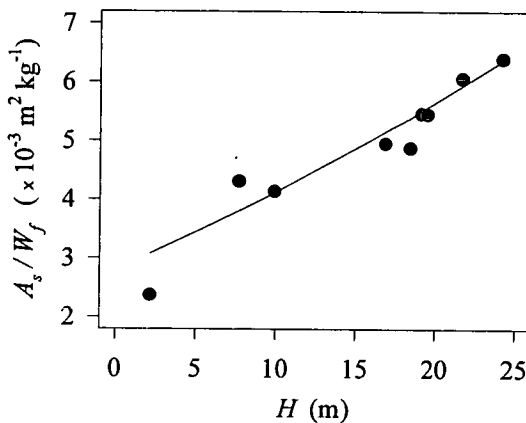
Values for all other parameters in the model were either directly measured or derived from the literature, as specified in Appendix 2.1.

### 2.4 Results and discussion

A rather clear picture of *P. sylvestris* stand dynamics emerges from the chronosequence of homogeneous plots (Fig. 2.1). Stand height is still increasing at an age of almost 60 years, albeith

at a reduced pace. As a consequence, sapwood biomass per unit surface is also increasing (data not shown), despite the concurrent decline in sapwood basal area. The estimated biomass of fine roots, on the contrary, is quite constant after a peak value of about  $0.7 \text{ kg m}^{-2}$  has been reached at an age of 30. A marked decline in leaf area index is observed after a maximum is reached at polestage; light interception is therefore lower in older stands (Mencuccini & Grace 1996b). Similar results have often been reported for *P. sylvestris* (Ovington 1957; Albrektson 1984; Vanninen *et al.* 1996) and several other species (Margolis *et al.* 1995; Ryan, Binkley & Fownes 1997).

**Figure 2.2** Height-related changes in sapwood area-to-  
foliage biomass ratio ( $A_s/W_f$ ). Experimental data are  
compared with model predictions (Eq. 2.18). A  
constant ratio would be expected from the pipe model  
theory.

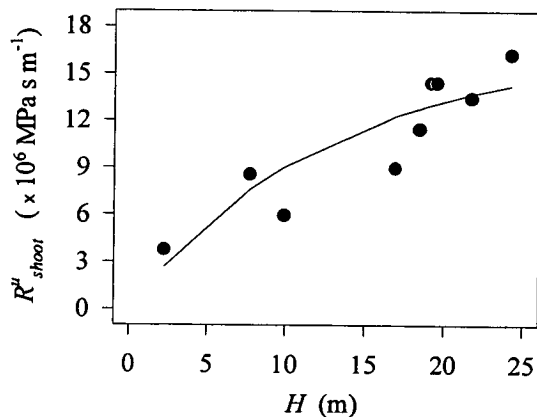


The different dynamics of plant compartments translate into marked changes in the functional structure of the stand.

The ratio between sapwood cross-sectional area at breast height and foliage biomass ( $A_s/W_f$ ) is not constant, as often assumed (Makela 1986; Margolis *et al.* 1995), but increases with stand height. This pattern is well explained by the hypothesis of optimal growth under hydraulic constraints (Fig. 2.2), as expressed in Eq. 2.18.

A re-analysis of published data-sets confirms this finding for Scots pine (Albrektson 1984; van Hees & Bartelink 1993; Vanninen *et al.* 1996) as well as for *P. taeda* (Shelburne, Hedden & Allen 1993) and *P. contorta* (Thompson 1989). The opposite pattern has been reported on the contrary for *Abies balsamea* (Coyea & Margolis 1992). A possible explanation for this different pattern lies in the age-related changes in xylem hydraulic characteristics elsewhere reported for this species (Pothier, Margolis & Waring 1989; Pothier *et al.* 1989): if sapwood conductivity  $k_s$  were assumed to increase markedly with height, the model would indeed predict a decline in the sapwood-to-foliage area ratio with stand development (data not shown). This result highlights the relevance of cell maturation and xylem anatomy not only for wood quality (Zobel & van Buijtenen 1989), but also

**Figure 2.3** Height-related changes in shoot hydraulic resistance per unit foliage area ( $R_{shoot}^u$ ). Experimental data are compared with model predictions (Eq. 2.20). A constant value would be expected from the model of Whitehead, Jarvis & Waring (1984).



$H$ (m)	$LAI$	Minimum $\Psi$ (MPa)	$R_{tot}^u$ ( $\times 10^7$ MPa s $m^{-1}$ )
15	2.4	- 1.8	3.2 <sup>1</sup>
15	3.1	- 1.5	1.8 <sup>1</sup>
10	2.59	- 1.5	4.9 <sup>2</sup>
seedling		- 1.2	1.6 <sup>3</sup>
seedling		- 1.8	1.8 <sup>4</sup>

<sup>1</sup> Whitehead *et al.* (1984), <sup>2</sup> Jackson *et al.* (1995b), <sup>3</sup> Jackson *et al.* (1995a), <sup>4</sup> Peña and Grace (1986)

**Table 2.2** Comparison of published values of hydraulic resistance per unit foliage biomass ( $R_{tot}^u$ ) in *P. sylvestris* plants of different dimensions, growing under similar climatic conditions (Scotland, U.K.). The large variability in tree height does not reflect in different values of minimum needle water potential or hydraulic resistance in the soil-plant continuum.

for forest function and productivity.

It is perhaps worth noting that a much larger change in the sapwood-to-foliage area ratio would be predicted by the model of Whitehead *et al.* (1984), which neglects the contribution of fine roots to total plant hydraulic resistance, since the effects of height would have to be entirely counterbalanced by the larger sapwood area. A constant shoot hydraulic resistance per unit foliage biomass is assumed by Whitehead *et al.* (1984); direct measurements, on the contrary, support the view that  $R_{shoot}^u$  increases with height, despite the larger conductive sapwood area (Fig. 2.3), as predicted by the hypothesis of functional balance and cavitation avoidance (Eq. 2.20).

The hydraulic resistance per unit foliage area in the soil-plant continuum, however, does not seem to be affected by plant dimensions, as demonstrated by a review of literature data for seedlings and mature *P. sylvestris* trees (Table 2.2). To draw a comparison, a 20-fold difference in  $R_{shoot}^u$  would be expected between a seedling 70 cm tall and a tree of 15 m based on the pipe model theory, if all

resistance were assumed to be located in the shoot, or a 10-fold difference if the additional assumptions were introduced that 50% of total plant resistance is belowground and that the ratio between feeder roots and foliage is constant.

As a consequence, the minimum water potential experienced by the needles under a wide range of conditions is almost constant at a value close to the threshold for xylem cavitation (- 2 MPa), as determined experimentally for Scots pine by Cochard (Cochard 1992). It is worth noting that the value of total plant resistance per unit foliage area estimated from Eq. 2.11 for the environmental conditions at Thetford Forest ( $3.0 \times 10^7$  MPa s m<sup>-1</sup> for  $h = 24$  m) is not far from the one derived from measurements by Jarvis (1976) for the same site ( $2.6 \times 10^7$  MPa s m<sup>-1</sup> for  $h = 16.5$  m). This functional homeostasis could be obtained by a concurrent shift in the balance between transpiring foliage and absorbing roots (Eq. 2.12), as suggested for Thetford Forest by the estimates reported in Fig. 2.4. This appears to be mainly the result of the

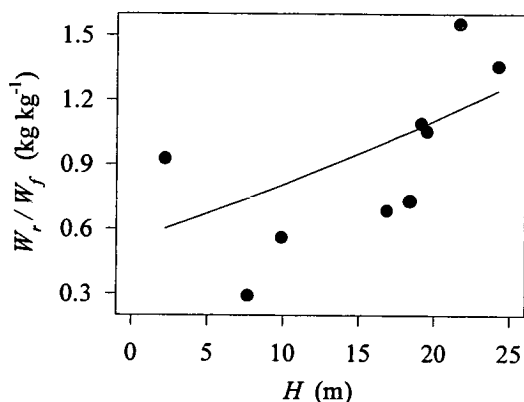


**Figure 2.4** Height-related changes in fine root-to-needle biomass ratio ( $W_r / W_f$ ). Experimental data are compared with model predictions (Eq. 2.19). A constant ratio would be expected from the functional balance model proposed by Givnish (1986).

marked decline in stand leaf area index, in the face of a constant fine root biomass (Fig. 2.1). Although not based on direct root measurements, these figures are consistent with the report by Ovington (1957), Persson (1983), Vanninen et al. (1996) and Usol'tsev and Vanclay (1995) of an increased allocation to fine roots in ageing *P. sylvestris* stands. The same pattern has been reported for several other species (Santantonio 1989; Gholz, Linder & McMurtrie 1994).

This picture would appear in contrast with the common assumption of a root-shoot functional balance (Wilson 1988; Makela 1990; Cannell & Dewar 1994), whereby foliage and fine root biomass and activity should be matched so as to provide a constant pool of carbon, water and nutrients for growth. It should be noted, on the other hand, that fine root activity in nutrient absorption could be lower in ageing stands. Gower *et al.* (1996) suggested that nutrient

**Figure 2.5.** Developmental changes in stand  $P_a$ . Estimated values (●) are compared with predictions of the equilibrium model (Eq. 2.1) when structural changes are either accounted for (○) or neglected (◇).

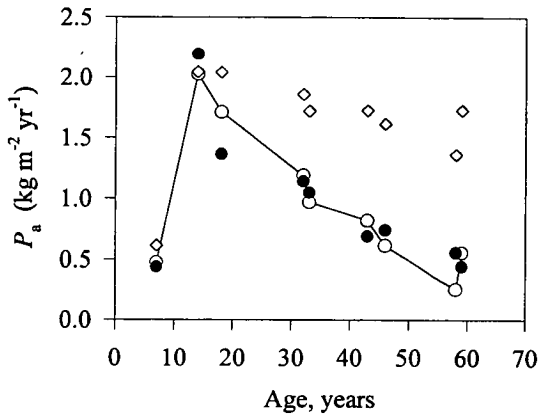
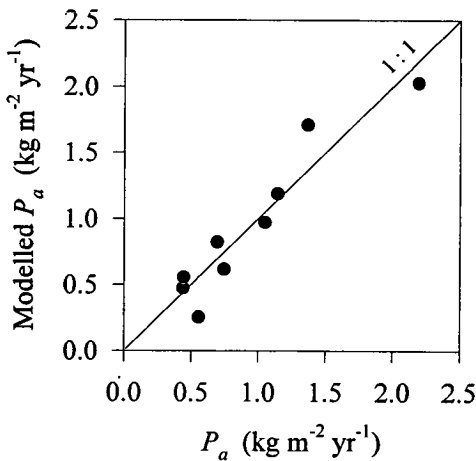


**Figure 2.6** Developmental changes in stand  $P_a$ . Estimated values are compared with predictions of the equilibrium model (Eq. 2.1) when structural changes are duly accounted for ( $R^2 = 0.89$ ,  $b = 0.99$ ).



the functional balance between foliage, sapwood and fine roots. In the absence of structural changes (i.e. with constant sapwood area-to-foliage biomass and fine root-to-foliage biomass ratios) the carbon balance model suggests that the observed drop in foliage biomass and light interception would have been largely compensated by

immobilization in soil litter could reduce the effectiveness of fine roots in ion uptake, thus requiring a higher belowground allocation and a lower leaf area index. Yet, this does not seem to be the case in the *P. sylvestris* chronosequence analyzed, since foliar nitrogen concentration was not lower in older than in young stands (Mencuccini & Grace 1996b).

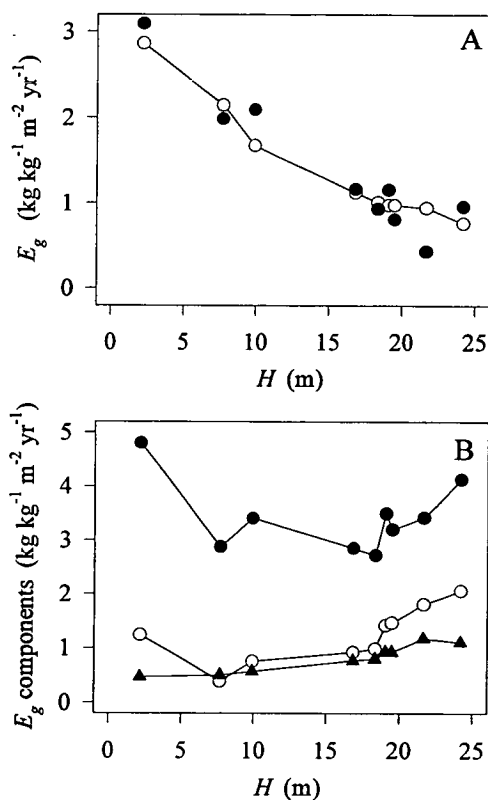
The increased allocation to fine roots would appear to contribute a large proportion of the observed decline in above-ground net primary production. Stand  $P_a$  dropped from 1.78 to 0.50  $\text{kg m}^{-2} \text{yr}^{-1}$  from age 14-18 to age 58-59 (Fig. 2.5). Similar values and dynamics have been reported for other species, both coniferous and broadleaf (Ryan, Binkley & Fownes 1997). The decline in  $P_a$  is well explained by concurrent changes in foliage biomass and functional structure, as predicted by the carbon balance model of Eq. 2.1 (Fig. 2.6). Reduced leaf area index and light interception accounted for 45 % of the observed change (Table 2.3), but most of the drop in  $P_a$  stemmed from a shift in



	Age		% of $P_a$ change
	14-18	58-59	
$P_a$ ( $\text{kg m}^{-2} \text{yr}^{-1}$ )	1.78	0.50 (-72%)	
$A$	2.61	2.01	- 45
$R_m$	0.41	0.48	- 12
$T_r$	0.51	1.13	- 43

**Table 2.3** Reduction in aboveground net primary productivity between age 14-18 and age 58-59 in *P. sylvestris* stands. Absolute values and percentage change are reported. Observed changes are partitioned among co-occurring processes, based on the model of Eq. 2.1: assimilation  $A$ , maintenance respiration  $R_m$  and root turnover  $T_r$ . Both  $A$  and  $R_m$  estimates have already been discounted for growth respiration (Eq. 2.1).

**Figure 2.7** Height-related changes in stand growth efficiency ( $E_g$ ). A Comparison of estimated values (●) and predictions of the equilibrium model of Eq. 2.6 (○). B Concurrent changes in unit carbon gain (●), unit respiratory costs (▲) and unit belowground costs (○), as estimated from Eq. 2.5.



reduced respiration and root turnover (Fig. 2.5).

It has been suggested that the risk of diffuse xylem embolism could be prevented by stomatal closure (Yoder *et al.* 1994; Williams *et al.* 1996), resulting in reduced radiation use efficiency (Landsberg & Waring 1997).

This possibility can not be ruled out. However, the value of maximum transpiration per unit leaf area derived from the literature for mature trees at Thetford (Stewart 1988; Jackson, Irvine & Grace 1995b) is in close agreement with what reported elsewhere for *P. sylvestris* seedlings (Pena & Grace 1986). Such indirect evidence suggests that stomatal mechanisms did not play a major role in maintaining a functional homeostasis in Scots pine.

The decline in stand productivity was partly explained by the development of  $E_g$  with age. Stand growth efficiency declined by more than 55 % from canopy closure at age 14-18 to age 58-59 (Fig. 2.7 A). A decline in  $E_g$  with age had already been reported by

**Table 2.4** Reduction in foliage biomass  $W_f$  and growth efficiency  $E_g$  between age 14-18 and age 58-59 in *P. sylvestris* stands. Absolute values and percentage changes are reported. Observed changes in  $E_g$  are also partitioned among co-occurring processes, based on the model of Eq. 2.5.

	Age		$E_g$ change explained, %
	14-18	58-59	
$W_f$ (kg m <sup>-2</sup> )	0.8	0.51 (-37%)	
$E_g$ (kg kg <sup>-1</sup> m <sup>-2</sup> yr <sup>-1</sup> )	1.91	0.85 (-55%)	
unit C gain	2.86	3.44	+ 47
unit respiratory costs	0.45	0.82	- 45
unit belowground costs	0.57	1.94	-102

Ovington (1957) for Thetford Forest and by Albrektson and Valinger (1985) for *P. sylvestris* in central Sweden, although with much slower dynamics in the latter case. In the present study, light interception and estimated photosynthesis per unit foliage biomass (i.e. unit carbon gain; Eq. 2.5) decreased quickly with canopy closure, but recovered to a large extent as self-shading declined in ageing stands. Because of changes in plant allometry, on the contrary, unit respiratory and belowground costs increased in ageing stands and more than offset the recovery in carbon gain (Fig. 2.7 B).

The increase in maintenance respiration determined by the larger sapwood and fine root biomass accounted for 12 % only of the change in  $P_a$ , in good agreement with estimates by Gower *et al.* (1996) for *P. contorta*, using the G'DAY model. Estimated fine root turnover and the resulting increase in belowground allocation, on the contrary, appear to play a key role in the reduction both of  $P_a$  and of  $E_g$  (Table 2.3, 2.4). Santantonio (1989) suggested that an increased belowground allocation and the resulting carbon loss through fine root turnover could largely explain the lower productivity of stands either ageing or on poor sites, a hypothesis supported by a growing body of experimental evidence (Gholz, Linder & McMurtrie 1994; Beets & Whitehead 1996). Despite all the uncertainties in the evaluation of model parameters and flux components, the results presented seem to confirm this view, shedding new light on causes and implications of the commonly observed change in plant functional

structure with age.

## 2.5 Conclusions

Several hypotheses have been put forward over the last few years to explain the age-related decline in stand productivity. The implications of the risk of diffuse embolism have been recognized, but the focus has been on the effects of hydraulic limitations on gas exchange only (Sperry & Pockman 1993; Yoder *et al.* 1994; Williams *et al.* 1996; Landsberg & Waring 1997). The new hypothesis presented, on the contrary, highlights the role of hydraulic limitations in structural acclimation and  $P_a$  reduction. The observed reduction in stand productivity appears indeed to be accounted for by allometric changes over the life-time of the stand. The principle of optimal growth under hydraulic constraints, based on the observation of functional homeostasis in water relations, seems to explain conveniently most of the observed structural acclimation: not only in the balance between foliage and fine roots, that could be explained also by the hypothesis of nutrient limitation (Gower, McMurtrie & Murty 1996), but also in the foliage-to-sapwood area ratio, often assumed to be constant. Only one of these components, on the contrary, had been accounted for in previous models of plant structure under hydraulic constraints (Whitehead, Jarvis & Waring 1984; Givnish 1986; Friend 1993).

The role of resource allocation in plant growth has been often neglected. Research has commonly focused on gas exchange processes, leading to an ever increasing understanding of light interception, photosynthesis and respiration. Little attention has been paid to the mechanisms of allocation, on the contrary, and no truly mechanistic model has been presented so far that can account for the experimental evidence available (Wilson 1988; Cannell & Dewar 1994). This severely limits our ability to understand and predict the growth and function of forest stands.

Whatever the processes involved, however, a complex web of feed-back mechanisms results in effective plant self-organisation and eventually in functional homeostasis (Grace & Magnani 1999). This enables to infer plant behavior and its response to the environment, treating the system as a black-box until a better understanding of the underlying mechanisms has emerged. The potential of such a top-down approach is demonstrated by the results presented.

## References

- Albrektson A. (1984) Sapwood basal area and needle mass of Scots pine (*Pinus sylvestris* L.) trees in central Sweden. *Forestry* **57**, 35-43.
- Albrektson A. & Valinger E. (1985) Relations between tree height and diameter, productivity and allocation of growth in a Scots pine (*Pinus sylvestris* L.) sample tree material. In *Crop Physiology of Forest Trees* (eds. P.M.A. Tigerstedt, P. Puttonen & V. Koski), pp. 95-105. University of Helsinki, Helsinki.
- Beets P.N. & Whitehead D. (1996) Carbon partitioning in *Pinus radiata* stands in relation to foliage nitrogen status. *Tree Physiology* **16**, 131-138.
- Bloom A.J., Chapin F.S. & Mooney H.A. (1985) Resource limitation in plants. An economic analogy. *Annual Review Ecology Systematics* **16**, 363-392.
- Braekke F.H. (1995) Response of understorey vegetation and Scots pine root systems to fertilization at multiple deficiency stress. *Plant and Soil* **168-169**, 179-185.
- Cannell M.G.R. & Dewar R.C. (1994) Carbon allocation in trees: a review of concepts for modelling. *Advances in Ecological Research* **25**, 50-104.
- Case K.E. & Fair R.C. (1989) *Principles of Economics*. Prentice-Hall, London.
- Chung H.-H. & Barnes R.L. (1977) Photosynthate allocation in *Pinus taeda*. I. Substrate requirements for synthesis of shoot biomass. *Canadian Journal of Forest Research* **7**, 106-111.
- Cochard H. (1992) Vulnerability of several conifers to air-embolism. *Tree Physiology* **11**, 73-83.
- Corbett W.M. (1973) *Breckland forest soils*. The Soil Survey, Rothamsted Experimental Station, Harpenden, Herts, U.K.
- Coyea M.R. & Margolis H.A. (1992) Factors affecting the relationship between sapwood area and leaf area of balsam fir. *Canadian Journal of Forest Research* **22**, 1684-1693.
- Eissenstat D.M. & Yanai R.D. (1997) The ecology of root lifespan. *Advances in Ecological Research* **27**, 1-60.
- Field C.B. & Mooney H.A. (1986) The photosynthesis-nitrogen relationship in wild plants. In *On the Economy of Plant Form and Function* (ed. T.J. Givnish), pp. 25-55. Cambridge Univ. Press, Cambridge.
- Friend A.D. (1993) The prediction and physiological significance of tree height. In *Vegetation Dynamics & Global Change* (eds. A.M. Solomon & H.H. Shugart), pp. 101-115. Chapman & Hall, New York.
- George E., Seith B., Schaeffer C. & Marschner H. (1997) Responses of *Picea*, *Pinus* and *Pseudotsuga* roots to heterogeneous nutrient distribution in the soil. *Tree Physiology* **17**, 39-45.
- Gholz H.L., Linder S. & McMurtrie R.E. (1994) *Environmental Constraints on the Structure and Productivity of Pine Forest Ecosystems: a Comparative Analysis*. *Ecological Bulletins No. 43*. Copenhagen.
- Givnish T.J. (1986) Optimal stomatal conductance, allocation of energy between leaves and roots, and the marginal cost of transpiration. In *On the Economy of Plant Form and Function* (ed. T.J. Givnish), pp. 171-213. Cambridge University Press, Cambridge.

- Gower S.T., McMurtrie R.E. & Murty D. (1996) Aboveground net primary production decline with stand age: potential causes. *Trends in Ecology & Evolution* **11**, 378-382.
- Grace J. & Magnani F. (1999) Plants as self-organising systems. In: *Leaf Development and Canopy Growth* (eds. B. Marshall, J. Roberts). Sheffield Academic Press, Sheffield. In press.
- Grier C.C., Vogt K.A., Keyes M.R. & Edmonds R.L. (1981) Biomass distribution and above- and below-ground production in young and mature *Abies amabilis* zone ecosystems of the Washington Cascades. *Canadian Journal of Forest Research* **11**, 155-167.
- Grulke N.E. & Miller P.R. (1994) Changes in gas exchange characteristics during the life span of giant sequoia: implications for response to current and future concentrations of atmospheric ozone. *Tree Physiology* **14**, 659-668.
- Helmisaari H.-S. & Siltala T. (1989) Variation in nutrient concentrations of *Pinus sylvestris* stems. *Scandinavian Journal of Forest Research* **4**, 443-451.
- Jackson G.E., Irvine J. & Grace J. (1995a) Xylem cavitation in Scots pine and Sitka spruce saplings during water stress. *Tree Physiology* **15**, 783-790.
- Jackson G.E., Irvine J. & Grace J. (1995b) Xylem cavitation in two mature Scots pine forests growing in a wet and a dry area of Britain. *Plant Cell and Environment* **18**, 1411-1418.
- Jalkanen R.E., Aalto T.O., Innes J.L., Kurkela T.T. & Townsend I.K. (1994) Needle retention and needle loss of Scots pine in recent decades at Thetford and Alice Holt, England. *Canadian Journal of Forest Research* **24**, 863-867.
- Jarvis P.G. (1976) The interpretation of the variations in leaf water potential and stomatal conductance found in canopies in the field. *Philosophical Transactions of the Royal Society of London Series B- Biological Sciences* **273**, 593-610.
- Jarvis P.G., James G.B. & Landsberg J.J. (1976) Coniferous forest. In *Vegetation and the Atmosphere* (ed. J.L. Monteith), Vol. 2, pp. 171-240. Academic Press, London.
- Kellomäki S. & Hari P. (1980) Eco-physiological studies on young Scots pine stands. I. Tree class as indicator of needle biomass, illumination, and photosynthetic capacity of crown system. *Silva Fennica* **14**, 227-242.
- Kira T. & Shidei T. (1967) Primary production and turnover of organic matter in different forest ecosystems of the western Pacific. *Japanese Journal of Ecology* **13**, 70-83.
- Kull O. & Koppel A. (1987) Net photosynthetic response to light intensity of shoots from different crown positions and age in *Picea abies* (L.) Karst. *Scandinavian Journal of Forest Research* **2**, 157-166.
- Landsberg J.J. & Waring R.H. (1997) A generalized model of forest productivity using simplified concepts of radiation-use efficiency, carbon balance and partitioning. *Forest Ecology and Management* **95**, 209-228.
- Magnani F., Centritto M. & Grace J. (1996) Measurement of apoplasmic and cell-to-cell components of root hydraulic conductance by a pressure clamp technique. *Planta* **199**, 296-306.
- Makela A. (1986) Implications of the pipe model theory on dry matter partitioning and height growth in trees. *Journal of Theoretical Biology* **123**, 103-120.
- Makela A. (1990) Modeling structural-functional relationships in whole-tree growth: resource allocation. In *Process Modelling of Forest Growth Responses to Environmental Stress* (eds. R.K. Dixon, R.S. Meldahl, G.A. Ruark & W.G.

- Warren), pp. 81-95. Timber Press, Portland.
- Margolis H., Oren R., Whitehead D. & Kaufmann M.R. (1995) Leaf area dynamics of conifer forests. In *Ecophysiology of Coniferous Forests* (eds. W.K. Smith & T.M. Hinckley), pp. 181-223. Academic Press, San Diego.
- McMurtrie R.E., Gholz H.L., Linder S. & Gower S.T. (1994) Climatic factors controlling the productivity of pine stands: a model-based analysis. *Ecological Bulletins* **43**, 173-188.
- Mencuccini M. & Grace J. (1995) Climate influences the leaf-area sapwood area ratio in Scots pine. *Tree Physiology* **15**, 1-10.
- Mencuccini M. & Grace J. (1996a) Developmental patterns of aboveground xylem conductance in a Scots pine (*Pinus sylvestris* L.) age sequence. *Plant Cell and Environment* **19**, 939-948.
- Mencuccini M. & Grace J. (1996b) Hydraulic conductance, light interception and needle nutrient concentration in Scots pine stands and their relations with net primary productivity. *Tree Physiology* **16**, 459-468.
- Murty D., McMurtrie R. & Ryan M.G. (1996) Declining forest productivity in aging forest stands: a modeling analysis of alternative hypotheses. *Tree Physiology* **16**, 187-200.
- Nooden L.D. (1988) Whole plant senescence. In *Senescence and Aging in Plants* (eds. L.D. Nooden & A.C. Leopold), pp. 391-439. Academic Press, San Diego.
- Ovington J.D. (1957) Dry-matter production by *Pinus sylvestris* L. *Annals of Botany* **21**, 287-314.
- Page J. & Lebens R. (eds) (1986) *Climate in the United Kingdom*. Department of Energy, London.
- Parker G.A. & Maynard Smith J. (1990) Optimality theory in evolutionary biology. *Nature* **348**, 27-33.
- Pena J. & Grace J. (1986) Water relations and ultrasound emissions of *Pinus sylvestris* L. before, during and after a period of water stress. *New Phytologist* **103**, 515-524.
- Persson H. (1980) Death and replacement of fine roots in a mature Scots pine stand. *Ecological Bulletins* **32**, 251-260.
- Persson H.A. (1983) The distribution and productivity of fine roots in boreal forests. *Plant and Soil* **71**, 87-101.
- Pothier D., Margolis H.A., Poliquin J. & Waring R.H. (1989) Relation between the permeability and the anatomy of jack pine sapwood with stand development. *Canadian Journal of Forest Research* **19**, 1564-1570.
- Pothier D., Margolis H.A. & Waring R.H. (1989) Patterns of change of saturated sapwood permeability and sapwood conductance with stand development. *Canadian Journal of Forest Research* **19**, 432-439.
- Roberts J. (1976) A study of root distribution and growth in a *Pinus sylvestris* L. (Scots pine) plantation in East Anglia. *Plant and Soil* **44X**, 607-621.
- Roberts J. (1977) The use of tree-cutting techniques in the study of the water relations of mature *Pinus sylvestris* L. *Journal of Experimental Botany* **28**, 751-767.
- Ryan M.G. (1990) Growth and maintenance respiration in stems of *Pinus contorta* and *Picea engelmannii*. *Canadian Journal of Forest Research* **20**, 48-57.
- Ryan M.G. (1991) A simple method for estimating gross carbon budgets for vegetation in forest ecosystems. *Tree Physiology* **9**, 255-266.
- Ryan M.G., Gower S.T., Hubbard R.M., Waring R.H., Gholz H.L., Cropper W.P. &

- Running S.W. (1995) Woody tissue maintenance respiration of four conifers in contrasting climates. *Oecologia* **101**, 133-140.
- Ryan M.G., Binkley D. & Fownes J.H. (1997) Age-related decline in forest productivity: pattern and processes. *Advances in Ecological Research* **27**, 213-262.
- Ryan M.G. & Waring R.H. (1992) Maintenance respiration and stand development in a subalpine lodgepole pine forest. *Ecology* **73**, 2100-2108.
- Saliendra N.Z., Sperry J.S. & Comstock J.P. (1995) Influence of leaf water status on stomatal response to humidity, hydraulic conductance, and soil drought in *Betula occidentalis*. *Planta* **196**, 357-366.
- Sands R., Fiscus E.L. & Reid C.P.P. (1982) Hydraulic properties of pine and bean roots with varying degrees of suberization, vascular differentiation and mycorrhizal infection. *Australian Journal of Plant Physiology* **9**, 559-569.
- Santantonio D. (1989) Dry-matter partitioning and fine-root production in forests - New approaches to a difficult problem. In *Biomass Production by Fast-Growing Trees*. (eds J.S. Pereira & J.J. Landsberg), pp. 57-72. Kluwer Academic Publishers, Dordrecht.
- Schoettle A.W. (1994) Influence of tree size on shoot structure and physiology of *Pinus contorta* and *Pinus aristata*. *Tree Physiology* **14**, 1055-1068.
- Schoettle A.W. & Fahey T.J. (1994) Foliage and fine root longevity of pines. *Ecological Bulletins* **43**, 136-153.
- Shelburne V.B., Hedden R.L. & Allen R.M. (1993) The effects of site, stand density, and sapwood permeability on the relationship between leaf area and sapwood area in loblolly pine (*Pinus taeda* L.). *Forest Ecology and Management* **58**, 193-209.
- Shinozaki K., Yoda K., Hozumi K. & Kira T. (1964) A quantitative analysis of plant form - The pipe model theory. I. Basic analyses. *Japanese Journal of Ecology* **14**, 97-105.
- Slatyer R.O. (1967) *Plant-Water Relationships*. Academic Press, New York.
- Smit-Spinks B., Swanson B.T. & Markhart III A.H. (1984) Changes in water relations, water flux, and root exudate abscisic acid content with cold acclimation of *Pinus sylvestris* L.. *Australian Journal of Plant Physiology* **11**, 431-441.
- Sperry J.S., Alder N.N. & Eastlack S.E. (1993) The effect of reduced hydraulic conductance on stomatal conductance and xylem cavitation. *Journal of Experimental Botany* **44**, 1075-1082.
- Sperry J.S. & Pockman W.T. (1993) Limitation of transpiration by hydraulic conductance and xylem cavitation in *Betula occidentalis*. *Plant Cell and Environment* **16**, 279-287.
- Stewart J.B. (1988) Modeling surface conductance of pine forest. *Agricultural and Forest Meteorology* **43**, 19-35.
- Thompson D.C. (1989) The effect of stand structure and stand density on the leaf area-sapwood area relationship of lodgepole pine. *Canadian Journal of Forest Research* **19**, 392-396.
- Thornley J.H.M. & Johnson I.R. (1990) *Plant and Crop Modelling*. Clarendon Press, Oxford.
- Troeng E. (1981) *Some Aspects of the Annual Carbon Balance of Scots Pine*. Ph.D. Thesis, University of Uppsala, Sweden.
- Tyree M.T. & Sperry J.S. (1988) Do woody-plants operate near the point of catastrophic xylem dysfunction caused by dynamic water-stress - answers from a model. *Plant Physiology* **88**, 574-580.
- Usol'tsev V.A. & Vanclay J.K. (1995) Stand biomass dynamics of pine plantations and

- natural forests on dry steppe in Kazakhstan. *Scandinavian Journal of Forest Research* **10**, 305-312X.
- van Hees A.F.M. & Bartelink H.H. (1993) Needle area relationships of Scots pine in the Netherlands. *Forest Ecology and Management* **58**, 19-31.
- Vanninen P., Ylitalo H., Sievanen R. & Makela A. (1996) Effects of age and site quality on the distribution of biomass in Scots pine (*Pinus sylvestris* L.). *Trees* **10**, 231-238.
- Waring R.H. (1983) Estimating forest growth and efficiency in relation to canopy leaf area. *Advances in Ecological Research* **13**, 327-354.
- Weatherley P.E. (1982) Water uptake and flow in roots. In *Vol. 12 B. Encyclopedia of Plant Physiology. New Series* (eds. O.L. Lange, P.S. Nobel, C.B. Osmond & H. Ziegler), pp. 79-109. Springer-Verlag, Berlin.
- Whitehead D., Edwards W.R.N. & Jarvis P.G. (1984) Conducting sapwood area, foliage area, and permeability in mature trees of *Picea sitchensis* and *Pinus contorta*. *Canadian Journal of Forest Research* **14**, 940-947.
- Whitehead D., Jarvis P.G. & Waring R.H. (1984) Stomatal conductance, transpiration, and resistance to water uptake in a *Pinus sylvestris* spacing experiment. *Canadian Journal of Forest Research* **14**, 692-700.
- Williams M., Rastetter E.B., Fernandes D.N., Goulden M.L., Wofsy S.C., Shaver G.R., Melillo J.M., Munger J.W., Fan S.-M. & Nadelhoffer K.J. (1996) Modelling the soil-plant-atmosphere continuum in a *Quercus-Acer* stand at Harvard Forest: the regulation of stomatal conductance by light, nitrogen and soil-plant hydraulic properties. *Plant Cell and Environment* **19**, 911-927.
- Wilson J.B. (1988) A review of evidence on the control of shoot:root ratio, in relation to models. *Annals of Botany* **61**, 433X-449.
- Yoder B.J., Ryan M.G., Waring R.H., Schoettle A.W. & Kaufmann M.R. (1994) Evidence of reduced photosynthetic rates in old trees. *Forest Science* **40**, 513-527.
- Zobel B.J. & van Buijtenen J.P. (1989) *Wood Variation. Its Causes and Control*. Springer-Verlag, Berlin.



## Appendix 2.1 Variables, parameters and units used in the model.

	<i>Definition</i>	<i>Units</i>	<i>Value</i>	<i>Source</i>
<i>A</i>	stand assimilation	$\text{kg m}^{-2} \text{yr}^{-1}$		
<i>A<sub>S</sub></i>	sapwood basal area	-		
<i>E<sub>g</sub></i>	stand growth efficiency (= $P_a / W_f$ )	$\text{yr}^{-1}$		
<i>E<sub>s</sub></i>	stand transpiration	$\text{m s}^{-1}$		
<i>E<sub>un</sub></i>	transpiration per unit foliage area	$\text{m s}^{-1}$	$4.2 \times 10^{-8}$	1, 2
<i>g</i>	acceleration due to gravity	$\text{m s}^{-2}$	9.8	
<i>h</i>	stand height	m		
<i>I</i>	incoming PAR over the growing season (mid April - mid October)	$\text{MJ m}^{-2} \text{yr}^{-1}$	2554	3
<i>k</i>	light extinction coefficient	-	0.46	4
<i>k<sub>r</sub></i>	specific hydraulic conductance of fine roots	$\text{m}^3 \text{s}^{-1} \text{MPa}^{-1} \text{kg}^{-1}$	$2.3 \times 10^{-7}$	5, 6
<i>k<sub>s</sub></i>	specific hydraulic conductivity of the sapwood	$\text{m}^2 \text{MPa}^{-1} \text{s}^{-1}$	$1.3 \times 10^{-3}$	7
<i>l<sub>r</sub></i>	fine root longevity	yr	0.65	8
<i>l<sub>s</sub></i>	sapwood longevity	yr	39	9
<i>N<sub>f</sub></i>	nitrogen concentration in foliage	$\text{kg N kg}^{-1}$	0.015	10
<i>N<sub>r</sub></i>	nitrogen concentration in fine roots	$\text{kg N kg}^{-1}$	0.0075	9
<i>N<sub>s</sub></i>	nitrogen concentration in sapwood	$\text{kg N kg}^{-1}$	0.0005	11
<i>P</i>	net primary production (subscript: a, above- ground, b, below-ground)	$\text{kg m}^{-2} \text{yr}^{-1}$		
<i>r<sub>g</sub></i>	growth respiration coefficient	-	0.28	12
<i>r<sup>m</sup></i>	specific maintenance respiration (subscript: f, foliage, r, fine roots, s, sapwood)	$\text{yr}^{-1}$		
<i>R<sub>m</sub></i>	maintenance respiration	$\text{kg m}^{-2} \text{yr}^{-1}$		
<i>R</i>	hydraulic resistance (superscript: u, per unit projected leaf area; subscript: root, shoot, total)	$\text{MPa s m}^{-1}$		
<i>T<sub>r</sub></i>	fine root turnover rate	$\text{kg m}^{-2} \text{yr}^{-1}$		
<i>W</i>	stand biomass (subscript: f, foliage, r, fine roots, s, sapwood)	$\text{kg m}^{-2}$		

$\epsilon_0$	gross light utilization coefficient	kg MJ <sup>-1</sup>	$1.7 \times 10^{-3}$	<sup>13</sup>
$\rho_S$	sapwood density	kg m <sup>-3</sup>	440	<sup>10</sup>
$\rho_W$	density of water	kg m <sup>-3</sup>	1000	
$\sigma$	specific leaf area	m <sup>2</sup> kg <sup>-1</sup>	4.5	<sup>7</sup>
$\Psi$	water potential (subscript: leaf, foliage, grav, gravitational)	MPa		
$\Psi_{soil}$	minimum soil water potential	MPa	-0.5	<sup>2</sup>
$\bar{\Psi}$	critical leaf water potential	MPa	-2.0	<sup>14</sup>

<sup>1</sup>Stewart (1988), <sup>2</sup>Jackson *et al.* (1995b), <sup>3</sup>Page and Lebens (1986), <sup>4</sup>Jarvis *et al.* (1976), <sup>5</sup>Roberts (1976), <sup>6</sup>Roberts (1977), <sup>7</sup>Mencuccini and Grace (1995), <sup>8</sup>Persson (1980), <sup>9</sup>Helmisaari and Siltala (1989), <sup>10</sup>Mencuccini and Grace (1996b), <sup>11</sup>Braekke (1995), <sup>12</sup>Chung & Barnes (1977), <sup>13</sup>McMurtrie *et al.* (1994), <sup>14</sup>Cochard (1992)

## Appendix 2.2 An analysis of the components of below-ground productivity.

Stand below-ground productivity  $P_b$  can be expressed as the sum of periodic biomass accumulation  $\Delta W$  and turnover  $T$

$$P_b = (\Delta W_{gr} + T_{gr}) + (\Delta W_r + T_r) \quad (\text{A.2.1})$$

where the subscripts  $gr$  and  $r$  refer to gross and fine roots, respectively.

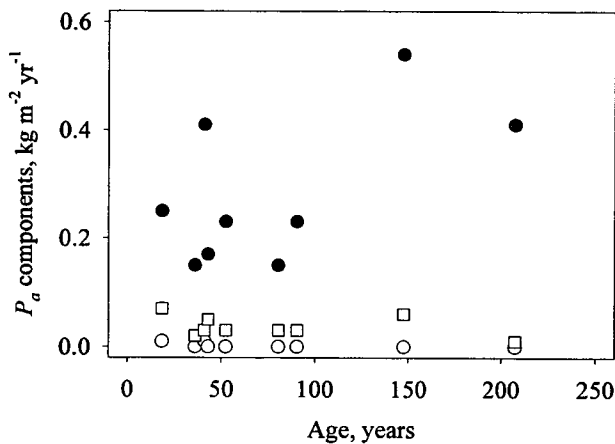


**Fig. A.2.1** Comparison of below-ground productivity components. Estimates of fine root turnover (●) and of the annual biomass accumulation of fine (○) and coarse roots (□) for a *P. sylvestris* chronosequence have been derived from allometric data in Vanninen *et al.* (1997) as described in the text.

although no figures are available for this component, it can be probably assumed to be rather negligible.

When the estimated values for the different components of  $P_b$  are compared (Fig. A.2.1), it is apparent that fine root turnover predominates over both coarse root production and fine root accumulation, lending support to the approximation introduced in Eq. 2.4.

To the best of our knowledge, no data are available in the literature on the productivity of fine versus coarse roots in *P. sylvestris*. However, some quantitative hints can be gained from Vanninen *et al.* (1997), who report detailed data on the standing biomass of different root components in a Scots pine chronosequence. The annual change in fine and coarse root biomass ( $\Delta W_i$ ) can be reasonably approximated by the mean annual increment of the compartment, i.e. the ratio between its standing biomass and stand age. The turnover rate of fine roots can be derived from fine root standing biomass and longevity, as discussed in the Theory section. As for the turnover rate of coarse roots,

### Chapter 3. On the causes of the age-related decline of forest growth. A meta-analysis of data from *Pinus sylvestris* L.

Science is built up with facts, as a house is with stones.  
But a collection of facts is no more a science than a  
heap of stones is a house.

Jules Henri Poincaré

#### 3.1 Introduction

The aboveground net primary production ( $P_a$ ) of forests is commonly observed to decline with stand age (Waring and Schlesinger 1985), resulting in the parallel reduction of current annual increments that all foresters know so well (Oliver and Larson 1996).

In polycarpic species such as forest trees, apical and secondary meristems ensure a continuous tissue turnover and largely prevent the detrimental effects of ageing at the individual cell and organ level (Nooden 1988). Forest ecologists have therefore long wondered what the functional basis of forest ageing at the whole tree and stand level could be (Gower *et al.* 1996).

Leaf area index and light interception have often been reported to decline after canopy closure (Margolis *et al.* 1995), reducing the amount of energy available to photosynthetic processes. Growth per unit leaf area, however, has also been reported to decline with age (Ryan *et al.* 1997). This could result from a reduction in the photosynthetic capacity of foliage or from increasing stomatal limitations to gas exchange. Changes in the functional balance between photosynthetic and allotrophic tissues (mainly sapwood and fine roots) have been also proposed as possible explanations, as they would result in higher respiratory and turnover costs (Gower *et al.* 1996). Nutrient limitations could be responsible for both processes (Murty *et al.* 1996), through a reduced leaf protein content, on the one hand, and because of the increased production of feeder roots that would be required to sustain plant growth. Hydraulic limitations have also been suggested as a possible cause (Yoder *et al.* 1994; Chapter 2): because of the increasingly long hydraulic pathway, tall trees need

to restrict water loss by closing their stomata or increase the conductivity of sapwood and fine roots to prevent extreme and potentially damaging leaf water potentials. How these processes interact in determining the observed decline in forest  $P_a$  has still to be ascertained.

Scots pine (*Pinus sylvestris* L.) is the most widely distributed pine species in the world (Vidakovic 1991) and has been the subject of much research; yet, ecological information on stand dynamics and on developmental changes in stand structure and productivity of this important species is scattered (Gower *et al.* 1994). The aim of the present study was therefore to review and organize published data on the age-related decline in Scots pine aboveground net primary production and on its possible causes, so as to attempt some general conclusions for the species.

### 3.2 Material and methods

Data on the age-related  $P_a$  decline in *P. sylvestris* were collated from four different studies (Tab. 3.1), covering both temperate and boreal conditions.

Values of stand  $P_a$  ( $\text{kg m}^{-2} \text{yr}^{-1}$ ) were directly obtained from Ovington (1957) and Mälkönen (1974). Values reported in Mencuccini and Grace (1996) had to be corrected for foliage biomass production, computed as the product of standing foliage biomass by average needle mortality. A value for the mortality of *P. sylvestris*

**Table 3.1.** Site characteristics of the *Pinus sylvestris* chronosequences analyzed: latitude, elevation, annual precipitation ( $P$ ) and average temperature ( $T$ ), height of dominant trees at the age of 50 ( $H_{50}$ ) and range of the age sequence.

Sequence	Location	Latitude °N	Elevation m	P mm yr <sup>-1</sup>	T °C	$H_{50}$ m	Age range years	Source
UK1	Thetford, U.K.	52	50	650	10	16	3-55	<sup>1</sup>
UK2						20	7-59	<sup>2</sup>
SW	Jädraås, Sweden	61	10-295	593-607	3.8-4.8	15	12-100	<sup>3,4</sup>
FI	Tammela, Finland	60	130	612	4.6	14	28-47	<sup>5</sup>

<sup>1</sup>Ovington (1957), <sup>2</sup>Mencuccini and Grace (1996), <sup>3</sup>Albrektson (1980, 1984), <sup>4</sup>Albrektson and Valinger (1985), <sup>5</sup>Mälkönen (1974)

needles in Thetford Forest was assumed from Jalkanen *et al.* (1994). For the Jädraås study (Albrektson 1980, 1984; Albrektson and Valinger 1985), the productivity of stemwood, needles and new shoot axes per unit foliage biomass (“fraction productivity”) of the *P. sylvestris* stands was derived from the empirical model fitted to data from 153 sampled trees by Albrektson and Valinger (1985) and multiplied by foliage biomass (Albrektson 1980) to obtain stand  $P_a$ . In addition, the fractional allocation of growth between foliage and sapwood ( $\lambda_s/\lambda_f$ , where  $\lambda_s$  and  $\lambda_f$  are coefficients of growth allocation to sapwood and foliage, respectively) could be derived from data in Ovington (1957) and Albrektson and Valinger (1985).

In order to understand the processes behind the observed pattern of  $P_a$  development, changes in stand foliage biomass were derived from the same sources. Stand specific productivity ( $P_s$ ,  $\text{yr}^{-1}$ ) was computed as the ratio between stand  $P_a$  and foliage biomass (Axelsson and Axelsson 1986); this index is akin to the stand growth efficiency proposed by Waring (1983) that has been widely used in the analysis of  $P_a$  dynamics (Ryan *et al.* 1997), although the latter is based on wood production only and is expressed on a foliage area basis. Following McMurtrie *et al.* (1994), a stand light utilization coefficient ( $\epsilon$ ,  $\text{kg GJ}^{-1}$ ;  $P_a$  per unit absorbed photosynthetically active radiation over the year) was also computed for the Thetford and Jädraås stands, assuming an exponential extinction of light inside the crown. A constant value of specific leaf area ( $4.7 \text{ m}^2 \text{ kg}^{-1}$ ; Kellomaki and Oker-Blom 1981) and of light absorption coefficient (0.46; Jarvis *et al.* 1976) was assumed for all sites. Estimates of total incoming photosynthetically active radiation (PAR) over the year at the two sites were derived from Page and Lebens (1986) and from McMurtrie *et al.* (1994), respectively; PAR was assumed to be a constant fraction of global radiation (Monteith and Unsworth 1990).

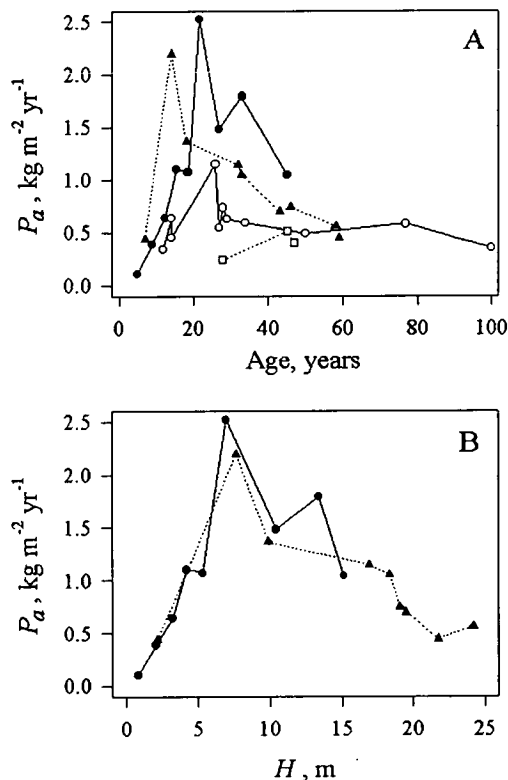
Additional data on developmental changes in plant structure and density were derived from the literature, as specified in the text, so as to try and explain the observed patterns of foliage biomass and light use efficiency. When published data referred to individual sample trees, an average for the whole stand was computed and used in comparisons.

### 3.3 Results and discussion

As a result of differences in the estimation process, some of the estimated values refer to slightly different quantities: increments in gross root biomass were included in the estimates by Mencuccini and Grace (1996), whilst the model proposed by Albrektson and Valinger (1985) neglected the contribution of cone production to stand  $P_a$ . Thinning regimes also differed among age-sequences and their effects were variously treated by the original authors. An analysis of the detailed data-set reported by Ovington (1957), however, suggests that these discrepancies are of little relevance and do not undermine the validity of the comparison.

At all four sites, above-ground net primary production reached a peak at canopy

**Figure 3.1.** Developmental changes in stand aboveground net primary production. A The pattern of  $P_a$  change at Thetford (sequence UK1, ●, and UK2, ▲), Jädraås (sequence SW, ○) and Tammela (sequence FI, □). B Effect of fertility on  $P_a$  dynamics: differences between sequence UK1 and UK2 tend to disappear when plotted against stand height.



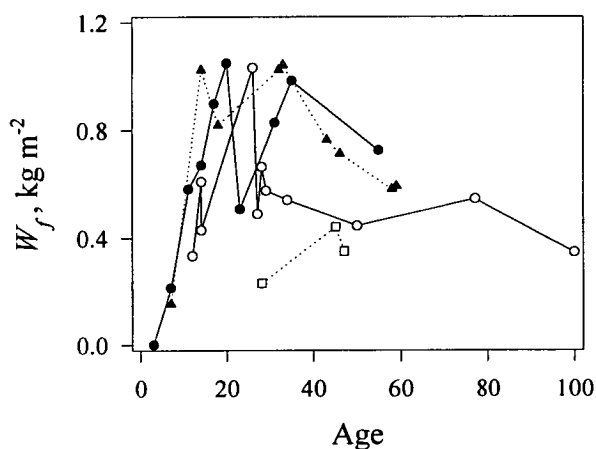
closure and then declined with age (Fig. 3.1 A), as reported for several other forest tree species (Ryan *et al.* 1997). The Finnish data-set, however, is too limited to draw any conclusions on developmental patterns and can only be used to confirm the absolute figures reported for boreal *P. sylvestris* forests at Jädraås.

Maximum  $P_a$  differed greatly among temperate and boreal sites. At the SW site  $P_a$  never exceeded  $1.2 \text{ kg m}^{-2} \text{ yr}^{-1}$ , about half that for the UK1 and UK2 chronosequences ( $2.2$  and  $2.5 \text{ kg m}^{-2} \text{ yr}^{-1}$ , respectively). To draw a comparison, the latter values are somewhat lower than those reported for another conifer, *Picea sitchensis*, under the wetter climate of southern Scotland (Ford 1982). Differences among temperate and boreal sites are only partly

attributable to lower decomposition rates and nutrient limitations: according to Axelsson and Axelsson (1986), for example, the application of both water and nutrients to a 20-year-old *P. sylvestris* stand at Jädraås resulted in a three-fold increase in  $P_a$ , from 0.3 to 0.9 kg m<sup>-2</sup> yr<sup>-1</sup>, but still well below the values reported for corresponding stands growing in the warmer Thetford climate. Higher mean annual temperatures and a more maritime climate presumably result in a longer growing season at the British site, which could have contributed to the observed differences. Moreover, the dynamics of  $P_a$  appear to be faster at the temperate site (Fig. 3.1 A), supporting the observation that the rate of age-related growth decline increases with temperature (Whittaker 1975). This relationship between site fertility and  $P_a$  dynamics is confirmed by a comparison of the two Thetford chronosequences: the UK2 series, characterized by a higher site index (Table 3.1), shows faster dynamics when chronological stand age is considered (Fig. 3.1 A). These differences parallel the faster longitudinal increments of the UK2 series and practically disappear when data are plotted against stand height (Fig. 3.1 B), suggesting a direct link between height and above-ground productivity under given environmental conditions (Chapter 2).

The age-related decline in  $P_a$  resulted from the interaction of an increasingly lower

**Figure 3.2.** Developmental changes in stand foliage biomass  $W_f$  at Thetford (sequence UK1, ●, and UK2, ▲), Jädraås (sequence SW, ○) and Tammela (sequence FI, □).



foliage biomass (and light interception) and a reduction in radiation use efficiency.

The same dynamics of leaf biomass development observed in the four chronosequences (Fig. 3.2) have been reported for other *P. sylvestris* stands (Vanninen *et al.* 1996) as well as for many other species (Gholz *et al.* 1994; Margolis *et al.* 1995). This pattern appears to be the result of the two co-occurring



**Figure 3.3.** Relationship between tree diameter at breast height ( $DBH$ ) and foliage biomass  $W_f^{tree}$ .  $W_f^{tree}$  was either directly measured or obtained by dividing stand foliage biomass by stand density. Data from Ovington (1957), Whitehead (1978), Albrektson (1980, 1984), van Hees and Bartelink (1993), Vanninen *et al.* (1996), Mencuccini & Grace (1996). Symbols refer to different studies.

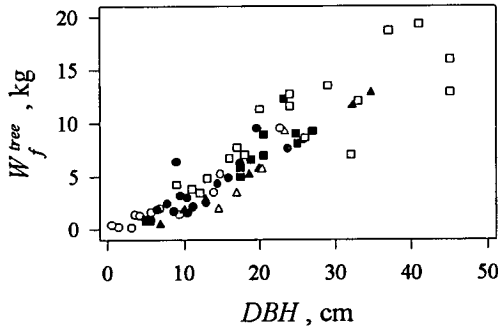
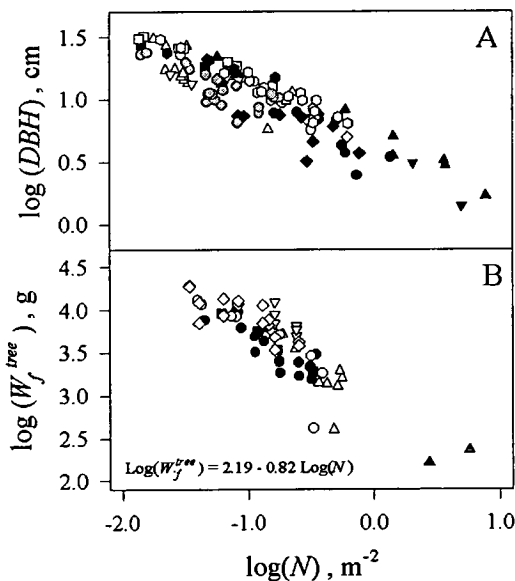


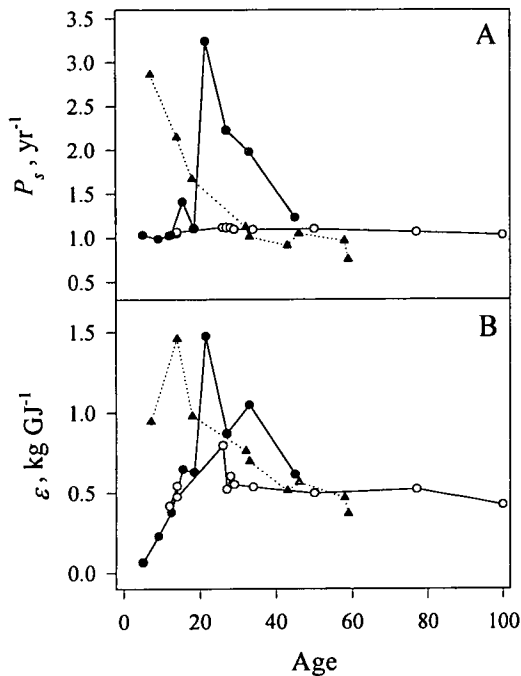
**Figure 3.4.** A Logarithmic relationship between stand density  $N$  and average diameter at breast height  $DBH$ . B Logarithmic relationship between tree foliage biomass  $W_f^{tree}$  and stand density. Data from Ovington (1957), Whitehead (1980), Albrektson (1980, 1984), Cannell (1982), Maddelein *et al.* (1990), Hynynen (1993), van Hees and Bartelink (1993), Berninger and Nikinmaa (1994), Usol'tsev and Vanclay (1995), Makela *et al.* (1995), Berninger *et al.* (1995), Vanninen *et al.* (1996), Mencuccini and Grace (1996). Symbols refer to different studies.



processes of individual tree growth and stand dynamics.

Foliage biomass per plant, on the one hand, increases almost linearly with tree dimensions, as demonstrated by a review of literature data for Scots pine (Fig. 3.3). Tree dimensions, on the other hand, are inversely related to stand density, as predicted by the self-thinning law (Westoby 1984). This is demonstrated for a number of *P. sylvestris* natural stands and plantations in Fig. 3.4A, taking tree diameter as an index of tree dimensions as already suggested by Reineke (1933). Because of the allometric relationship of Fig. 3.3, the self-thinning law can also be expressed in terms of plant foliage biomass (Westoby 1977; Waring and Running 1998): as the number of trees decreases in the ageing stand, the leaf area of individual trees increases exponentially. This is reviewed in Fig. 3.4 B for a number of *P. sylvestris* stands. The balance between these two contrasting processes is

**Figure 3.5.** Developmental change in  $P_a$  components at Thetford (sequence UK1, ●, and UK2, ▲), Jädraås (sequence SW, ○). A Changes in stand specific productivity ( $P_s$ ). B Changes in light utilization coefficient ( $\epsilon$ ).



determined by the slope of the self-thinning law in Fig. 3.4 B: a value less negative than -1 implies that the effect of self-thinning predominates and that stand leaf area index declines in ageing stands.

The initial rise in leaf area index often observed in plantations (Fig. 3.2) could be just the result of an initial low stocking density and incomplete canopy cover, as suggested by a comparison of natural stands and plantations at Thetford (Ovington 1957): naturally regenerated 11-year-old stands had a foliage biomass as high as  $1.33 \text{ kg m}^{-2}$ , well above the value of  $0.58$  in plantations of the same age and even higher than the

maximum value of  $1.05 \text{ kg m}^{-2}$  reached by plantations at canopy closure.

Stand specific productivity and light use efficiency also change over the life-time of the stand.

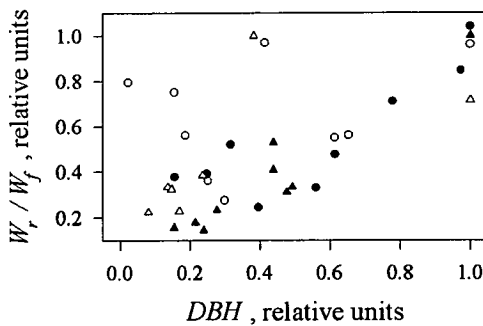
The pattern of specific productivity shows no consistency among the chronosequences analyzed (Fig. 3.5 A): the index peaks, then declines in the UK1 sequence, but decreases continuously for the UK2 sequence, whilst only small changes are observed at the Jädraås site. The comparison with the pattern of light use efficiency (Fig. 3.5 B), however, demonstrates how misleading can be the use of indices such as specific productivity that are purely allometric and lack any functional basis. All three chronosequences show the same trend in the coefficient of light utilization  $\epsilon$ , which peaks at or before canopy closure and then declines about 40-60 % by the age of 50 (Tab. 3.2). The decline is stronger in highly productive stands. The discrepancy between the two parameters stems from the nonlinear relationship between light interception and leaf area index, resulting in a higher

**Table 3.2.** Percentage reduction in  $P_a$ , stand foliage biomass ( $W_f$ , kg m<sup>-2</sup>), specific productivity ( $P_s$ , yr<sup>-1</sup>) and light utilization coefficient ( $\epsilon$ , kg GJ<sup>-1</sup>) at the age of 45-50 years, relative to the peak value at canopy closure. No estimates of  $\epsilon$  could be obtained for the FI sequence.

Sequence	Percentage reduction			
	$P_s$	$W_f$	$P_s$	$\epsilon$
UK1	58	12	62	58
UK2	70	38	65	65
SW	57	57	1	38
FI	22	20	1	-

the accumulation of woody litter of poor quality in ageing stands (Gower *et al.* 1996). In a collateral study at the Jädraås site, a much higher fine root biomass was indeed measured by Persson (1983; 1984) in a mature than in a young *P. sylvestris* stand (26.1 and 122.5 g m<sup>-2</sup>, respectively), and belowground productivity was estimated to decline between age 20 and age 120 by a mere 13 %, as compared to an

**Figure 3.6.** Height-related changes in the fine root -to- foliage biomass ratio ( $W_r / W_f$ ) in *P. sylvestris* stands. Data from Ovington (1957), Usol'tsev and Vanclay (1995) and Vanninen *et al.* (1996).



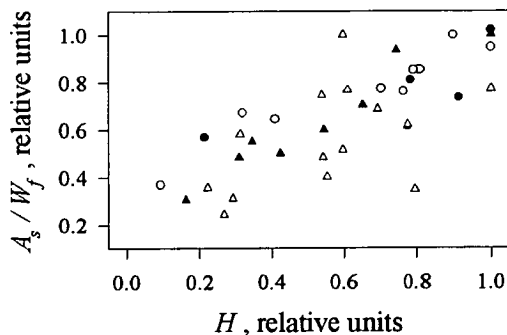
estimated 69 % decline in  $P_a$  between age 26 and age 100 in similar stands (Fig. 3.1). In combination with the reported decline in stand leaf biomass, this would determine a shift in the functional balance between the biomass of absorbing roots ( $W_r$ ) and assimilating needles ( $W_f$ ), with higher fine root:foliage ratios in old stands. A re-analysis of existing data-sets for *P. sylvestris* stands (Ovington 1957; Usol'tsev and Vanclay 1995; Vanninen *et al.* 1996) does confirm this trend (Fig. 3.6), demonstrating a significant global increase in the  $W_r / W_f$  with stem diameter when site-specific differences in absolute values are normalized.

sensitivity in sparse stands to even small changes in canopy closure.

Several explanations have been proposed over the years for the decline of the light utilization coefficient  $\epsilon$  in ageing stands (Ryan *et al.* 1997). It has been suggested that it could be the result of an increasing allocation of growth belowground, because of the reduced nutrient availability resulting from

the accumulation of woody litter of poor quality in ageing stands (Gower *et al.* 1996). In a collateral study at the Jädraås site, a much higher fine root biomass was indeed measured by Persson (1983; 1984) in a mature than in a young *P. sylvestris* stand (26.1 and 122.5 g m<sup>-2</sup>, respectively), and belowground productivity was estimated to decline between age 20 and age 120 by a mere 13 %, as compared to an estimated 69 % decline in  $P_a$  between age 26 and age 100 in similar stands (Fig. 3.1). In combination with the reported decline in stand leaf biomass, this would determine a shift in the functional balance between the biomass of absorbing roots ( $W_r$ ) and assimilating needles ( $W_f$ ), with higher fine root:foliage ratios in old stands. A re-analysis of existing data-sets for *P. sylvestris* stands (Ovington 1957; Usol'tsev and Vanclay 1995; Vanninen

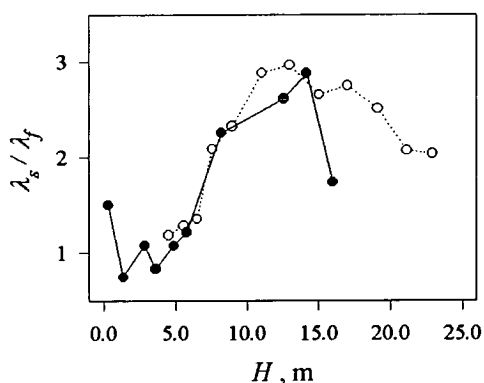
**Figure 3.7.** Height-related changes in the sapwood area-to-foilage biomass ratio ( $A_s/W_f$ ) in *P. sylvestris* stands. Data from Albrektson (1980), van Hees and Bartelink (1993), Vanninen *et al.* (1996), Mencuccini and Grace (1996).



Mencuccini and Grace 1996; Vanninen *et al.* 1996).

Such a structural change is the result of a marked shift in growth allocation between sapwood ( $\lambda_s$ ) and foliage ( $\lambda_f$ ), as can be derived from the detailed data reported in Ovington (1957) for entire stands and by Albrektson and Valinger (1985) for individual trees: the ratio  $\lambda_s/\lambda_f$  increases from a value of 1 to values close to 3 when tree height has reached values of 8-12 m, then declines again (Fig. 3.8). The

**Figure 3.8.** Height-related changes in the balance between allocation to sapwood ( $\lambda_s$ ) and allocation to foliage ( $\lambda_f$ ) for the UK1 (●) and the SW (○) chronosequence.



agreement both in trend and in absolute values between the two data-sets suggests a general consistency worthy of further investigation.

This is not, however, the only adjustment in the internal functional balance in ageing *P. sylvestris* stands: the ratio between sapwood cross-sectional area at breast height ( $A_s$ ) and foliage biomass is also not constant, as often assumed (Margolis *et al.* 1995), but increases significantly with stand height (Fig. 3.7), following approximately the same pattern in all four data-sets analyzed (Albrektson 1984; van Hees and Bartelink 1993;

The shift in the functional balance between sapwood and transpiring foliage cannot be explained by nutrient limitations, but could be related to the maintenance of a functional homeostasis in water transport, as first suggested by Whitehead *et al.* (1984): a larger area of conductive sapwood per unit area of transpiring foliage could counterbalance the detrimental effects of increasing tree height and help prevent the

onset of extreme needle water potentials and xylem cavitation (Tyree and Sperry 1989). It has indeed been demonstrated (Chapter 2, 4) that the minimum water potential experienced by *P. sylvestris* seedlings and mature trees over the season is rather conservative, despite large differences in tree dimensions, environmental conditions and transpiration rates per needle area. This threshold value appears to match quite closely the critical water potential for xylem cavitation.

The model by Whitehead *et al.* (1984), however, neglects the role of fine roots in water transport. This could be misleading: the root system of mature Scots pine trees has been reported to account for more than 50% of total plant hydraulic resistance (Roberts 1977). The observed changes in the balance between foliage and feeder roots (Fig. 3.6) could therefore play a major role in the maintenance of a functional homeostasis in water relations, since hydraulic resistance is inversely related to fine root biomass (Magnani *et al.* 1996). When the approach of Whitehead *et al.* (1984) is extended to take into account both components of plant hydraulic architecture, however, the principle of cavitation avoidance is found to explain conveniently the whole process of structural acclimation of ageing stands, suggesting an alternative explanation for the reduction in radiation use efficiency (Chapter 2). As trees age and grow taller, the greater length of the transport pathway is counterbalanced by a reduced allocation to foliage and a higher investment in sapwood and fine roots. This implies both a reduction in leaf area index (Chapter 4) and a shift in allometric ratios, in good agreement with the present review of *P. sylvestris* stands, providing an explanation for the observed decline in forest aboveground net primary production with age. Moreover, the same principle seems to account also for many features of tree response to temperature and water availability (Chapter 4).

### 3.4 Conclusions

The meta-analysis presented demonstrates how similar developmental patterns are recognizable in *P. sylvestris* stands growing under widely different climates, despite the large variability in growth rates observed. Under both maritime and boreal conditions the age-related decline in productivity appears to result from a parallel drop in light interception and light-use efficiency. The latter is likely to result largely from allometric changes, as reported for *P. sylvestris* stands under an even wider

range of conditions. These changes apparently depend upon a shift in resource allocation, rather than tissue mortality, as demonstrated for the balance between foliage and sapwood growth. Further research will be needed to assess how nutrient and hydraulic limitations combine in determining these structural changes and the resulting decline in  $P_a$  observed in ageing stands. The hypothesis of functional homeostasis in water transport, however, emerges as a strong candidate to explain the developmental pattern of productivity in coniferous forests.

Under this perspective, a pivotal role should be attributed to tree height, rather than age *per se*. Fast height increments are known to have a beneficial effect for the individual, because of the advantage they grant in plant competition for light. Even at the population level height increments are known to be positively related to the production of new foliage, in evergreen species at least, hence to light interception and growth. Because of the hydraulic limitations that it induces, on the other hand, height could be at the same time responsible for the developmental decline in stand productivity that has been commonly attributed to the effects of age. Such a negative feed-back control would appear to play a central role in the regulation of tree growth.

## References

- Albrektson A. (1980) Relations between tree biomass fractions and conventional silvicultural measurements. *Ecological Bulletins* 32: 315-327.
- Albrektson A. (1984) Sapwood basal area and needle mass of Scots pine (*Pinus sylvestris* L.) trees in central Sweden. *Forestry* 57: 35-43.
- Albrektson A., Valinger E. (1985) Relations between tree height and diameter, productivity and allocation of growth in a Scots pine (*Pinus sylvestris* L.) sample tree material. In *Crop Physiology of Forest Trees* (eds. P.M.A. Tigerstedt, P. Puttonen and V. Koski). University of Helsinki, Helsinki, pp 95-105.
- Axelsson E., Axelsson B. (1986) Changes in carbon allocation patterns in spruce and pine trees following irrigation and fertilization. *Tree Physiology* 2: 189-204.
- Berninger F., Mencuccini M., Nikinmaa E., Grace J., Hari P. (1995) Evaporative demand determines branchiness of Scots pine. *Oecologia* 102: 164-168.
- Berninger F., Nikinmaa E. (1994) Foliage area - sapwood area relationships of Scots pine (*Pinus sylvestris*) trees in different climates. *Canadian Journal of Forest Research* 24: 2263-2268.
- Cannell M.G.R. (1982) *World Forest Biomass and Primary Production Data*. Academic Press, New York.
- Ford E.D. (1982) High productivity in a polestage Sitka spruce stand and its relation to canopy structure. *Forestry* 55: 1-17.

- Gholz H.L., Linder S., McMurtrie R.E. (1994) Environmental Constraints on the Structure and Productivity of Pine Forest Ecosystems: a Comparative Analysis. *Ecological Bulletins* Vol. 43. Copenhagen.
- Gower S.T., Gholz H.L., Nakane K., Baldwin V.C. (1994) Production and carbon allocation patterns of pine forests. *Ecological Bulletins* 43: 115-135.
- Gower S.T., McMurtrie R.E., Murty D. (1996) Aboveground net primary production decline with stand age: potential causes. *Trends in Ecology and Evolution* 11: 378-382.
- Hynynen J. (1993) Self-thinning models for even-aged stands of *Pinus sylvestris*, *Picea abies* and *Betula pendula*. *Scandinavian Journal of Forest Research* 8: 326-336.
- Jarvis P.G., James G.B., Landsberg J.J. (1976) Coniferous forest. In Vol. 2. *Vegetation and the Atmosphere* (ed. J.L. Monteith). Academic Press, London, pp 171-240.
- Kellomaki S., Oker-Blom P. (1981) Specific needle area of Scots pine and its dependence on light conditions inside the canopy. *Silva Fennica* 15: 190-198.
- Maddelein D., Lust N., Meyen S., Muys B. (1990) Dynamics in maturing Scots pine monocultures in North-east Belgium. In *Proceedings XIX IUFRO World Congress, Montreal, Canada, August 1990*.
- Magnani F., Centritto M., Grace J. (1996) Measurement of apoplasmic and cell-to-cell components of root hydraulic conductance by a pressure clamp technique. *Planta* 199: 296-306.
- Makela A., Virtanen K., Nikinmaa E. (1995) The effects of ring width, stem position, and stand density on the relationship between foliage biomass and sapwood area in Scots pine (*Pinus sylvestris*). *Canadian Journal of Forest Research* 25: 970-977.
- Margolis H., Oren R., Whithead D., Kaufmann M.R. (1995) Leaf area dynamics of conifer forests. In *Ecophysiology of Coniferous Forests* (eds. W.K. Smith, T.M. Hinckley). Academic Press, San Diego, pp 181-223.
- Mälkönen E. (1974) Annual primary production and nutrient cycle in some Scots pine stands. *Communicationes Instituti Forestalis Fenniae* Vol. 84. Helsinki.
- McMurtrie R.E., Gholz H.L., Linder S., Gower S.T. (1994) Climatic factors controlling the productivity of pine stands: a model-based analysis. *Ecological Bulletins* 43: 173-188.
- Mencuccini M., Grace J. (1996) Hydraulic conductance, light interception and needle nutrient concentration in Scots pine stands and their relations with net primary productivity. *Tree Physiology* 16: 459-468.
- Monteith J.L., Unsworth M.H. (1990) *Principles of Environmental Physics*. Edward Arnold, London.
- Murty D., McMurtrie R.E., Ryan M.G. (1996) Declining forest productivity in aging forest stands: a modeling analysis of alternative hypotheses. *Tree Physiology* 16: 187-200.
- Nooden L.D. (1988) Whole plant senescence. In *Senescence and Aging in Plants* (eds. L.D. Nooden, A.C. Leopold). Academic Press, San Diego, pp 391-439.

- Oliver C.D., Larson B.C. (1996) *Forest Stand Dynamics*. John Wiley and Sons, New York.
- Ovington J.D. (1957) Dry-matter production by *Pinus sylvestris* L. *Annals of Botany* 21: 287-314.
- Page J., Lebens R. (eds) (1986) *Climate in the United Kingdom*. Department of Energy, London.
- Persson H. (1984) The dynamic fine roots of forest trees. In *State and Change of Forest Ecosystems* (ed. G.I. Ågren). Swed. Univ. Agric. Sci. Dept. Ecol. Envir. Res., pp 193-204.
- Persson H.A. (1983) The distribution and productivity of fine roots in boreal forests. *Plant and Soil* 71: 87-101.
- Reineke L.H. (1933) Perfecting a stand-density index for even-aged forests. *Journal of Agricultural Research* 46: 627-638.
- Roberts J. (1977) The use of tree-cutting techniques in the study of the water relations of mature *Pinus sylvestris* L. *Journal of Experimental Botany* 28: 751-767.
- Ryan M.G., Binkley D., Fownes J.H. (1997) Age-related decline in forest productivity: pattern and processes. *Advances in Ecological Research* 27: 213-262.
- Tyree M.T., Sperry J.S. (1989) Vulnerability of xylem to cavitation and embolism. *Annual Review of Plant Physiology and Plant Molecular Biology* 40: 19-38.
- Usolt'sev V.A., Vanclay J.K. (1995) Stand biomass dynamics of pine plantations and natural forests on dry steppe in Kazakhstan. *Scandinavian Journal of Forest Research* 10: 305-312X.
- van Hees A.F.M., Bartelink H.H. (1993) Needle area relationships of Scots pine in the Netherlands. *Forest Ecology and Management* 58: 19-31.
- Vanninen P., Ylitalo H., Sievanen R., Makela A. (1996) Effects of age and site quality on the distribution of biomass in Scots pine (*Pinus sylvestris* L.). *Trees* 10: 231-238.
- Vidakovic M. (1991) *Conifers*. Graficki Zavod Hrvatske, Zagreb.
- Waring R.H. (1983) Estimating forest growth and efficiency in relation to canopy leaf area. *Advances in Ecological Research* 13: 327-354.
- Waring R.H., Running S.W. (1998) *Forest Ecosystems. Analysis at Multiple Scales*. Academic Press, San Diego.
- Waring R.H., Schlesinger W.H. (1985) *Forest Ecosystems*. Academic Press, Orlando.
- Westoby M. (1977) Self-thinning driven by leaf area not by weight. *Nature* 265: 330-331.
- Westoby M. (1984) The self-thinning rule. *Advances in Ecological Research* 14: 167-225.
- Whitehead D. (1978) The estimation of foliage area from sapwood basal area in Scots pine. *Forestry* 51: 137-149.



- Whitehead D., Edwards W.R.N., Jarvis P.G. (1984) Conducting sapwood area, foliage area, and permeability in mature trees of *Picea sitchensis* and *Pinus contorta*. Canadian Journal of Forest Research 14: 940-947.
- Whittaker R.H. (1975) Communities and Ecosystems. MacMillan, New York.
- Yoder B.J., Ryan M.G., Waring R.H., Schoettle A.W., Kaufmann M.R. (1994) Evidence of reduced photosynthetic rates in old trees. Forest Science 40: 513-527.

## Chapter 4. Acclimation of coniferous tree structure to the environment under hydraulic constraints

*Non sunt multiplicanda entia praeter necessitatem.*  
("Ockham's razor")

William of Ockham

A model should be as simple as possible, but no simpler than that.

A. Einstein

### 4.1 Introduction

The response of trees to their physical environment has attracted much attention over recent decades. Significant progress has been made in understanding how gas exchange and gross primary production are affected by a variety of factors (Farquhar & von Caemmerer 1982; Monteith 1995; Ryan *et al.* 1996b). In comparison, allocation of growth among tree organs is poorly understood, despite the considerable effect that changes in resource allocation could have on the response of forest growth to climate change (Berninger & Nikinmaa 1997). A general lack of basic knowledge on complex topics such as phloem loading, transport and unloading (Van Bel 1993; Komor 1994; Patrick 1997) prevents translation of knowledge into simple operational models.

Many studies on the environmental control of allocation have focused on the final effect of the process, i.e. on the resulting changes in the allometric balance among tree parts (Wilson 1988; Cannell & Dewar 1994; Gower, Isebrands & Sheriff 1995). The allometry of the plant is known to be affected by a variety of environmental factors. Temperature, for example, is known to alter the balance between foliage and fine roots (Wilson 1988); fine root production is also enhanced by factors such as high light and nutrient deprivation, in such a way that the functional balance between carbon acquisition by foliage and nutrient acquisition from the soil is often maintained and tissue nutrient concentration is kept rather constant (Santantonio 1990; Dewar, Ludlow & Dougherty 1994). This

appears to be particularly true for conifers (Ägren & Ingestad 1987). The suggestion has been made that the same principle could drive the response of root-shoot ratios to soil drought (Cannell & Dewar 1994), which has been often reported to increase resource allocation to absorbing roots (Gower, Isebrands & Sheriff 1995). The hypothesis of a functional homeostasis in water transport constitutes the basis of models by Whitehead *et al.* (1984) and Givnish (1986). Whitehead *et al.* (1984) argued that a balance must exist between the amount of transpiring foliage, sapwood conducting area, tree height and humidity of soil and in the air. The balance should therefore change as a function of both the environment and stand age, rather than being constant as assumed by the pipe model theory (Shinozaki *et al.* 1964), with important implications for the response of forest growth to the environment (Berninger & Nikinmaa 1997). Moving from the assumption of a detrimental effect of water potential on leaf gas exchange, Givnish (1986) on the contrary predicted that optimal growth can only be achieved if the balance between foliage and conducting roots is tuned to the atmospheric environment experienced by the plant. Functional homeostasis was not assumed, but rather was an emergent property of the model. As can be seen, both hypotheses focused on only one component of the plant hydraulic continuum, either the sapwood or fine roots.

More recently, we have successfully combined the two approaches in a mathematical model of resource acclimation and growth in coniferous trees (Chapter 2). The analysis is based on the hypothesis of optimal growth and functional homeostasis in water transport: the assumption is made that minimum water potentials are constrained, possibly by the risk of destructive xylem embolism (Tyree & Sperry 1989), and that foliage production and tree growth are maximized within the limits imposed by this hydraulic constraint. Using this approach, model predictions of functional allometry and its changes over the lifetime of the tree have been successfully compared with available experimental evidence for *Pinus sylvestris* in natural conditions (Chapter 2, 3). The present paper will explore the implications of the hypothesis for the response of resource allocation and forest growth to the plant environment.

## 4.2 Theory

### 4.2.1 Optimal tree allometry under hydraulic constraints

The link between plant functional allometry and tissue water relations can be explored by means of a simple model. Let  $E_f$  be the amount of water transpired by a unit of leaf surface in the stand. If  $\Psi_{leaf}$  is the resulting leaf water potential and neglecting, for the sake of clarity, the effects of tree height and gravitational potential, we can then define  $R_{tot}^f$ , the hydraulic resistance per unit foliage area across the soil-plant continuum, as:

$$R_{tot}^f = W_f \cdot \sigma \cdot R_{tot} = \frac{\Psi_{soil} - \Psi_{leaf}}{E_f} \quad (4.1)$$

where  $W_f$  is stand foliage biomass,  $\sigma$  is specific leaf area and  $\Psi_{soil}$  is soil water potential. All parameters and variables are defined in Appendix 4.1. Stand hydraulic resistance  $R_{tot}$  (expressed on a ground surface basis) can be viewed as the sum in series of three distinct components located in the shoot, fine roots and soil, respectively. All of them are largely a function of plant allometry.

Shoot resistance ( $R_{shoot}$ ) is affected by the length of the hydraulic pathway, related to tree height  $h$ , and of the cross-sectional area  $A_s$  of conducting sapwood (Whitehead, Edwards & Jarvis 1984; Whitehead, Jarvis & Waring 1984):

$$R_{shoot} = \frac{r_s \cdot \eta \cdot h}{A_s} = \frac{r_s \cdot \eta \cdot h^2 \cdot \rho_s}{W_s} \quad (4.2)$$

where  $r_s$  is sapwood resistivity, here defined as the inverse of xylem permeability,  $\eta$  is water viscosity and  $W_s$  and  $\rho_s$  are sapwood biomass and sapwood density, respectively. A constant sapwood cross-sectional area along tree stem and branches has been assumed in Eq. 4.2 (Shinozaki *et al.* 1964; Makela & Hari 1986).

Root hydraulic resistance ( $R_{root}$ ) is mainly associated with the movement of water from the epidermis to the stele (Passioura 1988; Magnani, Centritto & Grace

1996); it is therefore inversely related to the surface of fine roots and, in first approximation, to fine root biomass  $W_r$ :

$$R_{root} = \frac{r_r \cdot \eta}{W_r} \quad (4.3)$$

where  $r_r$  is resistivity per unit root biomass.

Soil hydraulic resistance ( $R_{soil}$ ) is also influenced by the amount of fine roots exploring the soil. From single root theory,  $R_{soil}$  can be approximated as (Passioura & Cowan 1968):

$$R_{soil} = \frac{-\ln(\pi \cdot r^2 \cdot L)}{4 \cdot \pi \cdot L \cdot z} \cdot r_{soil} \cdot \eta = \frac{r_{soil}^r \cdot \eta}{W_r} \quad (4.4)$$

where  $r$  is root radius,  $L$  is fine root density in the soil,  $z$  is rooting depth and  $r_{soil}$  is soil hydraulic resistivity. Rooting depth is here assumed to increase with fine root biomass, implying a constant value of fine root density in the soil. Soil resistivity per unit root biomass ( $r_{soil}^r$ ) is therefore defined as:

$$r_{soil}^r = -\frac{1}{4} \cdot \ln(\pi \cdot r^2 \cdot L) \cdot r^2 \cdot \rho_r \cdot r_{soil} \quad (4.5)$$

where  $\rho_r$  is the basal density of fine roots and is assumed to be equal to sapwood density.

Soil hydraulic resistivity is a direct function of soil water potential and can be expressed as (Campbell 1985):

$$r_{soil} = r_{soil}^{sat} \cdot \left( \frac{\Psi_{soil}}{\Psi_e} \right)^{2+3/b} \quad (4.6)$$

where the resistivity of saturated soil ( $r_{soil}^{sat}$ ), soil entry potential ( $\Psi_e$ ) and the

empirical coefficient  $b$  are all function of soil texture (Campbell 1985). The coarser the soil, the steeper the relationship of Eq. 4.6 will be.

Experimental evidence (reviewed for *P. sylvestris* in the Results section) suggests that under natural conditions leaf water potential never exceeds a critical value  $\bar{\Psi}$ , which could be dictated in coniferous species by the risk of diffuse xylem embolism and tissue dieback (Tyree & Sperry 1988). The maintenance of such a functional homeostasis imposes a tight constraint on plant allometry, as it requires that hydraulic resistances do not exceed a limit given by (Eq. 4.1-4.4):

$$R_{tot}^f = W_f \cdot \sigma \cdot \eta \cdot \left( \frac{r_r + r_{soil}^r}{W_r} + \frac{h^2 \cdot \rho_s \cdot r_s}{W_s} \right) \leq \frac{\Psi_{soil} - \bar{\Psi}}{E_f} \quad (4.7)$$

This requirement could not be met unless new foliage growth were always supported by an adequate amount of sapwood and fine roots. The allocation of too many resources to conductive tissues, on the other hand, would allow the plant to produce less foliage than can be safely sustained under given environmental conditions, so reducing light interception and gross primary production and eventually resulting in a competitive disadvantage. The principle of optimality (Bloom, Chapin & Mooney 1985) therefore requires that the limit of Eq. 4.7 is not only not exceeded, but exactly met when new growth is allocated among plant organs.

Moreover, the reduction in hydraulic resistance that is needed to sustain new foliage will be achieved at the lowest possible cost, in order to reserve as many resources as possible for foliage growth and so maximize plant fitness (Parker & Maynard Smith 1990). This can be obtained by matching costs and returns of carbon allocation in transport tissues. The investment of carbon in fine roots or sapwood yields to the plant very different functional returns, both because of different hydraulic resistivities and because of the strong effect of plant height on shoot resistance (Eq. 4.2). Moreover, fine roots and sapwood have very different longevities and the cost of production, discounted for turnover, will differ accordingly.

Optimal growth under hydraulic constraints requires that the ratio of marginal

hydraulic returns to marginal annual cost for carbon investment in either roots or sapwood be the same (Case & Fair 1989), i.e.:

$$\frac{\partial R_{tot}}{\partial W_r} \bigg/ \frac{1}{l_r} = \frac{\partial R_{tot}}{\partial W_s} \bigg/ \frac{1}{l_s} \quad (4.8)$$

where  $l_r$  and  $l_s$  are fine root and sapwood longevity, respectively. From Eqs. 2-3, this corresponds to:

$$\frac{r_r + r_{soil}^r}{W_r^2} \cdot \frac{W_s^2}{h^2 \cdot \rho_s \cdot r_s} = \frac{l_s}{l_r} \quad (4.9)$$

After rearranging, Eq. 4.9 predicts a constant balance between sapwood area and fine root biomass, consistent with experimental evidence (Nikinmaa *et al.* 1996):

$$\frac{A_s}{W_r} = \frac{c}{\rho_s} \quad (4.10)$$

where the coefficient  $c$  is a function not only of tissue characteristics, but also of soil resistivity:

$$c = \sqrt{\frac{r_s}{r_r + r_{soil}^r} \cdot \frac{l_s}{l_r} \cdot \rho_s} \quad (4.11)$$

The balance between sapwood area and fine root biomass will therefore depend upon soil textural characteristics and will in general shift towards larger root biomass under dry conditions.

When combined with the general requirement of functional homeostasis of Eq. 4.7, Eq. 4.10 translates in two hydraulic constraints, representing the optimal balance between transpiring foliage and conductive tissues under given environmental conditions:

$$\frac{W_f}{W_r} = \frac{R_{tot}^f}{\sigma \cdot \eta \cdot (r_r + r_{soil}^r)} \cdot \left(1 + h \cdot c \cdot \frac{l_r}{l_s}\right)^{-1} \quad (4.12)$$

$$\frac{W_f}{A_s} = \frac{R_{tot}^f}{\sigma \cdot \eta \cdot r_s} \cdot \left(h + \frac{l_s}{c \cdot l_r}\right)^{-1} \quad (4.13)$$

The allometric balance between  $W_f$  and  $A_s$ ,  $W_r$  can be seen to depend markedly upon tree height, less carbon being allocated to foliage as the stand ages, as discussed in detail in Chapter 2 and 3.

A more complete model, which takes into account the direct effects of tree height on foliage water potential, will be applied henceforth, but the basic constraints captured by Eq. 4.10-4.13 are not significantly altered by this inclusion.

#### 4.2.2 Response of allometry to key environmental parameters

The hypothesis of optimal growth under hydraulic constraints allows us to predict the response of plant functional allometry to key environmental parameters. The effects of temperature, air humidity and soil water potential will be considered here.

Low temperatures are known to reduce dramatically the hydraulic conductance of the soil-plant continuum (Teskey, Hinckley & Grier 1984; BassiriRad, Radin & Matsuda 1991), leading in the short term to a marked reduction in foliage water potential both in agricultural crops (Markhart III *et al.* 1980) and in coniferous trees (Day, Heckathorn & De Lucia 1991). In temperate species, this is mainly the result of the temperature dependence of water viscosity  $\eta$ , which is known to decrease twofold in the range 5-35 °C (Douglas, Gasiorek & Swaffield 1985). The relationship can be well represented as:

$$\eta = \frac{1}{a + b \cdot T} \quad (4.14)$$

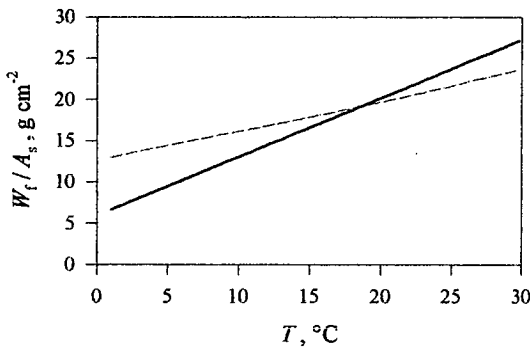
where  $T$  is temperature and  $a$  and  $b$  are empirical parameters. From Eq. 4.13, the



amount of foliage per unit sapwood area is therefore expected to increase linearly with temperature (Fig. 4.1):

$$\frac{W_f}{A_s} \propto \frac{1}{\eta} = a + b \cdot T \quad (4.15)$$

Fig. 4.1 Response of plant allometry to temperature. Simulated response to  $T$  of foliage biomass-to-sapwood area ratio ( $W_f/A_s$ ) when the parallel effects of temperature on air vapour pressure deficit are either neglected (—) or accounted for (---), assuming a constant 50 % relative humidity.



is reduced below its maximum value  $g_s^{\max}$  :

$$g_s = g_s^{\max} \cdot f_D \cdot f_{\Psi} \quad (4.16)$$

where the modifiers  $f_D$  and  $f_{\Psi}$  range in value between 0 and 1 and represent the effects of air vapour pressure deficit and of soil water potential, respectively. According to the Lohammar model (Lohammar *et al.* 1980) the reduction induced by air vapour pressure deficit can be expressed as:

$$f_D = \frac{D_0}{D + D_0} \quad (4.17)$$

The expected impact on plant allometry of air humidity and soil water strongly depends upon the response of transpiration to the plant's environment. Leaf transpiration can be well approximated in conifers by imposed transpiration, the product of stomatal conductance ( $g_s$ ) by air vapour pressure deficit (Whitehead & Jarvis 1981). As a result of air and soil humidity limitations, stomatal conductance

where  $D$  is air vapour pressure deficit and  $D_0$  is the value inducing a 50% stomatal closure. The response to soil water potential can be represented in first approximation by a simple linear function (Jones 1992):

$$f_{\psi} = 1 - \frac{\Psi_{soil}}{\Psi_0} \quad (4.18)$$

where the parameter  $\Psi_0$  represents the soil water potential corresponding to complete stomatal closure. Leaf transpiration can be therefore represented as:

$$E_f \approx g_s \cdot D = g_s^{\max} \cdot \frac{\Psi_0 - \Psi_{soil}}{\Psi_0} \cdot \frac{D_0 \cdot D}{D_0 + D} \quad (4.19)$$

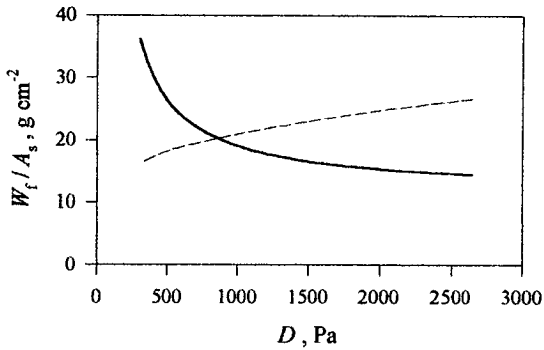
From Eq. 4.7, the hydraulic resistance per unit foliage area that can be safely maintained will decrease asymptotically as air vapour pressure deficit increases, mirroring the response of transpiration captured by Eq. 4.19. This constraint will result in a parallel decline in the amount of foliage supported by a unit sapwood area (Fig. 4.2):

$$\frac{W_f}{A_s} \propto R_{tot}^f \propto \frac{D_0 + D}{D_0 \cdot D} = \frac{1}{D} + \frac{1}{D_0} \quad (4.20)$$

From Eq. 4.10, the balance between foliage and absorbing roots is expected to respond in a completely similar way both to temperature and to  $D$ .

It should be stressed, however, that under natural conditions air vapour pressure deficit is generally not independent of air temperature (Kimball, Running & Nemani 1997). This partial dependence can lead to apparently puzzling results. If, for example, a constant value of relative humidity were to be assumed, a temperature increase would also induce higher vapour pressure deficits, leading to a positive, almost linear rise in transpiration rates. This would partly counterbalance the direct effects of temperature on tree water relations and functional allometry (Fig. 4.1, dashed line). Under this scenario, on the other

**Fig. 4.2** Response of plant allometry to vapour pressure deficit. Simulated response to  $D$  of foliage biomass-to-sapwood area ratio ( $W_f/A_s$ ) when the parallel effects of temperature on air vapour pressure deficit are either neglected (—) or accounted for (---), assuming a constant 50 % relative humidity.



hand, the direct effects of vapour pressure deficit on plant structure would be more than offset by the concurrent change in temperature, as shown in Fig. 4.2. This interaction of temperature and humidity should be kept in mind when interpreting results obtained under field conditions.

In response to soil drought, stomatal closure effectively prevents the onset of extreme leaf water potentials, despite the marked increase in soil-plant

hydraulic resistance that is often reported (Breda *et al.* 1993; Irvine *et al.* 1998). From Eq. 4.7 and 4.19, the maximum resistance that can be withstood by the plant under hydraulic constraints can be expressed as:

$$R_{tot}^f = \frac{\Psi_{soil} - \bar{\Psi}}{E_f} \propto \frac{\Psi_{soil} - \bar{\Psi}}{\Psi_{soil} - \Psi_0} = 1 + \frac{\Psi_0 - \bar{\Psi}}{\Psi_{soil} - \Psi_0} \quad (4.21)$$

If  $\bar{\Psi}$  is more negative than  $\Psi_0$  (as is the case for *P. sylvestris*), stomata will shut completely and  $R_{tot}^f$  will therefore increase in dry soil without triggering substantial cavitation (Fig. 4.3A), in good agreement with experimental evidence. In fine-textured soils, this will increase the amount of foliage that can be safely supported per unit sapwood area or fine root biomass (Fig. 4.3B, C). In coarse soils, however, the parallel increase in soil hydraulic resistivity (Eq. 4.6) will be so steep that plant resistance per unit foliage area will have to be reduced if the hydraulic constraints are to be met. Because of the parallel changes in the balance between sapwood and fine roots (Eq. 4.10) this will result in particular in a higher allocation to fine roots (Fig. 4.3B), as often reported under field

conditions.

### 4.2.3 Growth allocation under hydraulic constraints

When combined with a simple carbon balance model, the hydraulic constraints of Eq. 4.12-4.13 allow us to predict how growth is allocated among plant tissues in response to the environment, resulting in an adaptive model of forest growth.

Stand annual growth  $G$  results from the difference between gross primary production  $A$  and maintenance respiration  $M$ , further reduced for the effects of growth respiration:

$$G = \frac{(A - M) \cdot (1 - c_g)}{c_{DM}} \quad (4.22)$$

where  $c_g$  is a coefficient of growth respiration and  $c_{DM}$  is factor of conversion into dry matter.

Gross productivity can be assumed to be proportional to the cumulated photosynthetic active radiation (PAR) intercepted by the canopy over the year, reduced for the effects of soil water availability (McMurtrie *et al.* 1994):

$$A = \varepsilon \cdot I \cdot \left[ 1 - \exp(-k \cdot \sigma \cdot W_f) \right] \cdot f_\psi \quad (4.23)$$

where  $\varepsilon$  is a light utilization coefficient,  $I$  is annual incoming PAR,  $k$  is a coefficient of light extinction in the canopy. The effect of drought, which is assumed to reduce to the same extent stomatal conductance and assimilation, is captured by the multiplier  $f_\psi$ , as defined in Eq. 4.18. Maintenance respiration of tree components can be assumed to be proportional to tissue biomass:

$$M = m_f \cdot W_f + m_r \cdot W_r + m_s \cdot W_s \quad (4.24)$$

where the coefficients  $m_i$  represent specific maintenance respiration and will be a function of tissue nitrogen content (Ryan *et al.* 1996a). Eventually, the

exponential increase in maintenance respiration with temperature can be represented as (Ryan 1991):

$$m_i = m_i^{20} \cdot Q_{10}^{\frac{T-20}{10}} \quad (4.25)$$

where  $m_i^{20}$  is specific maintenance respiration at the reference temperature of 20 °C and  $Q_{10}$  is a coefficient of respiratory response to temperature.

The biomass of any plant tissue at the end of a growing season ( $W_i^{n+1}$ ) equals the value at the beginning of the year ( $W_i$ ), reduced by occurred mortality and increased by new growth:

$$W_i^{n+1} = W_i \cdot \left(1 - \frac{1}{l_i}\right) + \lambda_i \cdot G \quad (4.26)$$

where  $l_i$  is the average longevity of the tissue and the coefficient of allocation  $\lambda_i$  represents the fraction of  $G$  that is allocated to the compartment. Since growth must be distributed among foliage, sapwood and roots, it will hold:

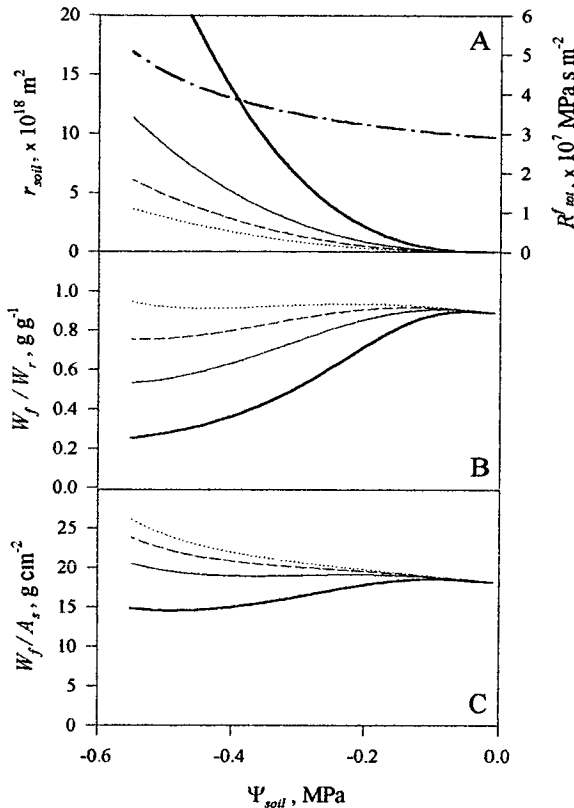
$$\lambda_f + \lambda_s + \lambda_r = 1 \quad (4.27)$$

As already noted, tree height strongly affects the functional allometry imposed by hydraulic constraints (Eq. 4.12-4.13). To model height growth over one year ( $\Delta h$ ), the assumption is made that new foliage production is evenly distributed over the canopy as an horizontal layer of thickness  $\Delta h$  and density  $\rho_f$  (Ludlow, Randle & Grace 1990). A re-analysis of *P. sylvestris* data in Ovington (1957) lends support to this assumption. Height increments can be therefore represented as:

$$\Delta h = (h^{n+1} - h) = \frac{\lambda_f \cdot G}{\rho_f} \quad (4.28)$$

When the hydraulic constraints of Eq. 4.12-4.13, the carbon constraint of Eq.

**Fig. 4.3** Response of plant allometry to soil water potential. A Simulated response to soil water potential  $\Psi_{soil}$  of total resistance per unit foliage area ( $-\cdot-$ ) and soil resistivity at a temperature of 20 °C for a sand fraction ranging from 0.8 ( $---$ ) to 0.2 ( $\cdots$ ), assuming a constant clay fraction of 0.15. Predicted response to  $\Psi_{soil}$  of (B) foliage-to-fine root biomass ratio ( $W_f/W_r$ ) and (C) foliage biomass-to-sapwood area ratio ( $W_f/A_s$ ) for the same range of soil textures.



4.26-4.27 and the height rule of Eq. 4.28 are combined, an analytical solution can be found for the allocation of growth among plant compartments in response to the environment, as outlined in detail in Appendix 2 and 3.

### 4.3 Materials and methods

#### 4.3.1 Test of the hypothesis of functional homeostasis

The hypothesis of functional homeostasis in plant water relations has been tested through a meta-analysis of minimum values of water potential reported in the literature for *P. sylvestris*. Sixteen values could be extracted from eleven papers (Jarvis 1976; Waring, Whitehead & Jarvis 1979; Bengston 1980; Hillerdal-Hagstromer, Mattson-Djos & Hellkvist 1982; Whitehead, Jarvis

& Waring 1984; Beadle *et al.* 1985; Örlander & Due 1986; Pena & Grace 1986; Jackson, Irvine & Grace 1995a, 1995b; Irvine *et al.* 1998), encompassing a large range of conditions from England to Finland and including both seedlings and mature trees. Results from short-term drought experiments on potted seedlings were not considered, because of the extreme and unnatural conditions that are forced upon the plants, leading to extensive cavitation and foliage dieback.

As a test of the hypothesis that minimum water potentials could be limited in conifers by the risk of diffuse xylem embolism, literature values of the critical

water potential for cavitation in *P. sylvestris* were also reviewed. Six values could be derived from five reports; results were variously based on the Sperry technique (Cochard 1992), on the detection of ultrasonic acoustic emissions (UAE) from living material (Pena & Grace 1986; Jackson, Irvine & Grace 1995a, 1995b) or on the gamma radiation technique (Borghetti *et al.* 1991); unpublished results obtained on excised material either by the UAE technique or by gravimetric methods were also used to complement the data-set (Caliari & Grace, unpublished results). Results based on UAE detection in living material are subject to background noise under field conditions. The critical water potential for cavitation was therefore subjectively defined as the value inducing at least 7 counts per minute.

#### 4.3.2 Test of forest growth model

The adaptive forest growth model outlined in the Theory section has been parameterized for *P. sylvestris* and used to explore the response of carbon allocation to selected environmental factors. For illustrative purposes, the model has been run under constant environmental conditions, i.e. neglecting any diurnal or seasonal variability, although the same approach can be extended to more realistic conditions. Baseline conditions are specified in Appendix 1.

Appropriate values for most parameters were either directly measured or derived from the literature, as detailed in Appendix 1. The estimation of fine root characteristics from literature data has been described in Chapter 2.

As a test of general consistency, basic runs of the model have been compared with growth and yield data for *P. sylvestris* growing in Britain (Edwards & Christie 1981), assuming no thinning and an initial spacing of 2 m. In the computation of merchantable volume, a woody biomass of up to 8 kg m<sup>-2</sup> has been assumed for the sum of branches, tree tops, bark and coarse roots. Model predictions have also been compared with structural data from a *P. sylvestris* chronosequence (Mencuccini & Grace 1996).

A more stringent test of model predictions has been based on the comparison of the structure and functionality of two mature Scots pine stands of the same genotype growing under contrasting conditions in Britain presented by

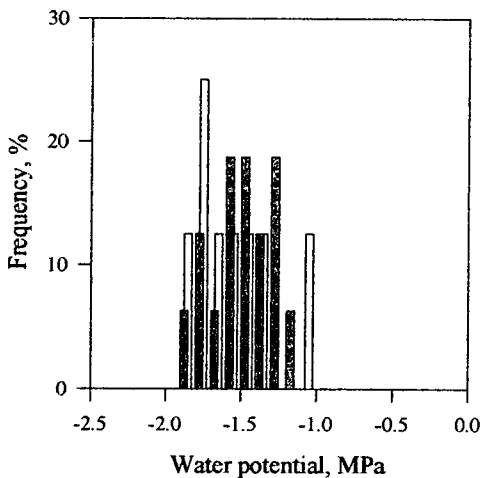
Mencuccini & Grace (1995) and by Jackson *et al.* (1995a). Typical summer values of air temperature and vapour pressure deficit and soil water potential at the study sites, needed to predict the functional allometry of *P. sylvestris* as a function of height, were derived from the same sources.

#### 4.4 Results and discussion

##### 4.4.1 Test of the hypothesis of functional homeostasis

In his review on plant water relations, Passioura (1982) noted that “the hydraulic resistance of a whole plant has often been found to be variable, with a tendency to keep  $\Psi_{leaf}$  constant over a wide range of transpiration rates”. This tendency has

Fig. 4.4 Evaluation of hypothesis of functional homeostasis. Review of literature data of minimum leaf water potential (shaded bars;  $-1.4 \pm 0.2$  MPa, mean  $\pm$  standard deviation,  $n = 16$ ) and critical water potential for cavitation (white bars;  $-1.5 \pm 0.2$  MPa, mean  $\pm$  standard deviation,  $n = 8$ ) in *P. sylvestris*.



been observed on herbaceous plants in response to changes both in air humidity (Tinklin & Weatherley 1966; Stoker & Weatherley 1971) and in root water potential (Macklon & Weatherley 1965), and Boyer (1985) noted that such a pattern is probably associated with growth processes. Subsequently, Whitehead *et al.* (1983) extended this observation to *P. radiata* seedlings acclimated to different air humidity conditions, coming to the conclusion that minimum leaf water potential is conserved irrespective of transpiration rates. This tendency is

confirmed by a review of literature data of minimum water potential in *P. sylvestris* (Fig. 4.4): despite large ontogenetic and environmental differences, data are grouped around a mean value of  $-1.4$  MPa, with a standard deviation of  $0.2$  MPa. This contrasts with the more than three-fold variation observed in  $R_{tot}^f$ , between  $1.6$  and  $4.9 \times 10^7$  MPa s m<sup>-1</sup>.

Two published long-term studies also allow to explore in more detail the



response of minimum water potential to changes in soil water availability under field conditions. Hillerdal-Hangstromer *et al.* (1982) irrigated mature *P. sylvestris* trees for three consecutive seasons, whilst an artificial drought stress was imposed by Irvine *et al.* (1998) over a whole season. In both cases, the effect of drought on daily minimum water potential was not statistically significant.

Tyree and Sperry (1988) suggested that minimum water potentials under field conditions closely match the critical threshold for xylem cavitation. Our meta-analysis of xylem vulnerability in *P. sylvestris* is consistent with this view (Fig. 4.4), suggesting an average water potential threshold of -1.54 MPa; the scatter in the results, however, is quite large (s.d. = 0.3 MPa), both because of the variety of techniques applied and as a result of an intrinsic variability that could have a genetic basis (Vander Willigen & Pammenter 1998).

The consequence of this close agreement is that extensive xylem embolism is uncommon in *P. sylvestris* under field conditions. Waring *et al.* (1979), for example, measured only small changes in xylem water content over a whole season, an observation confirmed by Irvine *et al.* (1998) in artificially droughted plants. An opposite result has been obtained on mature trees by Jackson *et al.* (1995a); most of the reports of extensive xylem cavitation, however, refer to potted seedlings subjected to extreme and rather unnatural drought conditions (Pena & Grace 1986; Borghetti *et al.* 1991; Sobrado, Grace & Jarvis 1992; Jackson, Irvine & Grace 1995b).

Evidence for cavitation avoidance can be found elsewhere. *Abies lasiocarpa*, *Larix laricina*, *Picea glauca* and *Juniperus scopulorum*, for example, all present low values of xylem embolism under natural conditions, in stark contrast with co-occurring broadleaf species (Sperry & Sullivan 1992; Sperry *et al.* 1994). Similarly, Panek and Waring (1995) and Panek (1996) in their analysis of *Pseudotsuga menziesii* stands along a climatic gradient could find significant seasonal changes in sapwood water content at only one out of six sites analyzed. Structural acclimation was also found to have effectively prevented the onset of diffuse embolism in *Abies lasiocarpa* seedlings experiencing a wide range of soil water availability in the field (Douglas, Gasiorek & Swaffield 1985), despite conditions drier than average. Reports, however, are not all consistent. Waring

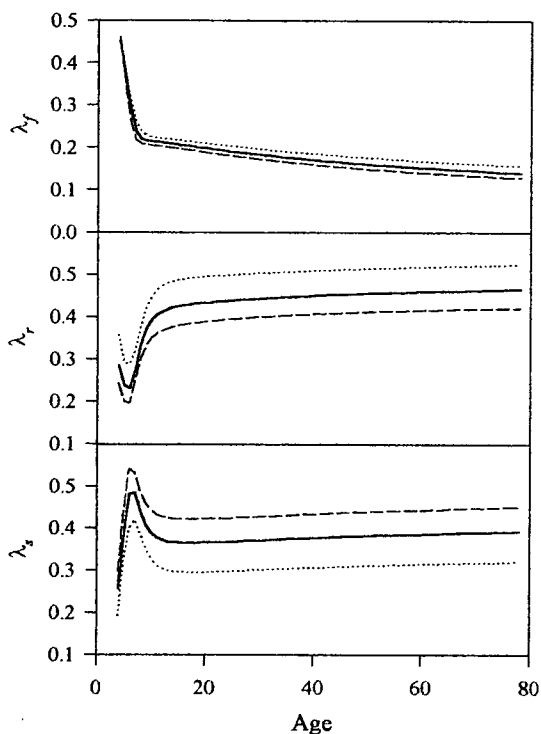


Fig. 4.5 Response of allocation to soil water potential. Developmental changes in carbon allocation to foliage ( $\lambda_f$ ), fine roots ( $\lambda_r$ ) and sapwood ( $\lambda_s$ ) when a constant soil water potential of -0.2 (---), -0.3 (—) or -0.4 MPa (····) is imposed. A soil sand fraction of 0.7 is assumed.

and Running (1978), for example, reported xylem relative water contents in *P. menziesii* down to about 50% and highly variable over the year. A different pattern has also been observed for *P. halepensis* under extremely dry conditions (Borghetti *et al.* 1998).

This strategy of cavitation avoidance is associated with a general lack of drought-induced leaf shedding in conifers. Leaf shedding is an important mechanism of drought resistance, enabling the plant to reduce transpiration and improve the water status of the remaining tissues (Kozłowski 1976). According to Kozłowski (1973), however, leaf shedding during droughts or as a response to hot and dry winds

(“scorching”) occurs more commonly in angiosperms than in gymnosperms. In the specific case of *P. sylvestris*, needle retention is highly variable, but most of this variability has a genetic basis (Pravdin 1964). To what extent it is also affected by environmental conditions and plant water relations is unsure. In the artificial drought experiment described by Irvine *et al.* (1998), however, needle loss was almost identical in droughted and control trees (unpublished results). Additional evidence comes from the study by Jalkanen *et al.* (1994) of needle retention over a period of more than 30 years in Southern England: changes in needle retention were not related to stem radial increments, suggesting that no direct link existed with drought conditions. A comparison of Scots pine trees growing at moist and dry sites in Finland (Jalkanen 1998) also seems to point to the same conclusions.

With all the caveats already discussed, the hypothesis that *P. sylvestris* (and possibly other coniferous species) has evolved a strategy of functional homeostasis and cavitation avoidance seems therefore supported by a strong body of experimental evidence.

Interestingly, the hypothesis seems to underline an important difference between conifers and broadleaves. Although several studies have demonstrated a pattern of hydraulic acclimation to the environment in broadleaf species (Shumway, Steiner & Abrams 1991; Shumway, Steiner & Kolb 1993; White *et al.* 1998), the proposed strategy of functional homeostasis and cavitation avoidance does not apply to this functional type: minimum water potential does largely fluctuate under drought conditions (Breda *et al.* 1993) and diffuse (albeit not destructive) embolism is commonly observed (Sperry *et al.* 1994; Magnani & Borghetti 1995). Foliage dieback under drought conditions has also been often reported (Kozłowski 1976; Tyree *et al.* 1993). Further research will be needed to explore the evolutionary consequences of this divergence.

#### **4.4.2 Implications for stand development**

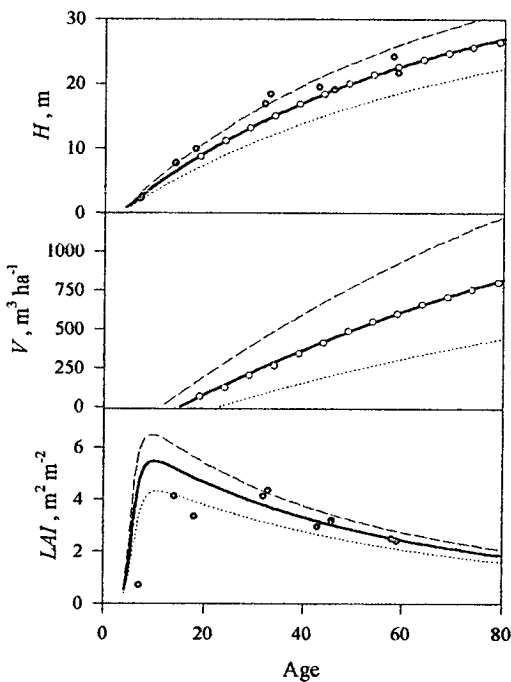
The implications of the hypothesis can be explored using the simple dynamic model described in the Theory section, and compared with available experimental evidence.

Allocation to foliage is predicted to decrease over the lifetime of the stand (Fig. 4.5), contributing to the observed decline in leaf area index (Fig. 4.6). In combination with the continuous rise in allocation to fine roots, this pattern could help explain the decline in above-ground net primary production that is commonly reported in ageing stands (Ryan, Binkley & Fownes 1997; Chapter 2 and 3). This reduced growth rate is the cause of the curvilinear trend of volume and height development that is well captured by model predictions (Fig. 4.6). The parallel agreement of height and *LAI* predictions with experimental data from the *P. sylvestris* chronosequence also lends support to the simple model of height increment of Eq. 4.28.

#### 4.4.3 Response of plant structure to soil water availability

The functional allometry of the plant is variously affected by soil water availability, depending upon soil textural characteristics (Fig. 4.3). In coarse soil, the ratio between foliage and conductive sapwood ( $W_f/A_s$ ) is predicted to decline with decreasing water availability. In *Abies lasiocarpa* seedlings in the Olympic

**Fig. 4.6** Response of stand structure and growth to soil water potential. Developmental changes in height  $H$ , stand cormometric volume  $V$  and leaf area index  $LAI$  when a constant soil water potential of -0.2 (---), -0.3 (—) or -0.4 MPa (····) is imposed. A soil sand fraction of 0.7 is assumed. For illustrative purposes, model results are compared with growth and yield data for *P. sylvestris* growing in Great Britain (○; Edwards & Christie 1981; yield class 12) and with direct measurements from a *P. sylvestris* chronosequence in Thetford Forest, U.K. (●; Mencuccini & Grace 1996).



Mountains, Kuuluvainen *et al.* (1996) did indeed observe significantly lower foliage-to-sapwood area ratios under conditions of soil drought, enough to prevent the onset of diffuse xylem embolism. Much more important, however, is the effect on the functional balance between transpiring foliage and absorbing roots, which is predicted to halve as soil water potential decreases from -0.1 to -0.5 Mpa.

Such a structural acclimation is the result of a marked shift in carbon allocation in response to drought (Fig. 4.5), consistent with experimental observations. Gower *et al.* (1995) reported a shift of allocation from stemwood to fine root production, whilst allocation to foliage was almost unaffected. The apparent paradox of a lower  $W_f/A_s$  despite the decline in  $\lambda_s$  with drought is the result of the parallel reduction in stand height (Fig. 4.6): sapwood production is spread along a shorter length, resulting in higher areal increments.

Axelsson (1986) and Axelsson and Axelsson (1986) also observed a reduced allocation to fine roots in mature *P. sylvestris* trees following irrigation, whilst

the effect on  $\lambda_f$  was very limited. The same effects have been reported for *P. menziesii* by Gower *et al.* (1992), in an analysis of tree response to irrigation, and by Santantonio and Hermann (1985) in their comparison of stands characterized by different water availabilities. These results seem to support the general view, put forward by Santantonio (1987), that as site conditions become less favourable, or as stands mature, resources are increasingly shifted from stemwood to fine root production. This, in combination with the already mentioned reduction in gross primary production, will have a major effect on stand volume increments (Fig. 4.6). On the contrary, the marked reduction in net leaf increments, stand leaf area index and height under drought conditions (Fig. 4.6) are predicted to arise from the drought-induced decline in gross primary production and not from changes in the allocation pattern.

Additional support to the hypothesis comes from the experimental results presented by Irvine *et al.* (1998). In response to an artificial drought, the total hydraulic resistance of *P. sylvestris* trees rooted in a sandy loam increased three-fold, but most of these changes appeared to be located in the soil compartment and all but disappeared upon rewatering. On the contrary, because of the reduction in leaf growth induced by drought, hydraulic resistance per unit foliage area was slightly lower in previously stressed trees. Growth measurements over two growing seasons are consistent with the prediction by the model of a medium-term acclimation to soil water availability in the foliage-to-sapwood area of trees rooted in a coarse soil. Drought resulted in a 21% reduction in needle elongation, but only a 11% reduction in girth increments. The difference was all the more important since current-year needles make up a considerable proportion of stand leaf area, whilst sapwood comprises up to 40 annual increments. The pattern was reversed upon rewatering: on the following year, needle length was reduced in previously droughted plots by 9% only, whilst radial increments were 19% lower than in control plots.

#### 4.4.4 Response of plant structure to air humidity

The dependence of functional allometry upon air vapour pressure deficit and transpiration rates had already been identified by Whitehead *et al.* (1984) and

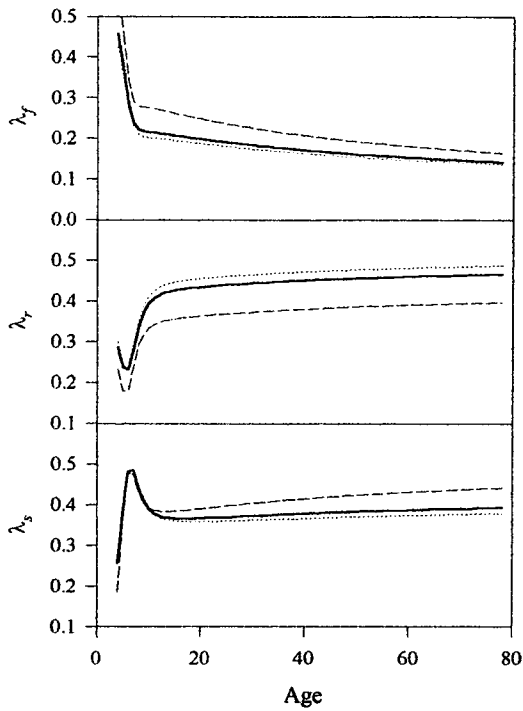


Fig. 4.7 Response of allocation to vapour pressure deficit. Developmental changes in carbon allocation to foliage ( $\lambda_f$ ), fine roots ( $\lambda_r$ ) and sapwood ( $\lambda_s$ ) when a constant vapour pressure deficit of 500 (---), 1500 (—) or 2500 Pa (····) is assumed.

Givnish (1986), who focused on the foliage relationship with sapwood and fine roots, respectively. When the stomatal response to  $D$  is accounted for (Eq. 4.19), foliage-to-sapwood area ratios are predicted to decline asymptotically in dry air, tending to a value about half that at 500 Pa (Fig. 4.2). The same applies to the ratio between foliage and fine roots, in good agreement with the predictions for *Phaseolus vulgaris* by Givnish (1986), also based on optimality theory but moving from wholly different assumptions. High vapour pressure deficits result in an increasingly large allocation to fine roots (Fig. 4.7); above 1500 Pa, however, transpiration and hence carbon allocation appear to be

almost insensitive to air humidity.

Few experimental studies have explicitly considered the effects of air humidity on plant structure. Lower values of total leaf specific conductance were observed by Bunce and Ziska (1998) in *Glycine max* and *Medicago sativa* plants grown under conditions of high vapour pressure deficit; as predicted by the hypothesis of homeostasis in water transport, this structural change was enough to offset the effects of humidity on transpiration rates, so that leaf water potential was not affected by the treatment. Darlington *et al.* (1997), on the contrary, observed a lower allocation to roots in *Picea mariana* and *Pinus banksiana* seedlings grown under high vapour pressure deficit. Coyea and Margolis (1992), finally, found no significant correlation between vapour pressure deficit and foliage-to-sapwood area ratios in *Abies balsamea* stands under field conditions. Available experimental evidence seems therefore insufficient to draw any conclusions in

favour or against the hypothesis proposed.

#### 4.4.5 Response of plant structure to temperature

Because of the effects of temperature on water viscosity, the amount of foliage that can be supported by a unit sapwood area is predicted to increase under warm climates; the effect is only partly counterbalanced by the parallel increase in air vapour pressure deficit and transpiration rates (Fig. 4.1). The functional balance between foliage and absorbing roots would be expected to behave just in the same way. This analysis is based on the assumption of a constant stand height. Under

warmer conditions, however, net primary production and height increments are reduced by respiratory costs. This tends to further redirect growth from sapwood to fine roots: since a constant balance between sapwood area and fine root biomass is expected from Eq. 4.10,  $W_s/W_r$  will change in proportion to tree height.

This explains the allocation pattern predicted by the dynamic model (Fig. 4.8): allocation to fine roots appears almost insensitive to temperature, in contrast with the large change observed in  $\lambda_s$ .

This reduced allocation to sapwood, together with higher tissue respiration and lower stand net primary production (Ryan *et al.* 1996b), contributes to the observed large reduction in stand volume increments under constantly warm conditions (Fig. 4.9).

Experimental studies on herbaceous species have indeed demonstrated higher

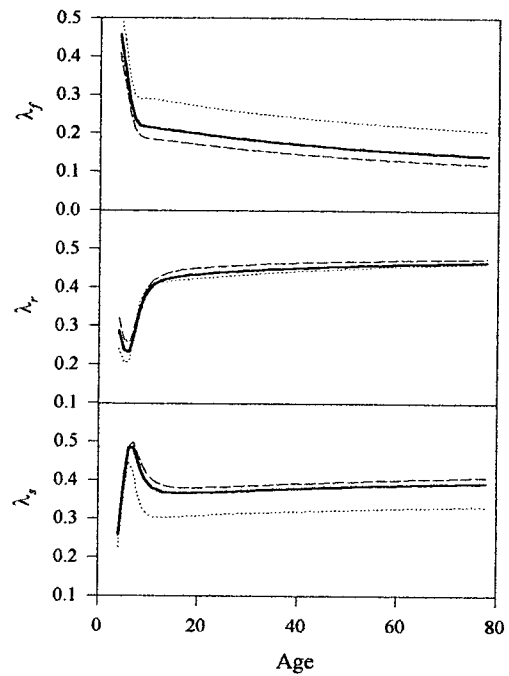


**Fig. 4.8** Response of allocation to temperature. Developmental changes in carbon allocation to foliage ( $\lambda_f$ ), fine roots ( $\lambda_r$ ) and sapwood ( $\lambda_s$ ) when a constant temperature of 5 (---), 10 (—) or 20 °C (····) is assumed. Air vapour pressure deficit is assigned a constant value of 1500 Pa, irrespective of temperature.

**Fig. 4.9** Response of stand structure and growth to temperature. Developmental changes in height  $H$ , stand main volume  $V$  and leaf area index  $LAI$  when a constant temperature of 5 (---), 10 (—) or 20 °C (···) is assumed. Air vapour pressure deficit is assigned a constant value of 1500 Pa, irrespective of temperature.

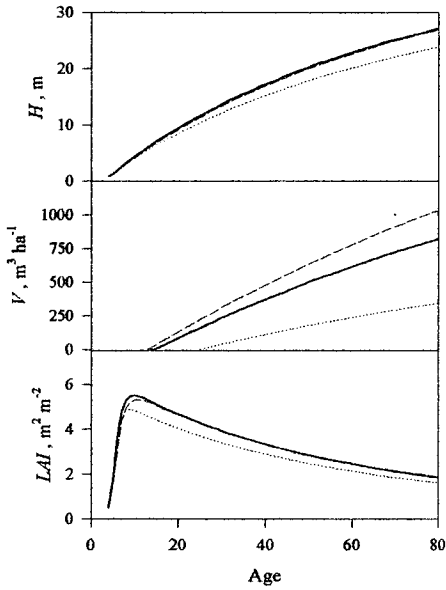
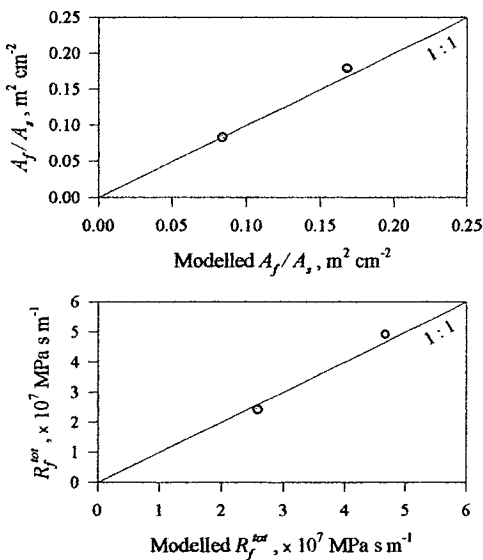


**Fig. 4.10** Response of plant structure and hydraulic architecture to climate. Measured values of foliage-to-sapwood area ratio ( $A_f/A_s$ ; Mencuccini & Grace 1995) and total hydraulic resistance per unit foliage area ( $R_f^{tot}$ ; Jackson, Irvine & Grace 1995) in two mature *P. sylvestris* stands growing in a wet and a dry area of Britain are compared with model predictions.



foliage-to-fine root ratios under warm conditions (Wilson 1988; Markhart III *et al.* 1980). This has been suggested to be the result of a functional balance between foliage assimilation and root nutrient uptake (Cannell & Dewar 1994), assuming a higher sensitivity of root processes to temperature. However, the effect is observed also when shoot temperature only is increased (Wilson 1988); this result runs contrary to the hypothesis of root-shoot functional balance, since the treatment would enhance leaf photosynthesis but not root function, but is well explained by the newly proposed model of optimal growth under hydraulic constraints.

Additional support to the hypothesis comes from the observation that the foliage-to-sapwood area ratio of *P. sylvestris* stands does indeed increase with mean annual temperature along a geographic gradient across Europe (Berninger *et al.* 1995; Berninger & Nikinmaa 1997). The conclusions of this meta-analysis of literature data have been



recently confirmed by Palmroth *et al.* (1999), who directly measured the functional allometry of stands ranging from Spain to Finland. Interestingly, the same pattern could be observed in a *P. sylvestris* provenance trial when average temperatures at the site of origin were considered. This finding seems to suggest that adaptation, rather than acclimation to current environmental conditions, is at work.

#### 4.4.6 Response of plant structure to climate

Under field conditions, the effects of temperature, air humidity and soil water availability are superimposed and jointly determine the response of plant structure and growth to the local climate. Great care should be therefore taken in the analysis of field results. Callaway *et al.* (1994), for example, reported a higher carbon allocation to sapwood in *P. ponderosa* stands under desert, relative to montane, conditions. It is difficult to say, however, whether this was the result of average site temperature (11 and 8 °C, respectively), soil water availability and precipitation (230 and 480 mm yr<sup>-1</sup>) or the higher vapour pressure deficit that is typical of desert climate (Kimball, Running & Nemani 1997). The relative role of contrasting processes can be ascertained, on the contrary, when enough site information is available.

Jackson *et al.* (1995a) and Mencuccini and Grace (1995) compared two *P. sylvestris* stands of the same age and from the same seed source growing under contrasting climatic conditions in Britain. Climate at the two sites differs under many respects. Annual precipitation in Aberfoyle is more than twice that in Thetford (1500 and 650 mm yr<sup>-1</sup>, respectively), although similar predawn water potential values were measured at the two sites. Average July temperature also differs among sites (14.4 and 17.0 °C in Aberfoyle and Thetford, respectively) and much higher values of vapour pressure deficit are commonly found in Thetford. As a result, maximum transpiration per unit foliage area at the dry site exceeded by almost 70% the values measured at the wet site (with values of 5.8 and  $3.4 \times 10^{-8} \text{ m}^3 \text{ m}^{-2} \text{ s}^{-1}$ , respectively; Jackson *et al.* 1995a). Tree functional allometry also differed. Trees in Thetford were taller but had a lower foliage-to-sapwood area ratio ( $A_f/A_s$ ) than in Aberfoyle (Fig. 4.10); besides, hydraulic

resistance per unit foliage area in Thetford was about half the value determined for Aberfoyle. It is worth noting that, since the two stands are genetically uniform, all differences observed are the result of plant acclimation to the environment, contrary to what suggested by the work of Palmroth *et al.* (1999). Clearly, further research is needed to elucidate this important question (Berninger & Nikinmaa 1997).

The differences in functional allometry among the two sites are well explained by

**Table 4.1** Partitioning of differences in  $A_f/A_s$  between Thetford and Aberfoyle among the effects of temperature and water viscosity, tree height and vapour pressure deficit and transpiration rates. Predictions of Eq. 4.13 when only one of the parameters is switched to the Thetford value are compared with the modelled value for Aberfoyle. Also reported is the value predicted for Thetford when all three parameters are changed, as well as observed values at both sites (between brackets).

	$A_f/A_s$ m <sup>2</sup> cm <sup>-2</sup>	% change
Aberfoyle	0.17 (0.18)	
$T$ as in Thetford	0.18	+ 8
$H$ as in Thetford	0.13	- 21
$E_f$ as in Thetford	0.10	- 41
Thetford	0.08 (0.08)	- 50

the model (Eq. 4.7 and 4.13) as a function of temperature and maximum vapour pressure deficit (Fig. 4.10). According to Eq. 4.15, temperature alone would have resulted in a foliage-to-sapwood area ratio about 8% larger at Thetford than at Aberfoyle (Table 4.1). The greater height of *P. sylvestris* trees in Thetford, on the other hand, would have in itself required a 21% reduction in  $A_f/A_s$  (Eq. 4.13); differences in vapour pressure

deficit and foliage transpiration, finally, explain a 41% reduction in  $A_f/A_s$ . All together, the three components well explain the 50% reduction in  $A_f/A_s$  observed at Thetford, relative to Aberfoyle.

#### 4.5 Conclusions

The newly proposed hypothesis of functional homeostasis for water transport in conifers seems to be supported by a large body of experimental evidence. Not only is the observation of a constancy in minimum leaf water potential confirmed by experimental results under a wide range of conditions; the implications of the hypothesis also help explain commonly observed changes in functional allometry

and stand productivity as a function of the environment.

The hypothesis proposed is based on the simple observation of a regularity in plant function. Once implemented into a mathematical model, however, its heuristic value becomes apparent. Plant's potential to acclimate is generally thought to be an important evolutionary feature, enabling long-lived, sessile trees to face the vagaries of the environment (Bradshaw 1965; Scheiner 1993). As a consequence, the new understanding of plant structural acclimation under hydraulic constraints could considerably improve our ability to predict tree and ecosystem response to climate and climate change. To this end, the simple scheme of resource allocation just explored will be thus combined in the next chapter with a more detailed representation of key functional processes and applied to the analysis of growth patterns of Scots pine across Europe.

#### References

- Axelsson B. (1986) Differences in yield at different sites: an irrigation-fertilization study of nutrient flux during fast growth. In *Forest Site and Productivity* (ed. S.P. Gessel), pp. 171-183. Martinus Nijhoff, Dordrecht.
- Axelsson E. & Axelsson B. (1986) Changes in carbon allocation patterns in spruce and pine trees following irrigation and fertilization. *Tree Physiology* **2**, 189-204.
- Ägren G.I. & Ingestad T. (1987) Root:shoot ratio as a balance between nitrogen productivity and photosynthesis. *Plant Cell and Environment* **10**, 579-586.
- BassiriRad H., Radin J.W. & Matsuda K. (1991) Temperature-dependent water and ion transport properties of barley and sorghum roots. *Plant Physiology* **97**, 426-432.
- Beadle C.L., Jarvis P.G., Talbot H. & Neilson R.E. (1985) Stomatal conductance and photosynthesis in a mature Scots pine forest. 2. Dependence on environmental variables of single shoots. *Journal of Applied Ecology* **22**, 573-586.
- Bengston C. (1980) Effects of water stress on Scots pine. *Ecological Bulletins* **32**, 205-213.
- Berninger F., Mencuccini M., Nikinmaa E., Grace J. & Hari P. (1995) Evaporative demand determines branchiness of Scots pine. *Oecologia* **102**, 164-168.
- Berninger F. & Nikinmaa E. (1997) Implications of varying pipe model relationships on Scots pine growth in different climates. *Functional Ecology* **11**, 146-156.
- Bloom A.J., Chapin F.S. & Mooney H.A. (1985) Resource limitation in plants. An economic analogy. *Annual Review Ecology Systematics* **16**, 363-392.
- Borghetti M., Edwards W.R.N., Grace J., Jarvis P.G. & Raschi A. (1991) The

- refilling of embolized xylem in *Pinus sylvestris* L. *Plant Cell and Environment* **14**, 357-369.
- Borghetti M., Cinnirella S., Magnani F. & Saracino A. (1998) Impact of long-term drought on xylem embolism and growth in *Pinus halepensis* Mill. *Trees* **12**, 187-195.
- Boyer J.S. (1985) Water transport. *Annual Review of Plant Physiology and Plant Molecular Biology* **36**, 473-516.
- Bradshaw A.D. (1965) Evolutionary significance of phenotypic plasticity in plants. *Advances in Genetics* **13**, 115-155.
- Breda N., Cochard H., Dreyer E. & Granier A. (1993) Water transfer in a mature oak stand (*Quercus petraea*). Seasonal evolution and effects of a severe drought. *Canadian Journal of Forest Research* **23**, 1136-1143.
- Bunce J.A. & Ziska L.H. (1998) Decreased hydraulic conductance in plants at elevated carbon dioxide. *Plant Cell and Environment* **21**, 121-126.
- Callaway R.M., De Lucia E.H. & Schlesinger W.H. (1994) Biomass allocation of montane and desert ponderosa pine: an analog for response to climate change. *Ecology* **75**, 1474-1481.
- Campbell G.S. (1985) *Soil Physics with BASIC. Transport Models for Soil-Plant Systems*. Elsevier, Amsterdam.
- Cannell M.G.R. & Dewar R.C. (1994) Carbon allocation in trees: a review of concepts for modelling. *Advances in Ecological Research* **25**, 50-104.
- Case K.E. & Fair R.C. (1989) *Principles of Economics*. Prentice-Hall, London.
- Chung H.-H. & Barnes R.L. (1977) Photosynthate allocation in *Pinus taeda*. I. Substrate requirements for synthesis of shoot biomass. *Canadian Journal of Forest Research* **7**, 106-111.
- Cochard H. (1992) Vulnerability of several conifers to air-embolism. *Tree Physiology* **11**, 73-83.
- Coyea M.R. & Margolis H.A. (1992) Factors affecting the relationship between sapwood area and leaf area of balsam fir. *Canadian Journal of Forest Research* **22**, 1684-1693.
- Darlington A.B., Halinska A., Dat J.F. & Blake T.J. (1997) Effects of increasing saturation vapour pressure deficit on growth and ABA levels in black spruce and jack pine. *Trees* **11**, 223-228.
- Day T.A., Heckathorn S.A. & De Lucia E.H. (1991) Limitations of photosynthesis in *Pinus taeda* L. (Loblolly pine) at low soil temperatures. *Plant Physiology* **96**, 1246-1254.
- Dewar R.C., Ludlow A.R. & Dougherty P.M. (1994) Environmental influences on carbon allocation in pines. *Ecological Bulletins* **43**, 92-101.
- Douglas J.F., Gasiorek J.M. & Swaffield J.A. (1985) *Fluid Mechanics*. Longman Scientific, Harlow.
- Edwards P.N. & Christie J.M. (1981) *Yield Models for Forest Management*. Forestry Commission Booklet 48
- Farquhar G.D. & von Caemmerer S. (1982) Modelling of photosynthetic response to environmental conditions. In *Encyclopedia of Plant Physiology. New Series. Vol. 12B. Physiological Plant Ecology II* (eds. O.L. Lange, P.S. Nobel, C.B. Osmond & H. Ziegler), pp. 549-587. Springer Verlag, Berlin.
- Givnish T.J. (1986) Optimal stomatal conductance, allocation of energy between leaves and roots, and the marginal cost of transpiration. In *On the Economy of*

- Plant Form and Function* (ed. T.J. Givnish), pp. 171-213. Cambridge University Press, Cambridge.
- Gower S.T., Isebrands J.G. & Sheriff D.W. (1995) Carbon allocation and accumulation in conifers. In *Resource Physiology of Conifers* (eds. W.K. Smith & T.M. Hinckley), pp. 217-254. Academic Press, San Diego.
- Gower S.T., Vogt K.A. & Grier C.C. (1992) Carbon dynamics of Rocky Mountain Douglas-fir: influence of water and nutrient availability. *Ecological Monographs* **62**, 43-65.
- Helmisaari H.-S. & Siltala T. (1989) Variation in nutrient concentrations of *Pinus sylvestris* stems. *Scandinavian Journal of Forest Research* **4**, 443-451.
- Hillerdal-Hagstromer K., Mattson-Djos E. & Hellkvist J. (1982) Field studies of water relations and photosynthesis in Scots pine. II. Influence of irrigation and fertilization on needle water potential of young pine trees. *Physiologia Plantarum* **54**, 295-301.
- Irvine J. (1998) Water relations of a pine plantation (*Pinus sylvestris* L.) during drought Ph.D. Thesis, University of Edinburgh.
- Irvine J., Perks M.P., Magnani F. & Grace J. (1998) The response of *Pinus sylvestris* to drought: stomatal control of transpiration and hydraulic conductance. *Tree Physiology* **18**, 393-402.
- Jackson G.E., Irvine J. & Grace J. (1995a) Xylem cavitation in two mature Scots pine forests growing in a wet and a dry area of Britain. *Plant Cell and Environment* **18**, 1411-1418.
- Jackson G.E., Irvine J. & Grace J. (1995b) Xylem cavitation in Scots pine and Sitka spruce saplings during water stress. *Tree Physiology* **15**, 783-790.
- Jalkanen R.E., Aalto T.O., Innes J.L., Kurkela T.T. & Townsend I.K. (1994) Needle retention and needle loss of Scots pine in recent decades at Thetford and Alice Holt, England. *Canadian Journal of Forest Research* **24**, 863-867.
- Jalkanen R.E. (1998) Fluctuation in the number of needle sets and needle shed in *Pinus sylvestris*. *Scandinavian Journal of Forest Research* **13**, 284-291.
- Jarvis P.G. (1976) The interpretation of the variations in leaf water potential and stomatal conductance found in canopies in the field. *Philosophical Transactions of the Royal Society of London Series B- Biological Sciences* **273**, 593-610.
- Jones H.G. (1992) *Plants and Microclimate*. Cambridge Univ. Press, Cambridge.
- Kimball J.S., Running S.W. & Nemani R. (1997) An improved method for estimating surface humidity from daily minimum temperature. *Agricultural and Forest Meteorology* **85**, 87-98.
- Komor E. (1994) Regulation by futile cycles: the transport of carbon and nitrogen in plants. In *Flux Control in Biological Systems* (ed. E.-D. Schulze), pp. 153-201. Academic Press, San Diego.
- Kozlowski T.T. (1973) Extent and significance of shedding of plant parts. In *Shedding of Plant Parts* (ed. T.T. Kozlowski), pp. 1-44. Academic Press, New York.
- Kozlowski T.T. (1976) Water supply and leaf shedding. In *Vol. Vol. IV. Water Deficits and Plant Growth* (ed. T.T. Kozlowski), pp. 191-231. Academic Press, New York.
- Kuuluvainen T., Sprugel D.G. & Brooks J.R. (1996) Hydraulic architecture and structure of *Abies lasiocarpa* seedlings in three subalpine meadows of different

- moisture status in the eastern Olympic Mountains, Washington, U.S.A. *Arctic and Alpine Research* **28**, 60-64.
- Larcher W. (1995) *Physiological Plant Ecology*. Springer-Verlag, Berlin.
- Lindroth A. (1985) Canopy conductance of coniferous forests related to climate. *Water Resources Research* **21**, 297-304.
- Lohammar T., Larsson S., Linder S. & Falk S.O. (1980) FAST - Simulation models of gaseous exchange in Scots pine. *Ecological Bulletins* **32**, 505-523.
- Ludlow A.R., Randle T.J. & Grace J.C. (1990) Developing a process-based growth model for Sitka spruce. In *Process Modeling of Forest Growth Responses to Environmental Stress* (eds. R.K. Dixon, R.S. Meldahl, G.A. Ruark & W.G. Warren), pp. 249-262. Timber Press, Portland, Oregon.
- Macklon A.E.S. & Weatherley P.E. (1965) Controlled environment studies of the nature and origins of water deficits in plants. *New Phytologist* **64**, 414-427.
- Magnani F. & Borghetti M. (1995) Interpretation of seasonal changes of xylem embolism and plant hydraulic resistance in *Fagus sylvatica*. *Plant Cell and Environment* **18**, 689-696.
- Magnani F., Centritto M. & Grace J. (1996) Measurement of apoplasmic and cell-to-cell components of root hydraulic conductance by a pressure clamp technique. *Planta* **199**, 296-306.
- Makela A. & Hari P. (1986) Stand growth model based on carbon uptake and allocation in individual trees. *Ecological Modelling* **33**, 205-229.
- Markhart III A.H., Peet M.M., Sionit N. & Kramer P.J. (1980) Low temperature acclimation of root fatty acid composition, leaf water potential, gas exchange and growth of soybean seedlings. *Plant Cell and Environment* **3**, 435-441.
- McMurtrie R.E., Gholz H.L., Linder S. & Gower S.T. (1994) Climatic factors controlling the productivity of pine stands: a model-based analysis. *Ecological Bulletins* **43**, 173-188.
- Mencuccini M. & Grace J. (1995) Climate influences the leaf-area sapwood area ratio in Scots pine. *Tree Physiology* **15**, 1-10.
- Mencuccini M. & Grace J. (1996) Hydraulic conductance, light interception and needle nutrient concentration in Scots pine stands and their relations with net primary productivity. *Tree Physiology* **16**, 459-468.
- Monteith J.L. (1995) A reinterpretation of stomatal responses to humidity. *Plant Cell and Environment* **18**, 357-364.
- Nikinmaa E., Kaipainen L., Mäkinen M., Ross J. & Sasonova T. (1996) Geographical variation in the regularities of woody structure and water transport. *Acta Forestalia Fennica* **254**, 49-78.
- Ovington J.D. (1957) Dry-matter production by *Pinus sylvestris* L. *Annals of Botany* **21**, 287-314.
- Örlander G. & Due K. (1986) Water relations of seedlings of Scots pine grown in peat as a function of soil water potential and soil temperature. *Studia Forestalia Suecica* **175**, 2-13.
- Page J. & Lebens R. (eds) (1986) *Climate in the United Kingdom*. Department of Energy, London.
- Palmroth S., Berninger F., Nikinmaa E., Lloyd J., Pulkkinen P. & Hari P. (1999) Structural adaptation rather than water conservation was observed in Scots pine over a range of wet to dry climates. *Oecologia* **121**, 302-309
- Panek J.A. (1996) Correlations between stable carbon-isotope abundance and

- hydraulic conductivity in Douglas-fir across a climate gradient in Oregon, USA. *Tree Physiology* **16**, 747-755.
- Panek J.A. & Waring R.H. (1995) Carbon isotope variation in Douglas-fir foliage: improving the  $\delta^{13}\text{C}$ -climate relationship. *Tree Physiology* **15**, 657-663.
- Parker G.A. & Maynard Smith J. (1990) Optimality theory in evolutionary biology. *Nature* **348**, 27-33.
- Passioura J.B. (1982) Water in the soil-plant-atmosphere continuum. In *Vol. Vol. 12B. Encyclopedia of Plant Physiology* (eds. O.L. Lange, P.S. Nobel, C.B. Osmond & H. Ziegler), pp. 5-33. Springer-Verlag, Berlin.
- Passioura J.B. (1988) Water transport in and to roots. *Annual Review of Plant Physiology and Plant Molecular Biology* **39**, 245-265.
- Passioura J.B. & Cowan I.R. (1968) On solving the non-linear diffusion equation for the radial flow of water to roots. *Agricultural Meteorology* **5**, 129-134.
- Patrick J.W. (1997) Phloem unloading. Sieve element unloading and post-sieve element transport. *Annual Review of Plant Physiology and Plant Molecular Biology* **48**, 191-222.
- Pena J. & Grace J. (1986) Water relations and ultrasound emissions of *Pinus sylvestris* L. before, during and after a period of water stress. *New Phytologist* **103**, 515-524.
- Persson H. (1980) Death and replacement of fine roots in a mature Scots pine stand. *Ecological Bulletins* **32**, 251-260.
- Pravdin L.F. (1964) *Scots Pine. Variation, Intraspecific Taxonomy and Selection*. Izdatel'stvo "Nauka", Moskva.
- Press W.H., Teukolsky S.A., Vetterling W.T. & Flannery B.P. (1992) *Numerical Recipes in FORTRAN*. Cambridge University Press, Cambridge.
- Roberts J. (1976) A study of root distribution and growth in a *Pinus sylvestris* L. (Scots pine) plantation in East Anglia. *Plant and Soil* **44**, 607-621.
- Roberts J. (1977) The use of tree-cutting techniques in the study of the water relations of mature *Pinus sylvestris* L. *Journal of Experimental Botany* **28**, 751-767.
- Ryan M.G. (1991) A simple method for estimating gross carbon budgets for vegetation in forest ecosystems. *Tree Physiology* **9**, 255-266.
- Ryan M.G., Hubbard R.M., Pongracic S., Raison R.J. & McMurtrie R.E. (1996a) Foliage, fine-root, woody tissue and stand respiration in *Pinus radiata* in relation to nitrogen status. *Tree Physiology* **16**, 333-343.
- Ryan M.G., Hunt E.R., McMurtrie R.E., Agren G.I., Aber J.D., Friend A.D., Rastetter E.B., Pulliam W.M., Raison R.J. & Linder S. (1996b) Comparing models of ecosystem function for temperate conifer forests. I. Model description and validation. In *Global Change: Effects on Coniferous Forests and Grasslands* (eds. A.I. Breymeyer, D.O. Hall, J.M. Melillo & G.I. Ågren), pp. 313-362. J. Wiley, Chichester.
- Ryan M.G., Binkley D. & Fownes J.H. (1997) Age-related decline in forest productivity: pattern and processes. *Advances in Ecological Research* **27**, 213-262.
- Santantonio D. (1990) Modeling growth and production of tree roots. In *Process Modelling of Forest Growth Responses to Environmental Stress*. (eds. R.K. Dixon, R.S. Meldahl, G.A. Ruark & W.G. Warren), pp. 124-141. Timber

Press, Portland.

- Santantonio D. & Hermann R.K. (1985) Standing crop, production, and turnover of fine roots on dry, moderate, and wet sites of mature Douglas-fir in western Oregon. *Annales des Sciences Forestieres* **42**, 113-142.
- Santantonio D. & Santantonio E. (1987) Effect of thinning on production and mortality of fine roots in a *Pinus radiata* plantation on a fertile site in New Zealand. *Canadian Journal of Forest Research* **17**, 928
- Scheiner S.M. (1993) Genetics and evolution of phenotypic plasticity. *Annual Review Ecology Systematics* **24**, 35-68.
- Shinozaki K., Yoda K., Hozumi K. & Kira T. (1964) A quantitative analysis of plant form - The pipe model theory. I. Basic analyses. *Japanese Journal of Ecology* **14**, 97-105.
- Shumway D.L., Steiner K.C. & Abrams M.D. (1991) Effects of drought stress on hydraulic architecture of seedlings from five populations of green ash. *Canadian Journal of Botany* **69**, 2158-2164.
- Shumway D.L., Steiner K.C. & Kolb T.E. (1993) Variation in seedling hydraulic architecture as a function of species and environment. *Tree Physiology* **12**, 41-54.
- Sobrado M.A., Grace J. & Jarvis P.G. (1992) The limits to xylem embolism recovery in *Pinus sylvestris* L. *Journal of Experimental Botany* **43**, 831-836.
- Sperry J.S., Nichols K.L., Sullivan J.E.M. & Eastlack S.E. (1994) Xylem embolism in ring-porous, diffuse porous, and coniferous trees of Northern Utah and interior Alaska. *Ecology* **75**, 1736-1752.
- Sperry J.S. & Sullivan J.E.M. (1992) Xylem embolism in response to freeze-thaw cycles and water stress in ring-porous, diffuse-porous, and conifer species. *Plant Physiology* **100**, 605-613.
- Stoker R. & Weatherley P.E. (1971) The influence of the root system on the relationship between the rate of transpiration and depression of leaf water potential. *New Phytologist* **70**, 547-554.
- Teskey R.O., Hinckley T.M. & Grier C.C. (1984) Temperature-induced change in the water relations of *Abies amabilis* (Dougl.) Forbes. *Plant Physiology* **74**, 77-80.
- Tinklin R. & Weatherley P.E. (1966) On the relationship between transpiration rate and leaf water potential. *New Phytologist* **65**, 509-517.
- Tyree M.T., Cochard H., Cruiziat P., Sinclair B. & Ameglio T. (1993) Drought-induced leaf shedding in walnut. Evidence for vulnerability segmentation. *Plant Cell and Environment* **16**, 879-882.
- Tyree M.T. & Sperry J.S. (1988) Do woody plants operate near the point of catastrophic xylem dysfunction caused by dynamic water stress? Answers from a model. *Plant Physiology* **88**, 574-580.
- Tyree M.T. & Sperry J.S. (1989) Vulnerability of xylem to cavitation and embolism. *Annual Review of Plant Physiology and Plant Molecular Biology* **40**, 19-38.
- Van Bel A.J.E. (1993) Strategies of phloem loading. *Annual Review of Plant Physiology and Plant Molecular Biology* **44**, 253-281.
- Vander Willigen C. & Pammenter N.W. (1998) Relationship between growth and xylem hydraulic characteristics of clones of *Eucalyptus* spp. at contrasting sites. *Tree Physiology* **18**, 595-600.



- Waring R.H. & Running S.W. (1978) Sapwood water storage: its contribution to transpiration and effect upon water and conductance through the stems of old growth Douglas fir. *Plant, Cell and Environment* 131-140.
- Waring R.H., Whitehead D. & Jarvis P.G. (1979) The contribution of stored water to transpiration in Scots pine. *Plant Cell and Environment* 2, 309-317.
- White D., Beadle C., Worledge D., Honeysett J. & Cherry M. (1998) The influence of drought on the relationship between leaf and conducting sapwood area in *Eucalyptus globulus* and *Eucalyptus nitens*. *Trees* 12, 406-414.
- Whitehead D., Edwards W.R.N. & Jarvis P.G. (1984) Conducting sapwood area, foliage area, and permeability in mature trees of *Picea sitchensis* and *Pinus contorta*. *Canadian Journal of Forest Research* 14, 940-947.
- Whitehead D. & Jarvis P.G. (1981) Coniferous forests and plantations. In *Water Deficits and Plant Growth* (ed. T.T. Kozlowski), Vol. 6, pp. 49-152. Academic Press, New York.
- Whitehead D., Jarvis P.G. & Waring R.H. (1984) Stomatal conductance, transpiration, and resistance to water uptake in a *Pinus sylvestris* spacing experiment. *Canadian Journal of Forest Research* 14, 692-700.
- Whitehead D., Sheriff D.W. & Greer D.H. (1983) The relationship between stomatal conductance, transpiration rate and tracheid structure in *Pinus radiata* clones grown at different water vapour saturation deficits. *Plant Cell and Environment* 6, 703-710.
- Wilson J.B. (1988) A review of evidence on the control of shoot:root ratio, in relation to models. *Annals of Botany* 61, 433X-449.

**Appendix 4.1** Variables, parameters and units used in the model. Baseline conditions of soil water potential, air vapour pressure deficit and temperature are also specified.

	<i>Definition</i>	<i>Units</i>	<i>Value</i>	<i>Source</i>
<i>A</i>	stand annual gross primary production	kgC m <sup>-2</sup> yr <sup>-1</sup>		
<i>A<sub>S</sub></i>	sapwood area	m <sup>2</sup> m <sup>-2</sup>		
<i>b</i>	empirical coefficient of soil water retention	-		
<i>c<sub>D</sub></i>	dry-matter conversion factor	kgC kg <sup>-1</sup>	0.5	1
<i>c<sub>g</sub></i>	growth respiration coefficient	-	0.28	2
<i>c<sub>p</sub></i>	specific heat capacity of air	J kg <sup>-1</sup> K <sup>-1</sup>	1012	
<i>D</i>	vapour pressure deficit	Pa	1500	

$D_o$	empirical coefficient for response to D	Pa	600	3, 4
$E_f$	transpiration per unit foliage area	$\text{m}^3 \text{m}^{-2} \text{s}^{-1}$		
$f$	reduction factor (subscript: D, for vapour pressure deficit; $\Psi$ , for soil water potential)	-		
$G$	stand annual growth (subscript: f, foliage)	$\text{kg m}^{-2} \text{yr}^{-1}$		
$g_s$	stomatal conductance	$\text{m s}^{-1}$		
$g_s^{\text{max}}$	maximum stomatal conductance	$\text{m s}^{-1}$	$8 \times 10^{-3}$	3, 4
$h$	stand height (superscript: n+1, after new growth)	m		
$I$	annual incoming PAR	MJ	1750	5
$k$	light extinction coefficient	-	0.5	6
$l_f$	foliage longevity	yr	2.6	7
$l_r$	fine root longevity	yr	0.65	8
$l_s$	sapwood longevity	yr	39	9
$L$	fine root density	$\text{m m}^{-3}$	5000	10
$m$	specific maintenance respiration (subscript: f, foliage; r, fine roots; s, sapwood; superscript: 20, at 20 °C)	$\text{kgC kg}^{-1} \text{yr}^{-1}$		
$M$	stand annual maintenance respiration	$\text{kgC m}^{-2} \text{yr}^{-1}$		
$Q_{10}$	coefficient of respiratory response to T	-	2	11
$r$	fine root radius	m	$2 \times 10^{-3}$	
$r_s$	sapwood resistivity	$\text{m}^{-2}$	$7 \times 10^{11}$	12
$r_r$	root resistivity per unit fine root biomass	$\text{kg m}^{-3}$	$4 \times 10^{14}$	10, 13
$r_{\text{soil}}$	soil resistivity (superscript: sat, saturated)	$\text{m}^{-2}$		
$r_{\text{soil}}^r$	soil resistivity per unit fine root biomass	$\text{kg m}^{-3}$		
$R$	hydraulic resistance (superscript: f, per unit projected leaf area; subscript: plant, root, shoot, soil, total)	$\text{MPa s m}^{-1}$		
$T$	temperature	°C	10	
$W$	stand biomass (subscript: f, foliage; r, fine roots; s, sapwood; superscript: n+1, after new growth)	$\text{kg m}^{-2}$		
$z$	rooting depth	m		
$\gamma$	psychrometer constant	$\text{Pa K}^{-1}$	65	
$\delta$	latent heat of vaporization	$\text{J m}^{-3}$	$2.5 \times 10^6$	
$\varepsilon$	light utilization coefficient	$\text{kgC MJ}^{-1}$	$1.8 \times 10^{-3}$	14
$\eta$	viscosity of water	$\text{MPa s}$		
$\lambda$	allocation coefficient (subscript: f, foliage; r, fine roots; s, sapwood)	-		
$\rho_a$	air density	$\text{kg m}^{-3}$	1.2	
$\rho$	density (subscript: s, sapwood; r, root)	$\text{kg m}^{-3}$	440	6
$\rho_f$	density of foliage in the canopy	$\text{kg m}^{-3}$	0.73	15
$\sigma$	specific leaf area	$\text{m}^2 \text{kg}^{-1}$	4.5	12
$\Psi$	water potential (subscript: e, entry, leaf, foliage; grav, gravitational)	MPa		
$\Psi_{\text{soil}}$	soil water potential	MPa	-0.3	

$\Psi_0$	$\Psi_{soil}$ for complete stomatal closure	MPa	-0.8	16
$\bar{\Psi}$	critical leaf water potential	MPa	-1.4	see text

<sup>1</sup>Larcher (1995), <sup>2</sup>Chung & Barnes (1977), <sup>3</sup>Lindroth (1985), <sup>4</sup>Irvine (1998), <sup>5</sup>Page and Lebens (1986), <sup>6</sup>Mencuccini & Grace (1996), <sup>7</sup>Jalkanen *et al.* (1994), <sup>8</sup>Persson (1980), <sup>9</sup>Helmisaari and Siltala (1989), <sup>10</sup>Roberts (1976), <sup>11</sup>Ryan (1991), <sup>12</sup>Mencuccini & Grace (1995), <sup>13</sup>Roberts (1977), <sup>14</sup>McMurtrie *et al.* (1994), <sup>15</sup>Ovington 1957, <sup>16</sup>Irvine *et al.* (1998)

## Appendix 4.2 Combination of hydraulic, carbon and height constraints

From Eq. 4.28, new foliage production ( $G_f$ ) can be expressed as:

$$G_f = \lambda_f \cdot G = G - \lambda_s \cdot G - \lambda_r \cdot G \quad (\text{A.4.2.1})$$

However, since fine root biomass is constrained by the relationship of Eq. 4.12, the production of new roots can be expressed as:

$$\begin{aligned} \lambda_r \cdot G &= W_r^{n+1} - W_r \cdot \left(1 - \frac{1}{l_r}\right) = \\ &= W_f^{n+1} \cdot \left(\frac{\sigma}{k_r \cdot R_{tot}^u}\right) \cdot \left(1 + h^{n+1} \cdot c \cdot \frac{l_r}{l_s}\right) - W_f \cdot \left(\frac{\sigma}{k_r \cdot R_{tot}^u}\right) \cdot \left(1 + h \cdot c \cdot \frac{l_r}{l_s}\right) \cdot \left(1 - \frac{1}{l_r}\right) \end{aligned} \quad (\text{A.4.2.2})$$

In a completely similar way, from Eq. 4.13, the production of new sapwood can be expressed as:

$$\begin{aligned} \lambda_s \cdot G &= W_s^{n+1} - W_s \cdot \left(1 - \frac{1}{l_s}\right) = \\ &= W_f^{n+1} \cdot \left(\frac{c \cdot h^{n+1} \cdot \sigma}{k_r \cdot R_{tot}^u}\right) \cdot \left(1 + h^{n+1} \cdot c \cdot \frac{l_r}{l_s}\right) - W_f \cdot \left(\frac{c \cdot h \cdot \sigma}{k_r \cdot R_{tot}^u}\right) \cdot \left(1 + h \cdot c \cdot \frac{l_r}{l_s}\right) \cdot \left(1 - \frac{1}{l_s}\right) \end{aligned} \quad (\text{A.4.2.3})$$

Eq. A.4.2.2 and A.4.2.3 capture the implications for plant growth of the hydraulic constraint: the principle of optimality requires that the production of new sapwood and fine roots exactly balances over one year the growth of new leaves. Eq. A.4.2.1 can now be reformulated as:

$$G_f \cdot \frac{k_r \cdot R_{tot}^u}{\sigma} = G - \left[ W_f \cdot \left( 1 - \frac{1}{l_f} \right) + G_f \right] \cdot \left( 1 + \left[ h + \frac{G_f}{\rho_f} \right] \cdot c \cdot \frac{l_r}{l_s} \right) \cdot \left( c \cdot \left[ h + \frac{G_f}{\rho_f} \right] + 1 \right) - W_f \cdot \left( 1 + h \cdot c \cdot \frac{l_r}{l_s} \right) \cdot \left[ c \cdot h \cdot \left( 1 - \frac{1}{l_s} \right) + \left( 1 - \frac{1}{l_r} \right) \right] \quad (\text{A.4.2.4})$$

After rearranging, Eq. A.4.2.4 yields a precise constraint on foliage growth as a function of plant structure and environment:

$$G_f^3 + a_1 \cdot G_f^2 + a_2 \cdot G_f + a_3 = 0 \quad (\text{A.4.2.5a})$$

$$a_1 = W_f \cdot \left( 1 - \frac{1}{l_f} \right) + \frac{\rho_f}{c} \cdot \left( 1 + 2 \cdot c \cdot h + \frac{l_s}{l_r} \right) \quad (\text{A.4.2.5b})$$

$$a_2 = W_f \cdot \left( 1 - \frac{1}{l_f} \right) \cdot \frac{\rho_f}{c} \cdot \left( 1 + 2 \cdot c \cdot h + \frac{l_s}{l_r} \right) + \frac{\rho_f^2}{c^2} \cdot (1 + c \cdot h) \cdot \left( c \cdot h + \frac{l_s}{l_r} \right) + \frac{\rho_f^2 \cdot l_s}{c^2 \cdot l_r} \cdot \frac{k_r \cdot R_{tot}^u}{\sigma} \quad (\text{A.4.2.5c})$$

$$a_3 = W_f \cdot \frac{\rho_f^2}{c^2} \cdot (1 + c \cdot h) \cdot \left( c \cdot h + \frac{l_s}{l_r} \right) \cdot \left( 2 - \frac{1}{l_s} - \frac{1}{l_f} \right) - \frac{\rho_f^2 \cdot l_s}{c^2 \cdot l_r} \cdot G \quad (\text{A.4.2.5d})$$

This cubic equation in  $G_f$  is amenable to an analytical solution, as outlined in Appendix 3. In the dynamic model, a slightly more complex but wholly similar formulation has been applied that takes into account the effects of gravitational potential.

### Appendix 4.3. Analytical solution of cubic equation

An efficient solution for cubic equations is presented by Press *et al.* (1992). Given a cubic equation with real coefficients  $a_1$ ,  $a_2$  and  $a_3$

$$x^3 + a_1 x^2 + a_2 x + a_3 = 0 \quad (\text{A.4.3.1})$$

let us first compute

$$Q = \frac{a_1^2 - 3a_2}{9} \quad (\text{A.4.3.2})$$

$$R = \frac{2a_1^3 - 9a_1 a_2 + 27a_3}{54} \quad (\text{A.4.3.3})$$

If  $R^2 < Q^3$ , then the cubic equation has three real roots. If we define

$$\theta = \arccos\left(\frac{R}{Q^{3/2}}\right) \quad (\text{A.4.3.4})$$

then the three roots are

$$\begin{aligned} x_1 &= -2\sqrt{Q} \cos\left(\frac{\theta}{3}\right) - \frac{a_1}{3} \\ x_2 &= -2\sqrt{Q} \cos\left(\frac{\theta + 2\pi}{3}\right) - \frac{a_1}{3} \\ x_3 &= -2\sqrt{Q} \cos\left(\frac{\theta - 2\pi}{3}\right) - \frac{a_1}{3} \end{aligned} \quad (\text{A.4.3.5})$$

Otherwise, let be

$$G = -\text{sgn}(R) \cdot \left[ |R| + \sqrt{R^2 - Q^3} \right]^{1/3} \quad (\text{A.4.3.6})$$

$$H = \begin{cases} Q/G & (G \neq 0) \\ 0 & (G = 0) \end{cases} \quad (\text{A.4.3.7})$$

In terms of which the single real root is

$$x = (G + H) - \frac{a_1}{3} \quad (\text{A.4.3.8})$$

## Chapter 5. Growth patterns of *Pinus sylvestris* across Europe.

### A functional analysis using the Hydrall model

Nature is, when reflected upon, unity within diversity, union of the manifoldness in form and variety, quintessence of things natural and natural forces, a living whole. The most important result of research on nature therefore is: to discover unity in the manifoldness, to recognize individual discoveries made in the past, to assess these without surrendering to their mass, and, mindful of the unique role of the human species, capture the essence of nature which is hidden under the surface of outward appearances.

Alexander von Humboldt

#### 5.1 Introduction

Forest growth is known to be affected in a complex way by a variety of climatic factors, resulting for every species in large differences in productivity across its natural range. A clear definition not only of what the physical limiting factors are, but also of the mechanisms that are involved is central to our understanding of forest function. Moreover, the analysis of regional patterns of growth could prove a useful tool for the prediction of the future effects of Climate Change on forest productivity (Breymer *et al.* 1996).

Scots pine (*Pinus sylvestris* L.) is the most widely distributed conifer in the world (Boratynski 1991), its range extending to large areas of Europe and Asia. The species extends as far north as 70°N on the Norwegian coast, reaching 37°N at its southern limit in the Sierra Nevada of Spain; the longitudinal range covers most of Europe, spreading over Siberia as far as 138°E.

Although unevenly distributed, Scots pine stands contribute a large proportion of European forests, comprising for example almost 65% of the total forest cover of Finland (Sevola 1998), about 20% of all high forests in the United Kingdom (Christie & Lines 1979) and 9% of the forested area of France (Bazire & Gadant 1991).

A wide variety of environmental conditions is covered within this natural range; this reflects in the large variability in productivity displayed by the species. Christie and

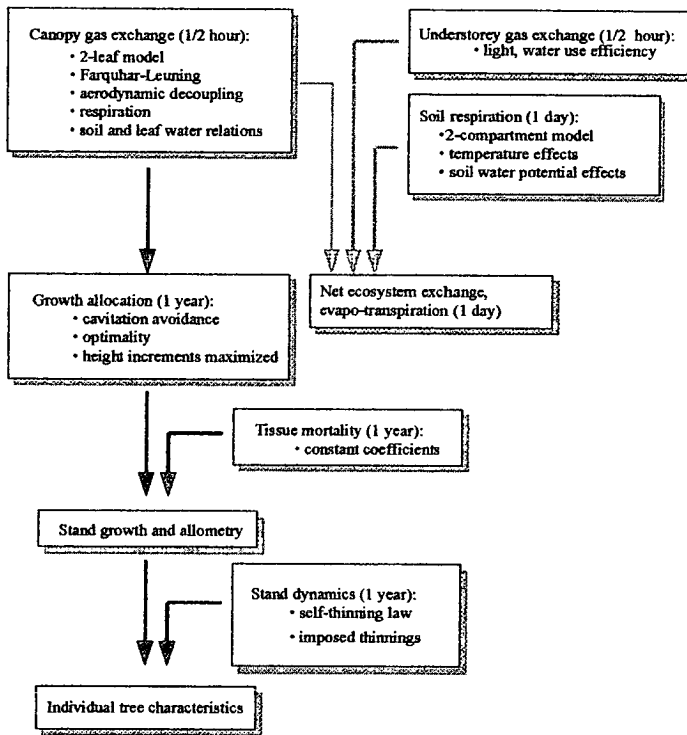
Lines (1979), for example, in a comparison of growth and yield data from several source all around Europe, reviewed national maximum mean annual increments ranging from just above 2 to more than 18 m<sup>3</sup> ha<sup>-1</sup> yr<sup>-1</sup>. Since all these figures refer to optimal fertility conditions at a national level, observed differences could be attributed to purely climatic factors. An interpretation of growth differences in terms of regional climate has been attempted by Ineson *et al.* (1984), who by multivariate statistical techniques identified winter temperature and precipitation as the two key limiting factors for Scots pine growth across Europe.

Such an empirical analysis, however, fails to exploit the understanding of tree and forest function that has been steadily gained over the last decades. Key processes like transpiration, photosynthesis and respiration have been partly dissected in their mechanisms, enabling to successfully predict the response of leaves to most environmental factors (Farquhar, von Caemmerer & Berry 1980; Monteith & Unsworth 1990; Leuning 1995). Moreover, simple schemes have been devised to up-scale leaf gas-exchange to the stand and ecosystem level (Choudhury & Monteith 1988; De Pury & Farquhar 1997; Wang & Leuning 1998), leading to the development of reliable models of canopy function.

The response to the plant environment of other processes such as carbon allocation is still poorly understood, although several approaches have been proposed (Cannell & Dewar 1994; Gower, Isebrands & Sheriff 1995). Recently, the hypothesis has been put forward that observed changes in growth allocation both over the lifetime of the plant (Chapter 3) and in response to the environment could be explained in coniferous species by a common framework, based on the observation of a functional homeostasis in water transport and on the assumption of optimal plant adaptation to a variable environment (Chapter 2 and 4). This hypothesis has been implemented in a detailed model of forest growth, which duly represents the acclimation not only of foliage function, but also of tree structure to the environment. In the present work, the newly developed model will be used to try and explain in detail the geographic variability of Scots pine growth across Europe. The results will highlight the sensitivity of the species to key environmental parameters, laying the ground for the prediction of its response to future Climate Change.

Fig. 5.1 General structure of the Hydrall model. The interconnection between stand function (black arrows) and ecosystem function (gray arrows) is shown. Individual tree characteristics directly result from stand structure and stand dynamics.

*HYDRALL - General model structure*



## 5.2 Model description

The HYDRALL (HYDRaulic constraints on ALlocation) model simulates the growth of a coniferous forest stand over a whole rotation. Key stand and ecosystem processes are nested according to their time constants, as represented in Fig. 5.1. The structure of the model reflects the need to combine realism with the greatest simplicity and generality (Sharpe 1990), focusing on what are believed to be the key determinants of plant growth: light interception and gas

exchange, water relations, growth allocation among functional tissues. All other processes are treated in a simplified way. The representation of stand structure also reflects a need for simplicity. The main focus of the model is on stand function; interindividual differences are therefore neglected, and stand dynamics are only considered for their effects on tissue mortality. Moreover, a specific treatment is given to only two of plant's organs, apart from photosynthesizing foliage: conducting sapwood and absorbing roots are considered in detail because of their role in stand water relations. Because of the strong impact on canopy gas-exchange, on the contrary, great attention is paid to the description of vertical gradients in leaf functional properties.

In comparison with other existing forest growth models, model generality is considerably improved by the recognition that growth allocation among tree organs is



**Table 5.1** Key references for the main components of the Hydrall model.

<b>Light interception</b>	De Pury and Farquhar 1997 Wang and Leuning 1998
<b>Gas exchange</b>	Farquhar <i>et al.</i> 1980 Wang and Leuning 1998
<b>Turnover and growth</b>	Thornley and Johnson 1990
<b>Growth allocation</b>	Magnani <i>et al.</i> , submitted
<b>Respiration</b>	Ryan 1991 Lloyd and Taylor 1994
<b>Stand dynamics</b>	Westoby 1984
<b>Soil carbon dynamics</b>	Andr�n and Paustian 1987 Andr�n and Katterer 1997
<b>Soil characteristic</b>	Campbell 1985

not fixed, but responds dynamically to the environment, resulting in the acclimation of plant's functional structure to local climatic conditions. The hypothesis of functional homeostasis in water transport, described in detail below, constitutes the basis to represent the changes in growth allocation both over the lifetime of the forest and in response to the environment.

The representation of specific processes is based on well established models, as summarized in Table 5.1. A brief description of key model features follows.

### 5.2.1 Light absorption by the canopy

The representation of global radiation absorption by the sunlit and the shaded portion of the coniferous canopy and by the understorey is based on the two-leaf model of Wang and Leuning (1998). The same approach is also used for the computation of absorbed long-wave radiation and foliage isothermal net radiation, a key variable in canopy transpiration. Light scattering and absorption in the visible, near-infrared and long-wave bands are modelled following Goudriaan (1977) and Goudriaan and van Laar (1994). In modelling light scattering, a same value has been assumed for leaf reflection and transmission. An extinction coefficient of direct radiation for non-horizontal black leaves has been computed following Ross (1981), assuming a spherical leaf angle distribution. In the computation of the extinction coefficient of diffuse radiation (Goudriaan & van Laar 1994), Standard Overcast Sky (SOC) conditions have been assumed. Reflection coefficients for visible and near-infrared radiation are also computed following Goudriaan and van Laar (1994), under the simplifying assumption of a common coefficient for the ground and the canopy, as could be expected if the soil is covered by a dense understorey.

### 5.2.2 Vertical functional gradients

Leaf photosynthetic parameters are integrated over sunlit and shaded foliage and adjusted as a function of absorbed photosynthetically active radiation (*PPFD*) and leaf temperature. The up-scaling of photosynthetic properties over the canopy is based on the approach of De Pury and Farquhar (1997). A vertical exponential profile of leaf nitrogen over the canopy is assumed, parallel to the reduction in diffuse *PPFD*, and both dark respiration and maximum carboxylation rate are assumed to be proportional to leaf nitrogen. Whilst the same approach is followed in up-scaling the electron transport of the sunlit big-leaf, the improved procedure proposed by Wang and Leuning (1998) is applied to shaded foliage, whereby the electron transport of a shaded leaf at the top of the canopy is first derived, based on the corresponding value of *PPFD* per unit leaf area, and the value so obtained is then up-scaled to the whole canopy.

### 5.2.3 Aerodynamic decoupling

Whilst the effects of aerodynamic decoupling are most strongly felt in broadleaf canopies (Magnani *et al.* 1998), the gas-exchange of short, dense coniferous forests could also be affected (Shaw & Pereira 1982). Stand aerodynamic conductance is therefore computed iteratively in the model, following Monteith and Unsworth (1990) and Garratt (1992), as a function of wind speed and sensible heat flux from the canopy. The temperature of sunlit and shaded foliage and the sensible heat flux from the canopy are derived from isothermal net radiation and aerodynamic conductance (Jones 1992), assuming an average value of canopy conductance. This simplifying assumption has been demonstrated to result in only minor errors. Appropriate values of zero plane displacement and roughness length as a function of stand leaf area index and height have been derived from Shaw and Pereira (1982). Near-field resistance to heat exchange is integrated over the whole canopy following the approach of Choudhury and Monteith (1988). Canopy aerodynamic conductance is partitioned among sunlit and shaded foliage based on leaf area index.

### 5.2.4 Stand gas-exchange and respiration

The conductance and gas-exchange of sunlit and shaded foliage are computed separately

on a half-hourly basis and summed up to a total value for the canopy. The representation of leaf assimilation is based on the Farquhar model (Farquhar, von Caemmerer & Berry 1980; Farquhar & von Caemmerer 1982), assuming a negligible internal resistance. The effects of temperature on photosynthesis are represented as described therein, whilst the response of leaf assimilation to *PPFD* follows Farquhar and Wong (1984). The dependence of stomatal conductance upon assimilation and air vapour pressure deficit is captured by the Leuning (1995) model, whilst a simple linear dependence of stomatal conductance upon soil water potential is assumed. A summary of key functional parameters and of their value as applied in the model is reported in Appendix 1. The effects of decoupling on leaf temperature, radiative heat dissipation and gas-exchange are also represented by an iterative procedure (Collatz *et al.* 1991). Finally, following Landsberg and Waring (1997), it is assumed that no gas-exchange takes place whenever minimum daily temperature falls below zero.

The respiration of sapwood and fine roots, on the contrary, are computed on a daily basis as a function of average daily temperature, tissue biomass and nitrogen content, as suggested by Ryan (1991). The assumption is made that stem and soil temperature are constant over the day, due to thermal inertia. The empirical model presented by Lloyd and Taylor (1994) is used to represent the dependence of tissue (and soil) respiration upon temperature, instead of the more common  $Q_{10}$  approach, to account for the often observed shift in  $Q_{10}$  with temperature (Breymer *et al.* 1996). Growth respiration, finally, is assumed to be a constant fraction of available carbon (Thornley & Johnson 1990).

### **5.2.5 Understorey gas-exchange and site water balance**

The representation of transpiration and net carbon exchange from a generic understorey is based on the approach proposed by Dewar (1997). The approach is based on the assumption that gas exchange is limited either by maximum potential photosynthesis, proportional to absorbed light, or by maximum potential transpiration, determined by root ability to extract water from the soil, itself a function of soil water content. Water use efficiency (the ratio between carbon and water fluxes) is modulated by both air humidity and atmospheric  $\text{CO}_2$  concentration as described by Jones (1992). The seasonal pattern of understorey foliage and root growth is derived from computed

assimilation, assuming a constant ratio between net and gross primary production (Waring, Landsberg & Williams 1998) and a constant coefficient of allocation to fine roots.

Site water balance is updated every day. Canopy interception is assumed to be a fixed proportion of incoming precipitation, and superficial runoff takes place whenever the water content of the single-layer of soil exceeds soil porosity. Water drainage to a water table at a constant depth of 20 m is represented following Campbell (1985). A rooting depth of 1 m and a soil sand fraction of 0.85 were assumed in all simulations.

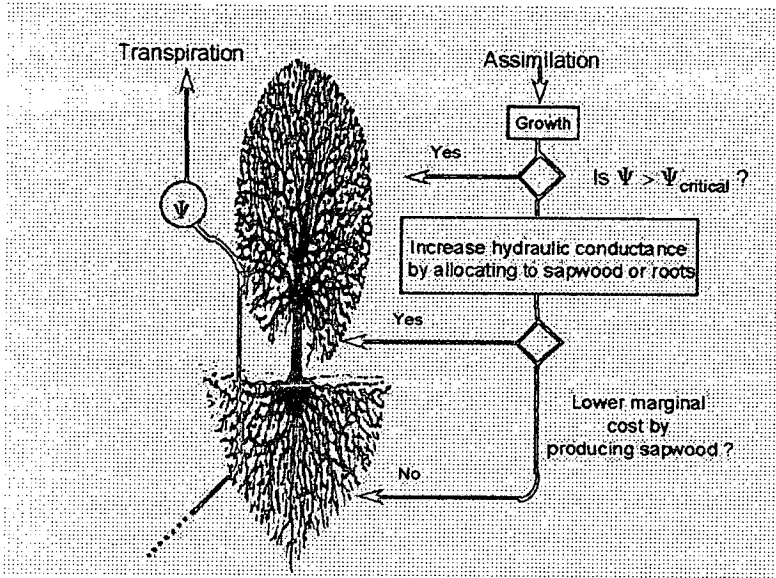
### **5.2.6 Foliage water relations**

The response of foliage water potential to the environment is central to the hypothesis of functional homeostasis in water transport, driving the structural acclimation of the tree to age and climate, as described below. The transport of water through the soil-plant continuum has been therefore modelled in detail as described in Chapter 2 and 4. Leaf water potential is the sum of soil water potential, gravitational potential and frictional potential losses, the product of leaf transpiration by the cumulated hydraulic resistance encountered by water flow across the soil and the plant. Soil water potential is a direct function of soil water content, the exact shape of the water retention curve being a function of soil texture; soil hydraulic resistance is also a function of water content, as well as of fine root density and dimensions (Campbell 1985). Root resistance is known to be inversely related to fine root biomass (Magnani, Centritto & Grace 1996), whilst aboveground resistance is assumed to be a simple function of sapwood basal area and tree height (Whitehead, Edwards & Jarvis 1984). Such a crude formulation has nevertheless been shown to be appropriate in the case of *P. sylvestris* (Chapter 2). The computed values of soil, root and sapwood hydraulic resistance are then adjusted for the effects of temperature on water viscosity.

### **5.2.7 Stand growth and allocation**

An annual time step has been chosen in the representation of tissue turnover and stand growth, a reasonable simplification in evergreen conifers. A fixed proportion of tissue biomass is lost every year through turnover (Makela 1986; Thornley & Johnson 1990). The growth of new tissues is sustained by the sum of stand net primary production over

**Fig. 5.2** Flow diagram illustrating the criteria for growth allocation according to the hypothesis of functional homeostasis in water transport. Allocation to foliage is maximized, as long as it does not induce leaf water potentials exceeding a safety range. Allocation between sapwood and fine roots, according to the principle of optimality, maximizes the return of new hydraulic conductance from carbon investment, so as to free more resources for foliage and height increments.



the year and internal reserves, which are remobilized at the beginning of the growing season and to which a fixed proportion of all available carbon is assumed to be partitioned for next year's growth.

Growth allocation among foliage, sapwood and fine roots is driven by the assumption of optimal plant growth under hydraulic constraints (Chapter 2 and 4). Evolution is assumed to have resulted in an allocation strategy that maximizes plant fitness within the limits

imposed by the species' functional characteristics and by the environment (Parker & Maynard Smith 1990). Height has been chosen as a fitness criterion to be maximized, because of its role in interindividual competition and plant survival in closed canopies. Height increments, however, are considered proportional to the annual production of new foliage in the stand (Ludlow, Randle & Grace 1990); this is equivalent to assuming that most of needle growth is concentrated at the top of the canopy, so that new foliage can be represented as a thin layer of fixed density and of thickness equal to the annual height increment.

The constraints imposed by the environment on foliage production and height increments are depicted in Fig. 5.2. As already discussed, foliage water potential  $\Psi$  results from the interaction of environmental boundary conditions with the hydraulic architecture of the plant, i.e. the balance between transpiring foliage and transport tissues in the shoot and the root system. Were all resources to be allocated to foliage growth, this would result in extremely negative values of leaf water potential over the course of

the year, which would pose a threat to the integrity of the entire system (Tyree & Sperry 1989). Minimum leaf water potential, on the contrary, has been found to be rather constant over a range of environmental conditions and developmental stages, as reviewed for *P. sylvestris* in Chapter 4. If this functional homeostasis is to be maintained, allocation has to favour transport tissues over foliage growth in ageing stands or under stress conditions, as often observed (Axelsson & Axelsson 1986; Mencuccini & Grace 1995; Mencuccini & Grace 1996a). Optimal height growth, on the other hand, requires that resources be allocated among transport tissues in an efficient way, in order to increase hydraulic conductance at the lowest possible carbon cost. An analysis of marginal costs and returns of sapwood and fine roots allocation (Chapter 2 and 4) has demonstrated that this optimal balance is strongly affected both by tree height and by environmental conditions, more carbon being allocated to feeder roots in aging stands and under stress conditions, in good agreement with experimental evidence (Santantonio 1989; Gholz, Linder & McMurtrie 1994).

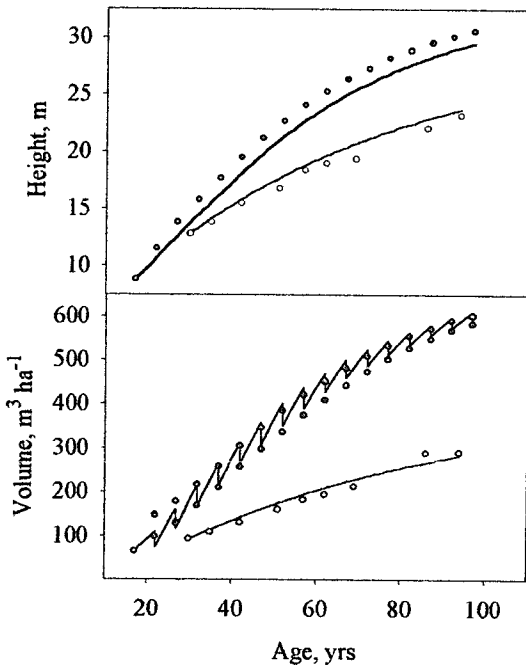
#### **5.2.8 Stand density**

Starting from an imposed stocking density, stand density is progressively reduced either by imposed thinnings or by distance-dependent mortality, represented by the self-thinning law (Westoby 1984). Self-thinning is driven by stand biomass, so as to avoid the positive feed-back that would result if computations were based on average tree characteristics. Both thinnings and mortality are assumed to reduce not only stand volume, but also foliage biomass and other living tissues to the same extent.

#### **5.2.9 Soil carbon dynamics**

Soil carbon dynamics have also been modelled in a simple way. The annual turnover of tree and understorey foliage and fine roots, together with tree mortality, periodically increases the amount of carbon that is stored in soil litter. The two-compartment model of Andrén and Kätterer (1997) has been chosen to represent soil respiration and the transition from young to old soil carbon pools. A constant humification coefficient is assumed. Decomposition of young and old organic matter and humification are affected to the same extent by soil temperature and soil water potential, as captured by the multiplicative model of Andrén and Paustian (1987).

**Fig. 5.3** Test of model predictions. The development of mean height and stand volume predicted by the model for Southeast England (thick line) and Central Finland (thin line) are compared with figures from British Growth & Yield tables (●; Edwards and Christie 1981, YC 14, intermediate thinning) and from Finnish permanent sample plots (○; R. Sievanen, unpublished data). Prescribed thinning was applied in the simulation for SE England, whilst self-thinning only was assumed for the Finnish stand.



### 5.2.10 Weather simulation

Detailed, half-hourly records of key meteorological variables are usually not available at forest sites. The model therefore relies for its input either on standard daily meteorological records or on monthly climatological data (maximum and minimum temperature, precipitation and number of rainy days, heliophany, average wind speed), as provided for the whole of Europe by the LINK data-set (Hulme *et al.* 1995). Daily data are simply derived from the monthly data-set by linear interpolation; in turn, they allow to simulate the diurnal course of all the meteorological variables needed in the model.

Air temperature is derived from daily maximum and minimum temperature as described by Goudriaan and van Laar (1994). An average daily value of

atmospheric transmissivity is obtained from relative heliophany, according to the Angstrom model (Maracchi, Benincasa & Zipoli 1983). Based on this value, instantaneous global radiation and the fraction of diffuse radiation are then computed (Goudriaan & van Laar 1994). Downward long-wave irradiance is derived from air temperature and atmospheric emissivity, which in turn is assumed to be under clear conditions a function of air vapour pressure and temperature, as predicted by the Brutsaert's model (Kustas, Jackson & Asrar 1989). The effect of cloudiness on atmospheric emissivity are represented following Monteith and Unsworth (1990).

Air vapour pressure is assumed to be constant over the day (Goudriaan & van Laar 1994). Dew-point temperature does not coincide with minimum daily temperature under

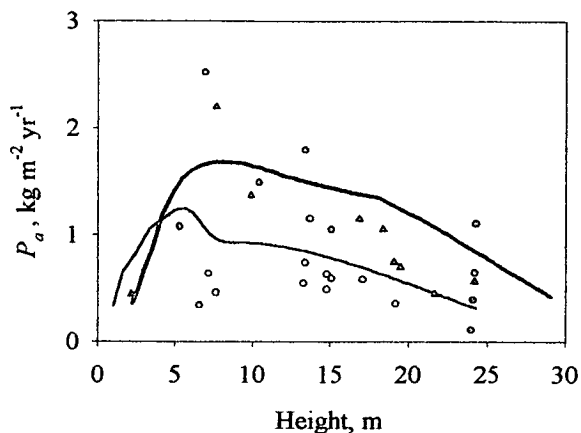


**Fig. 5.4** Test of model predictions. The development of stand above-ground net primary production ( $P_a$ ) predicted by the model for Southeast England (thick line) and Central Sweden (thin line) are compared with experimental data from a Scots pine chronosequence in Thetford Forest, UK (●, Ovington 1957; ▲, Mencuccini and Grace 1996) and from a series of sites around Jädraås, Sweden (○, Albrektson and Valinger 1985).

yield differences commonly observed in the species range. A summary of functional parameters applied in the model is reported in Appendix 1. These correspond to conditions of good nutrient availability, so as to be able to analyze the effects of climate alone. Model results for two locations in Southeast England and Central Finland, respectively, are reported in Fig. 5.3 and compared with predictions from local Growth & Yield tables (Edwards & Christie 1981) and permanent sample plots (Sievanen, unpublished data), respectively. The two stands differ considerably for latitude, climate and applied management regimes; the good agreement between modelled and measured data should be therefore viewed as a strong confirmation of the precision and generality of the model (Sharpe 1990). The systematic error in height predictions at the British site is partly explained by the fact that average stand height, as predicted by the model, is compared with tabulated values of top height.

Additional support for the model comes from a comparison (Fig. 5.4) with literature data of annual aboveground net primary production ( $P_a$ ) from a Scots pine chronosequence in Thetford Forest (Sussex, UK; Ovington 1957, Mencuccini and Grace 1996b) and from a series of sites around Jädraås (Sweden; Albrektson and Valinger 1985). Since the

dry conditions, but is computed as described by Kimball *et al.* (1997). Instantaneous vapour pressure deficit is then obtained as the difference from saturated air humidity, derived from the Teten's equation (Jones 1992).

### 5.3 Model results

The model has been parameterized for *P. sylvestris* and tested against growth and functional data corresponding to different conditions across Europe, then applied to simulate Scots pine growth along two regional transects and to explain



**Table 5.2** Sensitivity of selected growth variables to key environmental factors. Percentage changes in stand height ( $H$ ) and total volume at 100 years ( $V_{tot}$ ), average gross ( $GPP$ ) and net primary production ( $NPP$ ) and fraction allocated to fine root production ( $\lambda_r$ ) as a result of imposed changes in air temperature and precipitation. Sensitivity  $S$  is defined as:

$$S = \frac{O_1 - O_0}{O_0} \cdot 100$$

where  $O_0$  and  $O_1$  are model output under reference and changed conditions.

	$H$ %	$V_{tot}$ %	$GPP$ %	$NPP$ %	$\lambda_r$ %
Temperature + 2 °C	- 5.2	- 6.7	3.2	- 1.5	7.6
- 2 °C	- 8.6	- 21.4	- 22.7	- 19.0	- 0.4
Precipitation + 10 %	1.0	1.5	- 0.4	- 0.6	- 3.1
- 10 %	- 2.4	- 2.4	0.6	1.1	4.6

management history of the stands was not known, a high initial stocking density and no artificial thinning were assumed in the model simulations, partly explaining differences in  $P_a$  dynamics; both the age-related decline in productivity and the marked difference in  $P_a$  between the two locations, however, are well captured by the model.

Temperature and water availability are among the main limiting factors for plant growth on a regional scale. The sensitivity of model predictions to a temperature change of  $\pm 2$  °C and to a  $\pm 10$  % shift in precipitation has been therefore analyzed in detail (Table 5.2), taking the climate of Southeast England as a reference, so as to be able to interpret any differences observed along the European transects. Both height and total volume are negatively affected by a temperature change in either direction, but for different reasons: warming, on the one hand, would beneficially affect canopy photosynthesis, but because of the direct effect on respiration a slight reduction in net primary production would be expected. Moreover, allocation to fine roots is predicted to increase under warmer conditions, leading to an overall reduction in aboveground increments. Colder conditions, on the other hand, would mainly result in lower gross primary production, whilst only marginal changes in respiration and carbon allocation are predicted. Starting from the relatively mild British conditions, precipitation changes are predicted to have a relatively minor effect on growth, mainly the result of a shift in the allocation pattern. Moving from this general understanding, it is now possible to analyze the growth of Scots pine along two climatic gradients across Europe, spanning much of its natural range. Two regional transects have been identified (Fig. 5.5), exploring a latitudinal

**Fig. 5.5** Location of sites considered in the simulation. The range of sites encompasses a latitudinal transect from Northern Finland to Southern Germany, as well as a longitudinal transect from South-east England to Romania.

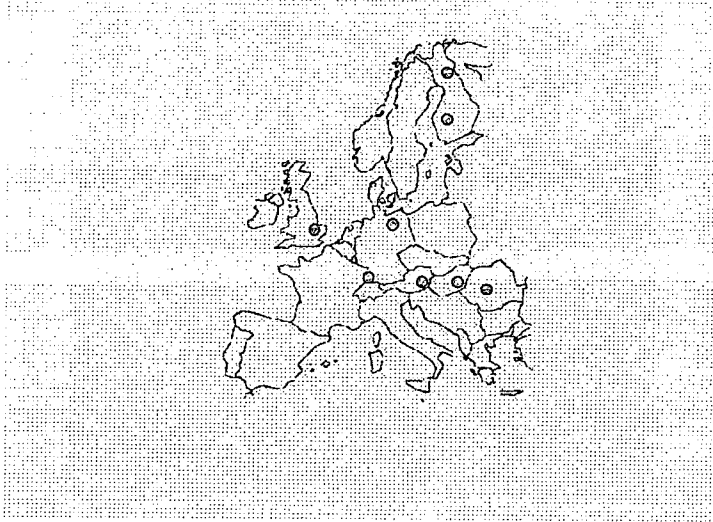


**Table 5.3** Location of sites considered in the simulation and key climatic characteristics: average annual temperature, July temperature, annual precipitation ( $P$ ), the ratio between potential evapotranspiration ( $PET$ ) and precipitation and maximum forest transpiration predicted by the Hydrall model ( $E$ ). Potential evapotranspiration is based on the Priestley and Taylor model, assuming an average net longwave irradiance of  $60 \text{ W m}^{-2}$ .

	Latitude	Longitude	Annual $T$	July $T$	$P$	$PET/P$	$E$
			$^{\circ}\text{C}$	$^{\circ}\text{C}$	$\text{mm yr}^{-1}$	-	$\text{mm yr}^{-1}$
N Finland	$67^{\circ} 15'$	$29^{\circ} 15'$	- 1.9	10.0	524	0.45	215
S Finland	$62^{\circ} 15'$	$24^{\circ} 15'$	3.2	14.1	503	0.69	258
N Germany	$53^{\circ} 15'$	$13^{\circ} 15'$	8.6	16.0	535	1.16	331
E England	$52^{\circ} 15'$	$0^{\circ} 45'$	9.1	14.0	564	0.94	359
S Germany	$47^{\circ} 15'$	$7^{\circ} 15'$	10.4	17.6	963	0.74	433
Austria	$47^{\circ} 15'$	$15^{\circ} 15'$	9.0	17.4	715	1.04	406
Hungary	$47^{\circ} 15'$	$21^{\circ} 15'$	10.3	18.7	481	1.83	337
Romania	$46^{\circ} 15'$	$24^{\circ} 15'$	9.5	18.0	476	1.72	341

gradient from Northern Finland to Southern Germany and a longitudinal one from the maritime climate of England to the more dry and continental climate of Romania, at the south-eastern limit of the species range. A list of the sites and of their key climatic characteristics, as derived from the LINK database (Hulme *et al.* 1995), is reported in Table 5.3. At all sites, climatic characteristics correspond to the lowest elevation in the data-base. A very high initial stocking density of  $5 \times 10^4$  trees  $\text{ha}^{-1}$ , as would be expected in a naturally regenerating stand (Ovington 1957), and no artificial thinning was assumed throughout, so as to neglect any national differences in management regimes.

When values of stand height and total (standing plus self-thinned) volume after 100 years are compared, a rather clear picture emerges (Fig. 5.6), with a marked decline in final height and even more in total volume moving northwards and eastwards. The lowest volume increments are predicted at the northern limit of the range (50 % of the maximum, corresponding to Southeast England), while modelled values for Romanian stands at the southeastern extreme are

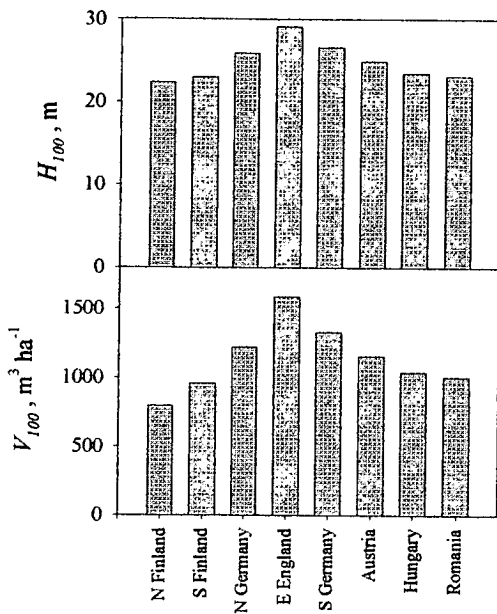


Fig. 5.6 Simulated height ( $H_{100}$ ) and total volume at age 100 ( $V_{100}$ ) for a range of sites along two latitudinal and longitudinal transects across Europe.

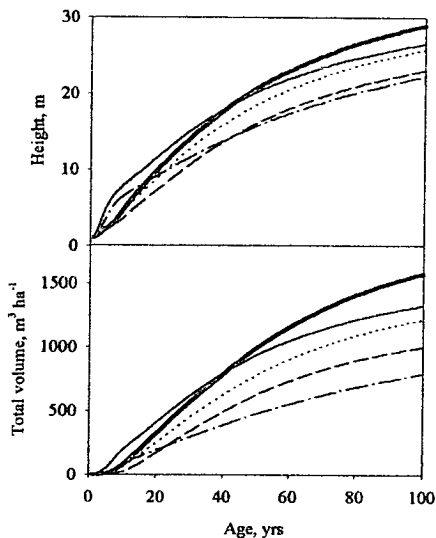


Fig. 5.7 Simulated development of stand height and total volume for a range of sites across Europe. Results are reported for Southeast England (continuous thick), Northern Finland (dash-dot), Northern Germany (dotted), Southern Germany (continuous thin) and Romania (dashed line).

still 63 % of the maximum. Differences between sites are not limited to final values but involve the dynamics of height and volume growth (Fig. 5.7).

The relationship between height and total volume increments is known to be rather constant at any particular site (Eichorn 1904), but quite variable at the regional scale, possibly as a result of climatic differences (Christie & Lines 1979). This variability is captured by the model, as shown in Fig. 5.8: the slope of the relationship is highest at the most productive sites, since total volume production is more strongly reduced than height under limiting environmental conditions (Fig. 5.6).

Contrasting processes seem to be involved in the response of forest growth to limiting conditions under different climates, as shown in Fig. 5.9. When figures are normalized to optimum values, it can be seen that at the northern limit of the range the reduction in gross primary production (-53 %) exceeds the corresponding value for growth (-50 %; Fig. 5.6), as low temperatures also reduce the proportion of available carbon that is lost through respiration. The opposite is true at the dry limit of the range, where a 26 % reduction in *GPP* translates in a 36

% decline in growth rates. In this case the discrepancy is the result not of respiration differences, but of higher belowground allocation (+ 13 %).

#### 5.4 Discussion

Both the dynamics of forest growth and the response to widely different environmental conditions are well captured by the model (Fig. 5.3 and 5.4), as already discussed in Chapter 2 and 4. Current annual increments culminate around the age of 30 at the British site, thinnings resulting in a more prolonged plateau. It is interesting to note that also the response of stand growth to thinning appears to be well represented. Despite the step decline in stand foliage biomass, because of the reduced self-shading light interception and photosynthesis are reduced less than respiration, which on the contrary is strictly proportional to tissue biomass. Moreover, carbon allocation to fine roots is also reduced by thinning (data not shown), probably because of the effects on transpiration and site water balance. Santantonio and Santantonio (1987) reported a very limited effect of thinning on allocation in *Pseudotsuga menziesii* under moist conditions. No reports could be found on the contrary of the effects at a site limited by water availability.

Another remarkable feature of the model is that no culmination in stand height is predicted. This is a direct consequence of the simple rule imposed for height growth, which would continue until the death of the stand, albeit at an increasingly reduced pace. Although in contrast with what generally assumed in empirical forest growth models (Vanclay 1994), this observation is in good agreement with direct experimental observations, as discussed by Robichaud and Methven (1993).

Scots pine seems to find near-optimal conditions in the English climate (Christie & Lines 1979). It is therefore not surprising that, according to the sensitivity analysis reported in Table 5.2, growth would be reduced at this site both by an increase and by a decrease in temperature, although by different mechanisms. Cold temperatures would mainly impair photosynthesis and net carbon exchange, whilst a climate warming would result in higher vapour pressure deficits, inducing higher transpiration rates and eventually resulting in a higher allocation belowground. This apparent sensitivity to water stress is confirmed by the response to changes in precipitation (Table 5.2) and is consistent with the conclusions by White (1982) that variations in *P. sylvestris* productivity in Great Britain are associated primarily with changes in solar radiation and

**Fig. 5.8** Simulated total volume production-height curves for a range of sites across Europe. See Fig. 6 for legends.

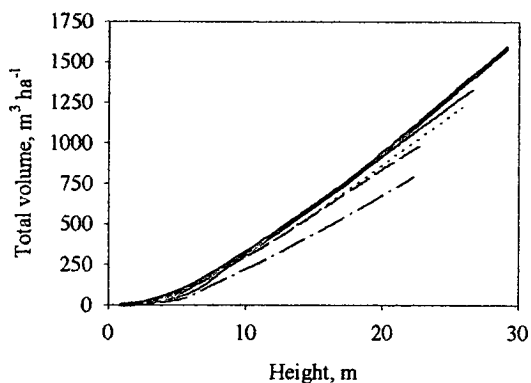
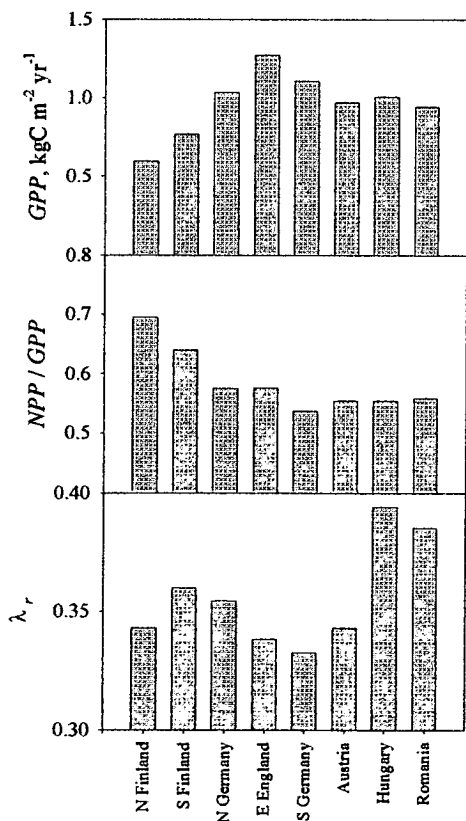


**Fig. 5.9** Simulated determinants of stand growth for a range of sites along two latitudinal and longitudinal transects across Europe. Mean values over 100 years of stand gross primary production (GPP), the ratio between net- and gross primary production ( $NPP / GPP$ ) and the fraction of growth allocated to fine root production ( $\lambda_r$ ) are reported.



soil water balance.

The predicted response to temperature, on the contrary, contradicts the suggestion by Cannell *et al.* (1989) that a 3 °C warming could result in a growth increase as high as 54% under British conditions. This prediction, however, was derived from an analysis of growth sensitivity to temperature under boreal conditions and the authors warned that the response to temperature could flatten off at a July temperature of 15 °C. Present results suggest that the relationship could be even reversed at higher temperatures.

A key role of low temperatures at the boreal (as well as at the altitudinal) limit (Grace 1988) and of water availability in the southern part of the range (Oberhuber, Stumböck & Kofler 1998) is confirmed by the site comparison across European transects. The sites considered encompass much of the natural range of the species in Western Europe (Boratynski 1991), covering a wide interval of latitude, temperature and water availability

(Table 5.3). Simulation results are in good agreement with the conclusions of Ineson *et al.* (1984), who studied the productivity of Scots pine across Europe. From a re-analysis of a data-set of 18 *P. sylvestris* stands throughout Europe (Cannell 1982) by principal component analysis (PCA), they found that almost 50% of the variability in productivity was explained by the first eigenvalue, related to temperature, whilst an additional 26% was associated to the second PCA axis, related to precipitation. Once referenced to the climate of Europe, their results show a good agreement with the pattern resulting from the present paper.

The results are only partly confirmed, on the contrary, by the review of *P. sylvestris* growth and yield tables across Europe presented by Christie and Lines (1979): height increments are quite similar across most of the temperate zone, but markedly lower in the boreal zone. Even larger differences are observed when volume increments are considered. On the other hand, the growth decline at southern and eastern locations predicted by the model is not apparent in growth and yield tables. This probably stems from the fact that simulations always refer to lowland sites, whilst *P. sylvestris* in these regions is more commonly found (and generally planted) at higher elevations and under moister conditions. The delayed rise and subsequent fall of height and volume increments under more maritime conditions (Southeast England, Northern Germany; Fig. 5.7), on the contrary, is confirmed by the results in Christie and Lines (1979). More simulations and experimental observations would be needed, however, to confirm this trend.

The use of a functional model makes it possible not only to predict, but also to understand the mechanisms behind such changes in forest productivity. Stand aboveground net primary production (and stand current annual increment, which is closely related to  $P_a$ ) is the result of three processes, acting in series: stand gross primary production ( $GPP$ ) is reduced by respiration to net primary production ( $NPP$ ) which is allocated above- and belowground. In mathematical terms:

$$ANPP = GPP \cdot \frac{NPP}{GPP} \cdot (1 - \lambda_r) \quad (5.1)$$

where  $\lambda_r$  represents the fraction of  $NPP$  allocated belowground. The three component

factors in which productivity has so been partitioned are affected in different ways by climatic conditions across Europe, as visualized in Fig. 5.9. Simulated gross primary production reaches its maximum at the British site and is elsewhere reduced by low temperatures and a short vegetative period, on the one hand, and by low air and soil humidity (as captured by the increasing  $PET/P$  values in Table 5.3) on the other. The ratio between net and gross net primary production, in turn, is quite constant across all of the temperate region and only increases in the boreal zone, reflecting the pattern of annual mean temperature. Under dry conditions, on the contrary, aboveground productivity is most seriously hampered by the need to allocate increasing amounts of resources to fine root production and maintenance.

The potential relevance of tree structural acclimation for forest growth under dry conditions has already been stressed by Berninger and Nikinmaa (1997), who considered in their simulations only potential changes in foliage-to-sapwood area ratio. In analogy with Hydrall predictions, they suggested that a strong reduction in volume increments at the southern limit can only be explained by climate-induced changes in tree functional structure. An additional increase in carbon allocation belowground, as predicted by the Hydrall model, could have even more important effects, because of the fast turnover rate of fine roots (Persson 1980; Schoettle & Fahey 1994).

Such changes in allocation, however, although of utmost importance under dry conditions, have only a minor and not so clear effect when other climates are considered. This explains why they have been generally neglected in forest growth models, traditionally applied to boreal or temperate moist conditions (Ågren *et al.* 1991; Breymeyer *et al.* 1996). Explicit consideration of structural acclimation, on the other hand, appears to extend the generality of the Hydrall model to a wider range of environments.

How general is the model, anyhow? Two important questions remain unanswered. First of all, it remains to be ascertained whether an optimal functional structure is achieved through long-term adaptation or medium-term acclimation. In other words, have local provenances tuned their structure to long-term local climatic conditions, or has the species evolved a strategy of constant adjustment to a variable climate? In the first case, any provenance should be viewed as an ecotype, that would fail to accommodate to any future changes, and model generality would be limited to geographic comparisons, but

would not extend in time (Berninger & Nikinmaa 1997). Much available experimental evidence (Axelsson & Axelsson 1986; Mencuccini & Grace 1995) suggests that acclimation is at work, on the contrary, implying that evolution under ever-changing environmental conditions has resulted in an optimal strategy of structural adjustment. The results of Palmroth *et al.* (1999), on the other hand, seem to point in the opposite direction. Moreover, it is well known from provenance trials that a considerable proportion of the variability in productivity across the range of the species is the result of long-term genetic differentiation (Giertych 1991).

On the other end of the spectrum, it has to be seen to what extent the conclusions reached for *P. sylvestris* also apply to other species and functional types. In this view, it is interesting to note that the pattern of forest productivity predicted by the Hydrall model mirrors the results for Europe of the empirical model of Paterson (1956), who correlated maximum forest productivity for a large number of species with summary climatic statistics. This seems to suggest that, irrespective of the species considered, the same basic processes are at work in determining the response to climate of forest ecosystems.

## 5.5 Conclusions

The results presented demonstrate the general ability of the Hydrall model to represent the growth of Scots pine over a wide range of climatic conditions. A thorough test of the model is a necessary step in model evaluation, in order to build confidence in its structure and predictions, and further tests of Hydrall results against eddy-covariance as well as long-term growth data are under way.

A process growth model, however, should not be judged solely from its agreement with field observations. An even better representation of experimental data can often be obtained from empirical models, as generally in use in the forestry sector. Functional models, on the other hand, have the twofold advantage of providing understanding, rather than mere representation, and of producing as a result reliable predictions of the response of the system to novel untested conditions.

As a pre-condition, the model must be based on our best understanding of individual processes one level down in the hierarchical scale, for which more refined information is available from controlled experiments. Chapters 2-4 have indeed provided this



background of general information for the core of the Hydrall model, its allocation routine, lending additional support to the predictions presented here.

Changes in resource allocation have resulted most relevant under warm and dry conditions. A correct representation of plant structural acclimation appears therefore crucial if the applicability of process growth models is to be extended to continental and Mediterranean climates. Moreover, it could prove important in the prediction of the effects of climate change, which could release the limitations presently induced by low temperatures and result at the same time in higher values of potential evaporation.

Two problems must be overcome, however, before the model can be applied to produce reliable predictions of the impact of climate change on coniferous forests. As already discussed, more research is needed to ascertain the role of acclimation and long-term adaptation in the response of plant structure to the environment. At the same time, novel methods should be devised to determine the value of highly sensitive functional parameters, such as the hydraulic properties of the roots, for which only scant experimental evidence is presently available. The last issue will be the subject of the next chapter.

### Acknowledgements

I gratefully thank the Climate Impacts LINK Project, UK Department of the Environment, Transport and the Regions (Contract Reference EPG 1/1/68) for producing the gridded climatology for Europe and Dr. R. Sievanen, Finnish Forest Research Institute, for providing the permanent plot data from the Vilppula site.

### References

- Ågren G.I., McMurtrie R.E., Parton W.J., Pastor J. & Shugart H.H. (1991) State-of-the-art of models of production-decomposition linkages in conifer and grassland ecosystems. *Ecological Applications* 1, 118-138.
- Albrektson A. & Valinger E. (1985) Relations between tree height and diameter, productivity and allocation of growth in a Scots pine (*Pinus sylvestris* L.) sample tree material. In *Crop Physiology of Forest Trees* (eds. P.M.A. Tigerstedt, P. Puttonen & V. Koski), pp. 95-105. University of Helsinki, Helsinki.
- Andrén O. & Kätterer T. (1997) ICBM: the introductory carbon balance model for exploration of soil carbon balances. *Ecological Applications* 7, 1226-1236.
- Andrén O. & Paustian K. (1987) Barley straw decomposition in the field: a comparison of models. *Ecology* 68, 1190-1200.

- Axelsson E. & Axelsson B. (1986) Changes in carbon allocation patterns in spruce and pine trees following irrigation and fertilization. *Tree Physiology* **2**, 189-204.
- Bazire P. & Gadant J. (1991) *La Forêt en France*. La Documentation Française, Paris.
- Berninger F. & Nikinmaa E. (1997) Implications of varying pipe model relationships on Scots pine growth in different climates. *Functional Ecology* **11**, 146-156.
- Boratynski A. (1991) Range of natural distribution. In *Genetics of Scots Pine* (eds. M. Giertych & C. Matyas), pp. 19-30. Elsevier, Amsterdam.
- Braekke F.H. (1995) Response of understorey vegetation and Scots pine root systems to fertilization at multiple deficiency stress. *Plant and Soil* **168-169**, 179-185.
- Breymeyer A.I., Hall D.O., Melillo J.M. & Ågren G.I. (eds.) (1996) *Global Change: Effects on Coniferous Forests and Grasslands*. J. Wiley, Chichester.
- Campbell G.S. (1985) *Soil Physics with BASIC. Transport Models for Soil-Plant Systems*. Elsevier, Amsterdam.
- Cannell M.G.R. (1982) *World Forest Biomass and Primary Production Data*. Academic Press, New York.
- Cannell M.G.R. & Dewar R.C. (1994) Carbon allocation in trees: a review of concepts for modelling. *Advances in Ecological Research* **25**, 50-104.
- Cannell M.G.R., Grace J. & Booth A. (1989) Possible impacts of climate warming on trees and forests in the United Kingdom: a review. *Forestry* **62**, 337-364.
- Choudhury B.J. & Monteith J.L. (1988) A four-layer model for the heat budget of homogeneous land surfaces. *Quarterly Journal of the Royal Meteorological Society* **114**, 373-398.
- Christie J.M. & Lines R. (1979) A comparison of forest productivity in Britain and Europe in relation to climatic factors. *Forest Ecology and Management* **2**, 75-102.
- Chung H.-H. & Barnes R.L. (1977) Photosynthate allocation in *Pinus taeda*. I. Substrate requirements for synthesis of shoot biomass. *Canadian Journal of Forest Research* **7**, 106-111.
- Collatz G.J., Ball J.T., Grivet C. & Berry J.A. (1991) Physiological and environmental regulation of stomatal conductance, photosynthesis and transpiration: a model that includes a laminar boundary layer. *Agricultural and Forest Meteorology* **54**, 107-136.
- De Pury D.G.G. & Farquhar G.D. (1997) Simple scaling of photosynthesis from leaves to canopies without the errors of big-leaf models. *Plant Cell and Environment* **20**, 537-557.
- Dewar R.C. (1997) A simple model of light and water use evaluated for *Pinus radiata*. *Tree Physiology* **17**, 259-265.
- Edwards P.N. & Christie J.M. (1981) *Yield Models for Forest Management*. Forestry Commission Report No. 48
- Eichorn F. (1904) Beziehungen zwischen Bestandeshöhe und Bestandesmasse. *Allgemeine Forst und Jagdzeitung* **80**:45-49.
- Farquhar G.D. & von Caemmerer S. (1982) Modelling of photosynthetic response to environmental conditions. In *Encyclopedia of Plant Physiology. New Series. Vol. 12B. Physiological Plant Ecology II* (eds. O.L. Lange, P.S. Nobel, C.B. Osmond & H. Ziegler), pp. 549-587. Springer Verlag, Berlin.
- Farquhar G.D., von Caemmerer S. & Berry J.A. (1980) A biochemical model of photosynthetic CO<sub>2</sub> assimilation in leaves of C<sub>3</sub> species. *Planta* **149**, 78-90.

- Farquhar G.D. & Wong S.C. (1984) An empirical model of stomatal conductance. *Australian Journal of Plant Physiology* **11**, 191-210.
- Garratt J.R. (1992) *The Atmospheric Boundary Layer*. Cambridge Univ. Press, Cambridge.
- Gholz H.L., Linder S. & McMurtrie R.E. (1994) *Environmental Constraints on the Structure and Productivity of Pine Forest Ecosystems: a Comparative Analysis*. Vol. 43. *Ecological Bulletins*, Copenhagen.
- Giertych M. (1991) Provenance variation in growth and phenology. In *Genetics of Scots Pine* (eds. M. Giertych & C. Matyas), pp. 87-101. Elsevier, Amsterdam.
- Goudriaan J. (1977) *Crop Micrometeorology: a Simulation Study*. PUDOC, Wageningen.
- Goudriaan J. & van Laar H.H. (1994) *Modelling Potential Crop Growth Processes*. Kluwer Academic Publ., Dordrecht.
- Gower S.T., Isebrands J.G. & Sheriff D.W. (1995) Carbon allocation and accumulation in conifers. In *Resource Physiology of Conifers* (eds. W.K. Smith & T.M. Hinckley), pp. 217-254. Academic Press, San Diego.
- Grace J. (1988) Temperature as a determinant of plant productivity. In *Plants and Temperature* (eds. S.P. Long & F.I. Woodward), pp. 91-107. Society for Experimental Biology, Great Britain.
- Helmisaari H.-S. & Siltala T. (1989) Variation in nutrient concentrations of *Pinus sylvestris* stems. *Scandinavian Journal of Forest Research* **4**, 443-451.
- Hulme M., Conway D., Jones P.D., Jiang T., Barrow E.M. & Turney C. (1995) Construction of a 1961-1990 European climatology for climate change modelling and impact applications. *International Journal of Climatology* **15**, 1333-1363.
- Ineson P., Jones H.F. & Heal O.W. (1984) Regional aspects of forests in Europe: a preliminary study of *Pinus sylvestris*. In *State and Change of Forest Ecosystems. Indicators in Current Research* (ed. G.I. Ågren), pp. 315-332. Swedish Univ. Agric. Sciences, Dept. Ecology & Environmental Research, Report No. 13.
- Irvine J., Perks M.P., Magnani F. & Grace J. (1998) The response of *Pinus sylvestris* to drought: stomatal control of transpiration and hydraulic conductance. *Tree Physiology* **18**, 393-402.
- Jones H.G. (1992) *Plants and Microclimate*. Cambridge Univ. Press, Cambridge.
- Kellomäki S. & Wang K.Y. (1998) Daily and seasonal CO<sub>2</sub> exchange in Scots pine grown under elevated O<sub>3</sub> and CO<sub>2</sub>: experiment and simulation. *Plant Ecology* **136**, 229-248.
- Kimball J.S., Running S.W. & Nemani R. (1997) An improved method for estimating surface humidity from daily minimum temperature. *Agricultural and Forest Meteorology* **85**, 87-98.
- Kustas W.P., Jackson R.D. & Asrar G. (1989) Estimating surface energy-balance components from remotely sensed data. In *Theory and Applications of Optical Remote Sensing* (ed. G. Asrar), pp. 604-627. Wiley, New York.
- Landsberg J.J. & Waring R.H. (1997) A generalized model of forest productivity using simplified concepts of radiation-use efficiency, carbon balance and partitioning. *Forest Ecology and Management* **95**, 209-228.
- Leuning R. (1995) A critical appraisal of a combined stomatal-photosynthesis model for C<sub>3</sub> plants. *Plant Cell and Environment* **18**, 339-355.
- Leuning R. (1997) Scaling to a common temperature improves the correlation

- between the photosynthesis parameters  $J_{max}$  and  $V_c^{max}$ . *Journal of Experimental Botany* **48**, 345-347.
- Lloyd J. & Taylor J.A. (1994) On the temperature dependence of soil respiration. *Functional Ecology* **8**, 315-323.
- Ludlow A.R., Randle T.J. & Grace J.C. (1990) Developing a process-based growth model for Sitka spruce. In *Process Modeling of Forest Growth Responses to Environmental Stress* (eds. R.K. Dixon, R.S. Meldahl, G.A. Ruark & W.G. Warren), pp. 249-262. Timber Press, Portland, Oregon.
- Magnani F., Centritto M. & Grace J. (1996) Measurement of apoplasmic and cell-to-cell components of root hydraulic conductance by a pressure clamp technique. *Planta* **199**, 296-306.
- Magnani F., Leonardi S., Tognetti R., Grace J. & Borghetti M. (1998) Modelling the surface conductance of a broad-leaf canopy: effects of partial decoupling from the atmosphere. *Plant Cell and Environment* **21**, 867-879.
- Makela A. (1986) Implications of the pipe model theory on dry matter partitioning and height growth in trees. *Journal of Theoretical Biology* **123**, 103-120.
- Maracchi G., Benincasa F. & Zipoli G. (1983) *Elementi di Agrometeorologia*. CNR-IATA, Firenze.
- Mencuccini M. & Grace J. (1995) Climate influences the leaf area-sapwood area ratio in Scots pine. *Tree Physiology* **15**, 1-10.
- Mencuccini M. & Grace J. (1996a) Developmental patterns of aboveground xylem conductance in a Scots pine (*Pinus sylvestris* L.) age sequence. *Plant Cell and Environment* **19**, 939-948.
- Mencuccini M. & Grace J. (1996b) Hydraulic conductance, light interception and needle nutrient concentration in Scots pine stands and their relations with net primary productivity. *Tree Physiology* **16**, 459-468.
- Monteith J.L. & Unsworth M.H. (1990) *Principles of Environmental Physics*. Edward Arnold, London.
- Oberhuber W., Stumböck M. & Kofler W. (1998) Climate-tree-growth relationships of Scots pine stands (*Pinus sylvestris* L.) exposed to soil dryness. *Trees* **13**, 19-27.
- Ovington J.D. (1957) Dry-matter production by *Pinus sylvestris* L. *Annals of Botany* **21**, 287-314.
- Palmroth S., Berninger F., Nikinmaa E., Lloyd J., Pulkkinen P. & Hari P. (1999) Structural adaptation rather than water conservation was observed in Scots pine over a range of wet to dry climates. *Oecologia* **121**, 302-309
- Parker G.A. & Maynard Smith J. (1990) Optimality theory in evolutionary biology. *Nature* **348**, 27-33.
- Paterson S.S. (1956) *The Forest Area of the World and its Potential Productivity*. Dept. of Geography, Royal Univ. of Gothenburgh, Sweden.
- Persson H. (1980) Death and replacement of fine roots in a mature Scots pine stand. *Ecological Bulletins* **32**, 251-260.
- Roberts J. (1976) A study of root distribution and growth in a *Pinus sylvestris* L. (Scots pine) plantation in East Anglia. *Plant and Soil* **44**, 607-621.
- Roberts J. (1977) The use of tree-cutting techniques in the study of the water relations of mature *Pinus sylvestris* L. *Journal of Experimental Botany* **28**, 751-767.
- Robichaud E. & Methven I.R. (1993) The effect of site quality on the timing of stand

- breakup, tree longevity, and the maximum attainable height of black spruce. *Canadian Journal of Forest Research* **23**, 1514-1519.
- Ross J. (1981) *The Radiation Regime and Architecture of Plant Stands*. Dr W. Junk Publishers, The Hague.
- Ryan M.G. (1991) A simple method for estimating gross carbon budgets for vegetation in forest ecosystems. *Tree Physiology* **9**, 255-266.
- Santantonio D. (1989) Dry-matter partitioning and fine root production in forests. New approaches to a difficult problem. In *Biomass Production by Fast-Growing Trees*. (eds. J.S. Pereira & J.J. Landsberg), pp. 57-72. Kluwer Academic Publishers, Dordrecht.
- Santantonio D. & Santantonio E. (1987) Effect of thinning on production and mortality of fine roots in a *Pinus radiata* plantation on a fertile site in New Zealand. *Canadian Journal of Forest Research* **17**, 919-928.
- Schoettle A.W. & Fahey T.J. (1994) Foliage and fine root longevity of pines. *Ecological Bulletins* **43**, 136-153.
- Sevola Y. (ed.) (1998) *Statistical Yearbook of Forestry*. Finnish Forest Research Institute, Helsinki
- Sharpe P.J.H. (1990) Forest modeling approaches: compromises between generality and precision. In *Process Modeling of Forest Growth Responses to Environmental Stress* (eds. R.K. Dixon, R.S. Meldahl, G.A. Ruark & W.G. Warren), pp. 180-190. Timber Press, Portland.
- Shaw R.H. & Pereira A.R. (1982) Aerodynamic roughness of a plant canopy: a numerical experiment. *Agricultural Meteorology* **26**, 51-65.
- Thornley J.H.M. & Johnson I.R. (1990) *Plant and Crop Modelling*. Clarendon Press, Oxford.
- Tyree M.T. & Sperry J.S. (1989) Vulnerability of xylem to cavitation and embolism. *Annual Review of Plant Physiology and Plant Molecular Biology* **40**, 19-38.
- Vanclay J.K. (1994) *Modelling Forest Growth and Yield*. CAB International, Wallingford.
- Wang K.Y. (1996) Canopy CO<sub>2</sub> exchange of Scots pine and its seasonal variation after four-year exposure to elevated CO<sub>2</sub> and temperature. *Agricultural and Forest Meteorology* **82**, 1-27.
- Wang K.Y., Kellomäki S. & Laitinen K. (1996) Acclimation of photosynthetic parameters in Scots pine after three years exposure to elevated temperature and CO<sub>2</sub>. *Agricultural and Forest Meteorology* **82**, 195-217.
- Wang Y.P. & Leuning R. (1998) A two-leaf model for canopy conductance, photosynthesis and partitioning of available energy. I. Model description and comparison with a multi-layered model. *Agricultural and Forest Meteorology* **91**, 89-111.
- Waring R.H., Landsberg J.J. & Williams M. (1998) Net primary production of forests: a constant fraction of gross primary production? *Tree Physiology* **18**, 129-134.
- Westoby M. (1984) The self-thinning rule. *Advances in Ecological Research* **14**, 167-225.
- White E.J. (1982) Relationship between height growth of Scots pine and site factors in Great Britain. *Forest Ecology and Management* **4**, 225-245.
- Whitehead D., Edwards W.R.N. & Jarvis P.G. (1984) Conducting sapwood area,

foliage area, and permeability in mature trees of *Picea sitchensis* and *Pinus contorta*. *Canadian Journal of Forest Research* 14, 940-947.

**Appendix 5.1** Summary of parameter values used in computations. Several photosynthetic parameters related to the properties of Rubisco are assumed to be invariant among C<sub>3</sub> species and a value has been therefore derived from detailed analyses published in the literature (see De Pury and Farquhar 1997). Maximum electron transport rate has been assumed to be linearly related to  $V_c^{max}$  (Leuning 1997).

	<i>Definition</i>	<i>Units</i>	<i>Value</i>	<i>Source</i>
$a_1$	coeff. in $g_s$ vs $A$ equation	Pa <sup>-1</sup>	$5.2 \times 10^5$	1
$D_0$	coeff. in $g_s$ response to vapour pressure deficit	Pa	1200	2
$g_0$	stomatal conductance to CO <sub>2</sub> in darkness	mol m <sup>-2</sup> s <sup>-1</sup>	$2.3 \times 10^{-3}$	1
$k_{fr}$	specific hydraulic conductance of fine roots	m <sup>3</sup> s <sup>-1</sup> MPa <sup>-1</sup> kg <sup>-1</sup>	$2.3 \times 10^{-7}$	3,4,5
$k_s$	specific hydraulic conductivity of sapwood	m <sup>2</sup> MPa <sup>-1</sup> s <sup>-1</sup>	$1.3 \times 10^{-3}$	6
$l_r$	fine root longevity	yr	0.65	7
$l_s$	sapwood longevity	yr	39	8
$N_f$	nitrogen concentration in foliage	kg N kg <sup>-1</sup>	0.015	9
$N_r$	nitrogen concentration in fine roots	kg N kg <sup>-1</sup>	0.0075	8
$N_s$	nitrogen concentration in sapwood	kg N kg <sup>-1</sup>	0.0005	10
$r_g$	growth respiration coefficient	-	0.28	11
$V_c^{max}$	maximum carboxylation rate	mol m <sup>-2</sup> s <sup>-1</sup>	$50 \times 10^{-6}$	1
$\alpha$	photosynthetic quantum efficiency	mol e <sup>-</sup> quantum <sup>-1</sup>	0.28	12
$\rho_f$	foliage density in the canopy (height vs foliage growth relationship)	kg m <sup>-3</sup>	0.73	13
$\bar{\Psi}$	critical leaf water potential	MPa	-1.4	14
$\Psi_0$	soil $\Psi$ for maximum stomatal closure	MPa	-1.0	15

<sup>1</sup>Kellomäki and Wang (1998), <sup>2</sup>Wang (1996), <sup>3</sup>Roberts (1976), <sup>4</sup>Roberts (1977), <sup>5</sup>Chapter 2, <sup>6</sup>Mencuccini and Grace (1995), <sup>7</sup>Persson (1980), <sup>8</sup>Helmisaari and Siltala (1989), <sup>9</sup>Mencuccini and Grace (1996), <sup>10</sup>Braekke (1995), <sup>11</sup>Chung and Barnes (1977), <sup>12</sup>Wang *et al.* (1996), <sup>13</sup>Ovington (1957), <sup>14</sup>Chapter 4, <sup>15</sup>Irvine *et al.* (1998)

## Chapter 6. Measurement of apoplastic and cell-to-cell components of root hydraulic conductance by a pressure clamp technique

What can we know? or what  
can we discern,  
When error chokes the windows  
of the mind?

Sir John Davies

### 6.1 Introduction

Much attention has been paid in the last two decades to the hydraulic architecture of plants, since the distribution of hydraulic conductances and capacitances across the plant determines the hydration patterns of tissues and consequently influences plant growth (Schulze *et al.* 1987). Quantitative studies of plant hydraulic architecture are also needed to parameterize SVATS (soil-vegetation-atmosphere transfer schemes) for use in climate models.

Several studies report that a considerable proportion of total plant resistance is located in the root system, both in herbaceous plants and in trees (Magnani and Borghetti 1995); in trees, in particular, the magnitude of root resistance is of great significance, as it also determines the daily contribution of water stored in the stem and the leaves to the water flow through the plant.

Root water uptake is driven by a combination of hydraulic and osmotic forces (Weatherley 1982). It is generally assumed that the root (like the cell) behaves like a two-compartment osmometer (Fiscus 1975; Dalton *et al.* 1975), where an internal compartment (the root xylem) is separated from an external compartment (the soil solution) by a membrane-like barrier. According to this model, at the endodermis a tight Casparian band forces water and solutes to enter the symplast and move along a cell-to-cell pathway; this cellular barrier, which results from the arrangement in series of several resistances, is supposed to act like a single equivalent membrane. Water uptake through the root system ( $J_v$ ) can therefore be described by the phenomenological equation (Kedem and Katchalsky 1963)

$$J_v = -AL_p \cdot (P - \sigma(\pi - \pi_m)) \quad (6.1)$$

where  $A$  is root surface area,  $L_p$  is root hydraulic conductivity (and  $A L_p$  is therefore total root hydraulic conductance),  $P$  is root hydrostatic pressure,  $\pi$  is root osmotic pressure and  $\pi_m$  is the osmotic pressure of the rooting medium;  $\sigma$  is the apparent reflection coefficient, which accounts for the non-ideal behavior of the osmometer.

Although this two-compartment model is attractive for its simplicity (Dainty 1985), more complex models have been proposed that include several resistances both in the radial pathway from the soil to the root stele and in the longitudinal pathway along the root xylem (e.g. Landsberg and Fowkes 1978; Powell 1978; Katou and Taura 1989; Alm *et al.* 1992; Steudle 1992).

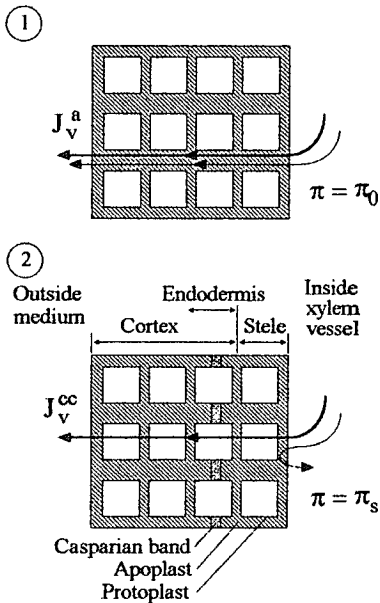
Of the several methods proposed for the measurement of root conductance, the root pressure probe technique has been most extensively used over the last few years for the measurement of water and solute exchange dynamics both on single apical roots and on entire root systems (Steudle and Jeschke 1983). The technique is an extension of the cell pressure probe (Steudle 1993). In pressure relaxation experiments a very small chamber is sealed to the cut end of a root system and a sudden water potential change is applied to the root system; root characteristics are derived from the changes in root pressure when the volume of the system is kept constant.

As an alternative to the pressure relaxation method, a pressure clamp technique was also proposed by Wendler and Zimmermann (1982) for use on single cells. In this variation of the technique, a constant pressure is applied to a cell and its hydraulic characteristics are inferred from the exponential decline of water flow over time, that results from the accumulation of solutes in the cell (Wendler and Zimmermann 1985; Moore and Cosgrove 1991; Zhang and Tyerman 1991). The pressure clamp technique has also been applied to segments of seminal roots of barley (Steudle and Jeschke 1983) and maize (Steudle and Frensch 1989), but a complete theory for the analysis of the results has not been proposed.

Experiments with the root pressure probe have indicated that in some species the apparent root hydraulic conductance (i.e. the ratio of root water uptake to water potential difference between soil and root) strongly depends on the nature of the driving force used to induce water flow (Steudle *et al.* 1987, 1993; Steudle and Frensch 1989; Zhu and Steudle 1991; Melchior and Steudle 1993; Rüdinger *et al.*



**Fig. 6.1** Diagrammatic representation of the composite membrane model of the root. (1) Under the hydrostatic pressure applied by the instrument, in the basal root compartment the flow of water along the apoplastic pathway ( $J_v^a$ ) is coupled to a flow of solutes (thin line). (2) In the apical root compartment water flows along the cell-to-cell pathway ( $J_v^{cc}$ ), but solutes are prevented from leaving the root by an equivalent membrane; as a result the osmotic pressure in the root xylem ( $\pi_s$ ) increases from its initial value  $\pi_0$ , until it counterbalances the hydrostatic pressure applied.



1994). When the osmotic pressure of the rooting solution is changed, the resulting flow of water is considerably smaller than observed for an applied pressure gradient. In these species the root deviates considerably from ideal behaviour, exhibiting reflection coefficients  $\sigma < 1$ , but does not appear to leak solutes, as indicated by fairly low solute permeabilities (Steudle 1993).

These results have been explained in terms of a composite membrane model of the root (Steudle *et al.* 1987; Steudle 1992; Steudle *et al.* 1993), which could account also for the observation of apparently

variable root conductances (Passioura 1982, 1988). The model assumes a composite transport of water in the root with two parallel pathways (Fig. 6.1): besides the cell-to-cell pathway, water and solutes also move along an apoplastic pathway, which does not cross any semi-permeable membrane. The resulting apoplastic flow is driven by purely hydraulic forces.

The existence of an apoplastic path has also been demonstrated by different techniques, using dyes (Peterson *et al.* 1981; Hanson *et al.* 1985; Häussling *et al.* 1988; Enstone and Peterson 1992), measuring solute absorption along the root (Sanderson 1983; Yeo *et al.* 1987; Häussling *et al.* 1988) or by the concurrent use of root pressure probe and cell pressure probe techniques (Jones *et al.* 1988; Radin and Matthews 1989).

The apoplastic path could be located at the emergence of root primordia from the stele of the primary root, where a flow of apoplastic tracers has been observed

(Peterson *et al.* 1981; Häussling *et al.* 1988), but other pathways have been proposed as well (Sanderson 1983; Häussling *et al.* 1988).

The distribution of root conductance between an apoplastic and a cell-to-cell component is worth investigating, since water and solute flow are coupled along the two pathways in completely different ways. The measurement of both components with the root pressure probe by the pressure relaxation technique would require osmotic experiments, which are not possible on plants grown in soil. The pressure clamp technique, on the other hand, would allow measurement of the two components but is difficult to apply to large root systems.

Our first aim was, therefore, to develop a simplified device for the application of the pressure clamp technique to large potted seedlings. A theoretical model for the interpretation of the results from pressure clamp experiments had first to be developed, based on the composite membrane model of the root proposed by Steudle *et al.* (1987).

The technique developed was used for the measurement of the apoplastic and cell-to-cell components of root hydraulic resistance of large cherry (*Prunus avium*) seedlings.

## 6.2 Theory

In the model, the cell-to-cell pathway for water and solute flow is supposed to be located in the apical root (apical root compartment), where no suberification has yet taken place; the apoplastic pathway is supposed to be located in a more basal region (basal root compartment), where the endodermal layer is interrupted by emerging lateral roots. As a consequence of this arrangement, the flow of solutes along the apoplastic pathway will not directly affect the solute concentration in the apical root compartment.

From the phenomenological equation for the flow of water through a membrane (Kedem and Katchalsky 1963) and the van t' Hoff relation, root water uptake through the cell-to-cell pathway ( $J_v^{\text{cc}}$ ,  $\text{m}^3 \text{s}^{-1}$ ) is represented by

$$\begin{aligned} J_v^{\text{cc}} &= -A^{\text{cc}} L_p^{\text{cc}} (P - \sigma(\pi_s - \pi_m)) = \\ &= -A^{\text{cc}} L_p^{\text{cc}} (P - \sigma \cdot RT \cdot C_s + \sigma \cdot \pi_m) \end{aligned} \quad (6.2)$$

where  $A^{cc}$  ( $\text{m}^2$ ) is the area of the equivalent membrane,  $L_p^{cc}$  ( $\text{m s}^{-1} \text{MPa}^{-1}$ ) is the hydraulic conductivity of the membrane, and the product  $A^{cc} L_p^{cc}$  is the hydraulic conductance of the membrane as a whole;  $P$  (MPa) is the hydrostatic pressure in the root,  $\pi_s$  and  $\pi_m$  (MPa) are the osmotic pressure in the apical root compartment and in the rooting medium, respectively,  $\sigma$  is the dimensionless reflection coefficient of the membrane, which accounts for its non-ideal selectivity,  $C_r$  ( $\text{mol m}^{-3}$ ) is the concentration of solutes in the root,  $R$  is the gas constant and  $T$  is absolute temperature of the solution. The negative sign accounts for the direction of water flow, which is assumed throughout the paper to be positive when entering the root system from the surrounding soil.

Where no semi-permeable membranes are involved, the flow of water through the apoplastic pathway ( $J_v^a$ ,  $\text{m}^3 \text{s}^{-1}$ ) is exclusively driven by the hydrostatic pressure  $P$  (MPa)

$$J_v^a = -A^a L_p^a \cdot P \quad (6.3)$$

where  $A^a L_p^a$  ( $\text{m}^3 \text{s}^{-1} \text{MPa}^{-1}$ ) is the overall conductance of the apoplastic pathway.

The total flow of water through the root system ( $J_v$ ,  $\text{m}^3 \text{s}^{-1}$ ) is the sum of an apoplastic and a cell-to-cell component:

$$J_v = J_v^{cc} + J_v^a = -A^{cc} L_p^{cc} (P - \sigma(\pi_s - \pi_m)) - A^a L_p^a \cdot P \quad (6.4)$$

If the root system is allowed to reach steady-state conditions, the initial concentration of solutes ( $C_0$ ,  $\text{mol m}^{-3}$ ) and the initial osmotic pressure in the root ( $\pi_s(0)$ , MPa) can be assumed to be constant throughout the root xylem.

If initially the flow of water out of the stem is artificially prevented, solutes will accumulate in the root and a hydrostatic root pressure  $P_0$  (MPa) will slowly build up. A small reverse flow out of the root system through the apoplastic pathway will result, counterbalanced by an inflow of water through the cell-to-cell pathway; the

initial osmotic force across the membrane is therefore

$$\sigma(\pi_s(0) - \pi_m) = P_0 \cdot \left( 1 + \frac{A^a L_p^a}{A^{cc} L_p^{cc}} \right) \quad (6.5)$$

Because xylem longitudinal conductance is usually large compared to root radial conductance (Steudle and Frensch 1989), the hydrostatic pressure can be assumed to be constant throughout the root system.

When a positive pressure  $P_{appl}$  (MPa) is applied from the base of the stem, water is forced backwards into the root system.

The sap originally in the basal root xylem will not mix with it, since the flow of water in xylem vessels is laminar; it is therefore assumed that its concentration remains at the initial concentration  $C_0$ , although it will decrease by a process of diffusion; diffusion is however slow over distances of several centimeters.

Solutes are dragged by the flow of water through the apoplasmic pathway. Along the cell-to-cell pathway, on the contrary, the flow of solutes across the endodermis is slow (Steudle *et al.* 1987) and over short time intervals it can be neglected, although this simplification will constitute a source of error that will be analyzed in the Discussion.

As water flows through the semi-permeable membrane an equivalent amount of solution at concentration  $C_0$  enters from the basal root into the apical root xylem, so increasing its concentration. Solute changes can then be expressed as

$$\frac{dn_s}{dt} = -J_v^{cc} \cdot C_0 \quad (6.6)$$

where  $n_s$  is the number of moles of solute in the apical root compartment.

As solutes are filtered at the endodermis and accumulate in the apical root tips, an osmotic pressure builds up which tends to counterbalance the applied hydrostatic pressure and to reduce the cell-to-cell flow.

$$\frac{dJ_v^{cc}}{dt} = A^{cc} L_p^{cc} \cdot \sigma \cdot RT \cdot \frac{dC_s}{dt} = \frac{A^{cc} L_p^{cc} \cdot \sigma \cdot RT}{V} \cdot \frac{dn_s}{dt} \quad (6.7)$$

$$\frac{dJ_v^{cc}}{dt} = -\frac{A^{cc} L_p^{cc} \cdot \sigma \cdot RT \cdot C_0}{V} \cdot J_v^{cc} = -\frac{A^{cc} L_p^{cc} \cdot \sigma \cdot \pi_s(0)}{V} \cdot J_v^{cc} \quad (6.8)$$

where  $V$  is the volume of solution in the apical root compartment.

This first-order differential equation can be easily integrated and yields

$$J_v^{cc} = J_v^{cc}(0) \cdot e^{-t/\tau} \quad (6.9)$$

where

$$\begin{aligned} J_v^{cc}(0) &= -A^{cc} L_p^{cc} \cdot (P_{appl} - \sigma(\pi_s(0) - \pi_m)) = \\ &= -A^{cc} L_p^{cc} \cdot (P_{appl} - P_0) + A^a L_p^a \cdot P_0 \end{aligned} \quad (6.10)$$

$$\tau = \frac{V}{A^{cc} L_p^{cc} \cdot \sigma \cdot \pi_s(0)} \quad (6.11)$$

The model predicts that cell-to-cell flow declines exponentially from the maximum value which is attained when the pressure is first applied, with time constant  $\tau$ .

Since the apoplastic flow of water is constant, the total flow of water under a constant applied hydrostatic pressure can be expressed as

$$J_v = J_v^{cc}(0) \cdot e^{-t/\tau} + J_v^a \quad (6.12)$$

Initial cell-to-cell flow and apoplastic flow can therefore be estimated by fitting the model to experimental data by non-linear regression techniques. Apoplastic conductance ( $A^a L_p^a$ ) and cell-to-cell conductance ( $A^{cc} L_p^{cc}$ ) can be derived from Eq.

6.3 and 6.10, respectively, as

$$A^a L_p^a = -\frac{J_v^a}{P_{appl}} \quad (6.13)$$

$$A^{cc} L_p^{cc} = -\frac{J_v^{cc}(0) - A^a L_p^a \cdot P_0}{(P_{appl} - P_0)} \cong -\frac{J_v^{cc}(0)}{(P_{appl} - P_0)} \quad (6.14)$$

where the approximation applies for very small values of initial root pressure.

A similar approach can be used in the analysis of flow dynamics when the applied pressure is released. When, under a constant applied pressure, a steady-state flow has been reached, the effect of the applied pressure is exactly counter-balanced by osmotic forces through the membrane (Eq. 6.2)

$$P_{appl} = \sigma(\pi_{seq} - \pi_m) \quad (6.15)$$

where  $\pi_{seq}$  (MPa) is the osmotic pressure at equilibrium of the solution adjacent to the membrane.

If the applied pressure is suddenly released, a reverse flow arises through the cell-to-cell pathway

$$J_v^{cc}(0) = A^{cc} L_p^{cc} \cdot \sigma \cdot (\pi_{seq} - \pi_m) \quad (6.16)$$

This determines a progressive dilution of solutes in the apical root compartment, which results in an exponential decrease of cell-to-cell flow, similar to that observed for applied pressure (Eq. 6.7). Solute are prevented from re-entering the apical root compartment by the semi-permeable membrane, but a solution with concentration  $C_s(t)$  flows out of the apical root compartment into the basal root, resulting in a net change of solute content

$$\frac{dn_s}{dt} = -C_s \cdot J_v^{cc} \quad (6.17)$$

If solute concentration is derived from Eq. 6.2 (for  $P_{appl} = 0$ ), we obtain

$$\frac{dn_s}{dt} = -\frac{J_v^{cc2}}{A^{cc} L_p^{cc} \cdot \sigma \cdot RT} - \frac{J_v^{cc} \cdot \pi_m}{RT} \quad (6.18)$$

and

$$\begin{aligned} \frac{dJ_v^{cc}}{dt} &= \frac{A^{cc} L_p^{cc} \cdot \sigma \cdot RT}{V} \cdot \left( -\frac{J_v^{cc2}}{A^{cc} L_p^{cc} \cdot \sigma \cdot RT} - J_v^{cc} \cdot \frac{\pi_m}{RT} \right) = \\ &= -\frac{1}{V} J_v^{cc} \cdot (J_v^{cc} + A^{cc} L_p^{cc} \cdot \sigma \cdot \pi_m) \end{aligned} \quad (6.19)$$

This non-linear differential equation is separable and by integration yields

$$J_v^{cc} = J_v^{cc}(0) \cdot e^{-t/\tau'} = A^{cc} L_p^{cc} \cdot P_{appl} \cdot e^{-t/\tau'} \quad (6.20)$$

where

$$\tau' = \frac{V}{A^{cc} L_p^{cc} \cdot \sigma \cdot \pi_m} \quad (6.21)$$

The cell-to-cell flow after the pressure is released, therefore, declines exponentially from its original value, with a time constant  $\tau'$ , which is similar to the time constant for applied pressure (Eq. 6.11) if

$$\pi_s(0) \cong \pi_m \quad (6.22)$$

No flow occurs though the apoplasmic pathway, since only osmotic forces are at work

in this case; as a result, total flow out of the root system consists of cell-to-cell flow alone and declines to zero exponentially.

From Eq. 6.20 a second estimate of cell-to-cell root conductance can be obtained.

### **6.3 Materials and methods**

#### **6.3.1 Plant material**

Cherry (*Prunus avium* L.) seeds were germinated in spring 1993 and grown for two years in a greenhouse at the University of Edinburgh (55 31' N, 3 12' W, 185 m a.s.l.). During the first year seedlings were transplanted into soil columns (7.5 dm<sup>3</sup>), regularly fertilized and watered with tap water to field capacity. In January 1994 the seedlings were transplanted before budburst into 15 dm<sup>3</sup> pots, regularly fertilized and watered to field capacity.

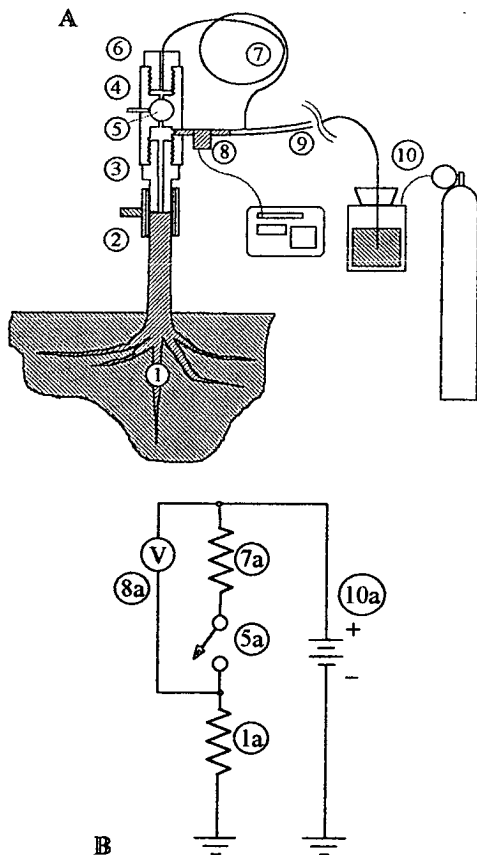
Root hydraulic conductance was measured on excised root systems in June 1994; plants were then harvested to enable comparison of shoot and root structural parameters. Leaf area was measured with a leaf area-meter (LI 3100; LI-COR Inc., Lincoln, Nebr., USA). Roots were washed from soil, divided into coarse and fine roots and dried at 80 °C to constant dry mass as measured to the nearest 0.01 g on an electronic balance (PJ360, Mettler, Goettingen, Germany).

#### **6.3.2 Description of the instrument**

A fast-response flow-meter was devised for the measurement of transient and steady-state root hydraulic conductance by the pressure clamp technique (Fig. 6.2). Distilled water, filtered to 0.2 µm to prevent clogging of xylem pit pores, was forced under pressure into the root system from a reservoir (10) placed in a pressure chamber (SKPM 1400; Skye Instruments, Llandrindod Wells, UK); from a large-diameter nylon tube (9), water was forced to flow through a fine nylon tube (7) (Mod. 800/200/100/100; Portex Ltd., Hythe, UK; 0.5 mm i.d., maximum pressure 11.5 MPa) into a stainless-steel body (4) connected to the root system by a silicone seal (2). The flow of water through the fine tubing resulted in a hydrostatic pressure drop which was measured by a temperature-corrected differential pressure transducer (24PC; Honeywell Micro Switch, Bracknell, UK) (8). The pressure transducer was fed with constant voltage and the output was recorded every half a second by a data-logger



**Fig. 6.2** Diagram of the root pressure clamp. (A) The instrument with an attached root system: water is forced under pressure into the root system from a reservoir (10) placed in a pressure bomb; from a large-diameter nylon tube (9), water is forced to flow through a hydraulic resistance (7) into a stainless steel body (4) closed by hollow bolts (3-6) and connected to the root system by a silicon seal (2). The frictional pressure drop across the resistance is measured by a differential pressure transducer (8) and recorded by a data-logger. A ball valve (5) allows to pressurize the instrument before the beginning of the measurements, whilst keeping the root system at ambient pressure. (B) An electrical analogue of the instrument: the measurement of the voltage difference across a resistance (7a) with a voltmeter (8a) allows estimation of the current through the system under a constant voltage (10a) and derivation of the value of the main resistance (1a); a step change in applied voltage is applied when the switch (5a) is closed.



(CR21X; Campbell Scientific, Shepshed, UK).

In order to minimize instrumental error arising from elastic distortion of components following a step pressure change, the steel body contained a ball valve (5) with a maximum working pressure of 13 MPa. A large part of the instrument could, therefore, be pressurized before the beginning of the measurements, whilst keeping the root system at ambient pressure.

When the valve was suddenly opened, however, the elastic expansion of instrument body and silicon seal still resulted in an apparent flow which declined over time with a very short time constant. This response time of the instrument was assessed when a metal rod was substituted for the root system.

The upstream pressure could be read continuously to 1 kPa with the pressure chamber gauge. When the valve (5) was closed, the system yielded a measurement of root pressure by difference. When the valve was open, it acted as a fast-response flow-meter, giving an exact

measurement of the hydrostatic pressure applied to the root system at the same time. Since the amounts of water moved were minimal in comparison with the volume of air in the pressure chamber, the pressure could be clamped to the desired level and kept

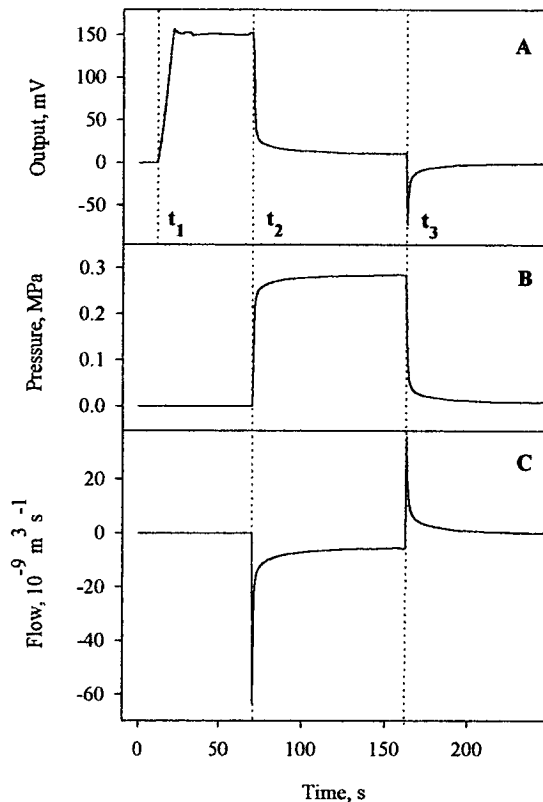


**Fig. 6.3** (A) Typical output from the instrument, (B) derived measurements of applied pressure and (C) water flow. At time  $t_1$  the pressure is increased and adjusted to the desired value, but the valve is closed and no pressure is applied to the root; when the instrument has acclimated to the new pressure, the valve is suddenly opened ( $t_2$ ). After a steady-state flow has been reached, the pressure is quickly released ( $t_3$ ) and a reverse flow of water is observed. Positive flows are from the soil into the root system.

constant throughout the whole experiment.

The flow-meter was calibrated against gravimetric measurements of water flow. A resistance made of a length of fine nylon tubing diverted the outflow from the instrument into a reservoir on an electronic balance (A120S; Sartorius, Goettingen, Germany) connected to a computer. When water was forced under pressure through the system, concurrent measures of water flow were taken with the flow-meter and as the difference between successive readings from the balance.

Plants were repeatedly watered to pot capacity and allowed to drain, in order to relieve any tensions in the soil or the root system. The stem was recut under water about 10 cm from the soil, a few cm of bark were removed and the instrument was fitted to the stump, taking great care to prevent any air bubbles from entering the system.

Root conductances were measured under five applied pressures from 0.1 to 0.5 MPa;

the complete measurement cycle took some 30 min per plant. After the instrument adjusted to the applied pressure, the valve was suddenly opened, imposing a step pressure change to the root system, and the flow of water into the root system was recorded. After a steady-state flow was reached the pressure was suddenly released at the pressure chamber and the reverse flow out of the root was measured (Fig. 6.3).

The presence of leaks in the seal could be easily detected, as a leak produced a marked deviation from the usual pattern of Fig. 6.3.

Soil temperature was recorded for each plant with a thermistor probe after the measurements and was fairly constant for all trees (19.0 to 19.6 °C).

### 6.3.3 Data analysis

The models of Eq. 6.12 and 6.20 were fitted to the untransformed data from the pressure clamp experiment by non-linear regression (SAS/STAT, SAS Institute Inc. 1988), in order to obtain unbiased estimates of the parameters (Johnson and Faunt 1992) and asymptotic standard errors of the estimates.

The nonlinear analysis yielded an estimate of initial cell-to-cell flow ( $J_s(0)$ ) and of constant apoplastic flow ( $J_a$ ) under a given applied pressure. To estimate hydraulic conductances with the highest accuracy, flows for the whole range of applied pressures were plotted against the relative effective pressure (Eq. 6.13, 6.14) and cell-to-cell and apoplastic conductances were estimated as the slope of the regression line.

## 6.4 Results

The instrument was calibrated against gravimetric measurements in the expected range of water flow. The response of the instrument was highly linear ( $R^2 = 0.999$ ), implying that flow through the resistance is always laminar.

The elastic response of the instrument was evaluated when operating it with a metal rod inserted in place of the root sample. The change in volume for a given change in pressure  $\Delta V/\Delta P$  was of the order of  $0.24 \times 10^{-6} \text{ m}^3 \text{ MPa}^{-1}$ , with a time constant of about one second. The output from the pressure transducer showed sinusoidal fluctuations of about 0.4 mV peak-to-peak, caused by instrumental noise.

A typical output from the instrument during the measurement of root conductance by the pressure clamp technique is shown in Fig. 6.3a. The voltage output was then

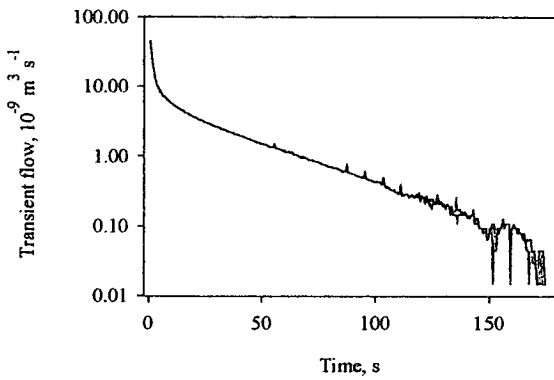
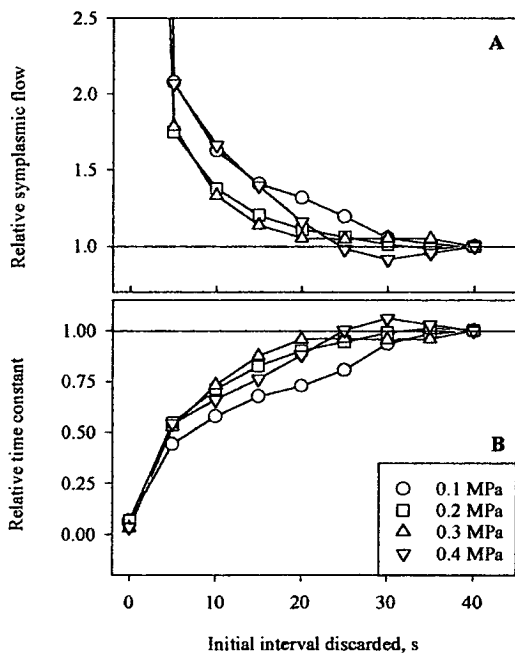


**Fig. 6.4** Semi-logarithmic plot of transient flow against time. Transient flow is the difference between measured and steady-state flow; it is the sum of cell-to-cell flow and instrumental response. Two phases can be separated: in (a) the instrumental response predominates, whilst the linear behaviour in (b) can be attributed to the exponential decay of cell-to-cell flow. In (c) the signal-to-noise ratio becomes too small for a meaningful analysis.

**Fig. 6.5** (A) Estimated initial cell-to-cell flow and (B) time constant of exponential decay of the flow for a range of applied pressures, when an initial interval of increasing length is discarded; values are normalized to the estimate for 40 s discarded.



converted to the corresponding values of water flow and hydrostatic pressure (Fig. 6.3B,C).

When the valve is opened (at time  $t_2$ ), water under pressure flows through the instrument into the root system and the flow slowly declines to a constant negative value (Fig. 6.3C). The change in applied pressure is not a perfectly square step because of frictional pressure losses, but within 15-20 seconds levels off to a constant value (Fig. 6.3B). When the pressure is released at the pressure chamber (at time  $t_3$ ), the applied pressure quickly drops to zero and the reverse flow of water into the instrument slowly declines to zero (Fig. 6.3C).

In order to analyze the behaviour of flow changes, the steady-state value was subtracted from total flow and the residual transient component was plotted against time on a semi-log plot (Fig. 6.4). Two relevant phases could be detected, an initial non-linear phase (a) related to the time response of the instrument, followed by a remarkably linear phase, indicative of an exponential decay (b). The fluctuations of increasing amplitude that eventually break the linear phase (phase c) are due

Plant	$A^{cc} L_n^{cc} \times$ ( $\text{m}^3 \cdot \text{MPa}^{-1} \cdot \text{s}^{-1}$ )	$R^2$	$A^a L_n^a \times 10^9$ ( $\text{m}^3 \cdot \text{MPa}^{-1} \cdot \text{s}^{-1}$ )	$R^2$	$T_{1/2}$ (s)
1	12.8 (1.00)	0.98	18.5 (0.76)	0.99	25.0 (1.5)
2	12.2 (1.7)	0.96	16.6 (0.7)	1.00	19.5 (1.5)
3	15.3 (1.3)	0.98	18.5 (0.5)	1.00	18.5 (1.3)
4	12.6 (0.9)	0.99	15.6 (1.6)	0.98	28.1 (4.9)
5	8.8 (0.9)	0.97	12.0 (0.5)	0.99	17.8 (1.4)
6	8.5 (0.4)	0.99	12.2 (1.2)	0.97	27.1 (3.7)

**Table 6.1.** Cell-to-cell hydraulic conductance ( $A^{cc} L_p^{cc}$ ) and apoplasmic conductance ( $A^a L_p^a$ ) of entire root systems of cherry seedlings. Conductances were computed by linear regression as the slope of the relationship between water flow and effective pressure (Eq. 6.13, 6.14); the standard error of the estimate is reported between brackets, together with the coefficient of determination of the regression ( $R^2$ ). For each plant, average and standard error of the half-times of cell-to-cell water flow ( $T_{1/2}$ ) under a range of applied pressures are reported.

conductances (Table 6.1).

The importance of discarding the initial interval dominated by instrumental response is demonstrated in Fig. 6.5: when initial intervals of increasing length are discarded, estimated values of both initial cell-to-cell flow and time constant of decay change greatly, but eventually level off to a constant value after 25 seconds, because of the very short time constant of instrumental response (1 second).

The model gives a good fit of experimental data (Fig. 6.6A). This is demonstrated by plotting residual errors (Fig. 6.6B). After the initial interval of instrumental response the error is negligible and appears to be mainly determined by the previously mentioned sinusoidal instrumental error. The elasticity of the device can be derived from the plot of residuals. For a given applied pressure, the total volume change of the instrument can be obtained by integrating the area beneath the curve of residuals. This yields the same value of  $\Delta V/\Delta P$  as determined in the preliminary assessment of the instrument, so confirming that (a) the initial fast phase is truly determined by instrumental response and (b) the elastic response of the root itself is of minor importance.

Both the initial cell-to-cell flow, as estimated by non-linear regression, and the steady-

to the sinusoidal instrumental error already mentioned. The same pattern is observed for both the application and release of pressure.

When the initial interval dominated by instrumental response was neglected, the model of Eq. 6.12 (pressure applied) and 6.20 (pressure released) could be fitted by non-linear regression on the data, yielding an estimate of initial flows (Fig. 6.7) and eventually of root cell-to-cell and apoplasmic

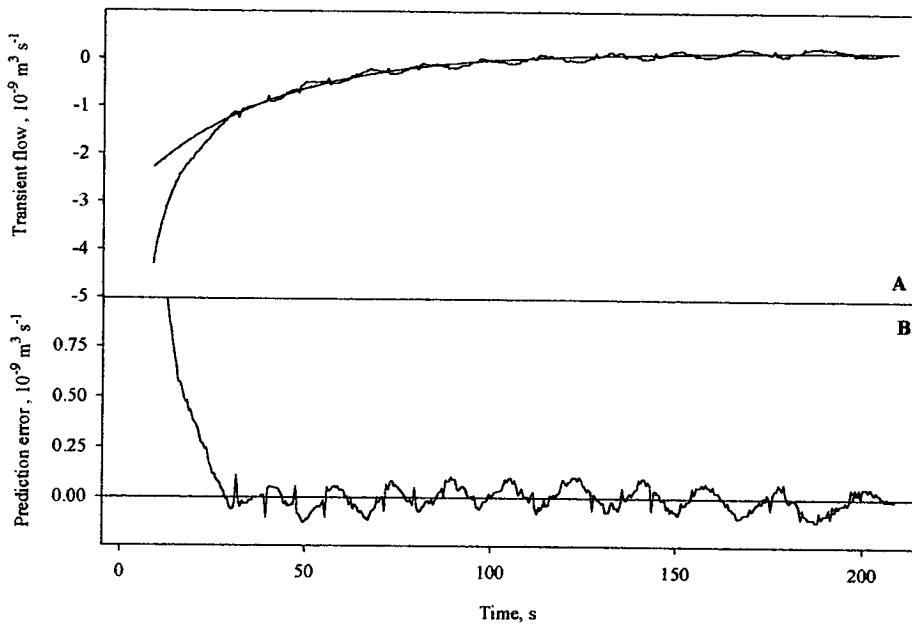


**Fig.6.6** Example of model fit to experimental data. (A) Measured flow under 0.2 MPa applied pressure and predicted flow and (B) prediction errors are plotted against time from pressure change. Instrumental error is very large, but declines sharply and is negligible after an initial interval which is discarded.

Plant	$AL_p \times 10^9$ ( $\text{m}^3 \cdot \text{MPa}^{-1} \cdot \text{s}^{-1}$ )	Fine root DW (g)	Total root DW (g)	Leaf area ( $\text{m}^2$ )	$LSC \times 10^8$ ( $\text{m} \cdot \text{MPa}^{-1} \cdot \text{s}^{-1}$ )
1	31.3	14.4	27.9	0.94	3.3
2	28.7	11.7	45.6	0.51	5.6
3	33.7	10.8	36.8	0.92	3.7
4	28.2	12.0	50.7	1.03	2.7
5	20.8	5.2	26.3	0.58	3.6
6	20.7	8.8	32.1	0.69	3.0

**Table 6.2.** Root hydraulic conductance ( $AL_p$ ), dry weight of fine roots and of the entire root system, leaf area and root leaf specific conductance ( $LSC$ ) of cherry seedlings. Root conductance is the sum of cell-to-cell and apoplastic components;  $LSC$  is the ratio of root conductance of the root system to plant leaf area.

state apoplastic flow are linearly related to effective pressure (Fig. 6.7); this implies (cf. Eq. 6.13 and 6.14) that cell-to-cell and apoplastic conductances are independent of pressure, and constant over the duration of the measurements.

Values of cell-to-cell and apoplastic root conductance for six cherry plants are reported in Tab. 6.1. Average apoplastic conductance is  $15.5 \times 10^{-9} \text{ m}^3 \text{ s}^{-1} \text{ MPa}^{-1}$ , with values ranging from  $12.0$  to  $18.5 \times 10^{-9} \text{ m}^3 \text{ s}^{-1} \text{ MPa}^{-1}$ ; average cell-to-cell

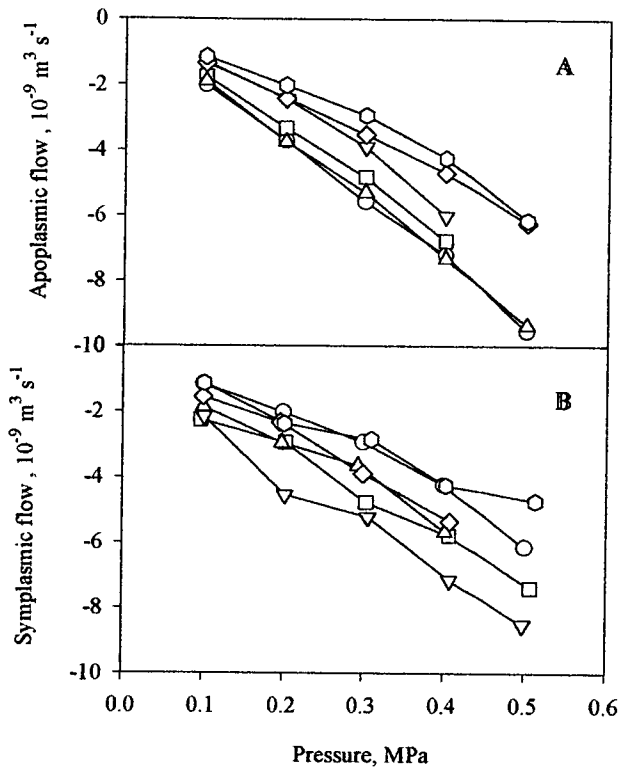


**Fig. 6.7** Plot of computed values of (A) apoplasmic flow and (B) of initial cell-to-cell flow against effective pressure (as from Eq. 6.13 and 6.14) for six young cherry trees. Apoplasmic and cell-to-cell conductances are obtained by linear regression of data from a single plant.

conductance (LSC, conductance per unit of leaf area supported) of the root systems ranges from  $2.7$  to  $5.6 \times 10^{-8} \text{ m s}^{-1} \text{ MPa}^{-1}$ , with an average of  $3.7 \times 10^{-8} \text{ m s}^{-1} \text{ MPa}^{-1}$  (Tab. 6.2).

### 6.5 Discussion

The proposed model of water movement through the root under a pressure clamp seems to explain satisfactorily the experimental observations. The model consists of two hypotheses (Fig. 6.1): (a) that the action of the semi-permeable barrier in the apical roots results in a change of solute concentration and in a decline of cell-to-cell flow that can be represented by an exponential function; and (b) that two different pathways act in parallel in the root and that the flow of water through the apoplasmic conductance is driven by purely hydrostatic forces.

conductance is  $11.7 \times 10^{-9} \text{ m}^3 \text{ s}^{-1} \text{ MPa}^{-1}$ , with values ranging from  $8.5$  to  $15.3 \times 10^{-9} \text{ m}^3 \text{ s}^{-1} \text{ MPa}^{-1}$ .

Cell-to-cell conductance amounts on average to 43 % of total root conductance; with values between 41 and 45 %. Half-times of exponential decay of cell-to-cell flow ( $T_{1/2} = 0.69 \tau$ ) range from 18 and 28 seconds (Tab. 6.1).

Root conductance is compared to structural shoot and root parameters in Tab. 6.2. Both components of root conductance are related to fine root biomass and more closely to plant leaf area, although the limited sample size does not allow significant conclusions. Leaf specific

An exponential decline of water flow under a pressure clamp has been consistently observed in the present research. This had previously been reported in pressure clamp experiments on single cells (Wendler and Zimmermann 1982, 1985; Moore and Cosgrove 1991; Zhang and Tyerman 1991), although the model then proposed predicted an exponential behaviour for an initial interval only. Mees and Weatherley (1957) observed the same transient response when the root system of tomato plants was pressurized in a pressure chamber, but were not able to explain the phenomenon and therefore neglected it.

The exponential decline observed cannot be attributed to the elastic response of the instrument. A quite large instrumental response was observed both in preliminary evaluations and during the measurements on root systems, but had a much shorter time constant and could be taken into account in analysis of the results. A very small time constant would also be expected for the elastic response of the xylem in the root system itself (Frensch and Hsiao 1993).

The presence of air bubbles, either in the instrument or in the root xylem, can also result in an apparent flow. The error resulting from bubble compression is discussed by Tyree *et al.* (1995). If we assume a negligible xylem resistance, the apparent flow should be proportional to the rate of change of applied pressure and can therefore be neglected if the first fast interval is discarded. The flow resulting from dissolution of bubbles under pressure, on the contrary, has a much longer time constant of hours (Tyree and Yang 1992).

The transient flow of water that we have attributed to an accumulation of solutes could have been the result of reversible changes in capacitance of living tissues. As a positive pressure is applied, water flows into cells until the resulting changes in osmotic pressure and cell turgor counter-balance the external pressure. This flow of water has been found to decline exponentially, both for single cells (Wendler and Zimmermann 1985) and for entire tissues (Tyree and Dainty 1973). When an estimate of root fresh volume is derived from their dry mass, it is apparent that the total amount of water moved in the transient phase could be easily accounted for by changes in living tissue capacitance in our experiment. Nevertheless, we think that this was not the case: the kinetics of capacitive exchange are always considerably slower and the time constant markedly increases with tissue length and longitudinal resistance (Tyree



*et al.* 1981; Stroshine *et al.* 1985). Similar results have been obtained by the cell pressure clamp technique. When a step pressure change is imposed, the half-time of water movement through the cell membrane is usually very long both in isolated algal cells (Wendler and Zimmermann 1982, 1985) and in shoot and root tissues (Moore and Cosgrove 1991; Zhang and Tyerman 1991), although a very short time response was observed in root tissues by Frensch and Hsiao (1993).

As already discussed, the constant flow ascribed to the apoplasmic pathway could not be attributed to leaks in the seal, which were easily detected. The model ignores for simplicity the effects of back-diffusion of solutes under the concentration gradient in the apical root compartment. Its effect would have been to maintain a non-null flow of water across the semi-permeable membrane even at equilibrium and this would have led to over-estimation of the apoplasmic flow and the corresponding conductance (Dainty 1963). The effect, however, would have been small, as it would have accounted for no more than a fraction of the initial cell-to-cell flow.

Cell-to-cell conductance amounts to about 40 % of total root conductance in cherry seedlings (Tab. 6.3). Values reported in the literature range from less than 1 % in entire root systems of *Picea abies* (Rüdinger *et al.* 1994) to 100 % in root segments of *Phaseolus coccineus* (Steudle and Brinckmann 1989) and *Hordeum distichon* (Steudle and Jeschke 1983).

The composite membrane model of the root has been proposed to explain the very low root conductances that have been observed in several species when the flow of water was driven by an osmotic pressure difference across the root, as opposed to hydraulic forces (Steudle 1993). Such differences have been observed by the pressure probe technique in maize (Steudle *et al.* 1987, 1993; Steudle and Frensch 1989; Zhu and Steudle 1991), onion (Melchior and Steudle 1993) and wheat (Jones *et al.* 1988) and they have also been reported in several tree species (Steudle 1993, 1994; Rüdinger *et al.* 1994). Comparable results have also been obtained by other techniques (Hanson *et al.* 1985; Yeo *et al.* 1987; Häussling *et al.* 1988; Radin and Matthews 1989).

Several experiments have detected an apoplasmic pathway for the flow of water and solutes where the continuity of the Casparian band is interrupted at the site of emergence of lateral roots. In *Zea mays* the entry of apoplasmic dyes into the stele was limited to lateral root initials (Peterson *et al.* 1981). The same results are reported for

*Picea abies* by Häussling *et al.* (1988); the relevance of this region of the root for water uptake was strongly affected by transpiration rate, as should be expected for an apoplastic pathway. A similar dependence was observed in roots of *Hordeum vulgare* by Sanderson (1983). No penetration of apoplastic dyes into the stele around emerging lateral roots was observed, on the contrary, in *Helianthus annuus* (Enstone and Peterson 1992) and in *Allium cepa* (Peterson and Moon 1993).

It has been suggested that, if apoplastic dyes cannot move along primary walls, their use could fail to detect an apoplastic pathway through the tip of the primary roots, where a Casparian band has not yet developed (Peterson *et al.* 1981; Häussling *et al.* 1988). Enstone and Peterson (1992) measured the diffusion of a highly mobile dye through the root tips of five exodermal and non-exodermal species; in all of them very little dye penetrated into the stele, even in the absence of a localized barrier. The restriction of tracer influx was ascribed to a high resistance to apoplastic movement in the young walls, where intermicrofibrillar spaces could have not developed yet; it is unclear if this restriction would also apply to the mass flow of the much smaller molecules of water and nutrients.

The relevance of the very tip of the root for water uptake is strongly reduced by the large axial resistance along immature xylem vessels (Frensch and Hsiao 1993; Peterson and Steudle 1993); this constraint is however limited to the first 20 mm in *Zea mays* (Frensch and Hsiao 1993), since the presence for a much greater length of immature vessels in the late metaxylem alone has little effect on water movement.

It has also been suggested (Sanderson 1983) that an apoplastic pathway could be across the suberin lamellae that are deposited inside the cells of the endodermis during the second stage of its development, and that it would be progressively occluded as waxes enter this structure. Alternative models that do not take into account the presence of an apoplastic pathway fail to explain different aspects of the observed root response. An exponential decline of water flow to a steady-state negative value is not predicted by the simple two-compartment model proposed by Fiscus (1975) and by Dalton *et al.* (1975). The three-compartment model proposed by Powell (1978), on the contrary, which assumes root conductivity to change with the turgor of endodermal cells, could explain this feature, but not the declining positive flow that was observed when the applied pressure was released.

**Table 6.3** Comparison of root hydraulic conductivity ( $L_p$ ,  $\text{m s}^{-1} \text{MPa}^{-1}$ ) and cell-to-cell hydraulic conductivity ( $L_p^{cc}$ ,  $\text{m s}^{-1} \text{MPa}^{-1}$ ) values for several species. When using the root pressure probe technique, cell-to-cell hydraulic conductivity is derived from osmotic experiments, according to the composite membrane model of the root (see text for details). For a comparison, relative values are derived for the present research from conductance measurements.

	$L_p \times 10^{-8}$ ( $\text{m s}^{-1} \text{MPa}^{-1}$ )	$L_p^{cc} \times 10^{-8}$ ( $\text{m s}^{-1} \text{MPa}^{-1}$ )	Reference
<i>Zea mays</i> ,			
seminal root	12.0 - 23.0	1.6 - 2.8	Zhu and Steudle (1991) <sup>a</sup>
segment of seminal root	4.3 - 43.8	0.2 - 5.1	Steudle and Frensch (1989) <sup>a</sup>
end segment of main root	1.2 - 4.6	0.1 - 4.5	Steudle <i>et al.</i> (1987) <sup>a</sup>
single excised root	4.18 - 9.0	2.72 - 5.5	Jones <i>et al.</i> (1988) <sup>b</sup>
segment of primary root	8.0 - 63.0	0.3 - 6.4	Steudle <i>et al.</i> (1993) <sup>a</sup>
<i>Pinus resinosa</i> ,			
entire root system		50 - 99% $L_p$	Hanson <i>et al.</i> (1985) <sup>c</sup>
<i>Picea abies</i> ,			
entire root system	4.9 - 7.8	0.002 - 0.026	Rüdinger <i>et al.</i> (1994) <sup>a</sup>
<i>Triticum aestivum</i> ,			
single excised root	5.6 - 11.8	3.6 - 7.0 <sup>c</sup>	Jones <i>et al.</i> (1988) <sup>b</sup>
<i>Phaseolus coccineus</i> ,			
segment of seminal root	2.7 - 6.8	1.8 - 8.4	Steudle and Brinckmann (1989) <sup>a</sup>
<i>Hordeum distichon</i> ,			
single excised root	0.4 - 1.3	0.5 - 4.3	Steudle and Jeschke (1983) <sup>a</sup>
<i>Prunus avium</i> ,			
entire root system		40.8 - 45.2% $L_p$	this paper <sup>d</sup>

<sup>a</sup> based on root pressure probe measurements, pressure relaxation and osmotic experiments

<sup>b</sup> total conductance measured with a back-flow technique; cell-to-cell conductance computed from cell pressure probe measurements

<sup>c</sup> estimated from dye absorption

<sup>d</sup> based on pressure probe measurements, pressure clamp experiments

The proposed model rests the assumption that the movement of solutes along the apoplasmic pathway does not affect the osmotic pressure acting across the cell-to-cell pathway; if the apoplasmic path is located either in root tips or in by-passes around the

Casparian band this view should probably be modified to take into account the process of solvent drag, as in the model outlined by Steudle (1992). The inclusion in the model of other processes such as solute diffusion, permeation and active transport (Molz and Ferrier 1982; Katou and Taura 1989; Steudle 1992), although realistic, would make it more difficult to evaluate the higher number of parameters involved.

The presence of a pathway for water and solute flow not bounded by a semi-permeable barrier has important ecophysiological implications. Solutes could enter the root by solvent-drag with the transpiration stream at no metabolic cost and with no concentration polarization effects at the endodermis even at high transpiration rates. The presence of an important apoplasmic path could also explain the absence of root pressure in some species (Rüdinger *et al.* 1994), since it would permit a reverse flow of water out of the root system into the soil as soon as solutes accumulate in the stele.

This enhanced reverse flow of water into the superficial soil could play a role in the phenomenon of so-called 'hydraulic lift' (Dawson 1993), in which water is absorbed at night by roots in moister deep horizons and released into superficial soil, where it is available for later use by the plant itself or its neighbours (Passioura 1988).

Fine root area was not measured in the present research, so a direct comparison with hydraulic conductivity values reported in the literature is not possible. When root conductance (sum of cell-to-cell and apoplasmic components) is related to plant leaf area, the resulting values of *LSC* (Tab. 6.2) are in very good agreement with those obtained for adult *Juglans regia* trees by a different technique (Tyree *et al.* 1994); similar results can be computed for *Picea abies* seedlings from the data reported by Rüdinger *et al.* (1994). Under steady-state transpiration, the water potential drop across the root system is equal to the transpiration flux (per unit leaf area) divided by the leaf specific conductance of the root; the observed constancy of *LSC* in different species has therefore important ecophysiological implications.

The proposed pressure clamp technique presents some advantages over other methods available for the measurement of root hydraulic conductance and its components. The use of the root pressure probe allows measurement of root conductance alone, without the effects of soil resistance (Steudle 1989). The measurement of cell-to-cell and apoplasmic components of root conductance with the pressure probe by the pressure relaxation method (Steudle *et al.* 1987) is based on the comparison of the results

obtained when applying either a hydrostatic or an osmotic driving force; osmotic experiments, however, require circulation of a solution of known osmotic pressure through the rooting medium and are suitable for root systems grown in hydroponics, but are difficult to apply to potted plants (Rüdinger *et al.* 1994) and are impossible in the field.

The pressure clamp technique, on the contrary, allows straightforward estimation of the two components. The technique had already been applied to root systems on a few occasions (Steudle and Jeschke 1983; Steudle and Frensch 1989) but appeared to be best suited for small cells (Wendler and Zimmermann 1985).

The instrument devised is simple and easily automated and seems to be best suited for use with the pressure clamp technique. The use on large seedlings requires an instrument of relatively large internal volume and this results in a considerable elastic response ( $\Delta V/\Delta P = 0.24 \times 10^{-6} \text{ m}^3 \text{ MPa}^{-1}$ , as compared to  $0.14 \times 10^{-8} \text{ m}^3 \text{ MPa}^{-1}$  for the root pressure probe applied by Steudle *et al.* (1987) on single apical segments of maize roots). We have demonstrated, however, that the elastic response of the instrument can be measured and taken into account and that it does not affect the validity of the results, as already suggested by Rüdinger *et al.* (1994) for the pressure relaxation technique.

Root cell-to-cell conductance can be evaluated by both application and release of pressure. The two estimates are generally in good agreement (data not shown), but for pressure release the instrumental error is larger because the whole chamber contracts, resulting in an apparent flow across the fine tube; as a consequence it is sometimes impossible to obtain accurate data. This demonstrates the utility of pressurization of the instrument prior to measurements.

The root pressure clamp technique, on the other hand, does not allow estimation of the solute exchange parameters that can be evaluated by the pressure relaxation technique (Steudle and Frensch 1989).

The proposed technique will be used to investigate the effects of drought and elevated CO<sub>2</sub> on the root conductance of *Prunus avium* and the implications of the composite membrane model for root pressure development and xylem refilling in adult *Pinus sylvestris* trees under field conditions.

## Acknowledgements

I gratefully thank Dr. Mauro Centritto (CNR-IBEV, Italy) for providing the plant material and measuring the biomass of root systems.

## References

- Alm DM, Cavelier J, Nobel PS (1992) A finite-element model of radial and axial conductivities for individual roots: development and validation for two desert succulents. *Ann Bot* 69: 87-92
- Dainty J (1963) Water relations of plant cells. *Adv Bot Res* 1: 279-326
- Dainty J (1985) Water transport through the root. *Acta Hort* 171: 21-31
- Dalton FN, Raats PAC, Gardner WR (1975) Simultaneous uptake of water and solutes by plants. *Agron J* 67: 334-339
- Dawson TE (1993) Hydraulic lift and water use by plants: implications for water balance, performance and plant-plant interactions. *Oecologia* 95: 565-574
- Enstone DE, Peterson CA (1992) The apoplastic permeability of root apices. *Can J Bot* 70: 1502-1512
- Fiscus EL (1975) The interaction between osmotic- and pressure-induced water flow in plant roots. *Plant Physiol* 55: 917-922
- Frensch J, Hsiao TC (1993) Hydraulic propagation of pressure along immature and mature xylem vessels of roots of *Zea mays* measured by pressure-probe techniques. *Planta* 190: 263-270
- Hanson PJ, Sucoff EI, Markhart III AH (1985) Quantifying apoplastic flux through red pine root systems using Trisodium, 3-hydroxy-5,8,10-pyrenetrisulfonate. *Plant Physiol* 77: 21-24
- Häussling M, Jorns CA, Lehmbecker G, Hecht-Buchholz C, Marschner H (1988) Ion and water uptake in relation to root development in Norway spruce (*Picea abies* (L.) Karst.). *J Plant Physiol* 133: 486-491
- Johnson ML, Faunt LM (1992) Parameter estimation by least-squares methods. *Methods Enzymol* 210: 1-37
- Jones H, Leigh RA, Jones RGW, Tomos AD (1988) The integration of whole-root and cellular conductivities in cereal roots. *Planta* 174: 1-7
- Katou K, Taura T (1989) Mechanism of pressure-induced water flow across plant roots. *Protoplasma* 150: 124-130
- Kedem O, Katchalsky A (1963) Permeability of composite membranes. Part 1. Electric current, volume flow and flow of solutes through membranes. *Trans Faraday Soc* 59: 1918-1930
- Landsberg JJ, Fowkes ND (1978) Water movement through plant roots. *Ann Bot* 42: 493-508
- Magnani F, Borghetti M (1995) Interpretation of seasonal changes of xylem embolism and plant hydraulic resistance in *Fagus sylvatica*. *Plant Cell Environ* 18: 689-696
- Mees GC, Weatherley PE (1957) The mechanism of water absorption by roots. I. Preliminary studies on the effects of hydrostatic pressure gradients. *Proc Roy Soc London Series B* 147: 367-380
- Melchior W, Steudle E (1993) Water transport in onion (*Allium cepa* L.) roots. *Plant Physiol* 101: 1305-1315

- Molz FJ, Ferrier JM (1982) Mathematical treatment of water movement in plant cells and tissues: a review. *Plant Cell Environ* 5: 191-206
- Moore PH, Cosgrove DJ (1991) Developmental changes in cell and tissue water relations parameters in storage parenchyma of sugarcane. *Plant Physiol* 96: 794-801
- Passioura JB (1982) Water in the soil-plant-atmosphere continuum. In: Lange OL, Nobel PS, Osmond CB, Ziegler H (eds) *Encyclopedia of plant physiology*. New series. Vol. 12B. *Physiological plant ecology II*. Springer-Verlag, Berlin, pp 5-33
- Passioura JB (1988) Water transport in and to roots. *Annu Rev Plant Physiol* 39: 245-265
- Peterson CA, Emanuel ME, Humpreys GB (1981) Pathway of movement of apoplastic fluorescent dye tracers through the endodermis at the site of secondary root formation in corn (*Zea mays*) and broad bean (*Vicia faba*). *Can J Bot* 59: 618-625
- Peterson CA, Moon GJ (1993) The effect of lateral root outgrowth on the structure and permeability of the onion root exodermis. *Bot Acta* 106: 411-418
- Peterson CA, Steudle E (1993) Lateral hydraulic conductivity of early metaxylem vessels in *Zea mays* L. roots. *Planta* 189: 288-297
- Powell DBB (1978) Regulation of plant water potential by membranes of the endodermis of young roots. *Plant Cell Environ* 1: 69-76
- Radin JW, Matthews MA (1989) Water transport properties of cortical cells in roots of nitrogen- and phosphorus-deficient cotton seedlings. *Plant Physiol* 89: 264-268
- Rüdinger M, Hallgren SW, Steudle E, Schulze E-D (1994) Hydraulic and osmotic properties of spruce roots. *J Exper Bot* 45: 1413-1425
- Sanderson J (1983) Water uptake by different regions of the barley root. Pathways of radial flow in relation to development of the endodermis. *J Exp Bot* 34: 240-253
- SAS Institute Inc (1988) SAS/STAT user's guide, release 6.03 edition. SAS Institute Inc, Cary, NC
- Schulze E-D, Robichaux RH, Grace J, Rundel PW, Ehleringer JR (1987) Plant water balance. *BioScience* 37: 30-37
- Steudle E (1989) Water transport in roots. In: Loughman BC *et al.* (eds) *Structural and functional aspects of transport in roots*. Kluwer Academic Publ., Dordrecht, pp 139-145
- Steudle E (1992) The biophysics of plant water: compartmentation, coupling with metabolic processes, and flow of water in plant roots. In: Somero GN *et al.* (eds.) *Water and life: comparative analysis of water relationships at the organismic, cellular, and molecular levels*. Springer-Verlag, Heidelberg, pp 173-204
- Steudle E (1993) Pressure probe techniques: basic principles and application to studies of water and solute relations at the cell, tissue and organ level. In: Smith JAC, Griffiths H (eds) *Water deficits. Plant responses from cell to community*. Bios Science Publ., Oxford, pp 5-36
- Steudle E (1994) Water transport across roots. *Plant Soil* 167: 79-90
- Steudle E, Brinckmann E (1989) The osmometer model of the root: water and solute relations of roots of *Phaseolus coccineus*. *Bot Acta* 102: 85-95
- Steudle E, Frensch J (1989) Osmotic responses of maize roots. Water and solute relations. *Planta* 177: 281-295
- Steudle E, Jeschke WD (1983) Water transport in barley roots. *Planta* 158: 237-248
- Steudle E, Murrmann M, Peterson CA (1993) Transport of water and solutes across maize roots modified by puncturing the endodermis. *Plant Physiol* 103: 335-349

- Steudle E, Oren R, Schulze E-D (1987) Water transport in maize roots. *Plant Physiol* 84: 1220-1232
- Stroshine RL, Rand RH, Cooke JR, Cutler JM, Chabot JF (1985) An analysis of resistance to water flow through wheat and tall fescue leaves during pressure chamber efflux experiments. *Plant Cell Environ* 8: 7-18
- Tyree MT, Cruiziat P, Benis M, LoGullo MA, Salleo S (1981) The kinetics of rehydration of detached sunflower leaves from different initial water deficits. *Plant Cell Environ* 4: 309-317
- Tyree MT, Dainty J (1973) The water relations of hemlock (*Tsuga canadensis*). II. The kinetics of water exchange between the symplast and the apoplast. *Can J Bot* 51: 1481-1489
- Tyree MT, Patino S, Bennink J, Alexander J (1995) Dynamic measurements of root hydraulic conductance using a high-pressure flowmeter in the laboratory and field. *J Exp Bot* 46: 83-94
- Tyree MT, Yang S (1992) Hydraulic conductivity recovery versus water pressure in xylem of *Acer saccharum*. *Plant Physiol* 100: 669-676
- Tyree MT, Yang S, Cruiziat P, Sinclair B (1994) Novel methods of measuring hydraulic conductivity of tree root systems and interpretation using AMAIZED. *Plant Physiol* 104: 189-199
- Weatherley PE (1982) Water uptake and flow in roots. In: Lange OL, Nobel PS, Osmond CB, Ziegler H (eds) *Encyclopedia of plant physiology*. New series. Vol. 12B. *Physiological plant ecology II*. Springer-Verlag, Berlin, pp 79-109
- Wendler S, Zimmermann U (1982) A new method for the determination of hydraulic conductivity and cell volume of plant cells by pressure clamp. *Plant Physiol* 69: 998-1003
- Wendler S, Zimmermann U (1985) Determination of the hydraulic conductivity of *Lamprothamnium* by use of the pressure clamp. *Planta* 164: 241-245
- Yeo AR, Yeo ME, Flowers TJ (1987) The contribution of an apoplastic pathway to sodium uptake by rice roots in saline conditions. *J Exp Bot* 38: 1141-1153
- Zhang WH, Tyerman SD (1991) Effect of low O<sub>2</sub> concentration and azide on hydraulic conductivity and osmotic volume of the cortical cells of wheat roots. *Aust J Plant Physiol* 18: 603-613
- Zhu GL, Steudle E (1991) Water transport across maize roots. *Plant Physiol* 95: 305-315



## Chapter 7. General discussion

I seem to have been only like a boy playing on the seashore, and diverting myself in now and then finding a smoother pebble or a prettier shell than ordinary, whilst the great ocean of truth lay all undiscovered before me.

Sir Isaac Newton

### 7.1 Introduction

Stand growth is the final result of several interconnected processes: assimilation, respiration, resource allocation, tissue and tree mortality. Over the last decades most ecophysiological research has focused on the processes of light absorption and photosynthesis, mainly because of the key role of gross primary production as the first determinant of growth, but also because of the difficulty in accessing and measuring processes such as phloem transport and allocation, heartwood formation and fine root mortality. As a result, it has been often suggested that research could focus on gross primary production alone, and that processes like allocation and autotrophic respiration could be treated as constant or easily estimated (Mäkelä 1986; Raich & Nadelhoffer 1989; Waring, Landsberg & Williams 1998).

Such an extreme view, however, has been questioned (Medlyn & Dewar 1999; Gower, Pongracic & Landsberg 1996). When a sufficiently large data-set is considered it is indeed apparent that allocation cannot be treated as constant but is highly variable, as a function of both age and environment, with a clear trade-off between stemwood and fine root production (Santantonio 1989).

Moving from this background, the objective of the present work was to present and test a novel hypothesis (Chapter 2), based on the assumption of functional homeostasis in water transport, that could help explain the response of allocation to age and the environment (Chapter 3-4), and to apply this new approach to improve existing process models of forest function and growth. The resulting simulation model was then tested against available experimental evidence and applied to explore the growth of *P. sylvestris*, a key European forest species, along a regional transect (Chapter 5).

The functional approach adopted allowed us to go beyond prediction of forest growth, to probe the possible underlying mechanisms and their responses to key environmental factors. A preliminary sensitivity analysis also allowed us to identify critical model parameters, root hydraulic conductivity in particular (data not shown). A new methodology was therefore developed for the experimental determination of this sensitive parameter under field conditions (Chapter 6).

In this chapter, some of the most interesting insights in forest function provided by the Hydrall model will be summarized, together with a few important gaps in present knowledge that were highlighted by model simulations. The critical assumptions of the hypothesis will be then discussed. Some of the limitations of the model in its present form will also be identified, and possible ways to overcome them will be eventually proposed.

## 7.2 Summary of key results

The commonly observed decline in forest aboveground net primary production ( $P_a$ ) in ageing stands is the result not only of reduced stand leaf area index and light interception, but also of a shift in resource allocation towards root production, as demonstrated by a review of literature data from several Scots pine chronosequences (Chapter 3). The fraction of  $P_a$  accounted for by new foliage production also decreases with age, leading to a continuous decline in the leaf-to-sapwood area ratio, contrary to the predictions of the so-called pipe model theory (Shinozaki *et al.* 1964; Margolis *et al.* 1995).

Such developmental changes in plant allometry are well accounted for by the hypothesis of optimal growth under hydraulic constraints (Chapter 2). The hypothesis is based on the assumption that homeostatic processes effectively maintain the water potential experienced by the leaves within a safety range, possibly dictated by the risk of destructive xylem embolism, irrespective of tree height and environmental conditions. A review of literature data has indeed demonstrated such a general homeostasis for *P. sylvestris* (Chapter 4).

According to the new hypothesis, a central role in age-related growth dynamics would be played by tree height rather than age *per se*; a comparison of two Scots pine chronosequences exposed to the same climatic conditions but differing in their height

growth dynamics seems to support this view (Chapter 3). A better understanding of height growth processes is therefore needed (Mäkelä & Sievänen 1992). The dynamics of xylem cell maturation could also play an important role and explain important differences between coniferous species (Chapter 2).

Of great relevance is also the observation of a strong interaction between age and the environment: the productivity decline with age is much more pronounced and takes place earlier in stands growing under more favourable conditions, as demonstrated by a comparison between British and Scandinavian chronosequences in Fig. 3.1. This interaction is well captured by the Hydrall model: faster height increments under milder climates are expected to exacerbate hydraulic limitations, thus increasing belowground allocation and reducing foliage production and light interception. This is reflected in model predictions for the regional transect analyzed in Chapter 5 (Fig. 5.7): curves of height and total volume development do not run parallel to each other, but cross and diverge.

Such a feed-back mechanism would have profound implications for the response of forest growth to climate change, as earlier maturation and senescence could largely offset the increase in productivity induced by higher CO<sub>2</sub> concentrations and temperatures. Medium-term experimental evidence from open-top chamber studies seems to support this view: faster initial growth rates under enriched conditions are indeed offset to a large extent by higher belowground allocation (Jarvis 1998).

The observation that minimum leaf water potentials are apparently not affected by elevated CO<sub>2</sub> and temperature (Kellomäki & Wang 1996) lends support to the view that such structural changes could be in fact the result of hydraulic limitations, as hypothesized in the Hydrall model.

Model predictions of the response of allocation and plant structure to other environmental variables are also generally consistent with experimental evidence reported in the literature, as discussed in Chapter 4 and 5. This rather thorough review, however, has highlighted the general lack of studies on the effects of individual environmental factors. Only a few studies have analyzed the response of allocation and plant structure to controlled conditions in coniferous seedlings. The information available for mature trees is even more scarce and commonly refers to broad climatic gradients, making it difficult to discriminate the effects of individual factors.

Functional models are the only suitable tool for analysis and interpretation of this kind of information, provided that all the relevant boundary conditions are duly considered. This illustrates the need to develop the Hydrall model to take into account the effects of nitrogen and nutrients in general, which are known to play a central role in forest growth.

Bearing these limitations in mind, the application of the Hydrall model over a regional transect has provided some interesting insights into forest response to climate (Chapter 5). As predicted by most models (Brey Meyer *et al.* 1996), reduced growth rates at high latitudes are mainly the result of low temperatures in the spring and in the autumn, which shorten the growing season and strongly inhibit the photosynthesis of older needles; the effect on gross primary production is only partly counterbalanced by reduced respiration rates. More interestingly, the results of the Hydrall model highlight the relevance of changes in resource allocation under warm and dry conditions, such as the ones experienced at the south-eastern European limit of the natural range. The response of the plant to water stress (demonstrated in Table 5.3 by increasing values of the ratio of potential evapotranspiration to precipitation) consists largely in an increased allocation of resources belowground, at the expense of wood and foliage production. The ensuing reduction in stand leaf area index (data not shown) combines with partial stomatal closure and results in a considerable decline in stand transpiration (Table 5.3), despite the higher transpirational demand. Stand gross primary production is less affected, on the contrary, because of higher water-use efficiency (a well-known response to stomatal closure; Jones 1992) and of reduced foliage self-shading.

While most forest growth models have been developed with boreal conditions in mind, there is clearly a need for greater attention to other climates, where different functional processes could play a dominant role and new modelling perspectives could be therefore needed.

Greater attention should also be paid to belowground processes: not only fine root growth and mortality, but also root hydraulic characteristics, which play an important role in the maintenance of functional homeostasis. It is hoped that the new technique presented in Chapter 6 for the measurement of the hydraulic conductance of plants rooted in the soil will prove useful in expanding this area of research. The technique

also allows us to quantify the apoplastic contribution to total root conductance, which could help explain the limited root pressure often observed in woody plants, especially conifers (Kramer & Boyer 1995). The lack of a root pressure capable of refilling any embolised xylem would make a strategy of cavitation avoidance all the more important for the plant.

In conclusion, there appears to be a good agreement between model predictions and experimental data. This, however, cannot be seen as a *definitive proof* of the hypothesis of optimal growth under hydraulic constraints, for as Popper pointed out, hypotheses cannot be proved but only supported or falsified (Popper 1972). There is clearly a need to test the model for other coniferous species, so as to falsify and eventually refine it. Alternative hypotheses have been proposed in the literature to explain both resource allocation (Wilson 1988; Cannell & Dewar 1994) and developmental changes in forest stand productivity (Gower, McMurtrie & Murty 1996; Ryan, Binkley & Fownes 1997), focusing on the effects of nutrient availability and stomatal control of gas-exchange. At present, such alternative mechanisms are explicitly excluded in the Hydrall model, which focuses for the sake of clarity on the effects of hydraulic limitations on allocation alone. These perspectives, however, should be viewed not as alternative but as complementary, different mechanisms possibly playing a central role under different conditions. Future efforts will therefore try to combine these different approaches, as outlined in Paragraphs 7.5 and 7.6.

### **7.3 Functional homeostasis in water transport and optimal growth: a critique**

The newly proposed approach to the representation of resource allocation is based on the hypothesis that a functional homeostasis exists in plant water relations (Chapter 2 and 4); this implies that a finely-tuned balance is maintained between the hydraulic properties of the soil and the conductive tissues in the plant, on the one hand, and soil water potential, foliage biomass and transpiration on the other. When combined with the assumption of optimal plant growth, these hydraulic limitations enable to predict the allocation of resources among foliage, sapwood and fine roots, which over time determines the functional allometry of the plant.

Our ability to predict the dynamics of resource allocation has been hampered by a general lack of understanding of the mechanisms driving phloem loading and

transport, as well as sink strength and carbon utilization (Mäkelä & Sievänen 1987; Cannell & Dewar 1994). The top-down approach proposed allows to circumvent this problem, moving from the observation of the emergent properties of the system to infer the behaviour and the interplay of its parts (Magnani & Grace 1999).

The assumption of homeostasis and optimal behaviour is undoubtedly questionable, under both a theoretical and an empirical point of view. Optimality is generally thought of as being always sought but never completely achieved in the dynamic game of evolution (Parker & Maynard Smith 1990). Moreover, it remains unclear whether a static or a dynamic adjustment should be expected, i.e. whether adaptation or acclimation predominates in nature (as discussed in Chapter 5). Empirical evidence, on the other hand, demonstrates that the assumption of full homeostasis in water transport is not generally met (Irvine *et al.* 1998). Rather, homeostatic processes tend to counter-balance the effect of external factors, whose impact is only contained but never completely offset.

These limitations will be hopefully overcome by future mechanistic models of resource allocation. It should be recognized, however, that a top-down approach such as the one proposed has a marked advantage over more detailed mechanistic schemes: simplicity. The number of parameters needed by the model is kept to a minimum, a crucial point when a model has to be applied at the regional level. Moreover, the parameters can be easily measured under field conditions or derived from the literature, making it possible to parameterize the model for mature trees and a wide range of species. The only notable exception is indeed root hydraulic conductance, which according to the new hypothesis would play a central role in functional homeostasis and plant growth, as further discussed below. To date this parameter has been studied on just a few species and most commonly on potted or hydroponically grown plants (Sands, Fiscus & Reid 1982; Smit-Spinks, Swanson & Markhart III 1984; Steudle & Meshcheryakov 1996; Steudle & Heydt 1997). It is hoped that the newly developed technique will help overcome these limitations.

From simplicity also comes hindsight. A simple scheme amenable to analytical solution makes it possible to understand the system, rather than simply relying on numerical simulations for the prediction of its behaviour.

Eventually, the discovery of functional homeostasis in water transport will provide an

additional criterion for the falsification of alternative functional hypotheses on sink strength and phloem transport. Magnani and Grace (2000) have demonstrated for example that functional homeostasis in water transport is compatible with the allocation model proposed by Dewar (1993) but apparently not with the scheme outlined by Komor (1994).

#### **7.4 Hydraulic limitations and tree function: model comparison**

The effects of hydraulic limitations resulting from tree height or high transpiration rates have been included explicitly or implied in several models of forest function.

A hydraulic constraint on carbon allocation is implicitly assumed, for example, in the plant growth model proposed by Dewar (1993). This interesting quasi-mechanistic model recognizes that higher transpiration rates result in more negative leaf water potentials, so restricting foliage growth and reducing the shoot:root ratio of the plant. Such a structural change, in turn, would reduce the total hydraulic resistance per unit foliage biomass of the plant and help re-establish a homeostatic balance in water relations, as discussed by Magnani and Grace (1999). Only a leaf and a root compartment, however, are considered in the model; any effects of stem length on xylem hydraulic resistance are therefore disregarded. Aboveground hydraulic conductance per unit foliage biomass is assumed to be constant, contrary to available experimental evidence for forest trees (Mencuccini & Grace 1996). As a result, the potential role of hydraulic limitations in the developmental pattern of productivity is not recognized.

The implications of stem length and resistance are duly recognized, on the contrary, in the canopy gas-exchange model proposed by Williams *et al.* (1996). Functional homeostasis is assumed to be achieved through the stomatal control of transpiration, triggered by negative leaf water potentials. A similar effect of stem length on canopy gas-exchange is implicitly assumed in the MBL-GEM forest growth model (Rastetter *et al.* 1991; Ryan *et al.* 1996). Foliage photosynthetic capacity is assumed to be modulated by tissue nitrogen concentration (Field & Mooney 1986), which in turn is determined by the exchange of carbon and nitrogen between foliage and roots. Resource translocation within the plant is represented in MBL-GEM by a scheme similar to the one first suggested by Thornley (1972): the flux is determined as the

ratio between the standing concentration gradient between the two compartments and an empirical resistance to carbon and nitrogen exchange, which is assumed to be linearly related to stem length. Foliage and roots would be therefore more strongly decoupled in tall trees and this, according to Mäkelä and Sievänen (1987), would result in a decline in tissue nitrogen content, which would eventually reduce leaf photosynthetic capacity and canopy net primary production.

The most complete, albeit empirical, description of the effects of hydraulic limitations on forest function and growth is to be found in the 3PG model proposed by Landsberg and Waring (1997). An empirical reduction coefficient is introduced to represent the detrimental effects of age *per se* on stomatal conductance and assimilation. Moreover, the fraction of growth allocated belowground is assumed to increase from a value of 0.2 to 0.8 (even under conditions of optimum nutrition) as age and other environmental factors reduce stomatal conductance and photosynthesis from their maximum potential value to zero.

High vapour pressure deficits, for example, are predicted to induce stomatal closure and to result at the same time in greater belowground allocation, in agreement with the hypothesis of functional homeostasis (Chapter 4). According to the 3PG model, however, soil dryness would affect to the same extent gas-exchange and allocation, whilst a strong interaction with soil texture is predicted by the Hydrall model, root production being strongly enhanced in coarse-textured soils. Moreover, no direct effects of soil and air temperature on either assimilation or allocation are considered in 3PG, contrary to available experimental evidence (Wilson 1988).

Similar conclusions can be drawn, however, from the two models: the shift towards greater belowground allocation in response to stress conditions is predicted to reinforce the effects of gas-exchange limitations on aboveground productivity. Figure 5.9 demonstrates this point for the Hydrall model: allocation to fine root production is lowest at the most favourable sites, where a peak in gross primary production is also observed. A notable exception is the northernmost site, where lower values of belowground allocation are predicted.

The comparison of the 3PG and the Hydrall model highlights three interesting areas of investigation and future model development. The representation of developmental changes is based in the 3PG model on a purely empirical approach: age rather than



height is assumed as a driving variable, so excluding any interaction with climatic conditions. In the Hydrall model, on the contrary, age and climate strongly interact, with accelerated dynamics under more favourable conditions. This seems to be consistent with experimental data (as discussed in Chapter 3), but further evidence will be needed to answer this important question.

The proposed hypothesis of functional homeostasis, on the other hand, excludes any direct effects of hydraulic limitations on stomatal conductance and gas-exchange. Although largely appropriate in the case of Scots pine, this could not be so for other coniferous species (Yoder *et al.* 1994; Walcroft *et al.* 1996; Alsheimer *et al.* 1998). Indeed, an optimal strategy of growth under hydraulic constraints would be expected to combine stomatal and structural changes, as a partial stomatal closure would allow the plant to reduce the investment in transport tissues and divert more resources to the production of more photosynthesizing foliage. A possible approach to represent such an optimal combined strategy will be described below.

What is even more important, the effects of nutrient availability are completely disregarded at present in the Hydrall model. This strongly limits the generality of the model, as soil fertility plays a central role in forest growth, in boreal ecosystems in particular (Gholz, Linder & McMurtrie 1994). Efforts are under way to expand the homeostatic approach applied in the Hydrall model to include the effects of soil nutrient availability, as outlined in the following paragraphs.

### **7.5 Future developments: optimal stomatal conductance and allocation under hydraulic constraints**

Both the hydraulic structure of the plant and maximum stomatal conductance have been reported to vary in ageing stands. Hydraulic limitations have been invoked to explain both phenomena (Chapter 2; Ryan, Binkley & Fownes 1997), since extremely negative (and potentially harmful) water potentials could be prevented both by stomatal limitations and by a shift of resources from transpiring foliage to transport tissues in the shoot and in the roots. The interaction between stomatal and structural mechanisms, however, has never been explored.

It is reasonable to assume that the plant has evolved an optimal strategy in order to maximize growth whilst preventing xylem cavitation and foliage die-back, through a

combination of stomatal regulation and structural adjustments.

Stomatal closure, on the one hand, could prevent extreme water potentials, but at the cost of lower intercellular CO<sub>2</sub> concentrations and reduced photosynthesis. This positive dependence of assimilation upon stomatal conductance can be viewed as an “assimilation constraint” on stomatal opening (fully equivalent to the “photosynthetic demand function” in Leuning 1990; 1995).

The construction of additional transport tissues, on the other hand, would enable the plant to maintain higher values of stomatal conductance and assimilation, but would require a greater investment in transport tissues. The amount of sapwood and fine roots that has to be produced to supply with water a unit of foliage, in order to prevent extreme water potentials, will be itself an increasing function of transpiration rates and stomatal conductance (Eq. 2.18 and 2.19). The production and maintenance cost of this transport structure will determine a second “hydraulic constraint” on stomatal opening.

An optimal strategy would maximize the net return from each unit of carbon invested in foliage growth, i.e. the difference between the amount of carbon assimilated by the leaf over its lifetime and the total production costs imposed by the need to avoid xylem cavitation. This will require a combination of stomatal and structural acclimation: as the plant grows taller both stomatal conductance and the ratio between transpiring foliage and conducting tissues will have to be reduced, as indeed suggested by experimental evidence (Chapter 3; Yoder *et al.* 1994).

### **7.6 Future developments: combining hydraulic and nutrient constraints**

Although Nadelhoffer *et al.* (1999) have cast doubts on the importance of nitrogen for forest growth, several studies (on *P. sylvestris* as well as other coniferous and broadleaf species) strongly suggest that growth is often limited by nutrient availability (Axelsson & Axelsson 1986; Linder & Rook 1984; McDonald & Davies 1996). Fertilization commonly results both in higher foliar nitrogen concentrations and faster assimilation rates (Field & Mooney 1986) and in reduced resource allocation to fine root production (Wilson 1988). Nutrient limitations have been suggested as a possible reason for the commonly observed age-related decline in productivity (Gower, McMurtrie & Murty 1996). Moreover, several studies have suggested that a crucial

role in the response of forest ecosystems to climate change could be played by the interaction between carbon and nitrogen dynamics (Kirschbaum *et al.* 1994; Curtis & Wang 1998; Stitt & Krapp 1999; but see Lloyd & Farquhar 1996 for a different opinion). Higher initial growth rates would result in a larger fraction of available nutrients being sequestered in living and dead biomass, so worsening stand nutrient limitations and accelerating the age-related decline in productivity. At the same time litter quality would be reduced by higher carbon and lower nutrient availability, resulting in slower decomposition rates that would aggravate the trend. Nitrogen availability, in summary, would play a homeostatic role similar to the one attributed to hydraulic limitations in the Hydrall model.

The effect of nutrient limitations is not presently considered in the Hydrall model. This could severely limit its ability to predict the growth of forest species on poor soils, although the effects of soil characteristics are already partly accounted for through their effects on soil hydraulic and water retention properties (Campbell 1985).

The hypothesis of homeostasis in water transport could be extended to take other resources, primarily nitrogen, into consideration. Two alternative approaches will be explored, as shortly outlined hereafter.

### 7.6.1 Functional balance in carbon and nutrient uptake

Quite early on, we see in the literature the idea of the plant as a wise investor, able to allocate resources to above- and below- ground organs in an optimal manner (Brenchley 1916; Blackman 1919). For example, Brenchley wrote "the plant makes every endeavor to supply itself with adequate nutrients and ...when the food supply is low, it strives to make as much root as possible". The idea of internal coordination resulting in a functional balance between absorbing roots and assimilating foliage was later formalized by Davidson (1969) as:

$$(W_r \cdot \alpha_r) = \pi \cdot (W_f \cdot \alpha_f) \quad (7.1)$$

where  $W_r$  and  $W_f$  are fine root and foliage biomass,  $\alpha_r$  and  $\alpha_f$  represent their activity in photosynthesis and nutrient uptake, respectively, and  $\pi$  is a proportionality coefficient.

The principle of functional balance in carbon and nutrient uptake has since been a central paradigm in the study of allocation response to nutrient availability (Cannell & Dewar 1994).

Under given environmental conditions, Equation 7.1 dictates the allometric balance between absorbing roots and photosynthesizing foliage, so imposing an additional constraint on resource allocation. According to the hypothesis of functional homeostasis in water transport, on the other hand, any changes in the ratio between foliage and absorbing roots would have to be balanced by sapwood production, so as to prevent the onset of extreme water potentials. In summary, the combination of hydraulic and nutrient constraints would fully determine the allocation of resources among foliage, sapwood and fine roots, without any need to assume that evolution has resulted in optimal plant behaviour.

The implications of the hypothesis of balanced activity can be easily understood: any environmental factor reducing root activity  $\alpha_r$  more than leaf photosynthesis would lead to increased belowground allocation. The effects of nutrient availability and shading would be therefore well explained by the hypothesis (Wilson 1988). In both cases, allocation to foliage would increase at the expenses of root growth. It remains to be seen whether the response of allocation to other environmental factors is consistent with the hypothesis of balanced activity. Drought is known to restrict nutrient supply and therefore root activity in nutrient uptake. It has also been suggested that this reduced availability of nutrients could lie behind the detrimental effects of drought on growth (Chapin 1991). Water availability has been indeed reported to have but a marginal effect on tissue nitrogen concentration, despite its large impact on carbon accumulation (Kramer & Boyer 1995). Balanced activity could also explain the response of allocation to atmospheric CO<sub>2</sub>: an increased allocation belowground has been often reported (Wilson 1988; Ceulemans & Mousseau 1994), although Eamus and Jarvis (1989) warned that such an effect is often not apparent when the plants are supplied with an adequate amount of nutrients.

High nutrient availability would be also expected to result in lower foliage-to-sapwood area ratios, by a combination of two mechanisms: enhanced fine root activity would reduce  $W_r$ , and fine root hydraulic conductance, leading to a compensatory increase in sapwood area. Moreover, according to the hypothesis of homeostasis in water

transport, the faster height increments commonly observed on fertile sites would also speed up the decline in the foliage-to-sapwood area ratio described in Chapter 3. The two effects have not yet been studied independently.

### **7.6.2 Effects of nitrogen on leaf and root function**

Thornley (1975) first demonstrated that the assumption of a functional balance in nutrient and carbon uptake also implies a constant nitrogen concentration in plant tissues, as discussed more recently by Cannell and Dewar (1994). Available experimental evidence, on the other hand, shows that tissue nitrogen content does change quite considerably in response to fertilization (Ågren 1985). At the leaf level this has a marked effect on potential assimilation (Field & Mooney 1986; Vapaavuori *et al.* 1995) as well as on leaf structure (Palomäki & Holopainen 1995). Tissue respiration is also known to be generally correlated with nitrogen content (Ryan 1991). Nitrogen availability, moreover, has a substantial effect also on root hydraulic conductance. This seems to result not from a change in root structure and specific root length (George *et al.* 1997), but from higher specific conductivities in fertilized plants (Radin & Matthews 1989; Radin 1990; Steudle & Meshcheryakov 1996). Nitrogen and phosphorus availability has been proved to affect the fluidity of plasma membranes (Carvajal, Cooke & Clarkson 1996a) and to regulate the activity of water channels (Carvajal, Cooke & Clarkson 1996b). Such an effect on fine root function has also been suggested as a possible explanation for the response of plant growth to nutrient availability (Radin & Boyer 1982; Chapin, Walter & Clarkson 1988).

A preliminary sensitivity analysis of the Hydrall model demonstrates that much of the growth variability at the local level could indeed be explained by lower photosynthetic potentials and root hydraulic conductivities under nutrient-poor conditions, which would respectively lead to a reduction in gross primary production and in aboveground allocation. Once expanded to take nitrogen uptake and translocation into account, the model could compute tissue nitrogen concentration from a simple carbon and nutrient balance and derive leaf and root properties from existing empirical relationships. This would require, however, more detailed and widespread studies of root hydraulic characteristics and their response to the environment. The novel technique outlined in Chapter 6 could provide a useful tool to address this challenging task.

## References

- Alsheimer M., Köstner B., Falge E. & Tenhunen J.D. (1998) Temporal and spatial variation in transpiration of Norway spruce stands within a forested catchment of the Fichtelgebirge, Germany. *Annales des Sciences Forestieres* **55**, 103-123.
- Axelsson E. & Axelsson B. (1986) Changes in carbon allocation patterns in spruce and pine trees following irrigation and fertilization. *Tree Physiology* **2**, 189-204.
- Ågren G.I. (1985) Theory for growth of plants derived from the nitrogen productivity concept. *Physiologia Plantarum* **64**, 17-28.
- Blackman V.H. (1919) The compound interest law and plant growth. *Annals of Botany* **33**, 353-360.
- Brenchley W.E. (1916) The effect of the concentration of the nutrient solution on the growth of barley and wheat in water cultures. *Annals of Botany* **30**, 77-90.
- Breymer A.I., Hall D.O., Melillo J.M. & Ågren G.I. (eds) (1996) *Global Change: Effects on Coniferous Forests and Grasslands*. J. Wiley, Chichester.
- Campbell G.S. (1985) *Soil Physics with BASIC. Transport Models for Soil-Plant Systems*. Elsevier, Amsterdam.
- Cannell M.G.R. & Dewar R.C. (1994) Carbon allocation in trees: a review of concepts for modelling. *Advances in Ecological Research* **25**, 50-104.
- Carvajal M., Cooke D.T. & Clarkson D.T. (1996a) Plasma membrane fluidity and hydraulic conductance in wheat roots: interactions between root temperature and nitrate or phosphorus deprivation. *Plant Cell and Environment* **19**, 1110-1114.
- Carvajal M., Cooke D.T. & Clarkson D.T. (1996b) Responses of wheat plants to nutrient deprivation may involve the regulation of water-channel function. *Planta* **199**, 372-381.
- Ceulemans R. & Mousseau M. (1994) Effects of elevated atmospheric CO<sub>2</sub> on woody plants. *New Phytologist* **127**, 425-446.
- Chapin F.S. (1991) Effects of multiple environmental stresses on nutrient availability and use. In *Response of Plants to Multiple Stresses* (eds. H.A. Mooney, W.E. Winner & E.J. Pell), pp. 67-88. Academic Press, San Diego.
- Chapin F.S., Walter C.H.S. & Clarkson D.T. (1988) Growth response of barley and tomato to nitrogen stress and its control by abscisic acid, water relations and photosynthesis. *Planta* **173**, 352-366.
- Curtis P.S. & Wang X. (1998) A meta-analysis of elevated CO<sub>2</sub> effects on woody plant mass, form, and physiology. *Oecologia* **113**, 299-313.
- Davidson R.L. (1969) Effects of soil nutrients and moisture on root/shoot ratios in *Lolium perenne* L. and *Trifolium repens* L. *Annals of Botany* **33**, 571-577.
- Dewar R.C. (1993) A root-shoot partitioning model based on carbon-nitrogen-water interactions and Münch phloem flow. *Functional Ecology* **7**, 356-368.
- Eamus D. & Jarvis P.G. (1989) The direct effects of increase in the global atmospheric CO<sub>2</sub> concentration on natural and commercial temperate trees and forests. *Advances in Ecological Research* **19**, 1-55.
- Field C.B. & Mooney H.A. (1986) The photosynthesis-nitrogen relationship in wild plants. In *On the Economy of Plant Form and Function* (ed. T.J. Givnish), pp. 25-55. Cambridge Univ. Press, Cambridge.
- George E., Seith B., Schaeffer C. & Marschner H. (1997) Responses of *Picea*, *Pinus*

- and *Pseudotsuga* roots to heterogeneous nutrient distribution in the soil. *Tree Physiology* **17**, 39-45.
- Gholz H.L., Linder S. & McMurtrie R.E. (1994) *Ecological Bulletins*. **43**. *Environmental Constraints on the Structure and Productivity of Pine Forest Ecosystems: a Comparative Analysis*. Copenhagen.
- Gower S.T., McMurtrie R.E. & Murty D. (1996) Aboveground net primary production decline with stand age: potential causes. *Trends in Ecology & Evolution* **11**, 378-382.
- Gower S.T., Pongracic S. & Landsberg J.J. (1996) A global trend in belowground carbon allocation: can we use the relationship at smaller scales? *Ecology* **77**, 1750-1755.
- Irvine J., Perks M.P., Magnani F. & Grace J. (1998) The response of *Pinus sylvestris* to drought: stomatal control of transpiration and hydraulic conductance. *Tree Physiology* **18**, 393-402.
- Jarvis P.G. (ed) (1998) *European Forests and Global Change*. Cambridge University Press, Cambridge.
- Jones H.G. (1992) *Plants and Microclimate*. Cambridge Univ. Press, Cambridge.
- Kellomäki S. & Wang K.Y. (1996) Photosynthetic responses to needle water potentials in Scots pine after a four-year exposure to elevated CO<sub>2</sub> and temperature. *Tree Physiology* **16**, 765-772.
- Kirschbaum M.U.F., King D.A., Comins H.N., McMurtrie R.E., Medlyn B.E., Pongracic S., Murty D., Keith H., Raison R.J., Khanna P.K. *et al.* (1994) Modelling forest response to increasing CO<sub>2</sub> concentration under nutrient-limited conditions. *Plant Cell and Environment* **17**, 1081-1099.
- Komor E. (1994) Regulation by futile cycles: the transport of carbon and nitrogen in plants. In *Flux Control in Biological Systems* (ed. E.-D.Schulze), pp. 153-201. Academic Press, San Diego.
- Kramer P.J. & Boyer J.S. (1995) *Water Relations of Plants and Soils*. Academic Press, San Diego.
- Landsberg J.J. & Waring R.H. (1997) A generalized model of forest productivity using simplified concepts of radiation-use efficiency, carbon balance and partitioning. *Forest Ecology and Management* **95**, 209-228.
- Leuning R. (1990) Modelling stomatal behaviour and photosynthesis of *Eucalyptus grandis*. *Australian Journal of Plant Physiology* **17**, 159-175.
- Leuning R. (1995) A critical appraisal of a combined stomatal-photosynthesis model for C<sub>3</sub> plants. *Plant Cell and Environment* **18**, 339-355.
- Linder S. & Rook D.A. (1984) Effects of mineral nutrition on carbon dioxide exchange and partitioning of carbon in trees. In *Nutrition of Plantation Forests* (eds. G.D.Bowen & E.K.S.Nambiar), pp. 211-236. Academic Press, London.
- Lloyd J. & Farquhar G.D. (1996) The CO<sub>2</sub> dependence of photosynthesis, plant growth responses to elevated CO<sub>2</sub> concentrations and their interaction with soil nutrient status. I. General principles and forest ecosystems. *Functional Ecology* **10**, 4-32.
- Magnani F. & Grace J. (2000) Plants as self-organising systems. In *Leaf Development and Canopy Growth* (eds. B.Marshall & J.Roberts) Sheffield Academic Press, Sheffield.
- Margolis H., Oren R., Whitehead D. & Kaufmann M.R. (1995) Leaf area dynamics of conifer forests. In *Ecophysiology of Coniferous Forests* (eds. W.K.Smith &

- T.M.Hinckley), pp. 181-223. Academic Press, San Diego.
- Mäkelä A. (1986) Implications of the pipe model theory on dry matter partitioning and height growth in trees. *Journal of Theoretical Biology* **123**, 103-120.
- Mäkelä A. & Sievänen R.P. (1987) Comparison of two shoot-root partitioning models with respect to substrate utilization and functional balance. *Annals of Botany* **59**, 129-140.
- Mäkelä A. & Sievänen R.P. (1992) Height growth strategies in open-grown trees. *Journal of Theoretical Biology* **159**, 443-467.
- McDonald A.J.S. & Davies W.J. (1996) Keeping in touch: responses of the whole plant to deficits in water and nitrogen supply. *Advances in Botanical Research* **22**, 229-300.
- Medlyn B.E. & Dewar R.C. (1999) Comment on the article by R. H. Waring, J. J. Landsberg and M. Williams relating net primary production to gross primary production. *Tree Physiology* **19**, 137-138.
- Mencuccini M. & Grace J. (1996) Developmental patterns of aboveground xylem conductance in a Scots pine (*Pinus sylvestris* L.) age sequence. *Plant Cell and Environment* **19**, 939-948.
- Nadelhoffer K.J., Emmett B.A., Gundersen P., Kjonaas O.J., Koopmans C.J., Schleppei P., Tietema A. & Wright R.F. (1999) Nitrogen deposition makes a minor contribution to carbon sequestration in temperate forests. *Nature* **398**, 145-148.
- Palomäki V. & Holopainen T. (1995) Effects of nitrogen deficiency and recovery fertilization on ultrastructure, growth, and mineral concentrations of Scots pine needles. *Canadian Journal of Forest Research* **25**, 198-207.
- Parker G.A. & Maynard Smith J. (1990) Optimality theory in evolutionary biology. *Nature* **348**, 27-33.
- Popper K.R. (1972) *The Logic of Scientific Discovery*. Hutchinson, London.
- Radin J.W. (1990) Responses of transpiration and hydraulic conductance to root temperature in nitrogen- and phosphorus-deficient cotton seedlings. *Plant Physiology* **92**, 855-857.
- Radin J.W. & Boyer J.S. (1982) Control of leaf expansion by nitrogen nutrition in sunflower plants. Role of hydraulic conductivity and turgor. *Plant Physiology* **69**, 771-775.
- Radin J.W. & Matthews M.A. (1989) Water transport properties of cortical cells in roots of nitrogen- and phosphorus-deficient cotton seedlings. *Plant Physiology* **89**, 264-268.
- Raich J.W. & Nadelhoffer K.J. (1989) Below ground carbon allocation in forest ecosystems: global trends. *Ecology* **70**, 1346-1354.
- Rastetter E.B., Ryan M.G., Shaver G.R., Melillo J.M., Nadelhoffer K.J., Hobbie J.E. & Aber J.D. (1991) A general biogeochemical model describing the response of the C and N cycles in terrestrial ecosystems to changes in CO<sub>2</sub>, climate, and N deposition. *Tree Physiology* **9**, 101-126.
- Ryan M.G. (1991) A simple method for estimating gross carbon budgets for vegetation in forest ecosystems. *Tree Physiology* **9**, 255-266.
- Ryan M.G., Binkley D. & Fownes J.H. (1997) Age-related decline in forest productivity: pattern and processes. *Advances in Ecological Research* **27**, 213-262.
- Ryan M.G., Hunt E.R., McMurtrie R.E., Ågren G.I., Aber J.D., Friend A.D., Rastetter E.B., Pulliam W.M., Raison R.J. & Linder S. (1996) Comparing models of



- ecosystem function for temperate conifer forests. I. Model description and validation. In *Global Change: Effects on Coniferous Forests and Grasslands* (eds. A.I. Breyer, D.O. Hall, J.M. Melillo & G.I. Ågren), pp. 313-362. J. Wiley, Chichester.
- Sands R., Fiscus E.L. & Reid C.P.P. (1982) Hydraulic properties of pine and bean roots with varying degrees of suberization, vascular differentiation and mycorrhizal infection. *Australian Journal of Plant Physiology* **9**, 559-569.
- Santantonio D. (1989) Dry-matter partitioning and fine root production in forests. New approaches to a difficult problem. In *Biomass Production by Fast-Growing Trees*. (eds. J.S. Pereira & J.J. Landsberg), pp. 57-72. Kluwer Academic,
- Shinozaki K., Yoda K., Hozumi K. & Kira T. (1964) A quantitative analysis of plant form - The pipe model theory. I. Basic analyses. *Japanese Journal of Ecology* **14**, 97-105.
- Smit-Spinks B., Swanson B.T. & Markhart III A.H. (1984) Changes in water relations, water flux, and root exudate abscisic acid content with cold acclimation of *Pinus sylvestris* L.. *Australian Journal of Plant Physiology* **11**, 431-441.
- Stedle E. & Heydt H. (1997) Water transport across tree roots. In *Trees. Contributions to Modern Tree Physiology* (eds. H. Rennenberg, W. Eschrich & H. Ziegler), pp. 239-255. Backhuys Publishers, Leiden.
- Stedle E. & Meshcheryakov A.B. (1996) Hydraulic and osmotic properties of oak roots. *Journal of Experimental Botany* **47**, 387-401.
- Stitt M. & Krapp A. (1999) The interaction between elevated carbon dioxide and nitrogen nutrition: the physiological and molecular background. *Plant Cell and Environment* **22**, 583-621.
- Thornley J.H.M. (1972) A balanced quantitative model for root:shoot ratios in vegetative plants. *Annals of Botany* **36**, 431-441.
- Thornley J.H.M. (1975) Comment on a recent paper by Hunt on shoot:root ratios. *Annals of Botany* **39**, 1149-1150.
- Vapaavuori E.M., Vuorinen A.H., Aphalo P.J. & Smolander H. (1995) Relationship between net photosynthesis and nitrogen in Scots pine. Seasonal variation in seedlings and shoots. *Plant and Soil* **169**, 263-270.
- Walcroft A.S., Silvester W.B., Grace J.C., Carson S.D. & Waring R.H. (1996) Effects of branch length on carbon isotope discrimination in *Pinus radiata*. *Tree Physiology* **16**, 281-286.
- Waring R.H., Landsberg J.J. & Williams M. (1998) Net primary production of forests: a constant fraction of gross primary production? *Tree Physiology* **18**, 129-134.
- Williams M., Rastetter E.B., Fernandes D.N., Goulden M.L., Wofsy S.C., Shaver G.R., Melillo J.M., Munger J.W., Fan S.-M. & Nadelhoffer K.J. (1996) Modelling the soil-plant-atmosphere continuum in a *Quercus-Acer* stand at Harvard Forest: the regulation of stomatal conductance by light, nitrogen and soil-plant hydraulic properties. *Plant Cell and Environment* **19**, 911-927.
- Wilson J.B. (1988) A review of evidence on the control of shoot:root ratio, in relation to models. *Annals of Botany* **61**, 433-449.
- Yoder B.J., Ryan M.G., Waring R.H., Schoettle A.W. & Kaufmann M.R. (1994) Evidence of reduced photosynthetic rates in old trees. *Forest Science* **40**, 513-527.

## Appendix A. Plant energetics and population density

Comments to the paper 'Allometric scaling of plant energetics and population density' by Enquist B.J., Brown J.H. and West G.B. (Nature 395, 163-165. 1998)

The paper by Enquist *et al.* <sup>1</sup> presents an interesting analysis of the link between plant size, allometry and mortality. Its claim to a functional basis, however, is misleading when upscaled to the population level.

Transpiration is known to be strongly driven by environmental conditions <sup>2</sup>. A comparison among species of transpiration rates per plant is therefore difficult, unless plants were exposed to the same environment. This does not seem to be the case, as transpiration rates were derived from a re-analysis of literature data. The confounding effect is negligible at the individual plant scale, given the wide range of rates and dimensions reviewed. When scaling-up to the canopy level, however, the relevance of environmental driving variables (radiation, water availability, site fertility) predominates and tends to obscure any effects of plant size on stand function. This appears quite clearly from the comparison of maximum conductances and assimilation rates among biomes in the world presented by Schulze *et al.* <sup>3</sup>.

It should also be noted that transpiration rates scaled-up to the population level, as presented in Figure 4, seem unrealistically high: rates of about  $100 \text{ l m}^{-2} \text{ d}^{-1}$  (i.e.  $\text{mm d}^{-1}$ ) are in stark contrast with maximum figures of 3-12  $\text{mm d}^{-1}$  reported by Jones <sup>4</sup> in a global comparison of plant canopies over the world. Kelliher *et al.* <sup>5</sup>, in their meta-analysis of evapo-transpiration from coniferous forests and grasslands, also present values never exceeding 6-7  $\text{mm d}^{-1}$ .

What is most important, however, is that the conclusions drawn by the Authors from their upscaling to the population level are misleading. It is not true that 'total energy use or productivity of plants in ecosystems is ... invariant with respect to body size'. This can be seen most clearly from stand chronosequences in forest tree species <sup>6</sup>: after canopy closure at the polestage, leaf area index tends to decline (as a result of self-thinning, among other processes). In mature canopies this has a marginal effect on the interception of radiant energy and gross primary production <sup>7</sup>. Net assimilation and above-ground allocation, however, are further reduced by increasing

respiratory costs, nutrient immobilization in soil litter and hydraulic constraints<sup>7-10</sup>, all a direct result of increasing body size, contributing to the well known decline in forest growth with tree dimensions and age<sup>6,8</sup>. Even the conservative nature of forest evapo-transpiration at the regional scale<sup>11</sup> seems to be true more at the community than at the population level, resulting from the interaction among overstorey and understorey processes<sup>3</sup>. On the contrary, considerable changes in transpiration with stand development have been reported<sup>12</sup>.

The data presented seem insufficient to subvert this picture.

## References

1. Enquist, B. J., Brown, J. H. & West, G. B. *Nature* **395**, 163-165 (1998)
2. Monteith, J. L. & Unsworth, M. H. *Principles of Environmental Physics*. (Edward Arnold, London, 1990)
3. Schulze, E.-D., Kelliher, F. M., Korner, C., Lloyd, J. & Leuning, R. *Annual Review Ecology Systematics* **25**, 629-660 (1994)
4. Jones, H. G. *Plants and Microclimate* (Cambridge Univ. Press, Cambridge, 1992)
5. Kelliher, F. M., Leuning, R. & Schulze, E.-D. *Oecologia* **95**, 153-163 (1993)
6. Ryan, M. G., Binkley, D. & Fownes, J. H. *Adv. Ecol. Res.* **27**, 213-262 (1997)
7. Mencuccini, M. & Grace, J. *Tree Physiol.* **16**, 459-468 (1996)
8. Gower, S. T., McMurtrie, R. E. & Murty, D. *Trends in Ecology & Evolution* **11**, 378-382 (1996)
9. Yoder, B. J., Ryan, M. G., Waring, R. H., Schoettle, A. W. & Kaufmann, M. R. *For. Sc.* **40**, 513-527 (1994)
10. Magnani, F., Borghetti, M. & Grace, J. in *System Analysis and Simulation for Agricultural Science: a Contribution of the RAISA Project* (eds Miglietta, F., van Laar, H.H. & Goudriaan, J.) (CABO-DLO, Wageningen, 1996)
11. Roberts, J. J. *Hydr.* **66**, 133-141 (1983)
12. Rauner, J. L. in *Vegetation and the Atmosphere* (ed Monteith, J.L.) 241-264 (Academic Press, London, 1976)

## Appendix B. HYDRALL model source code

### List of model components:

		Page
Main program	Hydrall	173
Subroutines	Aerodyn	175
	Gasflux	179
	Grstand	186
	Grtree	188
	Inclim	190
	Init	192
	Inparms	194
	Leuning	198
	Optimal	200
	Outhour	202
	Outyear	204
	Radenv	206
	Respsoil	210
	Resptree	212
	Rootfind	213
	Soilpsi	216
	Upscale	217
	Ustorey	221
Weather	223	
Functions	Psifun	227
	Tfun	228
Common blocks	Files	229
	Hydrall	230
Input files	Files.txt	234
	Parms.txt	234
	Photot.txt	234
	Run.txt	235

Note: the model takes advantage in input-output procedures of the TTUTIL library (van Kralingen D.W.G., Rappoldt C. 1998. Reference Manual of the FORTRAN utility library TTUTIL. AB-DLO Internal Report. AB-DLO, Wageningen, The Netherlands)

C \*\*\*\*\*

C FORTRAN main program      HYDRALL      (hydrall.for)      28/2/99

C

C

C -----  
C Purpose The model simulates the growth of a forest stand over a whole rotation.  
C Parameter input (sub INPARMS) - Input of functional and runtime parameters.  
C Initialization (sub INIT) - Initialization of state variables.  
C Climatic input (sub INCLIM) - Input of daily environmental variables.  
C Weather data (sub WEATHER) - Detailed half-hourly values of environmental  
C variables are derived from synoptic climate data.  
C Stand assimilation and transpiration (sub GASFLUX and LEUNING) - Computation of gas  
C exchange from simulated half-hourly weather data is based on Farquhar-Leuning  
C model and takes into account partial aerodynamic decoupling and light environment.  
C Derived site water balance and soil water potential (sub SOILPSI).  
C Stand respiration (sub GASFLUX) - Depends upon temperature.  
C Tissue turnover (sub GRSTAND) - Simple formulation, constant fraction.  
C Allocation (sub OPTIMAL) - Carbon allocated between foliage, sapwood and fine roots  
C with an optimization criterion under the hydraulic constraint of cavitation  
C avoidance (sub ROOTFIND). Height growth (fitness function) proportional to  
C production of foliage biomass.  
C Stand density (sub GRTREE) - Starting from an imposed stocking density, density-  
C dependent mortality progressively reduces the number of trees which approaches  
C asymptotically the self-thinning line. Stand biomass is the independent variable.  
C Thinning regimes can also be specified in input files.  
C Hourly output (sub OUTHOUR) - Selected meteo and gas-exchange variables from the  
C common block HYDRALL are output to file for the last year of simulations, one day  
C each month.  
C Annual output (sub OUTYEAR) - Selected annual variables from the common block  
C HYDRALL are output to file.

C

C Parameters and variables

C AGE            stand age (yr)  
C AGE0          initial stand age (yr)  
C NYRS          simulation length (yr)

C

C Linked subroutines (secondary links)

C GASFLUX      (LEUNING, OUTHOUR, SOILPSI)  
C GRTREE  
C GRSTAND      (OPTIMAL (ROOTFIND))  
C INCLIM  
C INIT  
C INPARMS  
C WEATHER  
C OUTYEAR

C \*\*\*\*\*

#### PROGRAM MAIN

C \*\*\*\*\*

C        Define parameters and variables

C \*\*\*\*\*

      INCLUDE 'HYDRALL.CMN'

C \*\*\*\*\*

C        Print logo

C \*\*\*\*\*

      WRITE (0, 1000)

C \*\*\*\*\*

C        Input parameters, initialize state variables

C \*\*\*\*\*

      CALL INPARMS                            !input parameters from file  
      CALL INIT                                !initialize variables  
      CALL OUTYEAR                            !output initial conditions

C \*\*\*\*\*

C        Annual increment of stand compartments

C \*\*\*\*\*

      DO 100, AGE=(AGE0+1), (AGE0+NYRS)  
          CALL INCLIM                        !read one year of meteo data from file  
          CALL GASFLUX                      !NPP, NEE, water rel parms for allocation  
          CALL GRSTAND                      !stand growth  
          CALL GRTREE                        !stand density, tree diameter  
          CALL OUTYEAR                      !output annual results



```

C *****
C FORTRAN subroutine      AERODYN      (aerodyn.for)      27/2/99
C -----
C Purpose The routine computes iteratively leaf temperature and sensible
C          heat flux from shaded and sunlit foliage and canopy aerodynamic
C          conductance, based on input values of:
C          (a) stand height and leaf area index
C          (j) average wind speed
C          (e) air temperature
C          (d) slope of vapour pressure vs temperature
C
C          Computation of zero plane displacement and roughness length as a function
C          of LAI and height based on Shaw & Pereira (1982)
C          Iterative computation of big-leaf temperature (sunlit and shaded) as a function
C          of isothermal net radiation and aerodynamic conductance based on Jones (1992)
C          Iterative computation of aerodynamic conductance as a function of wind speed
C          and sensible heat flux based on Monteith and Unsworth (1990) and Garratt (1992)
C          Computation of near-field resistance to heat exchange based on Choudhury and
C          Monteith (1988). Aerodynamic conductances are pooled over the whole canopy, value
C          for sunlit, shaded big-leaf proportional to its leaf area index.
C
C          NOTE: All fluxes and conductances are on a ground area basis
C          when not otherwise stated.
C
C Parameters and variables
C  A          multiplier for boundary-layer conduct (m s-1/2)
C  BETA       attenuation coefficient of wind speed inside the canopy (-)
C  CP         specific heat capacity of air (J mol-1 K-1)
C  DAY        Julian day
C  DELTAT1    leaf-to-air temperature difference, sunlit big-leaf (oC)
C  DELTAT2    leaf-to-air temperature difference, shaded big-leaf (oC)
C  DISPL      zero plane displacement (m)
C  FIH        stability function for heat (-)
C  FIM        stability function for momentum (-)
C  GAC        aerodynamic conductance to CO2 exchange of whole canopy (mol m-2 s-1)
C  GAC1       aerodynamic conductance to CO2 exchange of sunlit big-leaf (mol m-2 s-1)
C  GAC2       aerodynamic conductance to CO2 exchange of shaded big-leaf (mol m-2 s-1)
C  GAH        aerodynamic conductance for heat exchange of whole canopy (mol m-2 s-1)
C  GAH1       aerodynamic conductance for heat exchange of sunlit big-leaf (mol m-2 s-1)
C  GAH2       aerodynamic conductance for heat exchange of shaded big-leaf (mol m-2 s-1)
C  GAM        canopy aerodynamic conductance to momentum exchange (m s-1)
C  GAMMA      psychrometer constant (Pa K-1)
C  GBH        leaf boundary-layer conductance (m s-1)
C  GHR        total conductance to heat exchange of whole canopy (mol m-2 s-1)
C  GHR1       total conductance to heat exchange of sunlit big-leaf (mol m-2 s-1)
C  GHR2       total conductance to heat exchange of shaded big-leaf (mol m-2 s-1)
C  GR         radiative conductance (mol m-2 s-1)
C  H          stand height (m)
C  HOUR       1/2 hour interval number
C  HS(48)     sensible heat flux from the canopy (W m-2)
C  KARM       von Karman's constant (-)
C  L          Monin-Obukhov length (m)
C  LAI        canopy leaf area index (-)
C  LAI1       leaf area index of sunlit leaves (-)
C  LAI2       leaf area index of shaded leaves (-)
C  LATENT     latent heat of vaporization (J mol-1)
C  PSIH       deviation function for heat (-)
C  PSIM       deviation function for momentum (-)
C  RGAS       gas constant (Pa m3 mol-1 K-1)
C  RNI1       isothermal net radiation of sunlit leaves (W m-2)
C  RNI2       isothermal net radiation of shaded leaves (W m-2)
C  RSW        dummy value of stomatal conductance to H2O (molH2O m-2 s-1)
C  S(48)      slope of sat humidity dependence upon temperature (Pa K-1)
C  SIGMA      Stefan-Boltzmann constant (W m-2 K-4)
C  STIND      stomatal index (1= amphy-, 2= hypostomatous species)
C  TAIR(48)   air temperature (oC)
C  TLEAF1     temperature of sunlit leaves (K)
C  TLEAF2     temperature of shaded leaves (K)
C  USTAR      friction velocity (m s-1)
C  VPD(48)    vapour pressure deficit (Pa)
C  X          dummy variable
C  W          leaf width (m)
C  WND(12)    wind speed at reference height (m s-1)
C  WNDH       wind speed at canopy top (m s-1)

```

```

C   Y           dummy variable
C   ZETA        non-dimensional stability height (-)
C   ZREF        reference height (m)
C   Z0          roughness length (m)
C
C *****
      SUBROUTINE AERODYN(DAY, HOUR, LAI, LAI1, LAI2, RNI1, RNI2,
+                       GAC1, GAC2, GHR1, GHR2, TLEAF1, TLEAF2)
C *****
C           Define parameters and variables
C *****
C Parameters and variables
C -----
      INTEGER HOUR, I, DAY
      REAL  A, BETA, DELTAT1, DELTAT2, DISPL, DUM1, FIH, FIM,
+         GAC, GAC1, GAC2, GAH, GAH1, GAH2, GAM, GBH, GHR,
+         GHR1, GHR2, GR, KARM, L, LAI, LAI1, LAI2, PSIH,
+         PSIM, RNI1, RNI2, RSW, TLEAF1, TLEAF2, USTAR, X,
+         WNDH, Y, ZETA, ZREF, Z0
      PARAMETER (A= 0.0067,
+              BETA= 3.,
+              KARM= 0.41)
      INCLUDE 'HYDRALL.CMN'
C *****
C           Structural parameters
C *****
C           Ensure safety to the routine
C -----
      IF(WND(DAY).LT.1.E-4) WND(DAY)= 1.E-4
C
C           Reference height
C -----
      ZREF= H + 5.
C           Zero plane displacement and roughness length
C -----
      X= 0.2 * LAI
      DISPL= H * (LOG(1.+X**0.166) + 0.03*LOG(1+X**6))
      IF(DISPL.GE.H) DISPL= 0.99 * H
      IF(X.LT.0.2) THEN
        Z0= 0.01 + 0.28*SQRT(X) * H
      ELSE
        Z0= 0.3 * H * (1.-DISPL/H)
      END IF
C *****
C           Canopy energy balance.
C           Compute iteratively:
C           - leaf temperature (different for sunlit and shaded foliage)
C           - aerodynamic conductance (non-neutral conditions)
C *****
C           Initialize sensible heat flux and friction velocity
C -----
      HS(HOUR)= RNI1 + RNI2
      USTAR= KARM*WND(DAY)/LOG((ZREF-DISPL)/Z0)
      IF(USTAR.LE.1.E-4) THEN
        USTAR= 1.E-4
      END IF
C
      DO 50, I= 1,20
C           Monin-Obukhov length (m) and nondimensional height
C           Note: imposed a limit to non-dimensional height under stable
C           conditions, corresponding to a value of 0.2 for the generalized
C           stability factor F (=1/FIM/FIH)
C -----
      L= -(USTAR)**3*CP*PRESS/RGAS
+       / (KARM*9.8*HS(HOUR))
      ZETA= (ZREF-DISPL)/L
      IF(ZETA.GE.0.25) THEN
        ZETA= 0.25
      END IF
C           Non-stable conditions

```



```

C -----
C IF(ZETA.LT.0.) THEN
C   Stability function for momentum and heat (-)
C -----
C   FIM= (1.-16.*ZETA)**(-0.25)
C   FIH= FIM ** 2
C   X= 1./FIM
C   Y= 1./FIH
C   Deviation function for momentum and heat (-)
C -----
C   PSIM= 2.*LOG((1.+X)/2.) + LOG((1.+X**2)/2.)
+     - 2.*ATAN(X) + PI/2.
C   PSIH= 2.*LOG((1+Y)/2.)
C   Stable conditions
C -----
C ELSE
C   Stability function for momentum and heat (-)
C -----
C   FIM= (1.+5.*ZETA)
C   FIH= FIM
C   Deviation function for momentum and heat (-)
C -----
C   PSIH= - 5.*ZETA
C   PSIM= PSIH
C END IF
C Friction velocity (m s-1)
C -----
C USTAR= KARM*WND(DAY)/(LOG((ZREF-DISPL)/Z0)-PSIM)
C IF(USTAR.LE.1.E-4) THEN
C   USTAR= 1.E-4
C END IF
C Wind speed at canopy top (m s-1)
C -----
C WNDH= USTAR/KARM * LOG((H-DISPL)/Z0)
C IF(WNDH.LE.1.E-4) THEN
C   WNDH= 1.E-4
C END IF
C Average leaf boundary-layer conductance cumulated over the canopy (m s-1)
C -----
C GBH= A*SQRT(WNDH/W)*(2./BETA*(1-EXP(-BETA/2.))) * LAI
C Total canopy aerodynamic conductance for momentum exchange (s m-1)
C -----
C GAM= USTAR / (WND(DAY)/USTAR + (PSIM-PSIH)/KARM)
C Aerodynamic conductance for heat exchange (mol m-2 s-1)
C -----
C DUM1= PRESS/RGAS/(TAIR(HOUR)+273.2) !conversion factor m s-1 into mol m-2 s-1
C GAH= (GAM*GBH)/(GAM+GBH) * DUM1 !whole canopy
C GAH1= GAH * LAI1/LAI !sunlit big-leaf
C GAH2= GAH - GAH1 !shaded big-leaf
C
C Canopy radiative conductance (mol m-2 s-1)
C -----
C GR= 4.*S(HOUR)/GAMMA*SIGMA/CP*(TAIR(HOUR)+273.2)**3
C Total conductance to heat exchange (mol m-2 s-1)
C -----
C GHR= GAH + GR !whole canopy
C GHR1= GHR * LAI1/LAI !sunlit big-leaf
C GHR2= GHR - GHR1 !shaded big-leaf
C
C Temperature of big-leaf (approx. expression)
C -----
C IF(LAI1.GT.1.E-6) THEN !avoid instability
C   RSW= 10./LAI1 !dummy stom res for sunlit big-leaf
C   DELTAT1= ((RSW+1./GAH1)*GAMMA*RNI1/CP
+     - VPD(HOUR))
+     /GHR1/(GAMMA*(RSW+1./GAH1) + S(HOUR)/GHR1)
C ELSE
C   DELTAT1= 0.
C END IF
C TLEAF1= TAIR(HOUR) + DELTAT1 + 273.2 !sunlit big-leaf
C RSW= 10./LAI2 !dummy stom res for shaded big-leaf
C DELTAT2= ((RSW+1./GAH2)*GAMMA*RNI2/CP
+     - VPD(HOUR))
+     /GHR2/(GAMMA*(RSW+1./GAH2) + S(HOUR)/GHR2)

```

```

      TLEAF2= TAIR(HOUR) + DELTAT2 + 273.2           !shaded big-leaf
C      Sensible heat flux from the whole canopy
C      -----
50    HS(HOUR)= CP * (GAH1*DELTAT1 + GAH2*DELTAT2)
      CONTINUE

C      Aerodynamic conductance to CO2 exchange (mol m-2 s-1)
C      of whole canopy, sunlit and shaded big-leaf
C      -----
      IF(STIND.EQ.1) THEN                               !amphystomatous species
        GAC= 0.6 * GAH
      ELSE                                             !hypostomatous species
        GAC= 0.6 * (GAM*GBH)/(GBH + 2.*GAM) * DUM1
      END IF
      GAC1= GAC * LAI1/LAI                             !sunlit big-leaf
      GAC2= GAC * LAI2/LAI                             !shaded big-leaf

      RETURN
      END

C *****
C      References
C *****
C      Choudhury BJ, Monteith JL 1988. A four-layer model for the heat budget of
C      homogeneous land surfaces. Q J R Meteorol Soc 114,373-398
C      Garratt JR 1992. The Atmospheric Boundary Layer. Cambridge Univ Press,
C      Cambridge
C      Monteith JL, Unsworth M 1990. Principles of Environmental Physics.
C      E Arnold, London
C      Shaw RH, Pereira AR 1982. Aerodynamic roughness of a plant canopy.
C      A numerical experiment. Agric Meteorol 26,51-65

```

```

C *****
C FORTRAN subroutine      GASFLUX      (gasflux.for)      2/3/99
C -----
C Purpose (1) The routine computes canopy assimilation and ecosystem transpiration
C          over one year, based on input values of:
C          (a) foliage biomass (hence leaf area index)
C          (b) stand height
C          (c) initial soil water content
C          (d) daily values of minimum, maximum and mean temperature
C          (e) daily values of precipitation
C          (f) daily values of air relative humidity
C          (g) daily values of wind speed
C          (h) daily values of cumulated global radiation
C (2) The time course of leaf water potential and critical values of soil water
C     potential and transpiration for carbon allocation are also evaluated from
C     (k) sapwood biomass
C     (l) fine root biomass
C (3) Daily respiration of tree compartments is computed in subroutine RESPTREE.
C (4) Daily soil respiration is computed in subroutine RESPSOIL
C
C - The daily pattern of temperature, humidity and radiation is derived
C   in the subroutine WEATHER
C - Canopy and understory radiative environment computed in subroutine RADENV.
C - Leaf temperature and sensible heat flux from shaded and sunlit foliage and
C   canopy aerodynamic conductance computed in subroutine AERODYN.
C - Soil water content updated every day; soil water potential computed by subroutine
C   SOILPSI. Soil depth of 1 m, homogeneous soil water content. Capillary exchange
C   with a water table at a constant depth of 5 m.
C   Flux integration between the water table at null water potential and a node
C   at depth (1/2 SLDEP) and water potential PSISL follows Campbell (1985).
C   Runoff takes place when water content exceeds soil porosity.
C - Soil+root hydraulic conductance function of soil water potential and fine root
C   density and dimensions, based on Campbell (1985)
C   Shoot hydraulic resistance function of sapwood basal area and height, based
C   on Whitehead et al (1984).
C   The reference values of sapwood, soil and root hydraulic conductivities
C   (assumed at 20 oC) are adjusted for the effects of temperature on water viscosity.
C - Assimilation and transpiration of sunlit and shaded foliage are computed
C   by the subroutine LEUNING (based on the Leuning 1995 and Monteith 1995 models).
C   Photosynthetic parameters for sunlit and shaded foliage are scaled-up to the canopy
C   level in the subroutine SCALEUP, assuming an exponential gradient in the canopy
C   in parallel with diffuse PAR.
C - Critical soil water potential and transpiration rate for carbon allocation
C   correspond to annual minimum of leaf water potential
C - Sapwood and root respir are a function of tissue nitrogen content and temperature
C - Soil respiration is a function of soil water potential and daily temperature
C - It is assumed that no gas-exchange takes place on days with ground frost
C   (Landsberg & Waring 1997) and that this effect is additive to the direct effects
C   of air temperature; same assumptions for understory gas-exchange and growth.
C
C NOTE: All fluxes and conductances are on a _ground_ area basis
C       when not otherwise stated.
C
C Parameters and variables
C ADAY      canopy daily photosynthesis (mol m-2 d-1)
C ALPHAC    canopy quantum efficiency (-)
C APARDAY   canopy daily absorbed PPFD (mol m-2 d-1)
C APARUND   photosynth act rad absorbed by understory (W m-2)
C APARU2    absorbed PPFD per unit shaded leaf area at canopy top (mol m-2 s-1)
C APARYR    annual absorbed PAR (mol m-2 yr-1)
C APAR1     photosynth act rad absorbed by sunlit big-leaf (mol m-2 s-1)
C APAR2     photosynth act rad absorbed by shaded big-leaf (mol m-2 s-1)
C ATOT      canopy assimilation (mol m-2 s-1)
C AYR       annual assimilation (mol m-2 yr-1)
C A1        assimilation by sunlit big-leaf (mol m-2 s-1)
C A2        assimilation by shaded big-leaf (mol m-2 s-1)
C BSL       coefficient in soil water potential equation (-)
C COMP1     CO2 compensation point in dark for sunlit big-leaf (Pa)
C COMP2     CO2 compensation point in dark for shaded big-leaf (Pa)
C CONV      dry matter conversion efficiency (growth resp.)(-)
C DAY       day of simulation
C DAYTOT    total number of days in the year
C DAYCRIT   Julian day of critical water relations
C DRAIN     deep soil drainage with the water table (mm d-1)

```

C ECRIT critical transpir rate per unit foliage area (mol m<sup>-2</sup> s<sup>-1</sup>)  
C EDAY canopy daily transpiration (mm d<sup>-1</sup>)  
C ETDAY daily evapo-transpiration (mm d<sup>-1</sup>)  
C ETOT canopy transpiration (mol m<sup>-2</sup> s<sup>-1</sup>)  
C ETYR annual evapo-transpiration (mm yr<sup>-1</sup>)  
C EUDAY understorey daily transpiration (mm d<sup>-1</sup>)  
C EUYR annual understorey transpiration (mm yr<sup>-1</sup>)  
C EYR annual canopy transpiration (mm yr<sup>-1</sup>)  
C E1 transpiration by sunlit big-leaf (mol m<sup>-2</sup> s<sup>-1</sup>)  
C E2 transpiration by shaded big-leaf (mol m<sup>-2</sup> s<sup>-1</sup>)  
C EUND understorey transpiration (mol m<sup>-2</sup> s<sup>-1</sup>)  
C GAC1 aerodynamic conduct to CO2 of sunlit big-leaf (mol m<sup>-2</sup> s<sup>-1</sup>)  
C GAC2 aerodynamic conduct to CO2 of shaded big-leaf (mol m<sup>-2</sup> s<sup>-1</sup>)  
C GAMMA psychrometer constant (Pa K<sup>-1</sup>)  
C GPPYR annual gross primary production (kgC m<sup>-2</sup> yr<sup>-1</sup>)  
C GSCTOT canopy conductance to CO2 (mol m<sup>-2</sup> s<sup>-1</sup>)  
C GHR1 total conductance to heat exchange of sunlit big-leaf (mol m<sup>-2</sup> s<sup>-1</sup>)  
C GHR2 total conductance to heat exchange of shaded big-leaf (mol m<sup>-2</sup> s<sup>-1</sup>)  
C GSCD1 conductance in darkness of sunlit big-leaf (molCO2 m<sup>-2</sup> s<sup>-1</sup>)  
C GSCD2 conductance in darkness of shaded big-leaf (molCO2 m<sup>-2</sup> s<sup>-1</sup>)  
C GSC1 conductance of sunlit big-leaf (molCO2 m<sup>-2</sup> s<sup>-1</sup>)  
C GSC2 conductance of shaded big-leaf (molCO2 m<sup>-2</sup> s<sup>-1</sup>)  
C H stand height (m)  
C HOLD daily intercepted precipitation (mm d<sup>-1</sup>)  
C HOUR 1/2 hour interval number  
C J1 electron transport of sunlit big-leaf (mol m<sup>-2</sup> s<sup>-1</sup>)  
C J2 electron transport of shaded big-leaf (mol m<sup>-2</sup> s<sup>-1</sup>)  
C KB extinction coeff for canopy of black leaves, direct radiation (-)  
C KC1 Michaelis constant of carboxyl for sunlit big-leaf (Pa)  
C KC2 Michaelis constant of carboxyl for shaded big-leaf (Pa)  
C KDPAR canopy extinction coeff for PAR diffuse radiation (-)  
C KO1 Michaelis constant of oxygen for sunlit big-leaf (Pa)  
C KO2 Michaelis constant of oxygen for shaded big-leaf (Pa)  
C KS sapwood specific conductivity (m<sup>3</sup> MPa<sup>-1</sup> s<sup>-1</sup> m<sup>-1</sup>)  
C KSMAX max sapwood specific conductivity (m<sup>3</sup> MPa<sup>-1</sup> s<sup>-1</sup> m<sup>-1</sup>)  
C KSL soil specific hydraulic conductivity (m<sup>3</sup> MPa<sup>-1</sup> s<sup>-1</sup> kg<sup>-1</sup>)  
C KLSAT soil saturated conductivity (m<sup>3</sup> MPa<sup>-1</sup> s<sup>-1</sup> m<sup>-1</sup>)  
C KSLUNS soil conductivity (m<sup>3</sup> MPa<sup>-1</sup> s<sup>-1</sup> m<sup>-1</sup>)  
C KS\_R specific conductivity of soil+roots (m<sup>3</sup> MPa<sup>-1</sup> s<sup>-1</sup> kg<sup>-1</sup>)  
C LAI canopy leaf area index (-)  
C LAI1 leaf area index of sunlit big-leaf (-)  
C LAI2 leaf area index of shaded big-leaf (-)  
C LATENT latent heat of vaporization (J mol<sup>-1</sup>)  
C MW molecular weight of H2O (kg mol<sup>-1</sup>)  
C NEEDEDAY daily net ecosystem exchange (mol m<sup>-2</sup> d<sup>-1</sup>)  
C NEEYR annual net ecosystem exchange (mol,kgC m<sup>-2</sup> yr<sup>-1</sup>)  
C NPPDAY stand daily net primary production (mol m<sup>-2</sup> d<sup>-1</sup>)  
C NPPYR stand annual net primary production (mol,kgC m<sup>-2</sup> yr<sup>-1</sup>)  
C PENTRY soil entry water potential (MPa)  
C PRE(366) daily precipitation (mm d<sup>-1</sup>)  
C PSILMIN minimum leaf water potential over the year (MPa)  
C PSISCRIT critical soil water potential (MPa)  
C PSISMIN minimum soil water potential over the year (MPa)  
C PSISL soil water potential (MPa)  
C RADRT radius of fine roots (m)  
C RD1 dark respiration rate of sunlit big-leaf (mol m<sup>-2</sup> s<sup>-1</sup>)  
C RD2 dark respiration rate of shaded big-leaf (mol m<sup>-2</sup> s<sup>-1</sup>)  
C RESF hydraulic resistance per unit foliage area (MPa s m<sup>2</sup> m<sup>-3</sup>)  
C RGYR annual cumulated global radiation (J m<sup>-2</sup> yr<sup>-1</sup>)  
C RM stand mainten respir (mol m<sup>-2</sup> s<sup>-1</sup>)  
C RNI1 isothermal net radiation of sunlit big-leaf (W m<sup>-2</sup>)  
C RNI2 isothermal net radiation of shaded big-leaf (W m<sup>-2</sup>)  
C ROS wood density (kgDM m<sup>-3</sup>)  
C RSOIL soil respiration (mol m<sup>-2</sup> s<sup>-1</sup>)  
C SAPBA sapwood basal area (m<sup>2</sup> m<sup>-2</sup>)  
C SLA specific leaf area (m<sup>2</sup> kgDM<sup>-1</sup>)  
C SLDEP soil depth (m)  
C STOMWL coeff in gs vs A equation, limited by soil water (Pa<sup>-1</sup>)  
C TAU1 Rubisco specificity factor for sunlit big-leaf (-)  
C TAU2 Rubisco specificity factor for shaded big-leaf (-)  
C TLEAF1 temperature of sunlit big-leaf (K)  
C TLEAF2 temperature of shaded big-leaf (K)  
C TMEAN(366) daily mean air temperature (oC)  
C VCMAX1 max carboxyl of sunlit big-leaf (mol m<sup>-2</sup> s<sup>-1</sup>)

```

C VCMAX2    max carboxyl of shaded big-leaf (mol m-2 s-1)
C VWSL     soil volumetric water content (m3 m-3)
C VWSAT    saturated soil water content (m3 m-3)
C WF       foliage biomass (kgDM m-2)
C
C Linked subroutines and functions (secondary links)
C AERODYN
C LEUNING
C RADENV   (PSIFUN)
C RESPTREE
C RESPSOIL
C SOILPSI
C UPSCALE (PSIFUN)
C USTOREY
C WEATHER
C *****

```

SUBROUTINE GASFLUX

```

C *****
C Define parameters and variables
C *****
INTEGER DAY, HOUR
REAL ADAY, APARDAY, APARUND, APARU2, APAR1, APAR2,
+ AYR, A1, A2, COMP1, COMP2, DRAIN, EDAY, ETDAY,
+ EUDAY, E1, E2, GAC1, GAC2, GHR1, GHR2, GSC1, GSC2,
+ GSCD1, GSCD2, HOLD, J1, J2, KB, KC1, KC2, KDPAR,
+ KO1, KO2, KS, KSL, KSLUNS, KS_R, LAI, LAI1, LAI2,
+ NEEDAY, NPPDAY, RD1, RD2, RESF, RM, RNI1, RNI2,
+ RSOIL, STOMWL, TAU1, TAU2, TLEAF1, TLEAF2,
+ VCMAX1, VCMAX2
INCLUDE 'HYDRALL.CMN'

C *****
C Define structural parameters
C *****
LAI= WF * SLA !effective leaf area index
SAPBA= WS / (H * ROS) !sapwood basal area (m2 m-2)

C *****
C Zero values to be cumulated/maximized over the whole year
C *****
AYR= 0.
APARYR= 0.
ECRIT= 0.
ETYR= 0.
EUYR= 0.
EYR= 0.
NEEYR= 0.
NPPYR= 0.
PSILMIN= 0.
PSISMIN= 0.
PSISCRIT= 0.
RGYR= 0.

DO 200, DAY= 1, DAYTOT
C *****
C Preliminary computations
C *****
C Daily course of meteorological variables
C -----
CALL WEATHER(DAY)

C Stand respiration (sapwood+fine roots), constant over the day
C -----
CALL RESPTREE(DAY, RM)
C Soil respiration, constant over the day
C -----
CALL RESPSOIL(DAY, RSOIL)

C Soil water potential from soil water content
C -----
CALL SOILPSI
PSISMIN= MIN(PSISMIN, PSISL)

```

```

C      Soil and root hydraulic conductivity
C      -----
C      KSLUNS= KLSLST * (PENTRY/PSISL)**(2.+3./BSL)
C      KSL= KSLUNS / (1.625*ROS*RADRT*ADRT)
C      KS_R= 1. / (1./KR + 1./KSL)
C      Adjust for temp effects on water viscosity
C      -----
C      KS_R= KS_R * (0.5151+0.0242*TMEAN(DAY))
C      Sapwood specific conductivity as a function of height
C      -----
C      KS= KSMAX * (1.-EXP(-0.1127*H))
C      KS= KSMAX * (0.2 + 0.6 * H/18.3)
C      KS= KSMAX
C      Adjust for temp effects on water viscosity
C      -----
C      KS= KS * (0.5151+0.0242*TMEAN(DAY))
C      Leaf specific resistance
C      -----
C      RESF= (1./(WR*KS_R) + H/(SAPBA*KS)) * LAI

C      *****
C      Zero values to be cumulated over the day
C      *****
C      ADAY= 0.
C      APARDAY= 0.
C      EDAY= 0.
C      EUDAY= 0.
C      NPPDAY= 0.
C      NEEDAY= 0.

C      DO 100, HOUR= 1,48
C      *****
C      Photosynthesis, transpiration
C      *****
C      Canopy, understorey light interception
C      -----
C      CALL RADENV(HOUR, LAI,
+          APAR1, APAR2, APARUND, APARU2, KB,
+          KDPAR, LAI1, LAI2, RNI1, RNI2)

C      Canopy energy balance, aerodynamic decoupling
C      -----
C      CALL AERODYN(DAY, HOUR, LAI, LAI1, LAI2, RNI1, RNI2,
+          GAC1, GAC2, GHR1, GHR2, TLEAF1, TLEAF2)
C      Photosynthetic parameters scaled-up for sunlit, shaded big-leaf,
C      corrected for light, temperature effects
C      -----
C      CALL UPSCALE(APAR1, APARU2, HOUR, KB, KDPAR, LAI,
+          TLEAF1, TLEAF2,
+          COMP1, COMP2, GSCD1, GSCD2, J1, J2,
+          KC1, KC2, KO1, KO2, RD1, RD2, STOMWL,
+          TAU1, TAU2, VCMAX1, VCMAX2)
C      Assimilation, transpiration and conductance to CO2
C      for sunlit, shaded big-leaf
C      -----
C      IF(LAI1.GT.0.) THEN
+          CALL LEUNING(COMP1, GAC1, GHR1, GSCD1, HOUR, J1, KC1, KO1,
+          RD1, RNI1, STOMWL, TAU1, VCMAX1,
+          A1, GSC1, E1)                                     !sunlit big-leaf
C      ELSE
C          A1= 0.
C          GSC1= 0.
C          E1= 0.
C      END IF
C      CALL LEUNING(COMP2, GAC2, GHR2, GSCD2, HOUR, J2, KC2, KO2,
+          RD2, RNI2, STOMWL, TAU2, VCMAX2,
+          A2, GSC2, E2)                                     !shaded big-leaf
C      Canopy assimilation, transpiration and conductance to CO2 (mol m-2 s-1)
C      -----
C      ATOT(HOUR)= A1 + A2
C      ETOT(HOUR)= E1 + E2
C      GSCTOT(HOUR)= GSC1 + GSC2

C      Reduce canopy gas exchange and conductance for ground frost

```

```

C -----
C IF(TMIN(DAY).LT.0.) THEN
C   ATOT(HOUR)= 0.
C   ETOT(HOUR)= 0.
C   GSCTOT(HOUR)= 0.
C END IF

C Understorey transpiration, net C exchange
C -----
C CALL USTOREY (APARUND, DAY, HOUR)

C *****
C Cumulated daily values of
C   canopy assimilation (mol m-2 d-1),
C   canopy net primary production (mol m-2 d-1),
C   net ecosystem exchange (mol m-2 d-1)
C   absorbed PAR (mol m-2 yr-1),
C   canopy, understorey transpiration (mm d-1)
C *****
C ADAY= ADAY + 1800. * ATOT(HOUR)
C IF(ATOT(HOUR)-RM.GT.0.) THEN      !reduce positive stand NPP for growth respiration
C   NPPDAY= NPPDAY + 1800.*(ATOT(HOUR)-RM)*CONV
C ELSE
C   NPPDAY= NPPDAY + 1800.*(ATOT(HOUR)-RM)
C END IF
C NEEDAY= NPPDAY + 1800.*(AUND(HOUR) - RSOIL)
C APARDAY= APARDAY + 1800.*(APAR1+APAR2)
C EDAY= EDAY + 1800. * MW * ETOT(HOUR)
C EUDAY= EUDAY + 1800. * MW * EUND(HOUR)

C *****
C Minimum, critical leaf water potential
C *****
C Leaf water potential (MPa)
C -----
C PSILEAF= PSISL - (0.01 * H)
+   - (ETOT(HOUR)/LAI * 0.018/1000. * RESF)

C If leaf water potential is lowest in the year, store
C values of soil water potential and transpiration
C -----
C IF(PSILEAF.LT.PSILMIN) THEN
C   PSILMIN= PSILEAF
C   PSISCRIT= PSISL
C   ECRIT= ETOT(HOUR)/LAI
C   DAYCRIT= DAY
100 END IF
CONTINUE

C *****
C Output selected meteo and gas-exchange variables
C Note: only for last year of simulations, 15-th of each month
C *****
C IF(AGE.EQ.(AGE0+NYRS)) THEN
C   IF(DAY.EQ.15.OR.
+     DAY.EQ.46.OR.
+     DAY.EQ.74.OR.
+     DAY.EQ.105.OR.
+     DAY.EQ.135.OR.
+     DAY.EQ.166.OR.
+     DAY.EQ.196.OR.
+     DAY.EQ.227.OR.
+     DAY.EQ.258.OR.
+     DAY.EQ.288.OR.
+     DAY.EQ.319.OR.
+     DAY.EQ.349) CALL OUTHOUR
C END IF

C *****
C Site water balance
C *****
C Canopy rainfall interception (mm d-1)
C -----
C HOLD= 0.3 * PRE(DAY)

```

```

C      Update soil water content (m3 m-3) for precipitation
C      -----
C      VWSL= VWSL + (PRE(DAY)-HOLD)/SLDEP/1000.
C      Run-off
C      -----
C      IF(VWSL.GT.VWSAT) VWSL= VWSAT

C      Daily drainage (mm d-1)
C      -----
C      CALL SOILPSI
C      KSLUNS= KSLSAT * (PENTRY/PSISL)**(2.+3./BSL)
C      DRAIN= (0.01+PSISL/(20.-SLDEP/2.))/(1.+3./BSL) * KSLUNS !derived from Campbell 1985
C      DRAIN= DRAIN * 3600. * 24. * 1000. !convert into mm d-1
C      Update soil water content (m3 m-3)
C      for evapo-transpiration, capillary rise
C      -----
C      ETDAY= EDAY + EUDAY
C      VWSL= VWSL + (- DRAIN - ETDAY)/1000./SLDEP
C      IF(VWSL.LE.1.E-3) VWSL= 1.E-3
C      ETDAY= ETDAY + HOLD !add evaporation from wet canopy

C      *****
C      Cumulated annual values of
C      - canopy assimilation (mol m-2 yr-1)
C      - canopy net primary production (mol m-2 yr-1),
C      - net ecosystem exchange (mol m-2 yr-1),
C      - canopy, understorey transpiration (mm yr-1)
C      - site evapo-transpiration (mm yr-1)
C      - absorbed PAR (mol m-2 yr-1)
C      - precipitation (mm yr-1)
C      *****
C      AYR=      AYR      + ADAY
C      NPPYR=    NPPYR    + NPPDAY
C      NEEYR=    NEEYR    + NEE DAY
C      APARYR=   APARYR   + APARDAY
C      RGYR=    RGYR     + RGDAY(DAY)
C      EYR=     EYR      + EDAY
C      EUYR=    EUYR     + EUDAY
C      ETYR=    ETYR     + ETDAY
200 CONTINUE

C      *****
C      Final computations
C      *****
C      Impose non-negative GPP and NPP over the year
C      -----
C      IF(NPPYR.LT.0.) NPPYR= 1.E-6
C      IF(GPPYR.LT.0.) GPPYR= 1.E-6

C      Canopy quantum efficiency (-)
C      -----
C      ALPHAC= AYR/APARYR
C      Convert units of C exchange from moles into kgC m-2 yr-1
C      -----
C      GPPYR= AYR * 0.012
C      NPPYR= NPPYR * 0.012
C      NEEYR= NEEYR * 0.012

C      RETURN
C      END

C      *****
C      References
C      *****
C      Campbell GS 1985. Soil Physics with BASIC. Elsevier, Amsterdam
C      Choudhury BJ, Monteith JL 1988. A four-layer model for the heat budget of
C      homogeneous land surfaces. Q J R Meteorol Soc 114,373-398
C      Garratt JR 1992. The Atmospheric Boundary Layer. Cambridge Univ Press,
C      Cambridge
C      Landsberg JJ, Waring RH 1997. A generalized model of forest productivity
C      using simplified concepts of radiation-use efficiency, carbon balance
C      and partitioning. For Ecol Manag 95,209-228
C      Leuning R 1995. A critical appraisal of a combined stomatal-photosynthesis
C      model for C3 plants. Plant Cell Envir 18,339-355

```



- C Monteith JL 1995. A reinterpretation of stomatal responses to humidity.  
C Plant Cell Envir 18,357-364  
C Monteith JL, Unsworth M 1990. Principles of Environmental Physics.  
C E Arnold, London  
C Pothier D, Margolis HA, Waring RH 1989. Patterns of change of saturated  
C sapwood permeability and sapwood conductance with stand development.  
C Can J For Res 19,432-439  
C Shaw RH, Pereira AR 1982. Aerodynamic roughness of a plant canopy.  
C A numerical experiment. Agric Meteorol 26,51-65  
C Whitehead D, Edwards WRN, Jarvis PG 1984. Conducting sapwood area,  
C foliage area, and permeability in mature trees of *Picea sitchensis*  
C and *Pinus contorta*. Can J For Res 14,940-947

```

C *****
C FORTRAN subroutine   GRSTAND   (grstand.for)           26/6/98
C -----
C Purpose Given values for:
C   (a) initial biomass of stand compartments
C   (b) annual stand net primary production
C   (c) critical soil water potential
C   (d) critical transpiration rate (per unit leaf area) over the year
C the sub-routine simulates the growth of the compartments of the
C entire stand over one year.
C Turnover - Simplified formulation (Makela 1986,Thornley & Johnson 1990)
C Allocation (sub OPTIMAL) - Carbon allocated between foliage,
C   sapwood and fine roots with an optimization criterion
C   (Parker & Maynard-Smith 1990) under the hydraulic constraint of
C   cavitation avoidance (sub ROOTFIND). Height growth assumed as
C   fitness criterion, hence maximized.
C   Height growth assumed to be proportional to the difference between
C   foliage production and foliage turnover.
C Changes in content of young carbon in soil - Turnover of stand and
C   understorey tissues increases soil litter at the end of the year.

```

C Parameters and variables

```

C ALLF   coeff of allocation to foliage (-)
C ALLR   coeff of allocation to fine roots (-)
C ALLS   coeff of allocation to sapwood (-)
C CAI    stand current annual increment (m3 ha-1 yr-1)
C CSLY   young organic matter in soil (kgDM m-2)
C FC     coeff for conversion of carbon into DM (kgC kgDM-1)
C GST    annual gross stand growth (kgDM m-2 yr-1)
C H      stand height (m)
C LF     foliage longevity (yr)
C LR     fine root longevity (yr)
C LS     sapwood longevity (yr)
C MERCH  merchantable wood as fraction of stem biomass (-)
C NPPYR  stand annual net primary production (kgC m-2 yr-1)
C PSISCRIT critical soil water potential (MPa)
C ROF    foliage density (kgDM m-3)
C STORE  internal carbon storage (kgC m-2)
C VOL    stand volume (m3 ha-1)
C WF     stand foliage biomass (kgDM m-2)
C WFUND  understorey foliage biomass (kgDM m-2)
C WR     stand fine root biomass (kgDM m-2)
C WRUND  understorey fine root biomass (kgDM m-2)
C WS     stand sapwood biomass (kgDM m-2)
C WST    stand woody biomass (kgDM m-2)

```

C Linked subroutines (secondary links)

```

C   OPTIMAL   (ROOTFIND)

```

SUBROUTINE GRSTAND

```

C *****

```

Define parameters and variables

```

C *****
C   INTEGER COUNT
C   REAL   DUM1, DUM2, ALLFOLD, ALLROLD, ALLSOLD, STORE
C   SAVE   COUNT
C   INCLUDE 'HYDRALL.CMN'

```

```

C *****

```

C Annual stand growth

```

C *****

```

C Effects of understorey tissue turnover

```

C -----
C   CSLY= CSLY + (WFUND+WRUND)*0.9 !update soil carbon content
C   WFUND= 0.1 * WFUND             !reduce biomass of compartments
C   WRUND= 0.1 * WRUND

```

C Effects of stand tissue turnover

```

C -----
C   CSLY= CSLY + WF/LF + WR/LR !update soil carbon content
C   WF= WF - WF/LF             !reduce biomass of compartments
C   WR= WR - WR/LR

```

```

WS= WS - WS/LS

C   Net stand growth
C   -----
   IF(COUNT.EQ.1) THEN
     GST= (STORE + NPPYR)/2. / FC
   ELSE
     GST= NPPYR / FC
   END IF
   STORE= (STORE + NPPYR)/2.

C   Compute allocation coefficients under hydraulic constraint
C   -----
   ALLFOLD= ALLFNEW
   ALLROLD= ALLRNEW
   ALLSOLD= ALLSNEW
   CALL OPTIMAL
   IF(COUNT.EQ.1) THEN
     ALLFNEW= (ALLFNEW+ALLFOLD) / 2.
     ALLRNEW= (ALLRNEW+ALLROLD) / 2.
     ALLSOLD= (ALLSNEW+ALLSOLD) / 2.
   END IF

C   Compute stand height, allocate new growth
C   -----
   IF(ALLFNEW*GST.GT.0.) H= H + ALLFNEW*GST/ROF
   WF= WF + (ALLFNEW*GST)
   WR= WR + (ALLRNEW*GST)
   WS= WS + (ALLSNEW*GST)
   IF(WF.LT.1.E-6) WF= 1.E-6 !impose constraint of positive biomass
   IF(WR.LT.1.E-6) WR= 1.E-6
   IF(WS.LT.1.E-6) WS= 1.E-6

C   Compute woody biomass, stand volume and current annual increment
C   Note: 90% of woody biomass assumed to be in bole
C   -----
   DUM1= WST
   IF(ALLSNEW*GST.GT.0.) WST= WST + (ALLSNEW*GST)
   DUM2= MERCH * 10000. / ROS
   VOL= WST * DUM2 !stand volume (m3 ha-1)
   CAI= (WST-DUM1) * DUM2 !curr ann increm (m3 ha-1 yr-1)

C   Set flag high
C   -----
   COUNT= 1

   RETURN
   END

C *****
C   References
C *****
C Makela A. (1986) Implications of the pipe model theory on dry matter
C partitioning and height growth in trees. J. Theor. Biol. 123, 103-120.
C Parker G.A., Maynard Smith J. (1990) Optimality theory in evolutionary
C biology. Nature 348, 27-33
C Thornley J.H.M. & Johnson I.R. (1990) Plant and Crop Modelling. Clarendon
C Press, Oxford.

```

```

C *****
C FORTRAN subroutine      GRTREE      (grtree.for)          28/2/99
C -----
C Purpose Based on stand growth (as computed in sub-routine GRSTAND), the
C sub-routine partitions stand biomass among identical trees and
C computes average tree characteristics.
C Starting from an imposed stocking density, stand density is
C progressively reduced by distance-dependent mortality, represented
C by the self-thinning law (Westoby 1984). Self-thinning is driven by
C stand biomass, so as to avoid any positive feed-back.
C Constant values are assumed for the fraction of stem biomass in
C merchantable wood and for stem form factor.
C
C Parameters and variables
C DBH      average tree diameter at breast height (cm)
C FORM     stem form factor (-)
C H        stand height (m)
C MERCH    merchantable wood as fraction of stem biomass (-)
C ROS      wood density (kgDM m-3)
C STH      option for self-thinning (1 : included, 0 : neglected)
C STH0     intercept in self-thinning eq. (logN vs logWST) (m-2)
C STH1     slope in self-thinning eq. (logN vs logWST) (kgDM-1)
C THAGE    age for thinning (-)
C THN      thinning intensity, plants (-)
C THV      thinning intensity, volume (-)
C TREES    stand density (trees m-2)
C WF       foliage biomass of the stand (kgDM m-2)
C WFTR     foliage biomass of a tree (kgDM)
C WR       fine root biomass of the stand (kgDM m-2)
C WRTR     fine root biomass of a tree (kgDM)
C WS       sapwood biomass of the stand (kgDM m-2)
C WSTR     sapwood biomass of a tree (kgDM)
C WST      stemwood biomass of the stand (kgDM m-2)
C WSTR     stemwood biomass of a tree (kgDM)
C
C *****
C
C SUBROUTINE GRTREE
C
C *****
C Define parameters and variables
C *****
C INTEGER I
C REAL DUM1
C INCLUDE 'HYDRALL.CMN'
C
C *****
C Stand dynamics
C *****
C Compute tree biomass components and woody biomass
C -----
C WFTR= WF / TREES
C WRTR= WR / TREES
C WSTR= WS / TREES
C WSTR= WST / TREES
C
C (1) Impose a thinning regime
C -----
C DO 10, I=1,20
C IF(AGE.EQ.THAGE(I)) THEN
C TREES= TREES * (1.-THN(I))
C WF= WF * (1.-THV(I))
C WR= WR * (1.-THV(I))
C WS= WS * (1.-THV(I))
C WST= WST * (1.-THV(I))
C END IF
10 CONTINUE
C
C (2) If the stand is too dense, density is reduced by distance-dependent
C mortality (self-thinning).
C Note: self-thinning can be excluded by the user by setting STH= 0
C -----
C IF(STH.EQ.1) THEN
C DUM1= TREES

```

```

TRSTH= 10. ** (STH0 - STH1*LOG10(WST*MERCH))
IF(TRSTH.LT.TREES) THEN
  TREES= (TREES+TRSTH)/2.
  WF= WF - WFTR * (DUM1-TREES)
  WR= WR - WRTR * (DUM1-TREES)
  WS= WS - WSTR * (DUM1-TREES)
  WST= WST - WSTR * (DUM1-TREES)
END IF
END IF

C Average tree diameter at breast height
C Note: 10% of shoot carbon assumed to be in branches, stumps
C -----
WSTTR= WST / TREES
DBH= SQRT(4./PI*(WSTTR*MERCH)/(ROS*H*FORM)) *100.

RETURN
END

```

```

C *****
C References
C *****
C Westoby M 1984. The self-thinning rule. Adv Ecol Res 14, 167-225

```

```

C *****
C FORTRAN subroutine      INCLIM      (inclim.for)      10/3/99
C -----
C Purpose The routine reads from file one year of daily meteorological
C data. All variables are stored in common blocks.
C Air CO2 concentration is updated, based on input rate of change.
C
C Parameters and variables
C AGE      stand age (yr)
C CA      CO2 partial pressure in the atmosphere (Pa)
C DAY      day of month
C DAYTOT   total number of days in the year
C DCA      annual change in atmospheric CO2 (%)
C ICLIM,0  location of meteo data file (runs, initialization)
C IFILES   location of root input file
C INFILE   file to be read
C JDAY     Julian day
C PRE      daily precipitation (mm d-1)
C PREYR    annual precipitation (mm yr-1)
C RGDAY    daily total of global radiation (J m-2 d-1)
C RH       air relative humidity (%)
C TMAX     maximum daily temperature (oC)
C TMEAN    mean daily temperature (oC)
C TMIN     minimum daily temperature (oC)
C WND      monthly (constant) wind speed (m s-1)
C
C *****
C
C SUBROUTINE INCLIM
C *****
C Define parameters and variables
C *****
C INTEGER      COUNT, DAY, JDAY, MTH, YEAR
C CHARACTER*40 ICLIM, ICLIM0, INFILE
C SAVE         COUNT, ICLIM, ICLIM0, INFILE
C INCLUDE 'HYDRALL.CMN'
C INCLUDE 'FILES.CMN'
C *****
C Input weather data
C *****
C Upon first call, read specifications of input files
C -----
C IF(COUNT.EQ.0) THEN
C   CALL RDINIT (1 , 0, IFILES)
C   CALL RDSCHA ('ICLIM' , ICLIM )
C   CALL RDSCHA ('ICLIM0' , ICLIM0)
C   CLOSE (1)
C   INFILE= ICLIM0
C   COUNT= 1                               !set flag high
C END IF
C
C Reset meteo data-set after initialization
C -----
C IF(AGE.EQ.AGE0+1) THEN
C   CLOSE (1)
C   INFILE= ICLIM
C END IF
C
C Read one year of daily values of meteo variables
C -----
C OPEN(UNIT= 1,
C + FILE= INFILE,
C + STATUS= 'UNKNOWN',
C + ERR= 1000)
C PREYR= 0.
C DO 10, JDAY= 1,366
C   DAYTOT= JDAY                               !update number of days in the year
C   READ(UNIT= 1,
C + FMT= 2000,
C + END= 1000)
C + YEAR, MTH, DAY,
C + TMIN(JDAY) , TMEAN(JDAY) , TMAX(JDAY) , PRE(JDAY) ,

```

```

+      RH(JDAY),RGDAY(JDAY),WND(JDAY)
  RGDAY(JDAY)= RGDAY(JDAY) * 10000.    !change units in J m-2 d-1
  PREYR= PREYR + PRE(JDAY)             !annual precipitation (mm yr-1)
  IF(MTH.EQ.12.AND.DAY.EQ.31) GOTO 1000
10  CONTINUE
1000 CONTINUE

C      Update atmospheric CO2 for climate change effects (excluded during initialization)
C      -----
      IF(AGE.GE.AGE0+1)      CA= CA + DCA

C      Disconnect device upon last year of simulations
C      -----
      IF(AGE.EQ.AGE0+NYRS)  CLOSE (1)

C *****
C                               Formats
C *****
2000 FORMAT(T5,I4,
+          T15,I2,
+          T23,I2,
+          T28,F5.0,
+          T36,F5.0,
+          T44,F5.0,
+          T52,F5.0,
+          T60,F5.0,
+          T67,F6.0,
+          T77,F4.0 )

      RETURN
      END

```

```

C *****
C FORTRAN subroutine      INIT      (init.for)      10/3/99
C -----
C Purpose The routine assigns initial values to state variables.
C Sapwood and fine root biomass are derived from imposed
C foliage biomass so as to achieve set unit resistance with an
C optimal balance. Height derived from assumption of constant
C foliage density, cylindrical crown shape and fixed radius vs
C height ratio in young trees.
C The model is run with repeated meteo data until the initial conditions
C of stand height are reached. Initial stand woody biomass is then imposed.
C
C Parameters and variables
C A dummy variable
C ALLFNEW coefficient of allocation to foliage (-)
C ALLRNEW coefficient of allocation to fine roots (-)
C ALLSNEW coefficient of allocation to sapwood (-)
C BSL coeff. in soil water retention curve equation
C CSLO old organic matter in soil (kgDM m-2)
C CSLOO initial old organic matter in soil (kgDM m-2)
C CSLY young organic matter in soil (kgDM m-2)
C CSLYO initial young organic matter in soil (kgDM m-2)
C H stand height (m)
C HO initial stand height (m)
C KR root specific conductance (m3 MPa-1 s-1 kg-1)
C KS sapwood specific conductivity (m3 MPa-1 s-1 m-1)
C KSL soil specific hydr conduct (m3 MPa-1 s-1 kg-1)
C KLSAT satur soil hydr. conduct. (m3 MPa-1 s-1 m-1)
C KSMAX max sapwood specific conduct (m3 MPa-1 s-1 m-1)
C KS_R spec conduct of soil+roots (m3 MPa-1 s-1 kg-1)
C LR fine root longevity (yr)
C LS sapwood longevity (yr)
C MERCH merchantable wood as fraction of stem biomass (-)
C PENTRY soil entry water potential (MPa)
C PLANT planting density (m-2)
C PSISL soil water potential (MPa)
C RADRT root radius (m)
C RESF hydr resistance per unit leaf area (MPa s m2 m-3)
C ROF foliage density (kgDM m-3)
C ROS wood density (kgDM m-3)
C SLA specific leaf area (m2 kgDM-1)
C TREESO initial stand density (trees m-1)
C VOLO initial stand volume (m3 ha-1)
C VWSL soil volum water content (m3 m-3)
C WF stand foliage biomass (kgDM m-2)
C WFUND understorey foliage biomass (kgDM m-2)
C WR stand root biomass (kgDM m-2)
C WS stand sapwood biomass (kgDM m-2)
C WST stand woody biomass (kgDM m-2)
C
C Linked subroutines (secondary links)
C GRTREE
C SOILPSI
C *****
C
C SUBROUTINE INIT
C *****
C Define parameters and variables
C *****
C REAL A, KS, KSL, KS_R, RESF
C INCLUDE 'HYDRALL.CMN'
C *****
C Variables at planting
C *****
C Soil variables
C -----
C VWSL= 0.25 !initial soil water content, m3 m-3
C CALL SOILPSI !initial soil water potential (MPa)
C KSL= KLSAT / (1.625*ROS*RADRT*RADRT) *
C + (PENTRY/PSISL)**(2.+3./BSL) !soil hydr conductiv, m3 MPa-1 s-1 kg-1
C CSLO= CSLOO !old organic matter in soil, kgDM m-2
C CSLY= CSLYO !young organic matter in soil, kgDM m-2

```



```

C   Stand variables
C   -----
WFTR= 0.1                               !impose tree foliage biomass, kgDM
WF= WFTR * PLANT                         !compute stand foliage biomass, kgDM m-2
H= (9./PI * WFTR/ROF)**(1./3.)           !derive stand height, m
RESF= 1.E7                               !hydr res per unit leaf area, MPa s m2 m-3
KS_R= 1. / (1./KR + 1./KSL)             !soil+root hydr cond, m3 MPa-1 s-1 kg-1
KS= KSMAX                                !sapwood spec conductiv, m3 MPa-1 s-1 m-1
A= SQRT(KS_R/KS*LS/LR*ROS)
WR= WF * SLA / (KS_R*RESF) * (1.+H*A*LR/LS) !derive stand fine root biomass, kgDM
WS= WR * H * A                          !derive stand sapwood biomass, kgDM
WST= WS                                  !stand stem biomass, kgDM

C   Stand density, individual tree characteristics
C   -----
TREES= PLANT                             !initial stand density
CALL GRTREE                              !single tree characteristics

C   Understorey variables
C   -----
WFUND= 0.1                               !understorey foliage biomass, kgDM m-2

C *****
C   Initialize the model (run until initial height is reached)
C *****
DO 100, I= 1,50
  CALL INCLIM                            !read first year of meteo data from file
  CALL GASFLUX                           !NPP, NEE, water rel parms for allocation
  CALL GRSTAND                           !stand growth
  CALL GRTREE                            !stand density, tree diameter

  IF(H.GT.H0) THEN
    H= H0                                !impose initial height
    TREES= TREES0                        !impose initial density
    VOL= VOLO                             !impose volume
    WST= VOLO * ROS / MERCH / 10000.     !impose initial stand woody biomass
    CALL GRTREE                          !update stand density, tree diameter
    GOTO 200
  END IF
100 CONTINUE
200 CONTINUE

RETURN
END

```

```

C *****
C FORTRAN subroutine      INPARMS      (inparms.for)      26/2/99
C -----
C Purpose The routine sets physical constants, reads from file
C (a) general physiological and structural parameters
C (b) photosynthetic and stomatal parameters
C (c) runtime parameters (site location, initial values)
C Other parameters set or derived within the model:
C - constant photosynthetic parameters (dePury and Farquhar 1997)
C - photosynthetic parameters derived from input parms as suggested
C by de Pury and Farquhar (1997) and Leuning (1997)
C - convexity of light-response curve given a constant value of 0.7
C - parameters of self-thinning law assumed constant
C - growth respiration assumed constant
C - fine root diameter assumed constant
C - soil hydraulic characteristics derived from soil granulometry as
C described in Campbell (1985).
C All parameters and variables are stored in common blocks.
C
C Parameters and variables
C
C AGE0      initial stand age (yr)
C ALPHA     quantum efficiency of electron transport (mol mol-1)
C ALTIT     site altitude (m)
C BSL       coeff. in soil water retention curve equation
C CA        baseline CO2 partial pressure in the atmosphere (Pa)
C CLAY      soil fraction of clay particles (kg kg-1)
C CONV      dry matter conversion efficiency (growth resp.) (-)
C CP        specific heat capacity of air (J mol-1 K-1)
C CSLOO     initial old organic matter in soil (kgDM m-2)
C CSLYO     initial young organic matter in soil (kgDM m-2)
C DCA       annual change in atmospheric CO2 (%)
C DG        soil mean particle diameter (mm)
C FC        coeff for conversion of carbon into DM (kgC kgDM-1)
C FORM      stem form factor (-)
C GAMMA     psychrometer constant (Pa K-1)
C HA_JM     activation energy of electron transport (J mol-1)
C HA_KC     activation energy for carboxylation (J mol-1)
C HA_KO     activation energy for oxygenation (J mol-1)
C HA_RD     activation energy (J mol-1)
C HA_VCM    activation energy for carboxylation (J mol-1)
C HD_JM     deactivation energy of electron transport (J mol-1)
C H0        initial stand height (m)
C IFILES    location of root input file
C IPARMS    location of miscellaneous parameters file
C IPHOT     location of photosynthetic parameters file
C IRUN      location of run-time parameters file
C JM_OP     potential rate of electron transport at optimum temperature (mol m-2 s-1)
C KC_TO     Michaelis constant for carboxylation at reference temperature (Pa)
C KO_TO     Michaelis constant for oxygenation at reference temperature (Pa)
C KR        root specific conductance (m3 MPa-1 s-1 kg-1)
C KSMAX     max. sapwood specific conductivity (m3 MPa-1 s-1 m-1)
C KSLSAT    saturated soil hydr. conduct. (m3 MPa-1 s-1 m-1)
C LATENT    latent heat of vaporization (J mol-1)
C LATIT     site latitude (degrees x 100, then rad)
C LF        foliage longevity (yr)
C LONGIT    site latitude (degrees x 100)
C LR        fine root longevity (yr)
C LS        sapwood longevity (yr)
C MERCH     merchantable wood as fraction of stem biomass (-)
C MW        molecular weight of H2O (kg mol-1)
C NF        foliage nitrogen concentration (kg kgDM-1)
C NR        fine root nitrogen concentration (kg kgDM-1)
C NS        sapwood nitrogen concentration (molN kgDM-1)
C NYRS     simulation length (yr)
C OSS       oxygen part pressure in the atmosphere (Pa)
C PENTRY    soil entry water potential (MPa)
C PI        pi greek (-)
C PLANT     planting density (m-2)
C PRE       monthly precipitation (mm mth-1)
C PRESS     atmospheric pressure (Pa)
C PSITHR    water potential threshold for cavitation (MPa)
C PSIO     soil water potential for complete stomatal closure (MPa)
C PO        maximum photosynthetic efficiency (kgC MJ-1 global)

```

```

C RADRT    root radius (m)
C RD_TO    dark respiration at reference temp (mol m-2 s-1)
C RGAS     gas constant (Pa m3 mol-1 K-1)
C ROF      foliage density (kgDM m-3)
C ROS      wood density (kgDM m-3)
C SAND     soil fraction of sand particles (kg kg-1)
C SIGMA    Stefan-Boltzmann constant (W m-2 K-4)
C SIGMAG   geometric standard deviation in particle size distribution (mm)
C SILT     soil fraction of silt particles (kg kg-1)
C SLA      specific leaf area (project. leaf area basis)(m2 kgDM-1)
C SLDEP    depth of soil explored by roots (m)
C STH      option for self-thinning (1 : included, 0 : neglected)
C STH0     intercept in self-thinning eq. (logN vs logWST) (m-2)
C STH1     slope in self-thinning eq. (logN vs logWST) (kgDM-1)
C STIND    stomatal index (1= amphy-, 2= hypostomatous species)
C STOM0    stomatal conductance to CO2 in darkness (molCO2 m-2 s-1)
C STOM1    coeff in gs vs A equation (Pa)
C THETA    convexity factor of light response curve (-)
C THAGE    age for thinning (-)
C THN      thinning intensity, plants (-)
C THV      thinning intensity, volume (-)
C TREESO   initial stand density (m-2)
C T_JM     optimum temperature for electron transport (K)
C VCM_OP   max carboxylation rate at opt temp (mol m-2 s-1)
C VOL0     initial stand volume (m3 ha-1)
C VPD0     coeff in gs response to Ds (Pa)
C VWSAT    saturated soil water content (m3 m-3)
C W        leaf width (m)

```

```

C *****

```

```

SUBROUTINE INPARMS

```

```

C *****

```

```

C Define parameters and variables

```

```

C *****

```

```

INTEGER      DUM
REAL         CLAY, DG, DUM1, DUM2, SAND, SIGMAG, SILT
CHARACTER*40 IPARMS, IPHOT, IRUN
INCLUDE 'HYDRALL.CMN'
INCLUDE 'FILES.CMN'

```

```

C Assign physical and miscellaneous constants

```

```

C Note: the PARAMETER statement cannot be used, as parms are included in COMMON block

```

```

C -----

```

```

CP= 29.31
FC= 0.5
GAMMA= 66.2
LATENT= 43956.
MW= 0.018
OSS= 21176.
PI= 3.141593
PRESS= 101325.
RGAS= 8.3144
SIGMA= 5.6703E-8

```

```

C *****

```

```

C Input parameter; set output

```

```

C *****

```

```

C Read specifications of input and output files

```

```

C -----

```

```

WRITE (0, 100)
100 FORMAT(1H0, '          Type path of root input file'/
+       1H, '          between commas ('c:\...\files.txt'))
READ *, IFILES

CALL RDINIT (1, 0, IFILES)
CALL RDSCHA ('IPARMS'      , IPARMS      )
CALL RDSCHA ('IPHOT'      , IPHOT      )
CALL RDSCHA ('IRUN'       , IRUN       )
CLOSE (1)

```

```

C Read miscellaneous functional and structural parameters from file

```

```

C -----

```

```

CALL RDINIT (1 , 0 , IPARMS)
CALL RDSREA ('FORM'      , FORM      )
CALL RDSREA ('KR'       , KR       )
CALL RDSREA ('KSMAX'    , KSMAX   )
CALL RDSREA ('LF'       , LF       )
CALL RDSREA ('LR'       , LR       )
CALL RDSREA ('LS'       , LS       )
CALL RDSREA ('NF'       , NF       )
CALL RDSREA ('NR'       , NR       )
CALL RDSREA ('NS'       , NS       )
CALL RDSREA ('PSITHR'   , PSITHR  )
CALL RDSREA ('ROF'      , ROF      )
CALL RDSREA ('ROS'      , ROS      )
CALL RDSREA ('SLA'      , SLA      )
CALL RDSINT ('STIND'    , STIND    )
CALL RDSREA ('W'        , W        )
CLOSE (1)

```

C Unit conversion

```

C -----
NF= NF / 0.014           !foliage N content, molN kgDM-1
NR= NR / 0.014           !fine root N content, molN kgDM-1
NS= NS / 0.014           !sapwood N content, molN kgDM-1

```

C Define additional functional and structural parameters

```

C -----
CONV= 0.8                !dry matter conversion efficiency (growth resp.)(-)
MERCH= 0.85              !merchantable wood as fraction of stem biomass (-)
RADRT= 1.E-3             !root radius (m)
STHO= 0.8561             !intercept in self-thinn eq. (log(TREES) vs log(WST)) (m-2)
STH1= 1.9551             !slope in self-thinn eq. (log(TREES) vs log(WST)) (kgDM-1)

```

C Read photosynthesis/stomatal parameters from file

```

C -----
CALL RDINIT (1 , 0 , IPHOT)
CALL RDSREA ('ALPHA'    , ALPHA   )
CALL RDSREA ('PSIO'     , PSIO    )
CALL RDSREA ('STOMO'    , STOMO   )
CALL RDSREA ('STOM1'    , STOM1   )
CALL RDSREA ('VCMOP'    , VCMOP   )
CALL RDSREA ('VPDO'     , VPDO    )
CLOSE (1)

```

C Define additional photosynthetic parameters

```

C -----
THETA= 0.7               !convexity factor of light response curve (-)
HAVCM= 64800.            !activation energy of VCMOP (J mol-1)
JMOP= 2.68 * VCMOP       !pot rate of electr transp at opt temp (mol e m-2 s-1)
HAJM= 37000.             !activation energy of JMOP (J mol-1 e)
HDJM= 220000.            !deactivation energy of JMOP (J mol-1 e)
TJM= 304.16              !optimum temperature for electron transport (K)

KCT0= 40.4               !Michaelis constant for carboxylation at ref temp (Pa)
HAKC= 59400.             !activation energy of KCT0 (J mol-1)

KOT0= 24800.             !Michaelis constant for oxygenation at ref temp (Pa)
HAKO= 36000.             !activation energy of KOT0 (J mol-1)

RDT0= 0.0089 * VCMOP     !dark respiration at ref temp (mol m-2 s-1)
HARD= 66400.             !activation energy of RD0 (J mol-1)

```

C Read runtime parameters from file

```

C -----
CALL RDINIT (1 , 0 , IRUN)
CALL RDSINT ('AGE0'     , AGE0    )
CALL RDSREA ('ALTIT'    , ALTIT   )
CALL RDSREA ('CA'      , CA      )
CALL RDSREA ('CSLOO'    , CSLOO   )
CALL RDSREA ('CSLYO'    , CSLYO   )
CALL RDSREA ('DCA'     , DCA     )
CALL RDSREA ('HO'      , HO      )
CALL RDSREA ('LATIT'    , LATIT   )
CALL RDSREA ('LONGIT'   , LONGIT  )
CALL RDSINT ('NYRS'     , NYRS    )

```

```

CALL RDSREA ('PLANT' , PLANT )
CALL RDSREA ('SAND' , SAND )
CALL RDSREA ('SILT' , SILT )
CALL RDSREA ('SLDEP' , SLDEP )
CALL RDSINT ('STH' , STH )
CALL RDSREA ('TREES0' , TREES0 )
CALL RDAINT ('THAGE' , THAGE , 20, DUM)
CALL RDAREA ('THN' , THN , 20, DUM)
CALL RDAREA ('THV' , THV , 20, DUM)
CALL RDSREA ('VOLO' , VOLO )
CLOSE (1)

```

```

C Convert latitude into radians

```

```

C -----
LATIT= LATIT/100. * PI / 180.

```

```

C Derive soil hydraulic characteristics from soil granulometry

```

```

C -----
VWSAT= 0.4 !saturated soil water content (m3 m-3)
CLAY= 1.-SAND-SILT !soil fraction of clay (kg kg-1)
DUM1= CLAY*LOG(0.001) + SAND*LOG(1.025) + SILT*LOG(0.026)
DG= EXP(DUM1) !soil mean particle diameter (mm)
DUM2= SQRT(CLAY*LOG(0.001)**2 + SAND*LOG(1.025)**2
+ SILT*LOG(0.026)**2)
SIGMAG= EXP(DUM2) !geometr st dev in particle size distribution (mm)
PENRY= -0.5 / SQRT(DG) / 1000. !soil entry water potential (MPa)
BSL= -2. * (PENRY*1000.) + 0.2 * SIGMAG !coeff in soil water release curve (-)
KSLSAT= 0.004 * EXP(-6.9*CLAY-3.7*SILT) !sat soil hydr conduct (m3 MPa-1 s-1 m-1)

```

```

RETURN
END

```

```

C *****
C References
C *****
C Campbell GS 1985. Soil Physics with BASIC. Transport Models for Soil-Plant
C Systems. Elsevier, Amsterdam
C dePury DGG, Farquhar GD 1997. Simple scaling of photosynthesis from leaves to
C canopies without the errors of big-leaf models. Plant Cell Envir 20, 537-557
C Leuning R 1997. Scaling to a common temperature improves the correlation
C between the photosynthesis parameters Jmax and Vcmax. J Exp Bot 48, 345-347

```

```

C *****
C FORTRAN subroutine          LEUNING      (leuning.for)      7/3/99
C -----
C PURPOSE The program models leaf assimilation, stomatal conductance and
C transpiration as a function of environmental variables, taking into
C account the effects of partial aerodynamic decoupling.
C 1) assimilation represented by the Farquhar model (Farquhar et al 1980, 1982)
C    assuming negligible internal conductance
C 2) stomatal conductance represented by the Leuning model (Leuning 1995)
C 3) the effects of decoupling on leaf temperature and radiative heat
C    dissipation and CO2 and vapor exchange are considered (Collatz et al 1991)
C Input photosynthetic parameters have been corrected for temperature, PAR,
C soil water effects and scaled-up over the canopy in the subroutine UPSCALE.
C The model is solved iteratively.
C Computations are for a hypostomatous leaf.
C
C Parameters and variables
C
C ASS      assimilation rate (molCO2 m-2 s-1)
C CA       CO2 partial pressure in the atmosphere (Pa)
C CC       stromal CO2 concentration (Pa)
C COMP     CO2 compensation point in dark (Pa)
C CP       specific heat capacity of air (J mol-1 K-1)
C GAC      aerodynamic conductance to CO2 exchange (molCO2 m-2 s-1)
C GHR      total conductance to heat exchange (mol m-2 s-1)
C GSC      stomatal conductance to CO2 exchange (molCO2 m-2 s-1)
C GSCD     stomatal conductance in darkness (molCO2 m-2 s-1)
C HOUR     half/hour interval number
C J        electron transport rate (mol m-2 s-1)
C KC       Michaelis constant of carboxylation (Pa)
C KO       Michaelis constant of oxygenation (Pa)
C PRESS    atmospheric pressure (Pa)
C RD       dark respiration rate (mol m-2 s-1)
C RNI      isothermal net radiation (W m-2)
C S(48)    slope of sat vapor pressure vs temperature (Pa K-1)
C STOMWL   coeff in gs vs A equation, limited by soil water (Pa-1)
C TAU      Rubisco specificity factor (-)
C TR       transpiration rate (mol m-2 s-1)
C VC       carboxylation rate (mol m-2 s-1)
C VCMAX    maximum carboxylation rate (mol m-2 s-1)
C VPD(48)  vapour pressure deficit in the atmosphere (Pa)
C VPDS     vapor pressure deficit at leaf surface (Pa)
C VPDO     coeff in gs response to Ds (Pa)
C WC       Rubisco-limited carboxylation rate (mol m-2 s-1)
C WJ       electron transport-limited carboxylation rate (mol m-2 s-1)
C
C *****
      SUBROUTINE LEUNING (COMP, GAC, GHR, GSCD, HOUR, J, KC, KO, RD,
+          RNI, STOMWL, TAU, VCMAX,
+          ASS, GSC, TR)
C
C *****
C      Define parameters and variables
C *****
      INTEGER HOUR, I
      REAL ASS, CC,
+      COMP, DUM1, GAC, GHR, GSC, GSCD, J, KC, KO, RD, RNI,
+      STOMWL, TAU, TR, VC, VCMAX, VPDS, WC, WJ
      INCLUDE 'HYDRALL.CMN'
C
C *****
C      Day-time computations
C *****
      IF (J.GE.1.E-7) THEN
C      Initialize variables
C -----
      CC = 0.7 * CA
      VPDS = VPD(HOUR)
C
      DO 100, I = 1, 20
C      Assimilation
C -----
      WC = VCMAX * CC / (CC + KC * (1. + OSS/KO)) !RuBP-lim carboxyl (mol m-2 s-1)

```

```

WJ= J * CC / (4. * (CC + OSS/TAU))           !el transp-lim carboxyl (mol m-2 s-1)
VC= MIN(WC,WJ)                               !carboxylation rate (mol m-2 s-1)
ASS= VC * (1. - 0.5 * OSS / TAU / CC) - RD   !assimilation (mol m-2 s-1)
IF(ASS.LT.RD)  ASS= RD
CS= CA - PRESS * ASS / GAC                   !CO2 concentr at leaf surface (Pa)

C      Stomatal conductance
C      -----
GSC= GSCD + STOMWL * ASS / (CS-COMP) * VPD0 / (VPD0+VPDS) !CO2 st cond (mol m-2 s-1)
IF(GSC.LT.1.E-6)  GSC= 1.E-6

C      Stromal CO2 concentration
C      -----
CC= CS - PRESS * ASS / GSC                   !CO2 concentr at carboxyl sites (Pa)
IF(CC.LT.1.E-6)  CC= 1.E-6

C      Vapour pressure deficit at leaf surface
C      -----
DUM1= 1.6*S(HOUR)/GAMMA+GHR/GAC
VPDS= (S(HOUR)/CP*RNI + VPD(HOUR)*GHR)
+      / (GHR+GSC*DUM1)                       !VPD at the leaf surface (Pa)
100  CONTINUE

C      *****
C      Night-time computations
C      *****
ELSE
  ASS= -RD
  GSC= GSCD
  VPDS= VPD(HOUR)
END IF

C      Transpiration rate
C      -----
TR= (1.6 * GSC) * VPDS/PRESS                 !Transpiration rate (mol m-2 s-1)
IF(TR.LT.1.E-6)  TR= 1.E-6

RETURN
END

C      *****
C      References
C      *****
C Farquhar GD, von Caemmerer S, Berry JA (1980) A biochemical model of photosynthetic
C CO2 assimilation in leaves of C3 species. Planta 149, 78-90
C Farquhar GD, von Caemmerer S (1982) Modelling of photosynthetic response to
C environmental conditions. In Encyclopedia of Plant Physiology. New Series.
C Vol. 12B. Physiological Plant Ecology II (eds. OL Lange, PS Nobel, CB Osmond,
C H Ziegler), pp. 549-587. Springer Verlag, Berlin.
C Farquhar GD, Wong SC 1984. An empirical model of stomatal conductance. Aust J
C Plant Physiol 11, 191-210
C Leuning R (1995) A critical appraisal of a combined stomatal-photosynthesis model
C for C3 plants. Plant Cell and Environment 18, 339-355
C Collatz GJ, Ball JT, Griwet C, Berry JA (1991) Physiological and environmental
C regulation of stomatal conductance, photosynthesis and transpiration: a model
C that includes a laminar boundary layer. Agricultural and Forest Meteorology
C 54, 107-136

```

```

C *****
C FORTRAN subroutine      OPTIMAL      (optimal.for)      8/9/98
C -----
C Purpose The subroutine finds optimal allocation coefficients, subject to
C three constraints:
C (1) hydraulic constraint,
C (2) carbon balance constraint and
C (3) height growth constraint (formulation used is specified
C in subroutine ROOTFIND)
C The assumption of maximum allocation to foliage implies an
C optimal behaviour of the plant (Parker & Maynard Smith 1990),
C with foliage growth (hence height growth) as fitness function.
C Optimal solution is searched first with a stepwise method,
C then with a bisection method (Press et al. 1992).
C The ROOTFIND subroutine tests if the value of allocation to foliage
C being tested is either greater (SOL=1) or lower (SOL=-1) than
C would be possible if all residual resources were optimally allocated
C between sapwood and fine roots.
C If SOL=1 for ALLF=1, all new growth is allocated to foliage
C (this will still result in minimum water potentials below the
C cavitation threshold).
C Otherwise the search is refined so as to find the maximum value of
C ALLF that fulfils the hydraulic constraint.
C
C Parameters and variables
C ACC accuracy in bisection method
C DALLF interval in bisection method for ALLF
C INCR,-0 increment in stepwise exploration
C JMAX max. number of iterations in bisection method
C ALLF,-MID,-NEW,-OLD,-0 coefficient of allocation to foliage
C ALLR,-MID,-NEW coefficient of allocation to roots
C ALLS,-MID,-NEW coefficient of allocation to sapwood
C SOL,-MID index of solution (1=solution exists,-1=does not exist)
C
C Linked subroutines
C ROOTFIND
C *****
SUBROUTINE OPTIMAL
C *****
C Define parameters and variables
C *****
C Parameters and variables
C -----
C INTEGER J,JMAX,SOL,SOLMID
C REAL ACC,DALLF,INCR,INCRO,ALLF,
C + ALLFMID,ALLFOLD,ALLFO,ALLR,
C + ALLRMID,ALLS,ALLSMID
C PARAMETER (ACC= 1.E-6,
C + INCRO= 5.E-2,
C + JMAX= 40)
C INCLUDE 'HYDRALL.CMN'
C *****
C Compute optimal coefficients of allocation to plant compartments
C *****
C For ALLF decreasing stepwise from the maximum value of 1,
C test if a solution to the hydraulic constraint exists; find two
C values that bracket the optimum for ALLF.
C If no solution is found, try again with smaller search step.
C -----
C DO 200, J= 0,2
C ALLFOLD= 1.
C INCR= INCRO / 10**J
C DO 100, ALLF= 1.,0.,-INCR
C CALL ROOTFIND(ALLF,ALLR,ALLS,SOL)
C IF(SOL.GT.0) GOTO 300
C ALLFOLD= ALLF
100 CONTINUE
200 CONTINUE
300 CONTINUE
C
C IF(SOL.EQ.1) THEN

```



```

C      Find optimal allocation coefficients by bisection technique
C      -----
C      Set starting point and range
C      -----
      ALLF0= ALLF
      DALLF= (ALLFOLD - ALLF)

C      Bisection loop
C      -----
      DO 400, J= 1, JMAX
          DALLF= DALLF / 2.
          ALLFMID= ALLF0 + DALLF
          CALL ROOTFIND(ALLFMID, ALLRMID, ALLSMID, SOLMID)
          IF(SOLMID.GT.0.) THEN
              ALLF0= ALLFMID
              ALLF= ALLFMID
              ALLS= ALLSMID
              ALLR= ALLRMID
          END IF
          IF(ABS(DALLF).LT.ACC) GOTO 500
400    CONTINUE
500    CONTINUE
      END IF

C      Final values of allocation coefficients
C      -----
      ALLFNEW= ALLF
      ALLRNEW= ALLR
      ALLSNEW= ALLS

      RETURN
      END

```

```

C *****
C      References
C *****
C Parker G.A., Maynard Smith J. (1990) Optimality theory in evolutionary
C biology. Nature 348, 27-33
C Press W.H., Teukolsky S.A., Vetterling W.T. & Flannery B.P. (1992)
C Numerical Recipes in FORTRAN. 2nd Edition. pp.963. Cambridge Univ.
C Press, Cambridge.

```

```

C *****
C FORTRAN subroutine      OUTHOUR      (outhour.for)      27/2/1999
C -----
C Purpose The routine outputs 1/2 hourly meteo and gas-exchange variables
C for one day. Upon first call, the location of file for 1/2 hourly
C output is read. All variables are stored in the common block HYDRALL.
C
C Parameters and variables
C IFILES location of root input file
C HHOURL location of 1/2 hourly output file
C
C *****

      SUBROUTINE OUTHOUR

C *****
C Define parameters, include commn block
C *****
      INTEGER      COUNT,J
      CHARACTER*40 HHOURL
      SAVE         COUNT,HHOURL
      INCLUDE      'HYDRALL.CMN'
      INCLUDE      'FILES.CMN'

C *****
C On first access, read location of output file
C -----
      IF(COUNT.EQ.0) THEN
          COUNT= 1
          CALL RDINIT (3 , 0, IFILES)
          CALL RDSCHA ('HHOURL', HHOURL)
          CLOSE (3)
          OPEN(UNIT= 3,
+           FILE= HHOURL,
+           STATUS= 'UNKNOWN',
+           ERR= 1000)           !open file for 1/2 hourly output
          WRITE (UNIT= 3,
+           FMT= 2000,
+           ERR= 1000)           !write headings
          WRITE (UNIT= 3,
+           FMT= 3000,
+           ERR= 1000)           !write variable units
          END IF

C Output 1/2 hourly data to file
C -----
      DO 100, J=1,48
          WRITE (UNIT= 3,
+           FMT= 4000,
+           ERR= 1000)
          A TAIR(J),
          B VPD(J),
          C RGDIF(J)+RGDIR(J),
          D ATOT(J),
          E GSCTOT(J),
          F ETOT(J)

100 CONTINUE
1000 CONTINUE

C *****
C Formats
C *****
2000 FORMAT(T1, 'T', T10, ', ',
+ T12, 'D', T21, ', ',
+ T23, 'Rg', T32, ', ',
+ T34, 'A', T43, ', ',
+ T45, 'gsc', T54, ', ',
+ T56, 'E', T65 )
3000 FORMAT(T1, '°C', T10, ', ',
+ T12, 'Pa', T21, ', ',
+ T23, 'W/m2', T32, ', ',
+ T34, 'mol/m2/s', T43, ', ',
+ T45, 'mol/m2/s', T54, ', ',

```

```
+          T56, 'mol/m2/s', T65 )
4000 FORMAT(T1, G9.3, T10, ', ',
+          T12, G9.3, T21, ', ',
+          T23, G9.3, T32, ', ',
+          T34, G9.3, T43, ', ',
+          T45, G9.3, T54, ', ',
+          T56, G9.3, T65 )
```

```
RETURN
END
```

```

C *****
C FORTRAN subroutine      OUTYEAR      (outyear.for)      27/2/1999
C -----
C Purpose The routine outputs annual growth data for the simulation period.
C       Upon first call, the location of file for annual output is read.
C       All variables are stored in the common block HYDRALL.
C
C Parameters and variables
C COUNT      counter
C IFILES     location of root input file
C HHOURL     location of annual output file
C
C *****
C
C       SUBROUTINE OUTYEAR
C
C *****
C       Define parameters, include commn block
C *****
C       INTEGER      COUNT
C       CHARACTER*40 ANNUAL
C       SAVE         ANNUAL,COUNT
C       INCLUDE      'HYDRALL.CMN'
C       INCLUDE      'FILES.CMN'
C
C *****
C       On first access, read location of output file, print headings
C -----
C       IF(COUNT.EQ.0) THEN
C           COUNT= 1                !set banner high
C           CALL RDINIT (2 , 0, IFILES)
C           CALL RDSCHA ('ANNUAL', ANNUAL )
C           CLOSE (2)
C           OPEN(UNIT= 2,
C +           FILE= ANNUAL,
C +           STATUS= 'UNKNOWN',
C +           ERR= 1000)                !open file for output of annual data
C           WRITE (UNIT= 2,
C +           FMT= 2000,
C +           ERR= 1000)                !write headings
C           WRITE (UNIT= 2,
C +           FMT= 3000,
C +           ERR= 1000)                !write variable units
C       END IF
C
C       Output selected annual results
C -----
C       WRITE (UNIT= 2,
C +           FMT= 4000,
C +           ERR= 1000)
C       A TREES,
C       B H,
C       C DBH,
C       D VOL,
C       E CAI,
C       F GPPYR,
C       G NPPYR,
C       H ALLRNEW,
C       I WF*SLA,
C       J SAPBA,
C       K WR
C       1000 CONTINUE
C
C *****
C                               Formats
C *****
C 2000 FORMAT (T1, 'N', T10, ' ',
C +           T12, 'H', T21, ' ',
C +           T23, 'DBH', T32, ' ',
C +           T34, 'V', T43, ' ',
C +           T45, 'CAI', T54, ' ',
C +           T56, 'GPP', T65, ' ',
C +           T67, 'NPP', T76, ' ',
C +           T78, 'Lambdar', T87, ' ',

```

```

+      T89,'LAI', T98, ', ',
+      T100,'As', T109, ', ',
+      T111,'Wr' )
3000 FORMAT(T1, 'trees/m', T10, ', ',
+      T12,'m', T21, ', ',
+      T23,'cm', T32, ', ',
+      T34,'m3/ha', T43, ', ',
+      T45,'m3/ha/yr', T54, ', ',
+      T56,'kgC/m2/yr', T65, ', ',
+      T67,'kgC/m2/yr', T76, ', ',
+      T78,'-', T87, ', ',
+      T89,'-', T98, ', ',
+      T100,'-', T109, ', ',
+      T111,'kgDM/m2' )
4000 FORMAT(T1, G9.3, T10, ', ',
+      T12,G9.3, T21, ', ',
+      T23,G9.3, T32, ', ',
+      T34,G9.3, T43, ', ',
+      T45,G9.3, T54, ', ',
+      T56,G9.3, T65, ', ',
+      T67,G9.3, T76, ', ',
+      T78,G9.3, T87, ', ',
+      T89,G9.3, T98, ', ',
+      T100,G9.3, T109, ', ',
+      T111,G9.3 )

```

```

RETURN
END

```

```

C *****
C FORTRAN subroutine      RADENV      (radenv.for)      27/2/99
C -----
C Purpose Based on stand leaf area index and 1/2 hour values of:
C - global radiation (direct, diffuse)
C - incoming longwave radiation
C - air temperature
C - solar elevation
C the routine computes:
C - fraction of sunlit and shaded foliage
C - absorbed PPF of foliage classes
C - isothermal net radiation of foliage classes
C - global radiation absorbed by the understorey
C Light scattering and absorption in PAR, NIR and long-wave bands based
C on Goudriaan & van Laar 1994 and Wang & Leuning 1998.
C Scattering coefficients based on Goudriaan & van Laar 1994, p 100,
C assuming same value for leaf reflection and transmission.
C Extinction coefficients for direct and diffuse radiation, PAR and
C NIR based on Goudriaan & van Laar 1994, p 103.
C Extinction coefficient of diffuse radiation for non-horizontal, black
C leaves based on Goudriaan & van Laar 1994, p 99, assuming Standard
C Overcast Sky (SOC) conditions.
C Extinction coefficient of direct radiation for non-horizontal, black
C leaves based on Wang & Leuning 1998 and Ross 1981. Assumed spherical
C leaf angle distribution (CHI=0.)
C Reflection coefficients for PAR and NIR of canopy-soil system based on
C Goudriaan & van Laar 1994, p 105, assuming soil reflection coefficient
C is equal to canopy reflection coefficient (reasonable if soil is covered
C by the understorey).
C Absorption of long-wave radiation under isothermal conditions based on
C Wang & Leuning 1998.
C Fraction of sunlit vs shaded foliage based on Wang & Leuning 1998.
C
C NOTE: All fluxes and conductances are on a _ground_ area basis
C when not otherwise stated.
C
C Parameters and variables
C
C ANIR1 near infrared rad absorbed by sunlit big-leaf (W m-2)
C ANIR2 near infrared rad absorbed by shaded big-leaf (W m-2)
C APAR1 photosynth act rad absorbed by sunlit big-leaf (W m-2, then mol m-2 s-1)
C APAR2 photosynth act rad absorbed by shaded big-leaf (W m-2, then mol m-2 s-1)
C APARUND photosynth act rad absorbed by understorey (W m-2)
C APARU2 absorbed PPF per unit shaded leaf area at canopy top (mol m-2 s-1)
C ARLW1 long-wave radiation absorbed by sunlit big-leaf (W m-2)
C ARLW2 long-wave radiation absorbed by shaded big-leaf (W m-2)
C CHI parameter of leaf angle distribution (-0.4<CHI<0.6)
C DUM(17) dummy variables
C GROSS projection of unit leaf area in the direction of sun beam (-)
C HOUR 1/2 hour interval number
C KB extinction coeff for canopy of black leaves, direct radiation (-)
C KBNIR canopy extinction coeff for NIR direct radiation (-)
C KBPAR canopy extinction coeff for PAR direct radiation (-)
C KD extinction coeff for canopy of black leaves, diffuse radiation (-)
C KDNIR canopy extinction coeff for NIR diffuse radiation (-)
C KDPAR canopy extinction coeff for PAR diffuse radiation (-)
C LAI canopy leaf area index (-)
C LAIUND leaf area index of understorey (-)
C LAI1 leaf area index of sunlit big-leaf (-)
C LAI2 leaf area index of shaded big-leaf (-)
C NIRB incoming direct NIR (W m-2)
C NIRD incoming diffuse NIR (W m-2)
C OMPAR leaf scattering coefficient for PAR (-)
C OMNIR leaf scattering coefficient for NIR (-)
C PARB incoming direct PAR (W m-2)
C PARD incoming diffuse PAR (W m-2)
C PSIFUN function, returns the integral of exp function over the canopy
C RGDIF(48) incoming diffuse short-wave radiation (W m-2)
C RGDIF(48) incoming direct short-wave radiation (W m-2)
C RLW(48) incoming long-wave radiation (W m-2)
C RNI1 isothermal net radiation of shaded leaves (W m-2)
C RNI2 isothermal net radiation of sunlit leaves (W m-2)
C ROBNIR canopy+soil reflection coeff for direct NIR (-)
C ROBPAR canopy+soil reflection coeff for direct PAR (-)

```

```

C  RODNIR    canopy+soil reflection coeff for diffuse NIR (-)
C  RODPAR    canopy+soil reflection coeff for diffuse PAR (-)
C  SIGMA     Stefan-Boltzmann constant (W m-2 K-4)
C  SINBETA(48) sine of solar elevation (-)
C  TAIR(48)  air temperature (oC)
C
C Functions
C  PSIFUN
C *****
      SUBROUTINE RADENV(HOUR, LAI,
+                    APAR1, APAR2, APARUND, APARU2, KB,
+                    KDPAR, LAI1, LAI2, RNI1, RNI2)
C *****
C      Define parameters and variables
C *****
C Parameters and variables
C -----
      INTEGER HOUR
      REAL    ANIR1, ANIR2, APAR1, APAR2, APARUND, APARU2,
+           ARLW1, ARLW2, DUM(17), CHI, GROSS, KB, KBNIR,
+           KBPAR, KD, KDNIR, KDPAR, LAI, LAIUND, LAI1, LAI2,
+           NIRB, NIRD, OMPAR, OMNIR, PARB, PARD, PSIFUN,
+           RNI1, RNI2, ROBNIR, ROBPAP, RODNIR, RODPAR
      PARAMETER (CHI= 0.,
+              OMPAR= 0.2,
+              OMNIR= 0.8)
      INCLUDE 'HYDRALL.CMN'
C *****
C      Canopy radiative environment
C *****
C      Extinction coeff for canopy of black leaves, diffuse radiation
C      Note: assumed SOC conditions
C -----
      KD= - 1./LAI * LOG(0.178 * EXP(-1.93*LAI) +
+                    0.514 * EXP(-0.707*LAI) +
+                    0.308 * EXP(-0.518*LAI))
C
C      Extinction coeff for canopy of black leaves, direct radiation
C -----
      GROSS= 0.5 - CHI*(0.633-1.11*SINBETA(HOUR))
+           - CHI*CHI*(0.33-0.579*SINBETA(HOUR))
      IF(SINBETA(HOUR).LT.1.E-5) SINBETA(HOUR)= 1.E-5
      KB= GROSS / SINBETA(HOUR)
C
C      Extinction coefficients for diffuse PAR and NIR radiation
C -----
      DUM(1)= SQRT(1.-OMPAR)
      DUM(2)= SQRT(1.-OMNIR)
      KDPAR= KD * DUM(1)
      KDNIR= KD * DUM(2)
C
C *****
C      Day-time computations
C *****
      IF(SINBETA(HOUR).GT.1.E-3) THEN
      Leaf area index of sunlit (1) and shaded (2) big-leaf
C -----
      LAI1= PSIFUN(LAI, KB)
      LAI2= LAI - LAI1
C
C      Extinction coefficients for direct PAR and NIR radiation
C -----
      KBPAR= KB * DUM(1)
      KBNIR= KB * DUM(2)
C
C      Canopy+soil reflection coefficients for direct, diffuse PAR, NIR radiation
C -----
      DUM(3)= (1.-DUM(1)) / (1.+DUM(1))
      DUM(4)= (1.-DUM(2)) / (1.+DUM(2))
      DUM(5)= 2. * KB / (KB + KD)
      ROBPAP= DUM(5) * DUM(3)

```

```

RODPAR= ROBPAP
ROBNIR= DUM(5) * DUM(4)
RODNIR= ROBNIR

C      Incoming direct PAR and NIR (W m-2)
C      -----
PARB= RGDIR(HOUR) / 2.
NIRB= PARB

C      Incoming diffuse PAR and NIR (W m-2)
C      -----
PARD= RGDIF(HOUR) / 2.
NIRD= PARD

C      Preliminary computations
C      -----
DUM(6)= PARD * (1.-RODPAR) * KDPAR
DUM(7)= PARB * (1.-ROBPAP) * KBPAR
DUM(8)= PARB * (1.-OMPAR) * KB
DUM(9)= NIRD * (1.-RODNIR) * KDNIR
DUM(10)= NIRB * (1.-ROBNIR) * KBNIR
DUM(11)= NIRB * (1.-OMNIR) * KB
DUM(12)= PSIFUN(LAI,KDPAR+KB)
DUM(13)= PSIFUN(LAI,KBPAR+KB)
DUM(14)= PSIFUN(LAI,KDNIR+KB)
DUM(15)= PSIFUN(LAI,KBNIR+KB)
DUM(16)= PSIFUN(LAI,KB) - PSIFUN(LAI,2.*KB)

C      PAR absorbed by sunlit (1) and shaded (2) big-leaf (W m-2)
C      -----
APAR1= DUM(6) * DUM(12) +
+      DUM(7) * DUM(13) +
+      DUM(8) * DUM(16)
APAR2= DUM(6) * (PSIFUN(LAI,KDPAR) - DUM(12)) +
+      DUM(7) * (PSIFUN(LAI,KBPAR) - DUM(13)) -
+      DUM(8) * DUM(16)

C      PAR adsorbed by shaded leaves at canopy top (W m-2)
C      -----
APARU2= APAR2 / (PSIFUN(LAI,KDPAR) - DUM(12))

C      NIR absorbed by sunlit (1) and shaded (2) big-leaf
C      -----
ANIR1= DUM(9) * DUM(14) +
+      DUM(10) * DUM(15) +
+      DUM(11) * DUM(16)
ANIR2= DUM(9) * (PSIFUN(LAI,KDNIR) - DUM(14)) +
+      DUM(10) * (PSIFUN(LAI,KBNIR) - DUM(15)) -
+      DUM(11) * DUM(16)

C      Long-wave radiation absorbed by sunlit (1) and shaded (2) big-leaf
C      -----
DUM(17)= RLW(HOUR)-SIGMA*(TAIR(HOUR)+273.2)**4.
DUM(17)= DUM(17) * KD
ARLW1= DUM(17) * PSIFUN(LAI,KB+KD)
ARLW2= DUM(17) * PSIFUN(LAI,KD) - ARLW1

C      Isothermal net radiation for sunlit (1) and shaded (2) big-leaf
C      -----
RNI1= APAR1 + ANIR1 + ARLW1
RNI2= APAR2 + ANIR2 + ARLW2

C      PPFD absorbed by the understorey (W m-2)
C      Note: assumed for the understorey the same SLA than for the canopy
C      -----
LAIUND= WFUND * SLA
APARUND= DUM(6) * PSIFUN(LAI+LAIUND,KDPAR) +
+      DUM(7) * PSIFUN(LAI+LAIUND,KBPAR) -
+      APAR1 - APAR2

C      *****
C      Night-time computations
C      *****
ELSE

```



```

LAI1= 0.
APAR1= 0.
ANIR1= 0.
ARLW1= 0.
RNI1= 0.

LAI2= LAI
APAR2= 0.
APARU2= 0.
ANIR2= 0.
DUM(17)= RLW(HOUR)-SIGMA*(TAIR(HOUR)+273.2)**4.
DUM(17)= DUM(17) * KD
ARLW2= DUM(17) * (PSIFUN(LAI,KD) - PSIFUN(LAI,KB+KD))
RNI2= APAR2 + ANIR2 + ARLW2

```

```

APARUND= 0.
END IF

```

```

C Convert absorbed PAR into units of mol m-2 s-1
C -----

```

```

APAR1= APAR1 * 4.57E-6
APAR2= APAR2 * 4.57E-6
APARU2= APARU2 * 4.57E-6

```

```

RETURN
END

```

```

C *****

```

```

C References

```

```

C *****

```

```

C Goudriaan J., van Laar H.H. (1994) Modeling Potential Crop Growth Processes.
C pp. 238. Kluwer Academic Publ., Dordrecht
C Ross J 1981. The Radiation Regime and Architecture of Plant Stands. p 391.
C W Junk Publishers, The Hague
C Wang YP, Leuning R 1998. A two-leaf model for canopy conductance, photosynthesis
C and partitioning of available energy. I. Model description and comparison with
C a multi-layered model. Agr For Meteorol 91, 89-111
C

```

```

C *****
C FORTRAN subroutine      RESPSOIL      (respsoil.for)      2/3/99
C -----
C Purpose The routine computes instantaneous soil respiration and transition
C from young to old soil carbon pools, based on the two-compartments model
C of Andren and Katterer (1997). Input into the young carbon pool from
C stand and understory occurs at the end of each year (routine GRSTAND).
C A constant humification coefficient is assumed. Decomposition of young and
C old organic matter and humification are affected to the same extent by
C soil temperature and soil water potential, using the multiplicative model
C of Andren and Paustian (1987), parameterized as in Andren et al (1992).
C Only difference, the effect of temperature is represented (function TFUN)
C by the equation of Lloyd and Taylor (1994), to account for the shift
C in Q10 with temperature.
C Reference conditions are assumed at 10 oC and PSISL=PSIS1.
C NOTE: Fluxes are on a _ground_ area basis.
C
C Parameters and variables
C CSLO      old organic matter in soil (kgDM m-2)
C CSLY      young organic matter in soil (kgDM m-2)
C DAY       day of simulation
C FC        coeff for conversion of carbon into DM (kgC kgDM-1)
C HUMCOEF   humification coefficient (-)
C HUM       humification (mol m-2 s-1)
C PSICORR   resp correction factor for water potential effects (-)
C PSIS0     soil water potential for PSICORR=0 (MPa)
C PSIS1     soil water potential for PSICORR=1 (MPa)
C PSISL     soil water potential (MPa)
C RSLO      resp per unit old soil carbon (kgDM m-2 s-1)
C RSLY      resp per unit young soil carbon (kgDM m-2 s-1)
C ROSLO     resp per unit old soil carbon at ref conditions (kgDM kgDM-1 s-1)
C ROSLY     resp per unit young soil carbon at ref conditions (kgDM kgDM-1 s-1)
C RSOIL     soil respiration (mol m-2 s-1)
C TFUN      resp correction factor for temp effects (-)
C TMEAN(366) daily mean air temperature (oC)
C
C Linked subroutines and functions (secondary links)
C TFUN
C *****
      SUBROUTINE RESPSOIL(DAY,RSOIL)
C *****
C Define parameters and variables
C *****
      INTEGER DAY
      REAL HUM,HUMCOEF,PSICORR,PSIS0,PSIS1,RSLO,RSLY,
      + RSOIL,TFUN
      PARAMETER(HUMCOEF= 0.125,
      + PSIS0= -7.58,
      + PSIS1= -0.01,
      + ROSLO= 1.92E-10,
      + ROSLY= 1.5E-7 )
      INCLUDE 'HYDRALL.CMN'
C *****
C Effects of soil water potential
C -----
      IF(PSISL.GE.PSIS1) THEN
        PSICORR= 1.
      ELSE IF(PSISL.LE.PSIS0) THEN
        PSICORR= 0.
      ELSE
        PSICORR= LOG(PSIS0/PSISL) / LOG(PSIS0/PSIS1)
      END IF
C
C Fluxes for young soil carbon compartment
C -----
      RSLY= ROSLY * CSLY !respiration of young soil carbon
      RSLY= RSLY * TFUN(TMEAN(DAY)) * PSICORR
      HUM= RSLY * HUMCOEF / (1.-HUMCOEF) !humification of young soil carbon
      CSLY= CSLY + 1800. * (- HUM - RSLY) !update young soil carbon
C
C Fluxes for old soil carbon compartment

```

```

C -----
RSLO= ROSLO * CSLO !respiration of old soil carbon
RSLO= RSLO * TFUN(TMEAN(DAY)) * PSICORR
CSLO= CSLO + 1800. * (HUM - RSLO) !update old soil carbon

C Total soil respiration
C -----
RSOIL= RSLO + RSLY
RSOIL= RSOIL * FC / 0.012 !units from kgDM into mol C

RETURN
END

```

```

C *****
C References
C *****
C Andren O, Paustian K 1987. Barley straw decomposition in the field:
C a comparison of models. Ecology 68(5), 1190-1200
C Andren O, Katterer T 1997. ICBM: the introductory carbon balance model
C for exploration of soil carbon balances. Ecological Applications 7(4),
C 1226-1236
C Andren O, Steen E, Rajkai K 1992. Modelling the effects of moisture on barley
C straw and root decomposition in the field. Soil Biology Biochem 24(8), 727-736
C Lloyd J, Taylor JA 1994. On the temperature dependence of soil respiration.
C Funct Ecol 8,315-323

```

```

C *****
C FORTRAN subroutine      RESPTREE      (resptree.for)      2/3/99
C -----
C Purpose The routine computes daily respiration of sapwood and fine roots,
C (Ryan 1991), based on:
C - average daily temperature
C - tissue biomass
C - tissue nitrogen content
C Dependence of tissue and soil respiration upon temperature based
C on Lloyd and Taylor (1994). The assumption is made that stem and
C soil temperature are constant over the day, due to thermal inertia.
C Water potential is assumed to have no effects on tissue respiration.
C NOTE: Fluxes are on a _ground_ area basis.
C
C Parameters and variables
C DAY      day of simulation
C NR      fine root nitrogen concentration (molN kgDM-1)
C NS      sapwood nitrogen concentration (molN kgDM-1)
C RM      stand mainten respir (mol m-2 s-1)
C RMOR      fine root mainten respir at 10 oC (mol m-2 s-1)
C RMOS      sapwood mainten respir at 10 oC (mol m-2 s-1)
C TFUN      respiration correction factor for temp effects (-)
C TMEAN(366) daily mean air temperature (oC)
C WR      fine root biomass (kgDM m-2)
C WS      sapwood biomass (kgDM m-2)
C
C Linked subroutines and functions (secondary links)
C TFUN
C *****
C
C      SUBROUTINE RESPTREE(DAY, RM)
C
C      *****
C      Define parameters and variables
C      *****
C      INTEGER DAY
C      REAL    RM, RMOR, RMOS, TFUN
C      INCLUDE 'HYDRALL.CMN'
C
C      *****
C      Compute stand respiration at 10 oC
C      -----
C      IF(DAY.EQ.1) THEN !only after updating tissue biomass
C          RMOS= 0.0106/2. * WS * NS / 3600.
C          RMOR= 0.0106/2. * WR * NR / 3600.
C      END IF
C
C      Instantaneous canopy respiration (sapwood+fine roots)
C      -----
C      RM= RMOS + RMOR
C      RM= RM * TFUN(TMEAN(DAY)) !effects of temperature
C
C      RETURN
C      END
C
C *****
C      References
C      *****
C      Lloyd J, Taylor JA 1994. On the temperature dependence of soil respiration.
C      Funct Ecol 8, 315-323
C      Ryan MG 1991. A simple method for estimating gross carbon budgets for
C      vegetation in forest ecosystems. Tree Physiology 9, 255-266

```

```

C *****
C FORTRAN subroutine      ROOTFIND      (rootfind.for)      22/11/98
C -----
C Purpose Given values for
C (a) old stand biomass components
C (b) stand growth in the current year
C (c) critical transpiration rate per unit foliage biomass
C (d) critical soil water potential
C (e) a value of allocation coefficient to foliage ALLF
C the subroutine checks if any values of allocation to sapwood and
C to fine roots exist that satisfy the condition of optimality
C under hydraulic constraint.
C Tree height growth is assumed to be proportional to new foliage
C production
C Sapwood area at BH is linear function of sapwood volume and tree
C height (Ojansuu & Maltamo 1995).
C The expression of stem hydraulic conductance is derived from
C the analysis in Whitehead et al. (1984).
C Sapwood specific conductivity is assumed to increase with
C tree height (derived from Pothier et al. 1989a,b).
C The reference values of sapwood, soil and root hydraulic conductivities
C (assumed at 20 oC) are adjusted for the effects of temperature
C on water viscosity.

```

```

C Parameters and variables (I=input, O=output)

```

```

C A      coeff of quadratic equation in hydr. constraint
C ALLF   allocation coefficient to foliage compartment (-)
C ALLR   allocation coefficient to root compartment (-)
C ALLS   allocation coefficient to sapwood compartment (-)
C BSL    coefficient in soil water potential eq. (-)
C DAYCRIT Julian day of critical water relations
C ECRIT  critical inst. transp. per proj. leaf area (mol m-2 s-1)
C GST    annual gross stand growth (kgDM m-2 yr-1)
C HNEW   stand height after new growth (m)
C KR     root specific conductance (m3 MPa-1 s-1 kg-1)
C KS     sapwood specific conductivity (m2 MPa-1 s-1)
C KSL    specific conductivity of soil (m3 MPa-1 s-1 kg-1)
C KLSAT  soil saturated conductivity (m3 MPa-1 s-1 m-1)
C KSMAX  max. sapwood specific conductivity (m3 MPa-1 s-1 m-1)
C KS_R   spec. cond. of soil+roots (m3 MPa-1 s-1 kg-1)
C PENTRY soil entry water potential (MPa)
C PSISCRIT critical soil water potential (MPa)
C PSITHR water potential threshold for cavitation (MPa)
C RADRT  root radius (m)
C RESF   hydr res per unit foliage area (MPa s m2 m-3)
C ROF    foliage density (kgDM m-3)
C ROS    wood density (kgDM m-3)
C SLA    specific leaf area (projected) (m2 kgDM-1)
C SOL    index for reached solution
C WF,-NEW stand foliage biomass of a tree (kgDM m-2)
C WR,-NEW stand fine root biomass (kgDM m-2)
C WS,-NEW stand sapwood biomass (kgDM m-2)

```

```

C *****

```

```

SUBROUTINE ROOTFIND(ALLF,ALLR,ALLS,SOL)

```

```

C *****

```

```

C Define parameters and variables

```

```

C *****

```

```

C Parameters and variables

```

```

C -----

```

```

INTEGER SOL
REAL A, DUM1, HNEW, KS, KSL, KS_R, ALLF, ALLR, ALLS,
+ RESF, WFNEW, WRNEW, WSNEW
INCLUDE 'HYDRALL.CMN'

```

```

C *****

```

```

C Search for a solution to hydraulic constraint

```

```

C *****

```

```

C New foliage biomass of tree after growth

```

```

C -----

```

```

IF(ALLF.LT.0.) ALLF= 0.

```

```

WFNEW= WF + (ALLF*GST)

C   New tree height after growth
C   -----
IF(ALLF*GST.GT.0.) THEN
  HNEW= H + ALLF*GST/ROF
ELSE
  HNEW= H
END IF

C   Soil hydr. conductivity
C   -----
KSL= KLSAT / (1.625*ROS*RADRT*RADRT) *
+     (PENTRY/PSISCRIT)**(2.+3./BSL)

C   Specific hydraulic conductivity of soil+roots
C   -----
KS_R= 1. / (1./KR + 1./KSL)
KS_R= KS_R * (0.5151+0.0242*TMEAN(DAYCRIT)) !adjust for temp effects on water viscosity

C   New sapwood specific conductivity as a function of height
C   (three possible formulations)
C   -----
DUM1= KSMAX * (1.-EXP(-0.1127*HNEW))
DUM1= KSMAX * (0.2 + 0.6 * HNEW/18.3)
DUM1= KSMAX
KS= DUM1 * (0.5151+0.0242*TMEAN(DAYCRIT)) !adjust for temp effects on water viscosity

C   Optimal coefficient of allocation to fine roots and sapwood
C   for set allocation to foliage
C   -----
A= SQRT(KS_R/KS*LS/LR*ROS)
ALLR= (WS-A*HNEW*WR+GST*(1.-ALLF))/GST/(1.+A*HNEW)
IF(ALLR.LT.1.E-6) ALLR= 1.E-6 !bracket ALLR between (1-ALLF), small value
IF(ALLR.GT.1.-ALLF) ALLR= 1.-ALLF

ALLS= 1. - ALLF - ALLR
IF(ALLS.LT.1.E-6) ALLS= 1.E-6 !bracket ALLS between 1, small value
IF(ALLS.GT.1.) ALLS= 1.

C   Resulting fine root and sapwood biomass
C   -----
WRNEW= WR + ALLR * GST
IF(WRNEW.LT.1.E-6) WRNEW= 1.E-6
WSNEW= WS + ALLS * GST
IF(WSNEW.LT.1.E-6) WSNEW= 1.E-6

C   Resulting leaf specific resistance (MPa s m2 m-3)
C   -----
RESF= (1./(WRNEW*KS_R) + (HNEW*HNEW*ROS)/(WSNEW*KS))
+     * (WFNEW*SLA)

C   Resulting minimum leaf water potential
C   -----
PSILMIN= PSISCRIT - (0.01 * HNEW)
+     - (ECRIT * 0.018/1000.* RESF)

C   Check if given value of ALLF satisfies optimality constraint
C   -----
IF(PSILMIN.GE.PSITHR) THEN
  SOL= 1
ELSE
  SOL= -1
  ALLR= (WS+GST-WR*A*HNEW) / GST / (1.+A*HNEW)
  IF(ALLR.LT.1.E-6) ALLR= 1.E-6
  IF(ALLR.GT.1.) ALLR= 1.
  ALLS= 1.-ALLR
END IF

RETURN
END

C *****
C   References

```

C \*\*\*\*\*  
C Ojansuu R. & Maltamo M. (1995) Sapwood and heartwood taper in Scots pine  
C stems. Can. J. For. Res. 25, 1928-1943.  
C Pothier D., Margolis H.A. & Waring R.H. (1989a) Patterns of change of  
C saturated sapwood permeability and sapwood conductance with stand  
C development. Can. J. For. Res. 19, 432-439.  
C Pothier D., Margolis H.A., Poliquin J. & Waring R.H. (1989b) Relation  
C between the permeability and the anatomy of jack pine sapwood with  
C stand development. Can. J. For. Res. 19, 1564-1570.  
C Whitehead D., Edwards W.R.N. & Jarvis P.G. (1984) Conducting sapwood area,  
C foliage area, and permeability in mature trees of *Picea sitchensis*  
C and *Pinus contorta*. Can. J. For. Res. 14, 940-947.

```

C *****
C FORTRAN subroutine      SOILPSI      (soilpsi.for)      27/5/98
C -----
C Purpose Soil water potential is derived from soil water content; simple
C          formulation of soil water retention (Campbell 1985).
C
C Parameters and variables
C   BSL      coeff in soil water potential equation (-)
C   PENTRY   soil entry water potential (MPa)
C   VWSAT    saturated soil water content (m3 m-3)
C   PSISL    soil water potential (MPa)
C   VWSL     soil water content (m3 m-3)
C
C *****

      SUBROUTINE SOILPSI

C *****
C          Define parameters and variables
C *****
C Parameters and variables
C -----
      REAL      DUM
      INCLUDE 'HYDRALL.CMN'

C *****
C Compute soil water potential
C *****
      DUM= PENTRY * (VWSAT/VWSL)**BSL
      PSISL= MAX(DUM, PSIO)

      RETURN
      END

C *****
C          References
C *****
C Campbell G.S. (1985) Soil Physics with BASIC. pp 150. Elsevier, Amsterdam

```



```

C *****
C FORTRAN subroutine      UPSCALE      (upscale.for)      27/2/99
C -----
C PURPOSE The routine computes the integral of photosynthetic parameters
C over (1) sunlit and (2) shaded big-leaf, and adjusts them as a function
C of absorbed PPFD and leaf temperature.
C Up-scaling over the canopy based on the approach of dePury & Farquhar 1997,
C as improved by Wang & Leuning 1998.
C Leaf photosynthetic parameters are assumed to be proportional to leaf nitrogen.
C A vertical exponential profile of leaf nitrogen over the canopy is assumed,
C parallel to the reduction in diffuse PPFD.
C Effects of temperature on photosynthesis represented as in Farquhar et al (1980)
C and Farquhar & von Caemmerer (1982). Photosynthetic light response represented
C as in Farquhar and Wong 1984 (non-quadratic hyperbola).
C Scaling-up of electron transport different for (1) sunlit and (2) shaded
C big-leaf (Wang and Leuning 1998):
C (1) upscale potential electron transport, then derive actual electron
C transport, based on total PPFD absorbed by sunlit big-leaf;
C (2) derive actual electron transport for a shaded leaf at the top of the
C canopy, based on the corresponding value of PPFD per unit leaf area,
C then upscale it to the whole canopy.
C
C Note: suffixes 1 and 2 refer to sunlit and shaded big-leaf, respectively
C
C Parameters and variables
C
C ALPHA quantum yield of electron transport (mol e mol-1 quanta)
C APAR1 PPFD absorbed by sunlit big-leaf (mol m-2 s-1)
C APARU2 absorbed PPFD per unit shaded leaf area at canopy top (mol m-2 s-1)
C COMP1 CO2 compensation point in dark for sunlit big-leaf (Pa)
C COMP2 CO2 compensation point in dark for shaded big-leaf (Pa)
C DUM(7) dummy variables
C GSCD1 conductance in darkness of sunlit big-leaf (molCO2 m-2 s-1)
C GSCD2 conductance in darkness of shaded big-leaf (molCO2 m-2 s-1)
C HAJM activation energy of electron transport (J mol-1)
C HAKC activation energy for carboxylation (J mol-1)
C HAKO activation energy for oxygenation (J mol-1)
C HARD activation energy for dark respiration (J mol-1)
C HAVCM activation energy for carboxylation (J mol-1)
C HDJM deactivation energy of electron transport (J mol-1)
C HOUR 1/2 hour interval number
C J1 electron transport of sunlit big-leaf (mol m-2 s-1)
C J2 electron transport of shaded big-leaf (mol m-2 s-1)
C JMOP unit pot rate of electron transport at optimum temp (mol m-2 s-1)
C KB extinction coeff for canopy of black leaves, direct radiation (-)
C KC1 Michaelis constant of carboxyl for sunlit big-leaf (Pa)
C KC2 Michaelis constant of carboxyl for shaded big-leaf (Pa)
C KCT0 Michaelis constant of carboxyl at reference temp (Pa)
C KDPAR canopy extinction coeff for PAR diffuse radiation (-)
C KOT0 Michaelis constant of oxygenation at reference temp (Pa)
C KO1 Michaelis constant of oxygen for sunlit big-leaf (Pa)
C KO2 Michaelis constant of oxygen for shaded big-leaf (Pa)
C LAI canopy leaf area index (-)
C OSS oxygen part pressure in the atmosphere (Pa)
C PSIFUN function, returns the integral of exp function over the canopy
C PSISL soil water potential (MPa)
C PSIO soil water potential for complete stomatal closure (MPa)
C RD1 dark respiration rate of sunlit big-leaf (mol m-2 s-1)
C RD2 dark respiration rate of shaded big-leaf (mol m-2 s-1)
C RDT0 dark respir per unit leaf area at reference temp (mol m-2 s-1)
C RGAS gas constant (Pa m3 mol-1 K-1)
C SINBETA(12,48) sine of solar elevation (-)
C STOMWL coeff in gs vs A equation, limited by soil water (Pa-1)
C STOM0 stomatal conductance to CO2 in darkness (molCO2 m-2 s-1)
C STOM1 coeff in gs vs A equation (Pa)
C TAU1 Rubisco specificity factor for sunlit big-leaf (-)
C TAU2 Rubisco specificity factor for shaded big-leaf (-)
C THETA convexity factor of light response curve (-)
C TJM optimum temperature for electron transport (K)
C TLEAF1 temperature of sunlit big-leaf (K)
C TLEAF2 temperature of shaded big-leaf (K)
C T0 reference temperature (K)
C VCMAX1 max carboxyl of sunlit big-leaf (mol m-2 s-1)
C VCMAX2 max carboxyl of shaded big-leaf (mol m-2 s-1)

```

```

C  VCMOP  max carboxyl per unit leaf area at opt temp (mol m-2 s-1)
C
C  Linked subroutines and functions
C  PSIFUN
C  *****

      SUBROUTINE UPSCALE (APAR1, APARU2, HOUR, KB, KDPAR, LAI,
+
+           TLEAF1, TLEAF2,
+           COMP1, COMP2, GSCD1, GSCD2, J1, J2, KC1, KC2,
+           KO1, KO2, RD1, RD2, STOMWL, TAU1, TAU2,
+           VCMAX1, VCMAX2)

C  *****
C  Define parameters and variables
C  *****
      INTEGER HOUR
      REAL  APAR1, APARU2, COMP1, COMP2, DUM(9),
+         GSCD1, GSCD2, J1, J2, KC1, KC2, KB, KDPAR, KO1, KO2,
+         LAI, PSIFUN, RD1, RD2, STOMWL, TAU1, TAU2,
+         TLEAF1, TLEAF2, T0, VCMAX1, VCMAX2
      PARAMETER (T0= 293.3)

      INCLUDE 'HYDRALL.CMN'

C  *****
C  Computations
C  *****
C  Preliminary computations
C  -----
      DUM(1)= TLEAF1-T0
      DUM(2)= TLEAF2-T0
      DUM(3)= DUM(1)/(RGAS*TLEAF1*T0)
      DUM(4)= DUM(2)/(RGAS*TLEAF2*T0)

C  *****
C  Dark respiration rate
C  *****
C  Adjust unit dark respiration rate for temperature (mol m-2 s-1)
C  -----
      RD1= RDT0 * EXP(DUM(3)*HARD)
      RD2= RDT0 * EXP(DUM(4)*HARD)

C  Scale-up dark respir rate (mol m-2 s-1)
C  -----
      RD1= RD1 * PSIFUN(LAI,KB+KDPAR)
      RD2= RD2 * (PSIFUN(LAI, KDPAR) - PSIFUN(LAI,KB+KDPAR))

      IF(SINBETA(HOUR).GT.1.E-3) THEN !compute for day-time only
C  *****
C  Stomatal conductance
C  *****
C  Adjust stom conductance-photosynth ratio for soil water (Pa)
C  -----
      IF(PSISL.GT.0.) THEN
          STOMWL= STOM1
      ELSE IF(PSISL.LE.PSIO) THEN
          STOMWL= 0.
      ELSE
          STOMWL= STOM1 * (1. - PSISL/PSIO)
      END IF
C  Stomatal conductance to CO2 in darkness (molCO2 m-2 s-1)
C  -----
      GSCD1= STOM0 * PSIFUN(LAI,KB+KDPAR)
      GSCD2= STOM0 * (PSIFUN(LAI, KDPAR) - PSIFUN(LAI,KB+KDPAR))

C  *****
C  Carboxylation rate
C  *****
C  Adjust unit max carboxyl rate for temperature (mol m-2 s-1)
C  -----
      VCMAX1= VCMOP * EXP(DUM(3)*HAVCM)
      VCMAX2= VCMOP * EXP(DUM(4)*HAVCM)

C  Scale-up maximum carboxylation rate (mol m-2 s-1)

```

```

C -----
  VCMAX1= VCMAX1 * PSIFUN(LAI,KB+KDPAR)
  VCMAX2= VCMAX2 * (PSIFUN(LAI,KDPAR) - PSIFUN(LAI,KB+KDPAR))

C *****
C      CO2 compensation point in dark
C *****
C      Adjust Michaelis constant of carboxylation for temp (Pa)
C -----
  KC1= KCT0 * EXP(DUM(3)*HAKC)
  KC2= KCT0 * EXP(DUM(4)*HAKC)

C      Adjust Michaelis constant of oxygenation for temp (Pa)
C -----
  KO1= KOT0 * EXP(DUM(3)*HAKO)
  KO2= KOT0 * EXP(DUM(4)*HAKO)

C      Rubisco specificity factor (-)
C -----
  TAU1= 4.76 * KO1 / KC1
  TAU2= 4.76 * KO2 / KC2

C      CO2 compensation point in dark (Pa)
C -----
  COMP1= (0.5*OSS/TAU1 +KC1*RD1*(1.+OSS/KO1)/VCMAX1)
+        / (1.-RD1/VCMAX1)
  COMP2= (0.5*OSS/TAU2 +KC2*RD2*(1.+OSS/KO2)/VCMAX2)
+        / (1.-RD2/VCMAX2)

C *****
C      Electron transport
C *****
C      Adjust unit potential electron transport for temperature (mol m-2 s-1)
C -----
  DUM(6)= EXP(HAJM/RGAS*(1./TJM-1./TLEAF1))
  J1= JMOP * HDJM * DUM(6) / (HDJM-HAJM*(1.-DUM(6)))
  DUM(6)= EXP(HAJM/RGAS*(1./TJM-1./TLEAF2))
  J2= JMOP * HDJM * DUM(6) / (HDJM-HAJM*(1.-DUM(6)))

C      Scale-up potential electron transport of sunlit big-leaf (mol m-2 s-1)
C -----
  J1= J1 * PSIFUN(LAI,KB+KDPAR)

C      Adjust electr transp of sunlit big-leaf for PAR effects (mol m-2 s-1)
C -----
  DUM(7)= THETA
  DUM(8)= - J1 - APAR1 * ALPHA
  DUM(9)= J1 * APAR1 * ALPHA
  J1= (-DUM(8)-SQRT(DUM(8)*DUM(8)-4.*DUM(7)*DUM(9)))/(2.*DUM(7))

C      Adjust electr transp of individual shaded leaf at the top
C      of the canopy for PAR effects (mol m-2 s-1)
C -----
  DUM(7)= THETA
  DUM(8)= - J2 - APARU2 * ALPHA
  DUM(9)= J2 * APARU2 * ALPHA
  J2= (-DUM(8)-SQRT(DUM(8)*DUM(8)-4.*DUM(7)*DUM(9)))/(2.*DUM(7))

C      Scale-up potential electron transport of shaded big-leaf (mol m-2 s-1)
C -----
  J2= J2 * (PSIFUN(LAI,KDPAR) - PSIFUN(LAI,KB+KDPAR))

ELSE                                     !night-time computations
  J1= 0.
  J2= 0.
  RD1= 0.
  VCMAX1= 0.
END IF

RETURN
END

```

```

C *****

```

C           References

C \*\*\*\*\*  
C Farquhar GD, von Caemmerer S, Berry JA (1980) A biochemical model of photosynthetic  
C CO<sub>2</sub> assimilation in leaves of C<sub>3</sub> species. *Planta* 149, 78-90  
C Farquhar GD, von Caemmerer S (1982) Modelling of photosynthetic response to  
C environmental conditions. In *Encyclopedia of Plant Physiology. New Series.*  
C Vol. 12B. *Physiological Plant Ecology II* (eds. OL Lange, PS Nobel, CB Osmond,  
C H Ziegler), pp. 549-587. Springer Verlag, Berlin.  
C Farquhar GD, Wong SC 1984. An empirical model of stomatal conductance. *Aust J*  
C *Plant Physiol* 11, 191-210  
C Leuning R 1997. Scaling to a common temperature improves the correlation  
C between the photosynthesis parameters J<sub>max</sub> and V<sub>cmax</sub>. *J Exp Bot* 48, 345-347  
C Wang YP, Leuning R 1998. A two-leaf model for canopy conductance, photosynthesis  
C and partitioning of available energy. I. Model description and comparison with  
C a multi-layered model. *Agr For Meteorol* 91, 89-111  
C

```

C *****
C FORTRAN subroutine      USTOREY      (ustorey.for)      27/2/99
C -----
C Purpose The routine computes transpiration, growth and net C exchange from
C a generic understorey, based on input values of:
C - global radiation absorbed by the understorey
C - air vapour pressure deficit
C - soil water content
C Based on the RESCAP model (Monteith et al 1989; Dewar 1997)
C which implies:
C - constant ci/ca ratio
C - NPP is a fixed proportion of GPP (Waring et al 1998)
C However, the effects of atmospheric CO2 on water use efficiency
C has also been included as outlined in Jones 1992, assuming a
C C3 plant (ci/ca=0.7).
C It is assumed that no gas-exchange takes place on days with ground frost
C (Landsberg & Waring 1997).
C A value of light utilization coefficient for crops is derived
C from Jones 1992 (total aboveground dry matter vs intercepted
C global radiation), assuming allocation belowground is 30%.

```

C Parameters and variables

```

C APARUND photosynth act rad absorbed by understorey (W m-2)
C AUND net understorey CO2 exchange (molC m-2 s-1)
C CA CO2 partial pressure in the atmosphere (Pa)
C DAY day of simulation
C EUND understorey transpiration (mol m-2 s-1)
C EUNDW water-limited understorey transpiration (kg m-2 s-1)
C EPSUND understorey light utilization coeff (kgDM J-1)
C FC coeff for conversion of carbon into DM (kgC kgDM-1)
C FFERS reduction factor for ground frost (-)
C GUND understorey growth rate (kgDM m-2 s-1)
C GUNDL light-limited understorey growth rate (kgDM m-2 s-1)
C GUNDW water-limited understorey growth rate (kgDM m-2 s-1)
C HOUR half/hour interval number
C LRUND coeff allocation to roots in understorey (-)
C MW molecular weight of H2O (kg mol-1)
C RWEFF root efficiency in water extraction (kgH2O kgDM-1 s-1)
C VPD vapour pressure deficit in the atmosphere (Pa)
C VWSL soil volumetric water content (m3 m-3)
C VWMIN minimum soil water content (m3 m-3)
C WFUND understorey foliage biomass (kgDM m-2)
C WRUND understorey fine root biomass (kgDM m-2)

```

C \*\*\*\*\*

SUBROUTINE USTOREY (APARUND, DAY, HOUR)

C \*\*\*\*\*

Define parameters and variables

C \*\*\*\*\*

```

INTEGER DAY, HOUR
REAL APARUND, EUNDW, EPSUND,
+ GUND, GUNDL, GUNDW, LRUND, RWEFF,
+ VWMIN, WUEUND
PARAMETER (EPSUND= 1.8E-9,
+ LRUND= 0.3,
+ RWEFF= 1.25E-3,
+ VWMIN= 0.1)
INCLUDE 'HYDRALL.CMN'

```

C \*\*\*\*\*

Day-time computations

C \*\*\*\*\*

```

IF (APARUND.GT.0.) THEN
C Initial fine root biomass in understorey (kgDM m-2)
C -----
WRUND= WFUND * LRUND / (1.-LRUND)

```

C Water use efficiency (molC molH2O-1, then kgDM kgH2O-1)

```

C -----
WUEUND= CA * 0.3 / 1.6 / VPD(HOUR)
WUEUND= WUEUND * 0.012 / MW !units into kgC kgH2O-1

```

```

WUEUND= WUEUND * 0.47           !reduce for respiration
WUEUND= WUEUND / FC             !translate into kgDM kgH2O-1

C   Light-limited growth (kgDM m-2 s-1)
C   -----
GUNDL= EPSUND * APARUND

C   Water-limited transpiration (kg m-2 s-1) and growth (kgDM m-2 s-1)
C   -----
EUNDW= RWEFF * WRUND * MAX(VWSL-VWMIN,0.)
GUNDW= EUNDW * WUEUND

C   Underst growth, transp (mol m-2 s-1) and net CO2 exch (mol m-2 s-1)
C   -----
GUND= MIN(GUNDL,GUNDW)
EUND(HOUR)= GUND / WUEUND / MW
AUND(HOUR)= GUND * FC / 0.012

C   Reduce understorey gas exchange for ground frost
C   -----
IF(TMIN(DAY).LT.0.) THEN
    AUND(HOUR)= 0.
    EUND(HOUR)= 0.
END IF

C   Foliage biomass
C   -----
WFUND= WFUND + GUND * (1.-LRUND) * 1800.
IF(WFUND.LT.1.E-6) WFUND= 1.E-6

C *****
C   Night-time computations
C *****
ELSE
    GUND= 0.
    EUND(HOUR)= 0.
    AUND(HOUR)= 0.
END IF

RETURN
END

C *****
C   References
C *****
C Dewar R.C. 1997. A simple model of light and water use evaluated for
C   Pinus radiata. Tree Physiol 17,259-265
C Jones HG 1992. Plants and Microclimate. Cambridge Univ Press, Cambridge
C Landsberg JJ, Waring RH 1997. A generalized model of forest productivity
C   using simplified concepts of radiation-use efficiency, carbon balance
C   and partitioning. For Ecol Manag 95,209-228
C Monteith JL, Huda AKS, Midya D 1989. RESCAP: a resource capture model
C   for sorghum and pearl millet. In: Virmani SM, Tandon HLS, Alagarswamy G
C   (eds) Modelling the Growth and Development of Sorghum and Pearl Millet.
C   ICRISAT Research Bull 12 Patancheru, India, pp 30-34
C Waring RH, Landsberg JJ, Williams M 1998. Net primary production of
C   forests: a constant fraction of gross primary production? Tree Physiol
C   18, 129-134

```

```

C *****
C FORTRAN subroutine      WEATHER      (weather.for)      9/4/99
C -----
C Purpose The subroutine computes and tabulates the diurnal course of
C environmental variables (1/2 hourly values) needed by subroutine
C GASFLUX for the computation of stand assimilation and transpiration,
C based on user-defined constraints:
C   - minimum daily temperature
C   - maximum daily temperature
C   - air relative humidity at minimum temperature
C   - daily cumulated global radiation.
C Output from the subroutine are, for 12 months:
C   - 1/2-hourly values of air temperature;
C   - 1/2-hourly values of VPD;
C   - 1/2-hourly values of incoming direct global radiation;
C   - 1/2-hourly values of incoming diffuse global radiation;
C   - 1/2-hourly values of incoming longwave radiation.
C First element of arrays for time 00:00.
C
C Instantaneous global radiation computed from measured daily values as described
C in Goudriaan & van Laar (1994), forcing the value of average atmospheric
C transmissivity. Neglected the effects of variable optical air mass.
C Average atmospheric transmissivity computed from the relative heliophany,
C according to the Angstrom model (Maracchi et al. 1983). The fraction of diffuse
C radiation is a function of atmospheric transmissivity and is represented by
C the discontinuous function for daily totals in Goudriaan & van Laar (1994).
C
C Downward long-wave irradiance under cloud-free conditions function of air
C temperature and atmospheric emissivity, in turn a function of air vapour
C pressure and temperature, according to the Brutsaert's model (Kustas et al 1989).
C Effect of cloudiness on atmospheric emissivity represented according to
C Monteith & Unsworth (1990).
C
C The diurnal course of air temperature is derived from maximum and minimum
C temperatures and daylength as in Goudriaan & van Laar (1994). Different
C formulations apply for day- and night-time temperatures.
C
C Air vapour pressure assumed to be constant over the day (Goudriaan & van Laar 1994).
C Dew point temperature is computed as described by Kimball et al 1997, based on
C minimum, maximum temperature and on the balance between annual precipitation and
C daily potential evapotranspiration (derived from Priestley-Taylor equation).
C Vapour pressure deficit difference from saturated air humidity, computed with
C the Tetens' equation (Jones 1992).
C Note: the model applied by Kimball et al 1997 for the computation of PET contains
C an error, since net radiation is assumed equal to absorbed global radiation.
C The original formula has been retained, however, so as to be able to apply the
C empirical model for the computation of RH.
C
C Parameters and variables
C A1      solar shift with respect to the Equator (-)
C A2      amplitude of the sine of solar height (-)
C CLOUD   fraction of cloud cover (-)
C C1      factor for the computation of RADDIR
C C2      factor for the computation of night-time TAIR (-)
C DAY     Julian day (-)
C DLENGTH daylength (hours)
C EAIR    vapour pressure of the air (Pa)
C HELIO   relative heliophany (-)
C ESAT    saturated vapour pressure (Pa)
C EMISS   sky long-wave emissivity (-)
C ETPOT   daily potential evapotranspiration (Priestley-Taylor) (mm d-1)
C FDIF    fraction of diffuse global radiation (-)
C LATIT   latitude (radians)
C PREYR   annual precipitation (mm yr-1)
C RG      global radiation (W m-2)
C RGDIF(48) diffuse global radiation (W m-2)
C RGDIR(48) direct global radiation (W m-2)
C RGDAY   cumulated daily global radiation (J m-2 d-1)
C RGDMLX  daily global rad for unit transmissivity (J m-2 d-1)
C LW(48)  incoming long-wave radiation (W m-2)
C S(48)   slope of sat vapor pressure vs temperature (Pa K-1)
C SDAY    slope S at mean daily temperature (Pa K-1)
C SHIFT   time between solar noon and maximum temp. (hours)
C SIGMA   Stefan-Boltzmann constant (W m-2 K-1)

```

```

C SINBETA  sine of solar elevation (-)
C SINDELTA sine of declination of the sun to the Equator (-)
C TAIR(48) air temperature (oC)
C TAU      atmospheric transmissivity (-)
C TC      nocturnal time coefficient (hours)
C TDEW    daily dew-point temperature (oC)
C TIME    hour (hours)
C TMAX(366) daily maximum temperature (oC)
C TMEAN(366) daily average temperature (oC)
C TMIN(366) daily minimum temperature (oC)
C TSSET   temperature at sunset (oC)
C VPD(48) vapour pressure deficit (Pa)

```

```

C *****

```

```

SUBROUTINE WEATHER(DAY)

```

```

C *****

```

```

C Define parameters and variables

```

```

C *****

```

```

C Parameters and variables

```

```

C -----

```

```

      INTEGER    I, DAY
      REAL       CLOUD, C1, C2, DLENGTH, DUM1, DUM2, EAIR, EMISS,
+              ESAT, ETPOT, FDIF, HELIO, RG, RGMX, SHIFT,
+              SINDELTA, TAU, TC, TDEW, TIME, TSSET
      PARAMETER  (SHIFT= 1.5,
+              TC= 4.)
      INCLUDE 'HYDRALL.CMN'

```

```

C *****

```

```

C Compute half-hourly values of radiation, temperature and VPD

```

```

C *****

```

```

C Preliminary computations

```

```

C 1. Factor for the computation of RADDIR

```

```

C -----

```

```

      C1= 1367. * (1.+ 0.033 * COS(2.*PI*(DAY-10.)/365.))

```

```

C 2. Sine of declination of the sun to the Equator

```

```

C -----

```

```

      SINDELTA= - 0.4093 * COS(2.*PI*(DAY+10)/365.)

```

```

C 3. Solar shift with respect to the Equator

```

```

C -----

```

```

      A1= SIN(LATIT) * SINDELTA

```

```

C 4. Amplitude of the sine of solar height

```

```

C -----

```

```

      A2= COS(LATIT) * SQRT(1-(SINDELTA*SINDELTA))

```

```

C 5. Daylength

```

```

C -----

```

```

      IF(A1/A2.LT.-1.) THEN

```

```

          DLENGTH= 0.

```

```

      ELSE IF(A1/A2.GT.1.) THEN

```

```

          DLENGTH= 23.99

```

```

      ELSE

```

```

          DLENGTH= 12. * (1. + 0.6366 * ASIN(A1/A2))

```

```

      END IF

```

```

C 6. Temperature at sun-set

```

```

C -----

```

```

      TSSET= TMIN(DAY) + (TMAX(DAY)-TMIN(DAY)) *

```

```
+      SIN(PI*DLENGTH/(DLENGTH+2.*SHIFT))

```

```

C 7. Factor for the computation of night-time TAIR

```

```

C -----

```

```

      C2= EXP((DLENGTH-24.)/TC)

```

```

C 8. Maximum daily global radiation for unit transmissivity

```

```

C -----

```

```

      DUM1= 24. / PI

```

```

      RGMX= C1*3600.*(A1*DLENGTH+A2*DUM1*COS((DLENGTH-12.)/DUM1))

```

```

C 9. Average air transmissivity

```

```

C -----

```

```

      TAU= RGDAY(DAY) / RGMX

```

```

C 10. Relative heliophany (inverted Angstrom model), average cloud cover

```

```

C -----

```

```

      HELIO= (TAU - 0.2714) / 0.7571

```

```

      CLOUD= 1. - HELIO

```



```

IF(CLOUD.GT.1.) CLOUD= 1.
IF(CLOUD.LT.0.) CLOUD= 0.
C 11. Fraction of diffuse radiation
C -----
IF(TAU.LT.0.1) THEN
  FDIF= 1.
ELSE IF(TAU.GT.0.7) THEN
  FDIF= 0.2
ELSE
  FDIF= 1.133 - 1.33 * TAU
END IF

C 12. Daily dew-point temperature, air absolute humidity
C -----
SDAY= 2588464.2/(240.97+TMEAN(DAY))**2
+ * EXP(17.502* TMEAN(DAY)/(240.97+ TMEAN(DAY))) !slope of vapour at Tmean
ETPOT= 0.9072 * SDAY/(SDAY+GAMMA)/(LATENT/MW) * RGDAY(DAY) !daily PET
DUM2= ETPOT / PREYR
TDEW= (TMIN(DAY)+273.2) *
+ (0.9974 - 1.6187*DUM2 +
+ 13.8018*DUM2*DUM2 - 36.7307*DUM2**3. +
+ 0.0006*(TMAX(DAY)-TMIN(DAY))) !est dew-point temp (K)
TDEW= TDEW - 273.2 !convert units into oC
EAIR= 613.75 * EXP(17.502 * TDEW / (240.97+TDEW)) !air vapour pressure (Pa)

DO 100, I= 1,48
  TIME= 0.5 * (I-1)
C Compute RG separately for day-time and night-time
C -----
IF (TIME.GE.(12.-DLENGTH/2.).AND.
+ TIME.LE.(12.+DLENGTH/2.)) THEN
  SINBETA(I)= A1 + A2 * COS(0.2618 * (TIME-12.))
  RG= TAU * SINBETA(I) * C1
ELSE
  RG= 0.
END IF
RGDIF(I)= RG * FDIF
RGDIR(I)= RG - RGDIF(I)

C Compute air temperature separately for day-time and night time
C -----
IF (TIME.LE.(12.-DLENGTH/2.)) THEN
  TAIR(I)= (TMIN(DAY)-TSSET*C2+(TSSET-TMIN(DAY))
+ * EXP((DLENGTH/2.-12.-TIME)/TC)) / (1.-C2)
ELSE IF (TIME.GE.(12.+DLENGTH/2.)) THEN
  TAIR(I)= (TMIN(DAY)-TSSET*C2+(TSSET-TMIN(DAY))
+ * EXP((12.+DLENGTH/2.-TIME)/TC)) / (1.-C2)
ELSE
  TAIR(I)= TMIN(DAY) + (TMAX(DAY)-TMIN(DAY)) *
+ SIN(PI*(TIME-12.+DLENGTH/2.)/
+ (DLENGTH+2.*SHIFT))
END IF

C Compute vapour pressure deficit (a limit is imposed to air vapor
C pressure, based on minimum daily temperature)
C -----
ESAT= 613.75 * EXP(17.502 * TAIR(I) / (240.97+TAIR(I)))
IF (ESAT.GT.EAIR) THEN
  VPD(I)= ESAT - EAIR
ELSE
  VPD(I)= 1.E-6
END IF

C Slope of saturated vapor pressure vs temperature relationship
C -----
S(I)= 2588464.2/(240.97+TAIR(I))**2
+ * EXP(17.502* TAIR(I)/(240.97+ TAIR(I)))

C Compute downward long-wave radiation from cloudy sky
C -----
EMISS= 1.24*(EAIR/100./(TAIR(I)+273.2))**(1./7.)
EMISS= (1. - 0.84*CLOUD) * EMISS + 0.84 * CLOUD
RLW(I)= EMISS * SIGMA * (TAIR(I)+273.2)**4

```

100 CONTINUE

RETURN  
END

C \*\*\*\*\*  
C           REFERENCES  
C \*\*\*\*\*  
C Goudriaan J, van Laar HH (1994) Modeling Potential Crop Growth  
C     Processes. pp. 238. Kluwer Academic Publ., Dordrecht  
C Jones HG (1992) Plants and Microclimate. 2nd Ed. pp. 428. Cambridge  
C     University, Cambridge  
C Kimball JS, Running SW, Nemani R 1997. An improved method for estimating  
C     surface humidity from daily minimum temperature. Agr For Meteor 85,87-98  
C Kustas WP, Jackson RD, Asrar G 1989. Estimating surface energy-balance  
C     components from remotely sensed data. In: Asrar G (ed) Theory and  
C     Applications of Optical Remote Sensing. pp 604-627 JWiley, New York  
C Maracchi G, Benincasa F, Zipoli G 1983. Elementi di Agrometeorologia.  
C     pp 76. CNR-IATA, Firenze  
C Monteith J, Unsworth M 1990. Principles of Environmental Physics. 2nd Ed.  
C     pp 291 Arnold, London

```

C *****
C FORTRAN function      PSIFUN      (psifun.for)          13/10/98
C -----
C Purpose Returns the function Psi of Wang & Leuning 1998, integral of an
C      exponential function over the canopy.
C
C Parameters and variables
C
C LAI canopy leaf area index (-)
C Z argument to be integrated over the canopy
C *****

      FUNCTION PSIFUN(LAI,Z)

C *****
C      Define parameters and variables
C *****
      REAL    LAI,PSIFUN,Z

C *****
C      Computations
C *****
      PSIFUN= (1. - EXP(-Z*LAI)) / Z

      RETURN
      END

C *****
C      References
C *****
C Wang YP, Leuning R 1998. A two-leaf model for canopy conductance, photosynthesis
C      and partitioning of available energy. I. Model description and comparison with
C      a multi-layered model. Agr For Meteorol 91, 89-111

```

```

C *****
C FORTRAN function      TFUN      (tfun.for)                3/3/99
C -----
C Purpose Returns a correction factor for temperature effects on
C respiration. The formulation of Lloyd & Taylor (1994) is applied,
C to account for the shift in Q10 with temperature.
C Reference conditions are assumed at a temperature of 10 oC.
C
C Parameters and variables
C
C T      temperature (oC)
C
C *****
C
C      FUNCTION TFUN(T)
C *****
C      Define parameters and variables
C *****
C      REAL      T,TFUN
C *****
C      Computations
C *****
C      TFUN= 308.56 * (1./56.02 - 1./(T+46.02))
C      TFUN= EXP(TFUN)
C
C      RETURN
C      END
C *****
C      References
C *****
C      Lloyd J, Taylor JA 1994. On the temperature dependence of soil respiration.
C      Funct Ecol 8,315-323

```

```
C FILES.CMN
C -----
C Include common block
C -----
C Location of input files
C -----
C IFILES location of root input file

      CHARACTER*40 IFILES

C Common block
C -----
      COMMON /FILES/ IFILES
```

```

C HYDRALL.CMN
C -----
C Include common block
C -----
C Physical constants and parameters
C -----
C CA      baseline CO2 partial pressure in the atmosphere (Pa)
C CP      specific heat capacity of air (J mol-1 K-1)
C DCA     annual change in atmospheric CO2 (%)
C FC      coeff for conversion of carbon into DM (kgC kgDM-1)
C GAMMA   psychrometer constant (Pa K-1)
C LATENT  latent heat of vaporization (J mol-1)
C MW      molecular weight of H2O (kg mol-1)
C OSS     oxygen part pressure in the atmosphere (Pa)
C PI      pi greek (-)
C PRESS   atmospheric pressure (Pa)
C RGAS    gas constant (Pa m3 mol-1 K-1)
C ROS     wood density (kgDM m-3)
C SIGMA   Stefan-Boltzmann constant (W m-2 K-4)

```

```

      REAL CA, CP, DCA, FC, GAMMA, LATENT, MW, OSS, PI,
+      PRESS, RGAS, ROS, SIGMA

```

```

C Miscellaneous parameters input from file
C -----

```

```

C AGE0    initial stand age (yr)
C ALTIT   site altitude (m)
C BSL     coeff. in soil water retention curve equation
C CONV    dry matter conversion efficiency (growth resp.) (-)
C CSLOO   initial old organic matter in soil (kgDM m-2)
C CSLYO   initial young organic matter in soil (kgDM m-2)
C FORM    stem form factor (-)
C H0      initial stand height (m)
C KR      root specific conductance (m3 MPa-1 s-1 kg-1)
C KSMAX   max. sapwood specific conductivity (m3 MPa-1 s-1 m-1)
C KLSLAT  saturated soil hydr. conduct. (m3 MPa-1 s-1 m-1)
C LATIT   site latitude (rad)
C LF      foliage longevity (yr)
C LONGIT  site latitude (degrees x 1.00)
C LR      fine root longevity (yr)
C LS      sapwood longevity (yr)
C MERCH   merchantable wood as fraction of stem biomass (-)
C NF      foliage nitrogen concentration (kg kgDM-1)
C NR      fine root nitrogen concentration (molN kgDM-1)
C NS      sapwood nitrogen concentration (molN kgDM-1)
C NYRS    simulation length (yr)
C PENTRY  soil entry water potential (MPa)
C PLANT   planting density (m-2)
C PSITHR  water potential threshold for cavitation (MPa)
C ROF     foliage density (kgDM m-3)
C RADRT   root radius (m)
C SLA     specific leaf area (project. leaf area basis) (m2 kgDM-1)
C SLDEP   depth of soil explored by roots (m)
C STH     option for self-thinning (1 : included, 0 : neglected)
C STH0    intercept in self-thinning eq. (logN vs logWST) (m-2)
C STH1    slope in self-thinning eq. (logN vs logWST) (kgDM-1)
C STIND   stomatal index (1= amphy-, 2= hypostomatous species)
C THAGE   age for thinning (-)
C THN     thinning intensity, plants (-)
C THV     thinning intensity, volume (-)
C TREESO  initial stand density (m-2)
C VOLO    initial stand volume (m3 ha-1)
C VWSAT   saturated soil water content (m3 m-3)
C W       leaf width (m)

```

```

      INTEGER  AGE0, NYRS, STH, STIND, THAGE (20)
      REAL    ALTIT, BSL, CONV, CSLOO, CSLYO, FORM, H0, KR, KSMAX, KLSLAT,
+           LATIT, LF, LONGIT, LR, LS, MERCH, NF, NR, NS, PENTRY, PLANT,
+           PSITHR, RADRT, ROF, SLA, SLDEP, STH0, STH1,
+           THN (20), THV (20), TREESO, VOLO, VWSAT, W

```

```

C Photosynthesis/stomatal parameters input from file
C -----

```

C ALPHA quantum efficiency of electron transport (mol e mol<sup>-1</sup> quanta)  
 C HAJM activation energy of electron transport (J mol<sup>-1</sup>)  
 C HAKC activation energy for carboxylation (J mol<sup>-1</sup>)  
 C HAKO activation energy for oxygenation (J mol<sup>-1</sup>)  
 C HARD activation energy (J mol<sup>-1</sup>)  
 C HAVCM activation energy for carboxylation (J mol<sup>-1</sup>)  
 C HDJM deactivation energy of electron transport (J mol<sup>-1</sup>)  
 C JMOP potential rate of electron transport at optimum temperature (mol m<sup>-2</sup> s<sup>-1</sup>)  
 C KCTO Michaelis constant for carboxylation at reference temperature (Pa)  
 C KOTO Michaelis constant for oxygenation at reference temperature (Pa)  
 C PSIO soil water potential for complete stomatal closure (MPa)  
 C RDTO dark respiration at reference temp (mol m<sup>-2</sup> s<sup>-1</sup>)  
 C STOMO stomatal conductance to CO<sub>2</sub> in darkness (molCO<sub>2</sub> m<sup>-2</sup> s<sup>-1</sup>)  
 C STOM1 coeff in g<sub>s</sub> vs A equation (Pa)  
 C THETA convexity factor of light response curve (-)  
 C TJM optimum temperature for electron transport (K)  
 C VCMOP max carboxylation rate at opt temp (mol m<sup>-2</sup> s<sup>-1</sup>)  
 C VPDO coeff in g<sub>s</sub> response to D<sub>s</sub> (Pa)

REAL ALPHA, HAJM, HAKC, HAKO,  
 + HARD, HAVCM, HDJM, JMOP,  
 + KCTO, KOTO, PSIO, RDTO, STOMO,  
 + STOM1, THETA, TJM, VCMOP, VPDO

C Environmental variables read from file

C -----  
 C DAYTOT total number of days in the year  
 C PRE daily precipitation (mm d<sup>-1</sup>)  
 C RGDAY daily total of global radiation (J m<sup>-2</sup> d<sup>-1</sup>)  
 C RH air relative humidity (%)  
 C TMAX maximum daily temperature (oC)  
 C TMEAN mean daily temperature (oC)  
 C TMIN minimum daily temperature (oC)  
 C WND monthly (constant) wind speed (m s<sup>-1</sup>)

INTEGER DAYTOT  
 REAL PRE(366), RGDAY(366), RH(366), TMAX(366),  
 + TMEAN(366), TMIN(366), WND(366)

C Half-hourly values of environmental variables from subroutine WEATHER

C -----  
 C RGDIF diffuse global radiation (W m<sup>-2</sup>)  
 C RGDIR direct global radiation (W m<sup>-2</sup>)  
 C RLW incoming long-wave radiation (W m<sup>-2</sup>)  
 C S slope of sat vapor press vs temp (Pa K<sup>-1</sup>) from GASFLUX  
 C SINBETA sine of solar elevation (-)  
 C TAIR air temperature (oC)  
 C VPD vapour pressure deficit (Pa)

REAL RGDIF(48), RGDIR(48), RLW(48), S(48),  
 + SINBETA(48), TAIR(48), VPD(48)

C Annual output

C -----  
 C AGE stand age (yrs)  
 C ALPHAC canopy quantum efficiency (-)  
 C ALLENEW coefficient of allocation to foliage (-)  
 C ALLRNEW coefficient of allocation to fine roots (-)  
 C ALLSNEW coefficient of allocation to sapwood (-)  
 C APARYR annual absorbed PAR (mol m<sup>-2</sup> yr<sup>-1</sup>)  
 C CAI current annual increment (m<sup>3</sup> ha<sup>-1</sup> yr<sup>-1</sup>)  
 C CSLO old organic matter in soil (kgDM m<sup>-2</sup>)  
 C CSLY young organic matter in soil (kgDM m<sup>-2</sup>)  
 C DAYCRIT Julian day of critical water relations  
 C DBH average tree diameter at breast height (cm)  
 C ECRIT critical transpiration rate (mol m<sup>-2</sup> s<sup>-1</sup>)  
 C ETYR annual site evapo-transpiration (mm yr<sup>-1</sup>)  
 C EUYR annual understorey transpiration (mm yr<sup>-1</sup>)  
 C EYR annual canopy transpiration (mm yr<sup>-1</sup>)  
 C GPPYR annual gross primary production (kgC m<sup>-2</sup> yr<sup>-1</sup>)  
 C GST annual gross stand growth (kgDM yr<sup>-1</sup> m<sup>-2</sup>)  
 C H tree height (m)  
 C NEEYR annual net ecosystem exchange (kgC m<sup>-2</sup> yr<sup>-1</sup>)

C NPPYR stand annual net primary production (kgC m<sup>-2</sup> yr<sup>-1</sup>)  
 C PREYR annual precipitation (mm yr<sup>-1</sup>)  
 C PSILMIN minimum leaf water potential over the year (MPa)  
 C PSISCRIT critical soil water potential (MPa)  
 C PSISMIN minimum soil water potential over the year (MPa)  
 C RGYR annual cumulated global radiation (J m<sup>-2</sup> yr<sup>-1</sup>)  
 C SAPBA sapwood basal area (m<sup>2</sup> m<sup>-2</sup>)  
 C TREES stand density (trees m<sup>-1</sup>)  
 C VOL stand volume (m<sup>3</sup> ha<sup>-1</sup>)  
 C WF stand foliage biomass (kgDM m<sup>-2</sup>)  
 C WFTR tree foliage biomass (kgDM)  
 C WFUND understorey foliage biomass (kgDM m<sup>-2</sup>)  
 C WR stand fine root biomass (kgDM m<sup>-2</sup>)  
 C WRTR tree fine root biomass (kgDM)  
 C WRUND understorey root biomass (kgDM m<sup>-2</sup>)  
 C WS stand sapwood biomass (kgDM m<sup>-2</sup>)  
 C WSTR tree sapwood biomass (kgDM)  
 C WST stand stemwood biomass (kgDM m<sup>-2</sup>)  
 C WSTTR tree stemwood biomass (kgDM)

INTEGER AGE  
 REAL ALLFNEW, ALLRNEW, ALLSNEW, ALPHAC, APARYR, CAI, CSLO,  
 + CSLY, DAYCRIT, DBH, ECRIT, ETYR, EUYR, EYR, GPPYR, GST, H,  
 + NEEYR, NPPYR, PREYR, PSILMIN, PSISCRIT, PSISMIN, RGYR, SAPBA,  
 + TREES, VOL, WF, WFTR, WFUND, WR, WRTR, WRUND, WS, WSTR, WST,  
 + WSTTR

C Half-hourly or daily output

C -----  
 C ATOT canopy net photosynthesis (mol m<sup>-2</sup> s<sup>-1</sup>)  
 C AUND understorey net photosynthesis (mol m<sup>-2</sup> s<sup>-1</sup>)  
 C ETOT canopy transpiration (mol m<sup>-2</sup> s<sup>-1</sup>)  
 C EUND understorey transpiration (mol m<sup>-2</sup> s<sup>-1</sup>)  
 C GSCTOT canopy conductance to CO<sub>2</sub> (mol m<sup>-2</sup> s<sup>-1</sup>)  
 C HS total flux of sensible heat from the canopy (W m<sup>-2</sup>)  
 C PSISL soil water potential (MPa)  
 C VWSL soil volumetric water content (m<sup>3</sup> m<sup>-3</sup>)

REAL ATOT(48), AUND(48), ETOT(48), EUND(48),  
 + GSCTOT(48), HS(48), PSISL, VWSL

C Dummy variables for output

C -----  
 C DUMH1..8 dummy variable for half-hourly output  
 C DUMY1..4 dummy variable for annual output

REAL DUMH1(48), DUMH2(48), DUMH3(48), DUMH4(48),  
 + DUMH5(48), DUMH6(48), DUMH7(48), DUMH8(48),  
 + DUMH9(48), DUMH10(48), DUMH11(48),  
 + DUMY1, DUMY2, DUMY3, DUMY4

C Common blocks

C -----  
 COMMON /PHYS/ CA, CP, DCA, FC, GAMMA, LATENT, MW, OSS,  
 + PI, PRESS, RGAS, ROS, SIGMA  
  
 COMMON /PARMS/ AGE0, ALTIT, BSL, CONV, CSLO0, CSLY0, FORM, HO, KR,  
 + KSMAX, KSLSAT, LATIT, LF, LONGIT, LR, LS, MERCH, NF, NR, NS,  
 + NYRS, PENTRY, PLANT, PSITHR, RADRT, ROF, SLA, SLDEP, STH,  
 + STH0, STH1, STIND, THAGE, THN, THV, TREES0, VOL0, VWSAT, W  
  
 COMMON /ENVIR/ DAYTOT, PRE, RGDAY, RH, TMAX, TMEAN, TMIN, WND,  
 + RGDIF, RGDIF, RLW, S, SINBETA, TAIR, VPD  
  
 COMMON /PHOTO/ ALPHA, HAJM, HAKC, HAKO,  
 + HARD, HAVCM, HDJM, JMOP, KCT0,  
 + KOT0, PSIO, RDT0, STOMO, STOM1,  
 + THETA, TJM, VCMOP, VPD0  
  
 COMMON /HHOURLY/ ATOT, AUND, ETOT, EUND, GSCTOT, HS, PSISL, VWSL  
  
 COMMON /ANNUAL/ AGE, ALLFNEW, ALLRNEW, ALLSNEW, ALPHAC, APARYR,  
 + CAI, CSLO, CSLY, DAYCRIT, DBH, ECRIT, ETYR, EUYR, EYR,  
 + GPPYR, GST, H, NEEYR, NPPYR, PREYR, PSILMIN, PSISCRIT,



```
+          PSISMIN, RGYR, SAPBA, TREES, VOL, WF, WFTR, WFUND, WR,  
+          WRTR, WRUND, WS, WSTR, WST, WSTTR  
  
COMMON /DUMMY/ DUMH1, DUMH2, DUMH3, DUMH4,  
+          DUMH5, DUMH6, DUMH7, DUMH8, DUMH9, DUMH10, DUMH11,  
+          DUMY1, DUMY2, DUMY3, DUMY4
```

### Input file "Files.txt"

```
IPARMS = 'c:\temp\parms.txt'      !file for miscellaneous parameter input
IPHOT = 'c:\temp\photo.txt'      !file for photosynthesis/conductance parms input
IRUN = 'c:\temp\run.txt'         !file for runtime parms
ICLIMO = 'c:\temp\climate.prn'   !input of daily meteo data, initialization
ICLIM = 'c:\temp\climate.prn'   !input of daily meteo data, runs
HHOUR = 'c:\temp\hourly.txt'    !output file, 1/2 hourly data
ANNUAL = 'c:\temp\annual.txt'    !output file, annual data
```

### Input file "Parms.txt"

\*Pinus sylvestris, Thetford, UK

\*Tree structure

```
*-----
FORM= 0.4      !stem form factor (-)
ROF = 0.73     !foliage density (kgDM m-3)
ROS = 440.     !wood density (kg DM m-3)
SLA = 4.7      !specific leaf area (project. leaf area basis)(m2 kg-1)
STIND= 1       !stomatal index (1= amphy-, 2= hypostomatous species)
W = 0.02       !average leaf width (m)
```

\*Hydraulic properties

```
*-----
KR = 2.3E-7    !root specific conductance (m3 MPa-1 s-1 kg-1)
KSMAX = 1.2E-3 !max. sapwood specific conductivity (m2 MPa-1 s-1)
PSITHR = -1.4  !water potential threshold for cavitation (MPa)
```

\*Tissue mortality and respiration

```
*-----
LF = 2.6       !foliage longevity (yr)
LR = 0.65      !fine root longevity (yr)
LS = 39.       !sapwood longevity (yr)
NF = 0.015     !foliage nitrogen concentration (kg kgDM-1)
NR = 0.0075    !fine root nitrogen concentration (kg kgDM-1)
NS = 0.0005    !sapwood nitrogen concentration (kg kgDM-1)
```

\* Source of parameters:

```
* FORM= 0.5 from Edwards & Christie 1981, assuming MERCH= 0.9
* ROF= 0.1 from Ovington 1957
* ROS= 450. from Mencuccini & Grace 1995
* SLA= 4.7 from Mencuccini & Grace 1995
* W= 0.03 from Kellomaki & Wang 1998
* KR= 2.3E-7 from Magnani, Mencuccini & Grace 1999
* KSMAX= 1.2E-3 from Mencuccini & Grace 1995
* PSITHR= -1.5 from Magnani, Borghetti & Grace 1999
* NF= 0.015 from Mencuccini & Grace 1996
* NR= 0.0075 from Helmisaari & Siltala 1989
* NS= 0.0005 from Braekke 1995
* LF= 2.6 from Jalkanen et al 1994
* LS= 39 from Helmisaari & Siltala 1989
* LR= 0.65 from Persson 1980
```

### Input file "Photo.txt"

\*Pinus sylvestris, Thetford, UK

\*Photosynthetic and stomatal characteristics

```
*-----
ALPHA = 0.28   !quantum efficiency (mol mol-1)
PSIO = -1.5    !threshold of soil water potential for maximum stomatal closure (MPa)
STOMO = 2.3E-3 !stomatal conductance to CO2 in darkness (molCO2 m-2 s-1)
STOMI = 5.2E5  !coeff in gsc vs A equation (Pa-1)
VCMOP = 50.E-6 !max carboxylation rate at opt temp (mol m-2 s-1)
VPDO = 1200.   !coeff in gsc response to Ds (Pa)
```

```

*Source of photosynthetic parameters for Pinus sylvestris (see Psylvestris.xls)
*-----
* ALPHA= 0.28 value for Pinus sylvestris in Ecocraft database
* PSI0= -1. estimate based on Irvine 1999
* STOM0= 2.3E-3 Kellomaki & Wang 1998
* STOM1= 5.E5 Kellomaki & Wang 1998 (Fig. 6)
* VCMOP= 60.3E-6 Ecocraft database
* VCMOP= 60.E-6 maximum value in Kellomaki & Wang 1998 (Fig. 10)
* VCMOP= 37.5E-6 Wang et al 1996
* VPD0= 1200. value for Pinus sylvestris in Ecocraft database, derived from Wang (1996)

```

### Input file "Run.txt"

```

* Pinus sylvestris
*-----
*Site geographic location
*-----
Site: E. England (Thetford)
LATIT = 5242.      !site latitude (degrees x 100)
LONGIT = 0067.    !site longitude (degrees x 100)
ALTIT = 50.       !site altitude (m)

*Soil characteristics
*-----
CSLOO = 4.1       !initial old organic matter in soil (kgDM m-2)
CSLYO = 0.35      !initial young organic matter in soil (kgDM m-2)
SAND = 0.9        !soil fraction of sand particles (m3 m-3)
SILT = 0.1        !soil fraction of silt particles (m3 m-3)
SLDEP= 1.         !depth of soil explored by roots (m)

*Initial values, run duration (YC 14, intermediate thinning)
*-----
AGE0 = 1          !initial stand age (yr)
HO = 1.           !initial stand height (m)
NYRS = 100       !simulation length (yr)
PLANT = 10.       !planting density (m-2)
TREESO = 10.     !initial stand density (m-2)
VOL0 = 0.1       !initial stand volume (m3 ha-1)

*AGE0 = 17        !initial stand age (yr)
*HO = 8.8         !initial stand height (m)
*NYRS = 80        !simulation length (yr)
*PLANT = 0.3      !planting density (m-2)
*TREESO = 0.2159 !initial stand density (m-2)
*VOL0 = 64.77    !initial stand volume (m3 ha-1)

*Thinning regime
*-----
STH = 1           !option for self-thinning (1 : included, 0 : excluded)
THAGE = 22,27,32,37,42,47,52,57,62,67,72,77,82,87,92,97 !age for thinning (-)
THN = 0.38,
      0.34,
      0.26,
      0.21,
      0.17,
      0.15,
      0.14,
      0.11,
      0.10,
      0.08,
      0.07,
      0.06,
      0.05,
      0.05,
      0.04,

```

```
0.03      !thinning intensities by number (-)
THV =    0.33,
         0.28,
         0.23,
         0.19,
         0.16,
         0.14,
         0.13,
         0.11,
         0.09,
         0.08,
         0.07,
         0.06,
         0.05,
         0.04,
         0.04,
         0.03      !thinning intensities by volume (-)
```

\*Climate Change scenario

```
*-----
CA =     35.      !baseline atmospheric CO2 concentration (Pa)
DCA=     0.       !percent annual change in atmospheric CO2 (%)
```